

EDWARDS UNDERGROUND
WATER DISTRICT

Report 92-02

Investigation of the
Fresh/Saline-Water Interface
in the Edwards Aquifer in
New Braunfels and San Marcos, Texas

Report



**INVESTIGATION OF THE FRESH/SALINE-WATER INTERFACE IN THE
EDWARDS AQUIFER IN NEW BRAUNFELS AND SAN MARCOS, TEXAS**

by Diane Poteet, Hughbert Collier, and Robert Maclay

Edwards Underground Water District Report 92-02

TABLE OF CONTENTS

	Abstract	1-1
1.0	Introduction	1-1
1.1	Hydrogeologic Setting	1-1
1.2	Historical Perspective	1-4
1.3	Objectives	1-5
1.4	Acknowledgements.	1-5
2.0	Study Site Locations and Geology Setting	2-1
2.1	Study Site Locations and Geological Setting.	2-1
2.2	Overview of Geologic History.	2-5
3.0	Regional Geology	3-1
3.1	Geologic Setting	3-1
3.2	Diagenesis of the Edwards Aquifer.	3-4
3.3	Hydrogeologic Framework of the Edwards Aquifer	3-7
3.3-1	Lithofacies.	3-7
3.3-2	Hydrostratigraphic Units.	3-12
3.3-2.1	Confining Formations.	3-12
3.3-2.2	Internal Stratigraphic Units	3-15
3.4	Structural Geometry	3-19
3.5	Barrier Faults	3-19
3.6	Hydraulic Characterization	3-21
3.7	Regional Ground-Water Flow.	3-26
3.7.1	Water Levels and Ground-Water Flow.	3-26
4.0	Data Collection	4-1
5.0	Pump Tests, Water Quality Data, and Cutting Descriptions.	5-1
5.1	Pump Tests Results	5-1
5.1-1	Recovery Tests Performed at Various Depth Intervals	5-1
5.1-2	Pump Tests Performed with Observation Wells at Total Depth	5-7
5.2	Inorganic Water Sample Results.	5-14
5.2-1	Specific Conductance	5-14
5.2-1.1	Values Recorded at the End of Each Pump or Air-lift Test.	5-17
5.2-1.2	Values Recorded During Pump or Air-lift Testing	5-19
5.2-2	Temperature.	5-20
5.2-3	Ionic Concentrations	5-20
5.2-3.1	Stiff Diagrams.	5-22
5.2-3.2	Schoeller Diagrams.	5-22
5.2-3.3	Piper Diagrams	5-26
5.2-4	Saturation Indices.	5-30
5.3	Cutting and Thin Section Descriptions.	5-34
6.0	Petrophysical and Petrographic Analysis	6-1
6.1	Petrographic Analysis of the Cuttings	6-1

6.1-1	Methodology	6-1
6.1-2	Petrographic Analysis	6-3
6.1-2.1	Georgetown Formation	6-8
6.1-2.2	Person Formation	6-14
6.1-2.2-1	Cyclic, Marine, Leached and Collapsed Members (Undifferentiated)	6-14
6.1-2.2-2	Regional Dense Member	6-20
6.1-2.3	Kainer Formation	6-20
6.1-2.3-1	Grainstone Member	6-20
6.1-2.3-2	Kirschberg and Dolomitic Members (Undifferentiated)	6-24
6.1-2.3-3	Basal Nodular Member	6-27
6.2	Analysis of the Borehole Geophysical Logs	6-30
6.2-1	Methodology	6-30
6.2-2	Petrophysical Analysis	6-53
6.2-2.1	Lithology Variations	6-53
6.2-2.2	Porosity	6-58
6.2-2.3	Water Quality	6-60
6.3	Effectiveness of the Logging Program at the Transect Sites	6-60
7.0	Summary and Conclusions	7-1
7.1	Summary	7-1
7.2	Discussion	7-6
7.2-1	Important Lithologic Characteristics of the Edwards Group	7-6
7.2-2	Effects of Lithology on Transmissivity and Storativity	7-6
7.2-3	Important Chemical Considerations for the Fresh/Saline-Water Interface	7-7
7.3	Conclusions	7-8
7.4	Recommendations	7-12
	Bibliography	B-1

LIST OF FIGURES

1-1	Hydrologic boundaries of the Edwards Aquifer	1-3
2-1	Study site locations	2-2
2-2	New Braunfels study area - plan-view	2-3
2-3	New Braunfels study area - cross-section Y - Y'	2-4
2-4	San Marcos study area - plan-view	2-6
2-5	San Marcos study area - cross-section Z - Z'	2-7
2-6	Universal land mass Pangea	2-9
2-7	Break-up of Pangea after 20 million years ago	2-10
3-1	Early Cretaceous Central Texas Platform	3-2
3-2	Depositional province of Edwards Limestone and equivalent rocks	3-3
3-3	Major faults	3-5
3-4	Stratigraphy correlations	3-16
3-5	Displacements of major fault	3-20
3-6	Layered heterogeneity of the Edwards Aquifer on the San	

	Marcos Platform, Castle Hills Test Hole (AY-68-29-910)	3-22
3-7	Layered heterogeneity - within the Maverick Basin, Uvalde Test Hole YP-69-42-709	3-23
3-8	Layered heterogeneity of the Edwards Aquifer within the Devils River Trend, Sabinal Test Hole, YP-69-37-402	3-24
3-9	Simulated flow vectors at each cell in the mode	3-27
4-1	Drilling procedures	4-2
4-2	Drilling methods employed on the Bad-Water Line transect	4-6
4-3	Completion procedures	4-8
5-1	Pumping test analysis - recovery - New Braunfels C-1, packer test/interval 821-959.35 feet	5-4
5-2	Pumping test analysis - recovery - New Braunfels C-1, packer test/interval 618-706.33 feet	5-6
5.3	Transmissivity values for New Braunfels wells	5-8
5.4	Transmissivity values for San Marcos wells	5-9
5-5	Drawdown versus time for the New Braunfels seven-hour pump test	5-12
5-6	Theis Curve - $1/u$ versus $W(u)$	5-13
5-7	Specific conductance versus depth	5-18
5-8	Stiff diagrams for New Braunfels	5-23
5-9	Stiff diagrams for San Marcos	5-24
5-10	Schoeller diagrams by Clement	5-25
5-11	Schoeller diagrams for New Braunfels	5-27
5-12	Schoeller diagrams for San Marcos	5-28
5-13	USGS Piper diagram	5-29
5-14	Piper diagrams for New Braunfels	5-31
5-15	Piper diagrams for San Marcos	5-32
6-1	Type 1 - no visible porosity, NBA-1, 626-31	6-4
6-2	Type 1 - no visible porosity, NBC-1, 561.7-71.7	6-4
6-3	Type 2 - very little porosity, NBC-1, 540.7-71.7	6-5
6-4	Type 2 - very little porosity, NBA-1, 516.2-26.2	6-5
6-5	Type 3 - low to medium porosity & permeability, NBC-1, 540.7-51.7	6-6
6-6	Type 3 - low to medium porosity & permeability, NBC-1, 581.7-91.5	6-6
6-7	Type 3 - low to medium porosity & permeability, NBA-1, 586-906	6-7
6-8	Type 3 - low to medium porosity & permeability, NBC-1, 756-66	6-7
6-9	Type 4 - high porosity & permeability, NBC-1, 591.5-601.5	6-9
6-10	Type 4 - high porosity & permeability, NBC-1, 571.7-81.7	6-9
6-11	Type 4 - high porosity & permeability, SMD, 668-79.5	6-10
6-12	Type 4 - high porosity & permeability, SMD, 482-96	6-10
6-13	Type 4 - high porosity & permeability, NBA-1, 516.2-26.2	6-11
6-14	Type 4 - high porosity & permeability, NBA-1, 5472.25-86.2	6-11
6-15	Georgetown Formation, SMC, 425-35	6-12
6-16	Georgetown Formation, NBA-1, 446.2-47.2	6-12
6-17	Georgetown Formation, NBC-1, 530.5-40.7	6-13
6-18	Georgetown Formation, SMC, 419-25	6-13
6-19	Person Formation, Cyclic, Marine, Leached & Collapsed Members, NBC-1, 555.7-61.7	6-15

6-20	Person Formation, Cyclic, Marine, Leached & Collapsed Members, NBC-1, 561.7-71.7	6-15
6-21	Person Formation, Cyclic, Marine, Leached & Collapsed Members, NBA-1, 506.2-26.2	6-16
6-22	Person Formation, Cyclic, Marine, Leached & Collapsed Members, NBA-1, 516.2-26.2	6-16
6-23	Person Formation, Cyclic, Marine, Leached & Collapsed Members, SMC, 477-89	6-17
6-24	Person Formation, Cyclic, Marine, Leached & Collapsed Members, SMC, 457-67	6-17
6-25	Person Formation, Cyclic, Marine, Leached & Collapsed Members, NBB-1, 551.7-61.7	6-18
6-26	Person Formation, Cyclic, Marine, Leached & Collapsed Members, SMD, 506-16	6-18
6-27	Person Formation, Regional Dense Member, NBC-1, 706.5-16.3	6-21
6-28	Kainer Formation, Grainstone Member, NBA-1, 646.5-56.8	6-22
6-29	Kainer Formation, Grainstone Member, NBC-1, 726.3-36.3	6-22
6-30	Kainer Formation, Grainstone Member, NBB-1, 706.7-11.4	6-23
6-31	Kainer Formation, Grainstone Member, SMC, 622.6-32.6	6-23
6-32	Kainer Formation, Kirschberg & Dolomitic Member, NBC-1, 939.1-49.1	6-25
6-33	Kainer Formation, Kirschberg & Dolomitic Member, NBA-1, 706.5-16.3	6-25
6-34	Kainer Formation, Kirschberg & Dolomitic Member, NBA-1, 746.5-56.5	6-26
6-35	Kainer Formation, Kirschberg & Dolomitic Member, NBC-1, 918.1-28.1	6-26
6-36	Kainer Formation, Kirschberg & Dolomitic Member, SMD, 763-74.6	6-28
6-37	Kainer Formation, Kirschberg & Dolomitic Member, SMD, 731-43.1	6-28
6-38	Kainer Formation, Basal Nodular Member, NBC-1, 949.1-59.1	6-29
6-39	Kainer Formation, Basal Nodular Member, SMC, 886.4-97	6-29
6-40	Neutron porosity-bulk density, neutron porosity-gamma ray, and gamma ray-bulk density crossplots (excluding the Regional Dense Member)	6-35
6-41	Neutron porosity-bulk density, neutron porosity-gamma ray, and gamma ray-bulk density crossplots (excluding the Regional Dense Member)	6-36
6-42	Neutron porosity-bulk density, neutron porosity-gamma ray, and gamma ray-bulk density crossplots (excluding the Regional Dense Member)	6-37
6-43	Neutron porosity-gamma ray crossplots of the Regional Dense Member	6-38
6-44	Neutron porosity-bulk density crossplots of the Regional Dense Member	6-39
6-45	Gamma ray-bulk density crossplots of the Regional Dense Member	6-40
6-46	Neutron porosity-bulk density crossplots of the Kainer Formation (excluding the Basal Nodular Member)	6-41
6-47	Neutron porosity-gamma ray crossplots of the Kainer Formation (excluding the Basal Nodular Member)	6-42
6-48	Gamma ray-bulk density crossplots of the Kainer Formation (excluding the Basal Nodular Member)	6-43

6-49	Normalized histograms of the gamma ray and apparent grain density values of the Edwards Aquifer (excluding the Georgetown Formation and the Basal Nodular Member)	6-45
6-50	Normalized histograms of density-neutron crossplot porosity and photoelectric factor values of the Edwards Aquifer (excluding the Georgetown Formation and the Basal Nodular Member).	6-46
6-51	Normalized histograms of gamma ray and apparent grain density values of the Person Formation (excluding the Regional Dense Member).	6-47
6-52	Normalized histograms of the density-neutron crossplot and photoelectric factor value of the Person Formation (excluding the Regional Dense Member).	6-48
6-53	Normalized histograms of gamma ray and apparent grain density values of the Regional Dense Member	6-49
6-54	Normalized histograms of the density-neutron crossplot and photoelectric factor value of the Regional Dense Member	6-50
6-55	Normalized histograms of gamma ray and apparent grain density values of the Kainer Formation (excluding the Basal Nodular Member)	6-51
6-56	Normalized histograms of the density-neutron crossplot and photoelectric factor value of the Kainer Formation (excluding the Basal Nodular Member)	6-52
6-57	A comparison of a normal gamma ray curve (GR), a spectral gamma ray curve that does not contain a uranium count (GRKT), and a caliper curve (CALI).	6-54
6-58	Lithology plots for two different gamma ray constants	6-55
6-59	A comparison of resistivity values measured by a microspherically focused log (MSFL) and an unaveraged spherically focused log (SFLU).	6-63
6-60	A comparison of porosity values calculated with an electromagnetic propagation tool (EPHI) and a density-neutron crossplot (D-NPOROS)	6-64
6-61	A formation microscanner (FMS) image of portions of the New Braunfels C-1 well	6-65
6-62	A comparison of averaged spherically focused (SFLA) and unaveraged spherically focused (SFLU) resistivity values	6-67
6-63	A comparison of the vertical resolution of the 16 inch short normal (SH NORM), 64 inch long normal (LONG NOR), deep phasor induction (IDPH), and unaveraged spherically focused (SFLU) curves	6-69
6-64	A comparison of resistivity values measured by a deep induction (ILD), a phasor deep induction (IDPH), and a deep laterolog (LLD).	6-70
6-65	A comparison of resistivity values measured by a deep induction (ILD), a phasor deep induction (IDPH), and a deep laterolog (LLD).	6-71
7-1	New Braunfels Proposed Saline Zone Boundary	7-92
7-2	San Marcos Proposed Saline Zone Boundary	7-10

LIST OF TABLES

3-1	Summary of geologic processes in the development of rocks in the Edwards Aquifer.	3-8
3-2	Summary of the lithology and hydrostratigraphy of the of the San Marcos Platform in the Balcones Fault Zone	3-9
3-3	Porosity of the typical lithofacies of rocks in the Edwards Aquifer	3-13
3-4	Porosity, permeability, and lithology of the hydrologic subdivisions of the Edwards Aquifer in Bexar County.	3-17
4-1	Depths of the stratigraphic units encountered above the Edwards Group at the New Braunfels and San Marcos Transects	4-4
4-2	Depths of the stratigraphic units encountered within the Edwards Group at the New Braunfels and San Marcos Transects	4-5
5-1	Recovery tests results from New Braunfels.	5-2
5-2	Recovery tests results from San Marcos	5-3
5-3	Results of pump tests performed with observation wells for both sites.	5-11
5-4	Water quality data from the New Braunfels wells	5-15
5-5	Water quality data from the San Marcos wells	5-16
5-6	Balance error	5-21
5-7	General lithologic composition of the wells	5-36
6-1	Borehole geophysical logs ran in each well logging suites.	6-31
6-2	Log-response constants for various lithologies.	6-34

LIST OF PLATES

5-1	Lithologic descriptions of rock cuttings - New Braunfels well A-1
5-2	Lithologic descriptions of rock cuttings - New Braunfels well B-1
5-3	Lithologic descriptions of rock cuttings - New Braunfels well C-1
5-4	Lithologic descriptions of rock cuttings - San Marcos well B
5-5	Lithologic descriptions of rock cuttings - San Marcos well C
5-6	Lithologic descriptions of rock cuttings - San Marcos well D
6-1	Composite plate of New Braunfels well A-1 and C-1
6-2	Composite plate of New Braunfels well A-1 and

6-3	San Marcos well C New Braunfels well B-1 (Lithology, SFLU, IDPH, PEF, and D-NPOROS curves)
6-4	New Braunfels well A-1 (Lithology, SFLU, IDPH, PEF, and D-NPOROS curves)
6-5	New Braunfels well C-1 (Lithology, SFLU, IDPH, PEF, and D-NPOROS curves)
6-6	San Marcos well C (Lithology, SFLU, IDPH, PEF, and D-NPOROS curves)
6-7	San Marcos D (Lithology, SFLU, IDPH, PEF, and D-NPOROS curves)
6-8	New Braunfels well A-1 (GR, CALI, DRHO, DPHI, NPHI, and PEF curves)
6-9	New Braunfels well B-1 (GR, CALI, DRHO, DPHI, NPHI, and PEF curves)
6-10	New Braunfels well C-1 (GR, CALI, DRHO, DPHI, NPHI, and PEF curves)
6-11	San Marcos well C (GR, CALI, DRHO, DPHI, NPHI, and PEF curves)
6-12	San Marcos well D (GR, CALI, DRHO, DPHI, NPHI, and PEF curves)
6-13	New Braunfels well A-1 (FLUIDRES, TEMP, RWA, SH NORM, LONG NOR, D-NPOROS, and PEF curves)
6-14	New Braunfels well B-1 (FLUIDRES, TEMP, RWA, SH NORM, LONG NOR, D-NPOROS, and PEF curves)
6-15	New Braunfels well C-1 (FLUIDRES, TEMP, RWA, SH NORM, LONG NOR, D-NPOROS, and PEF curves)
6-16	San Marcos well C (FLUIDRES, TEMP, RWA, SH NORM, LONG NOR, D-NPOROS, and PEF curves)
6-17	San Marcos well D (FLUIDRES, TEMP, RWA, SH NORM, LONG NOR, D-NPOROS, and PEF curves)
6-18	New Braunfels well A-1 (GR, CALI, DT, PEF, SPHI WYI, SPHI RH, D-NPOROS curves)
6-19	New Braunfels well B-1 (GR, CALI, DT, PEF, SPHI WYI, SPHI RH, D-NPOROS curves)

APPENDICES

I	Charts containing water level, conductance, and temperature measurements for recovery tests performed at various depth intervals with: 1) residual drawdown versus time graphs which include transmissivity calculations; and 2) graphs plotted for conductivity versus time	I - 1
II	Charts containing water level, conductance, and temperature measurements for pump tests performed with observation wells with drawdown and Theis curves.	II - 1
III	Summary of video tapes.	III - 1
IV	Thin section descriptions for wells A-1, B-1, C-1 from New Braunfels, and no. C from San Marcos.	IV - 1

Section 1

INVESTIGATION OF THE FRESH/SALINE-WATER INTERFACE IN THE EDWARDS AQUIFER IN NEW BRAUNFELS AND SAN MARCOS, TEXAS

ABSTRACT

Two well transects, one in New Braunfels and one in San Marcos, were drilled for the purpose of: 1) collecting hydrogeologic data regarding the interface between the fresh and saline zones of the Edwards Aquifer; and 2) monitoring the movement of the interface over a long period of time. Water samples, drill cuttings, and conductivity measurements were collected at various intervals during the drilling of each well. Thin sections were made from the drill cuttings and then analyzed. Pump tests and geophysical logging were also performed at each well at various depths within the Edwards Aquifer. The data and resulting analyses presented in this report, therefore, details the hydrogeologic setting at each transect site, and lays a technical foundation for the long-term monitoring of the fresh/saline interface, as well as for other hydrogeologic studies regarding the Edwards Aquifer.

For both sites, the transmissivity values were lower in the saline-water zone than in the fresh-water zone which corresponded with the lithology and porosity conditions observed in the geophysical logs, thin sections, and rock cutting descriptions. The water quality evidence also correlated with the trends related to the rock properties. In addition, the petrographic evidence revealed that at both San Marcos and New Braunfels, the rock where the wells were drilled was once exposed to fresh water. The drilling of both transects proved that the fresh/saline boundary was much closer to the major springs than previously believed.

The most significant information regarding the New Braunfels transect is that the interface between the fresh/saline zones was well defined and that a bottom saline layer persisted underneath the the fresh-water zone where the wells were drilled. Thus, during some of the pump tests, the conductivity values in the wells increased. This change in water quality lead to a conservative conclusion that public supply wells in the same fault block should be monitored.

The San Marcos transect did not cross an interface between the fresh/saline zone, rather only saline water was found. The transect however, did reveal a trend of increased transmissivity toward the San Marcos Springs Fault. Moreover, though the quality of water was saline in the well closest to this fault, the water quality did improve over time during some of the pump tests. This is believed to be caused by the increase of transmissivity near such a major fault. However, communication from the lower block, where the wells were drilled, up the San Marcos Springs Fault to the spring orifices have yet to be established.

SECTION 1.0 INTRODUCTION

1.1 HYDROGEOLOGIC SETTING

In a west to northeast direction, the porous and faulted limestones of the Edwards Aquifer arc across south-central Texas from parts of Kinney County to parts of Uvalde, Medina, Bexar, Comal, and Hays Counties. The 180-mile expanse of the Edwards Aquifer is hydrogeologically bounded by: 1) ground-water divides in Kinney County to the west and in Hays County to the northeast; 2) the faulted outcrop of the aquifer known as the recharge zone to the

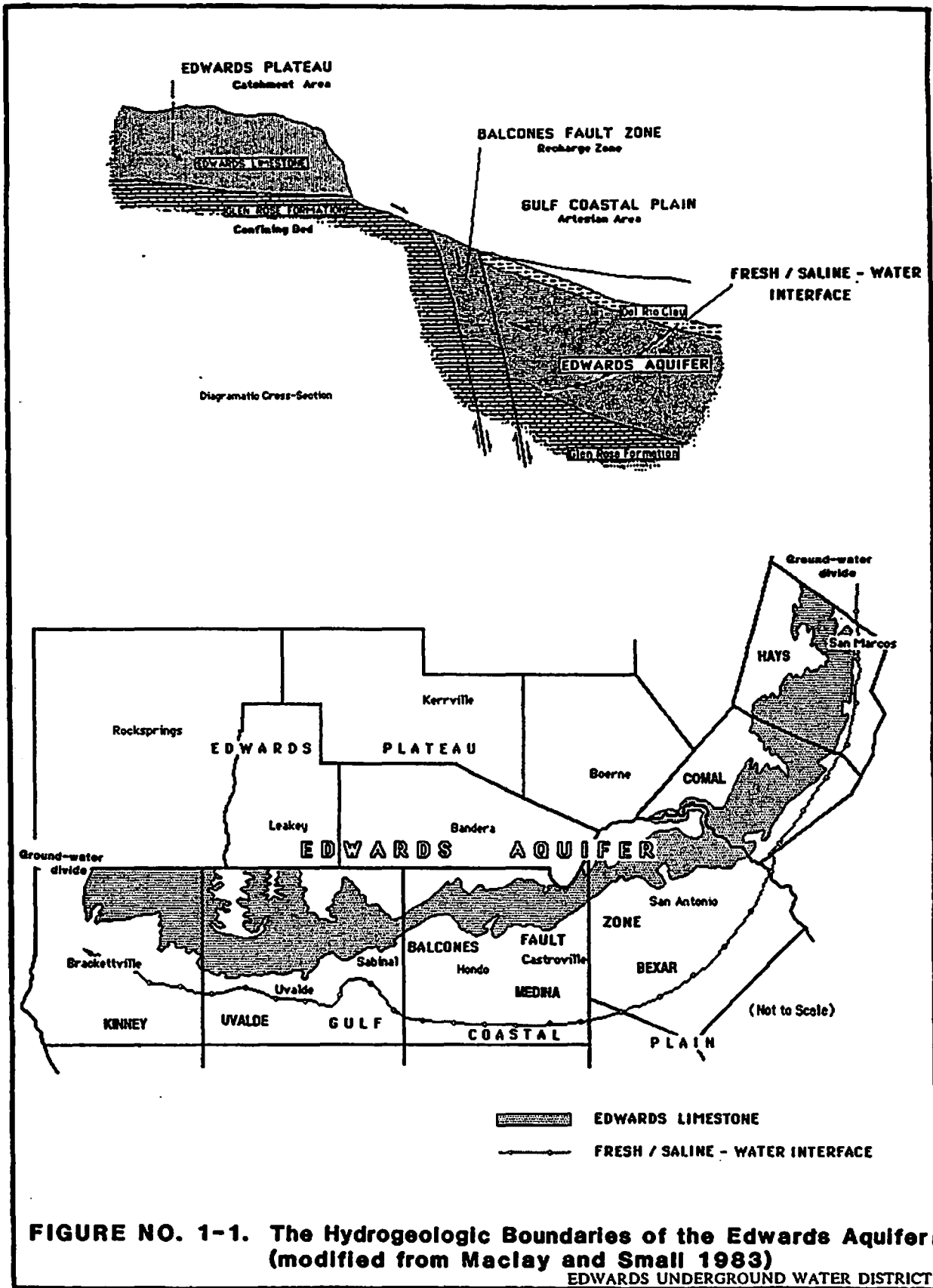
north and northwest; 3) the interface between the fresh water and saline water to the south and southeast; and bounded stratigraphically by the older Glen Rose Formation below, and the younger Del Rio Formation above (see Figure No. 1-1).

The arbitrary subsurface boundary between the fresh-water and saline-water zones in the downdip artesian portion of the aquifer is defined by a 1000 mg/l dissolved-solids-concentration contour. This contour is sometimes referred to as the "bad-water line," or more accurately, the fresh/saline-water interface. In the fresh-water zone, void spaces in the rocks are better connected, where as in the saline zone, the opposite is true. Thus, the circulation of ground water in the fresh-water zone is much greater than in the saline-water zone.

Recharge enters the aquifer from the north and west, and the flow in the aquifer is generally from the west to east and northeast. In Comal and Hays Counties, major discharge points for the fresh-water zone occur at Comal Springs and San Marcos Springs, respectively.

The fresh-water zone of the Edwards Aquifer is highly productive, and over a million people depend on it as their sole source of drinking water. The aquifer is also an important source of water for agriculture and commercial uses. The Edwards Underground Water District (EUWD) was created by the state legislature in 1959 to protect and preserve the waters of the Edwards Aquifer. Thus, the EUWD is concerned about the quality and quantity of water in the aquifer, and has reason to study the interface between the fresh-water and saline-water zones.

As population numbers increase, pumpage demands increase, and as periodic drought conditions arise, recharge amounts decrease. Over time, the overall effect on the artesian reservoir from these phenomena is a decrease in hydraulic head values. Because water circulates faster in the fresh-water zone than in the saline-water zone, a greater response to the decrease in head values results in the fresh-water zone. In turn, the heads in the fresh-water zone could become much less than those in the saline zone, and a reversal of the hydraulic gradients between them could occur. If this reversal were to happen in the vicinity of large pumping supply wells, intrusion of saline waters into the fresh zone could threaten the quality and quantity of the water used for public supply. Very little is known about this relationship in New Braunfels and San Marcos, where the fresh/saline-water interface is relatively close to public supply wells and springs that support commercial activities and several endangered species.



1.2 HISTORICAL PERSPECTIVE

By joining together their technical resources for the purpose of learning more about the Edwards Aquifer, the EUWD, the City Water Board/City of San Antonio (with technical support from William F. Guyton and Associates, Inc.), the United States Geological Survey (USGS), and the Texas Department of Water Resources (TDWR), recognized that two phases of research were needed to study the hydrogeologic relationships between the fresh and saline zones. The first one involved the drilling, testing, and completion of monitoring wells to characterize the hydrogeological properties of the interface between the two zones. The second phase would then involve the long term monitoring of the potentiometric surfaces and water quality characteristics at this interface.

The first monitoring wells were drilled in San Antonio, and then later in New Braunfels and San Marcos. From 1984 to 1986, the EUWD participated with the City Water Board/City of San Antonio, the USGS, and the TDWR in the drilling and testing of 7 wells. The project leader for the USGS was Robert Maclay, and the primary administrator and technical director of the program for the City Water Board was Dr. W. L. Guyton (deceased) of William F. Guyton Associates, Incorporated. Later, from 1989 to 1990, the EUWD drilled and tested 4 wells in New Braunfels and 2 wells in San Marcos, with John Hoyt as the project manager. A third well was drilled and tested in 1992 by the EUWD, with Diane Poteet as the project manager.

The drilling, testing, and completion of these monitoring wells began the first phase of study. Two separate reports were published on the 7 wells that were drilled in San Antonio. These reports, one written by William F. Guyton and Associates, Inc. in 1986, and the other by Dianne Pavlicek, Ted Small, and Paul Rettman for the USGS in 1987, describe the project work and present the data collected. Through further cooperation between the EUWD, the City Water Board, and the USGS, an interpretive report by George Groschen of the USGS regarding the San Antonio data was funded and is presently under review.

Unlike the previously mentioned reports, the present EUWD report combines several phases of research concerning the 6 wells drilled in New Braunfels and San Marcos: data collection, data analysis, and data interpretation.

The second phase is the long term collecting and analyzing of water levels and water quality data. This process has been on-going since the inception of all the wells by the EUWD with the cooperation of the USGS.

1.3 OBJECTIVES

This study had three major objectives. The first was to delineate the interface between the fresh and saline zones. The second objective was to characterize this interface by describing and analyzing the hydrogeological and chemical data collected during the drilling of each monitoring well. The last objective was to estimate from the data, if possible, the potential of the saline waters to intrude upon the fresh waters of the Edwards Aquifer, particularly near the springs and public supply wells in New Braunfels and San Marcos, Texas.

1.4 ACKNOWLEDGEMENTS

The following individuals are recognized for their important contributions to this report: 1) John Hoyt, Senior Geologist: EUWD Project Manager for the data collected at the New Braunfels well sites and the San Marcos B and C well sites; 2) Hughbert Collier, Associate Professor of Geology, Abilene Christian University: Author on the section regarding petrographic and petrophysical analysis; and 3) Robert Maclay, retired USGS hydrogeologist: Contractor and author of the section regarding the regional geology. The other EUWD staff who participated in this study and in the preparation of this report are also recognized for their support, and they as follows in alphabetical order: David Burgess, Jim O'Connor, Earl Parker, Maggie Ruiz, and Randy Williams.

Section 2

SECTION 2.0 STUDY SITE LOCATIONS AND GEOLOGY SETTING

2.1 STUDY SITE LOCATIONS AND GEOLOGICAL SETTING

The transects for the monitoring wells are located in the townships of New Braunfels and San Marcos, Texas (see Figure No. 2-1).

NEW BRAUNFELS

The four wells in New Braunfels are located near Landa Park. The state well numbers for the A-1, B-1, B-2, and C-1 wells are respectively: DX-68-23-616, DX-68-23-617, DX-68-23-618, and DX-68-23-619. A plan-view and cross-section of the sites are presented in Figures Nos. 2-2 and 2-3, respectively. In both figures, the boundary between the fresh and saline zones has been drawn within the Edwards Group based on the geophysical well logs and water quality data collected from each well in the transect. The boundary represents a change in water quality from between a range of 500 to 2000 microsiemens per centimeter ($\mu\text{S}/\text{cm}$) to between 2000 and over 5000 $\mu\text{S}/\text{cm}$. The boundary also represents a correlating change in total dissolved solids range of 320 to 1,190 milligrams/liter (mg/l) to between 1,190 to over 3,600 mg/l.

A major fault called the Comal Springs Fault lies approximately 680 feet to the west of the sites, trending in a northeast to southwest direction with approximately 800 feet of displacement. On the west side of the fault, the limestones of the Edwards Group crop out, whereas on the east side, the Edwards has been completely displaced, lying approximately 460 feet below the surface. Emerging from the fault are the Comal Springs, the origin of the Comal River.

After the wells were drilled and geophysically logged, displacements of the geologic units were noted and compared to a well owned by the Lower Colorado River Authority (LCRA). The displacements were determined to be: 40 feet between wells A-1 and B-1, 25 feet between B-1 and C-1, and 120 feet between the LCRA well and well C-1. Hence, between each EUWD well and the LCRA well, faults were inferred.

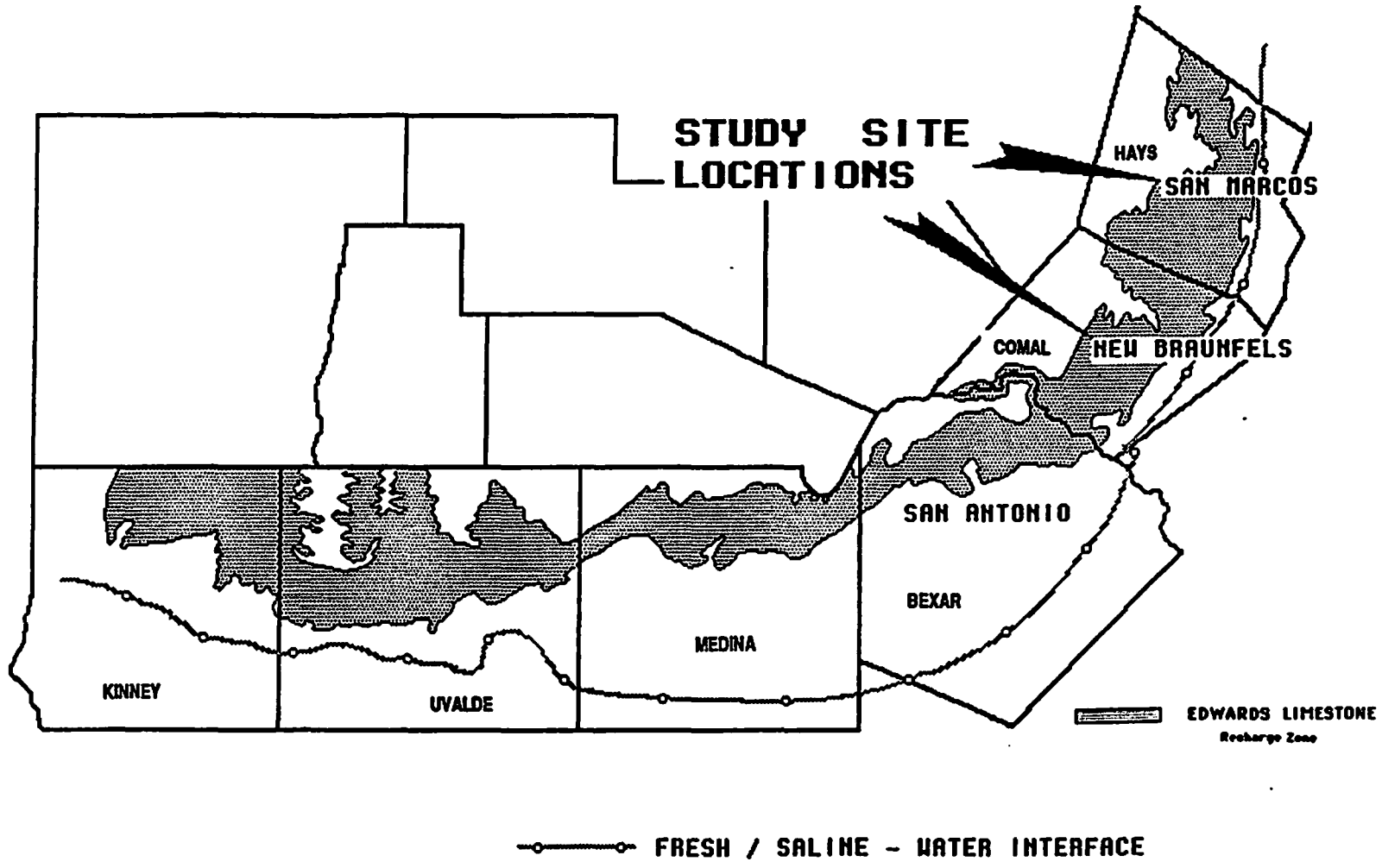


FIGURE NO. 2-1. Study Site Locations.

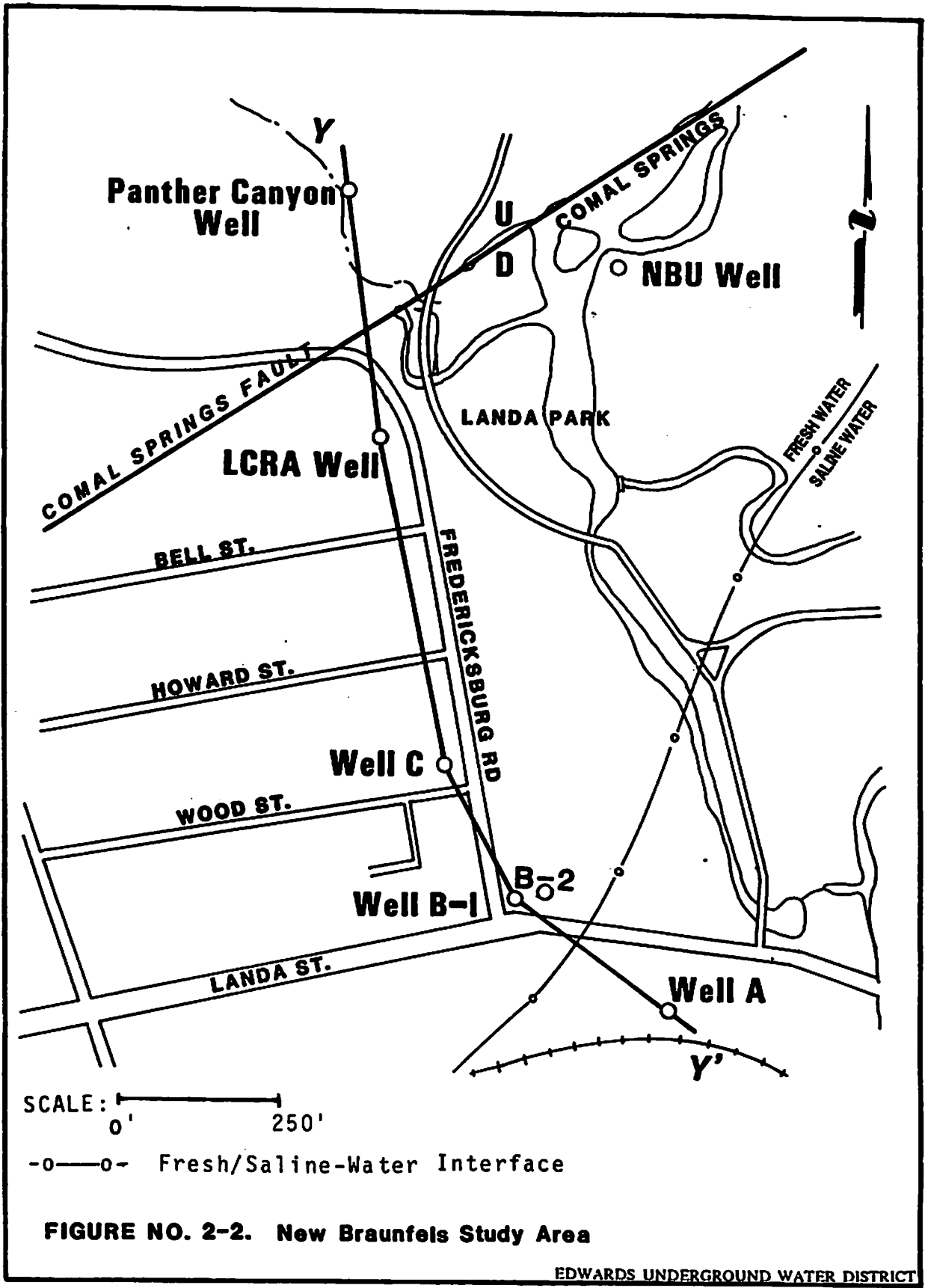
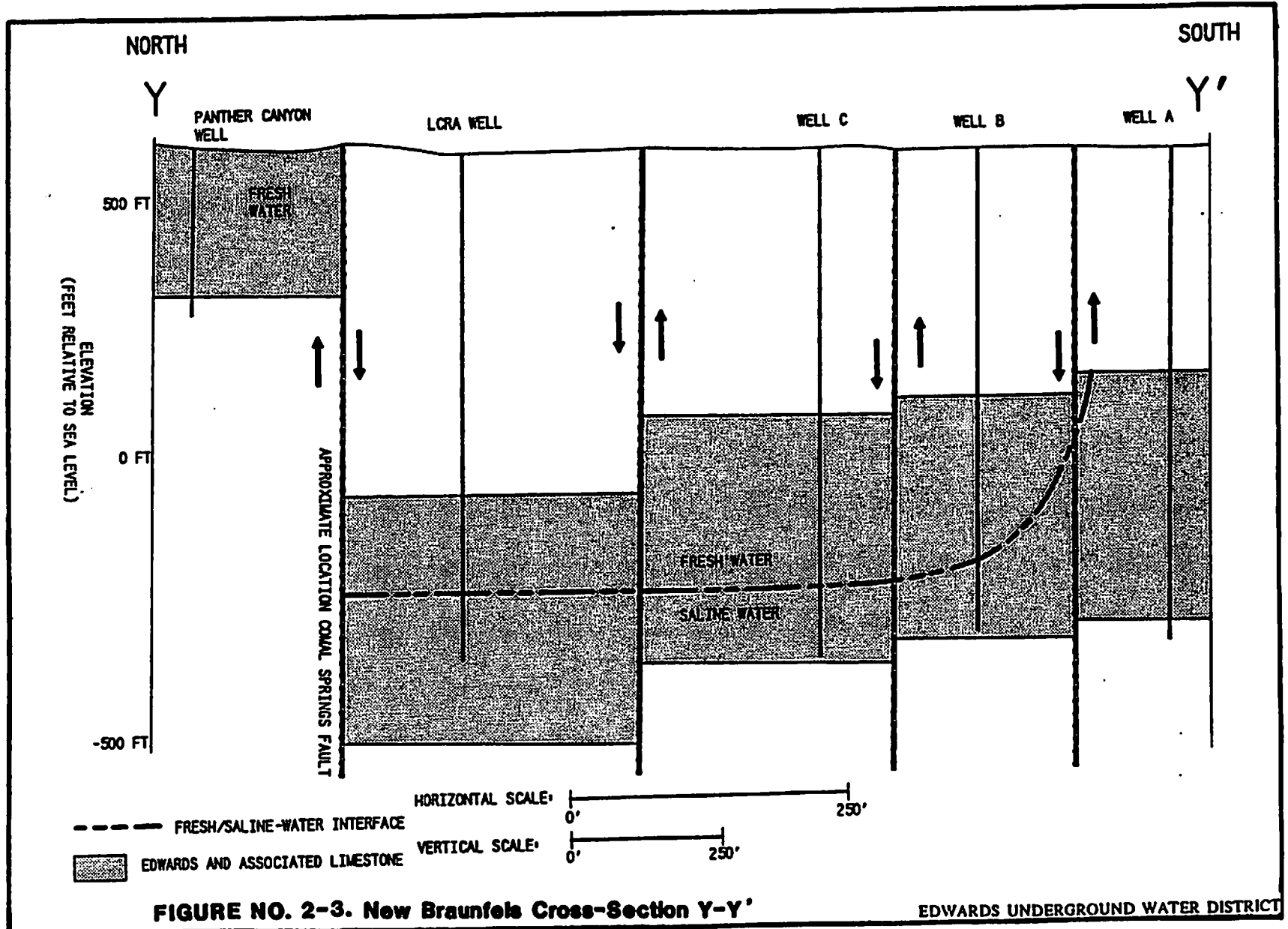


FIGURE NO. 2-2. New Braunfels Study Area

EDWARDS UNDERGROUND WATER DISTRICT



SAN MARCOS

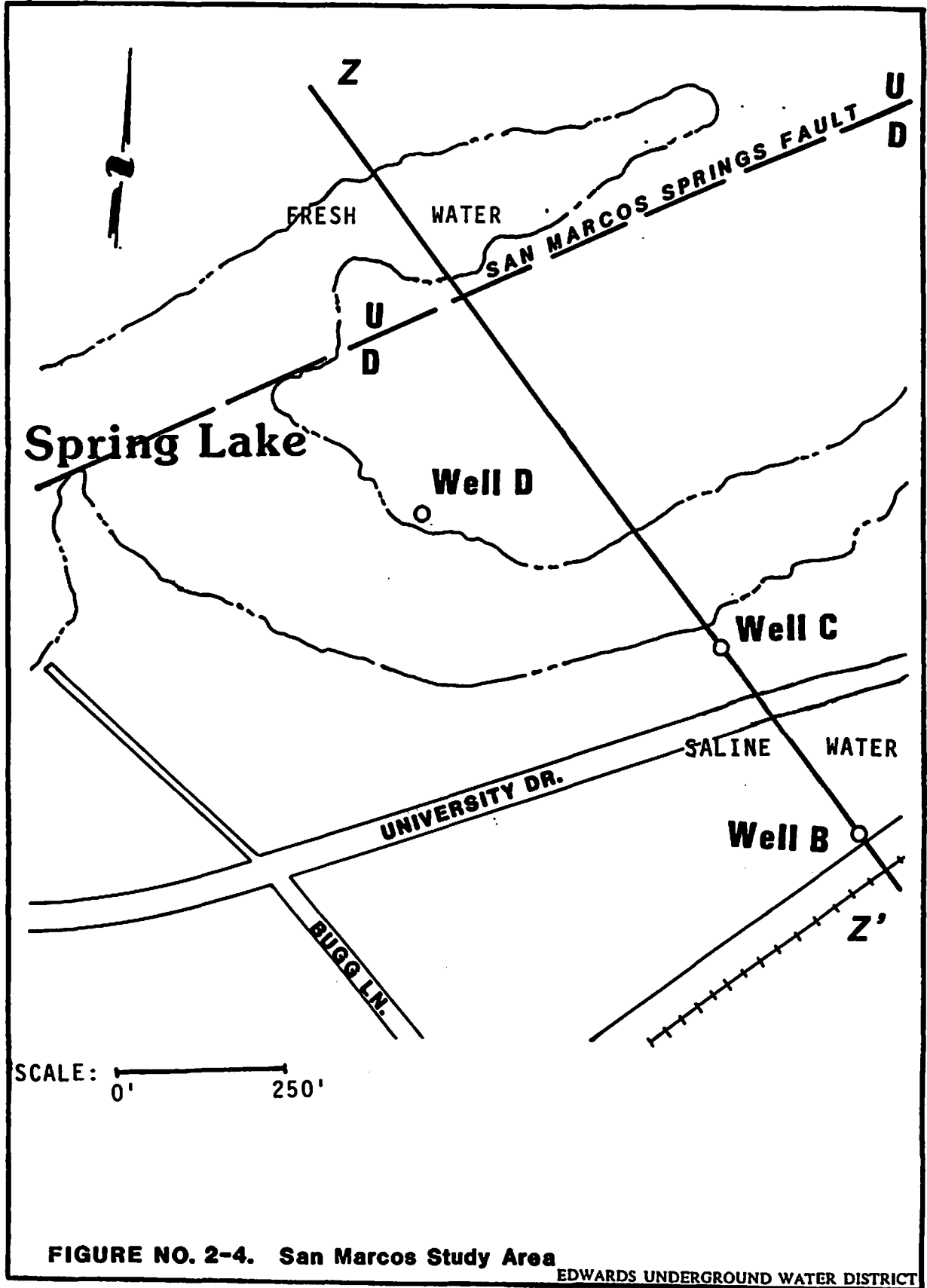
The wells in San Marcos are located near Spring Lake. The state well number for B is LR-67-01-812, the number for C is LR-67-01-813, and the number for D is LR-67-01-814. A plan-view and cross-section of the sites are presented in Figure Nos. 2-4 and 2-5, respectively. In both of these figures, the boundary between the fresh and saline zone within the Edwards Group near the EUWD transect is believed to follow the fault plane of the San Marcos Springs Fault. This boundary is based on the geophysical well log and water quality data collected from the two wells drilled in this transect and a third well just recently drilled by the EUWD. The boundary between the two zones represents a change in water quality from approximately 500 to over 13,000 $\mu\text{S}/\text{cm}$ (or total dissolved solids range of 300 to over 8,800 mg/l).

A major fault called the San Marcos Springs Fault lies approximately 650 feet to the west of the sites trending in a northeast to southwest direction with approximately 470 feet of displacement. On the west side of the fault, the top of the Edwards Group crops out, whereas, on the east side, the top of the Edwards Group lies approximately 460 feet below the surface. Emerging from the fault are the San Marcos Springs, the origin of the San Marcos River. After the C and B wells were drilled and logged, no displacements were observed between them. However, after the drilling of the D well, displacement of the geologic formations between the D and C well were observed. In addition, due to approximately 40 feet of section missing in the Grainstone Member of the Kainer Formation, another fault was believed to have been crossed when drilling in the lower half of the Edwards Group took place.

2.2 OVERVIEW OF GEOLOGIC HISTORY

The Texas craton is comprised of Pre-Cambrian metamorphic and igneous basement rocks which have been dated at approximately 1 billion years old (Ellis, 1981). These rocks were covered by sea deposits through the lower Paleozoic (1/2 billion years ago). At the shelf edge, approximately where the Balcones Fault Zone is today, a hingeline known as the Ouachita Belt developed between the shallow and deep water environments due to the overloading of sediments on the continental shelf (Burgess, 1966). Most of the deposits during this period were carbonate in nature.

The upper Paleozoic (340 million years ago) brought a change in the tectonic relationship between the continents as they existed at that time. During Mississippian and early



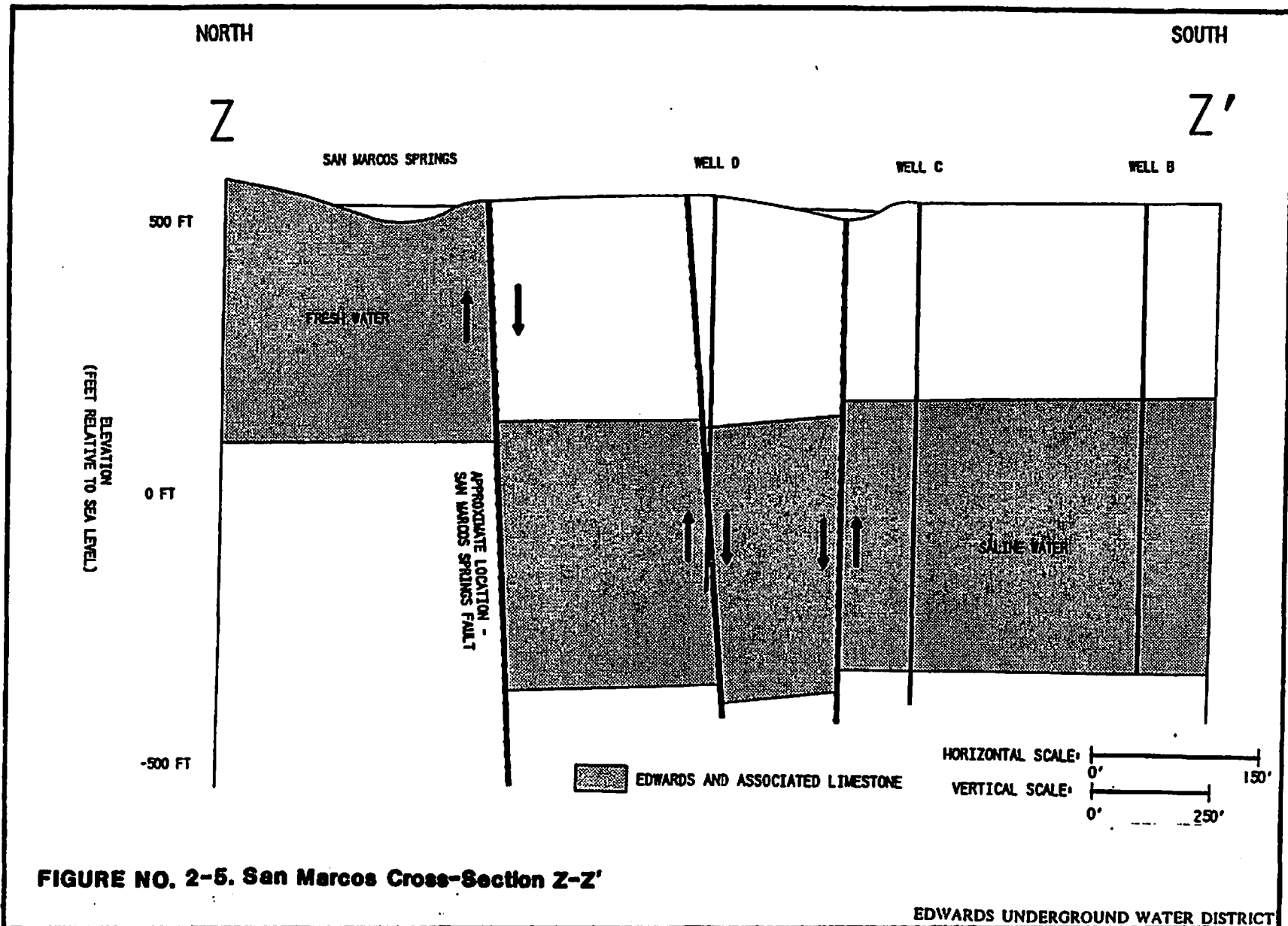


FIGURE NO. 2-5. San Marcos Cross-Section Z-Z'

Pennsylvanian time, the African-South American-European continent and the North American continent began to come together to form one land mass called Pangea (see Figure No. 2-6) (Dietz and Holden, 1970). A great basin where much sediment accumulated was formed as the African-South American-European plate began subducting under the North American plate. Collision occurred early on, and welding of the Ouachita rock facies onto Africa caused the creation of a suture zone (Burgess, 1976).

From late Pennsylvanian through the early Triassic (250-190 million years ago), Pangea broke apart (see Figure No. 2-7)(Dietz and Holden, 1970). The continents began to separate due to the formation of a rift and graben zone south of the Ouachita hingeline (Burgess, 1966). Texas had been largely a land mass and most of the rocks were of terrigenous origin and deposited by rivers, such as the Triassic Red Beds (Sheldon, 1982). As the seas invaded, Triassic salts were formed as the seas were intermittently trapped in the grabens. After exposure to deep burial and high temperatures, these salt deposits have been squeezed upward to form today's salt domes (Burgess, 1976, and Sheldon, 1982).

By the late Triassic and early Jurassic (190-140 million years ago), the continents had spread far enough apart to allow for normal marine sedimentation. Then from mid-Jurassic to early Cretaceous (140-120 million years ago), terrigenous sediments were deposited due to up-lift of the North American continent (Burgess, 1966). During the Mid-Cretaceous, carbonate deposition over a large area of the Gulf Coast occurred from the Glen Rose through the Edwards time (Burgess, 1966). The limestones of the Edwards Aquifer were deposited as tidal-flat and shallow-water marine environments. After deposition, the rocks were buried.

From late Cretaceous to the Cenozoic (65-2 million years ago), the Rocky Mountains were being formed. As a result, deposits were formed from terrigenous sediments and regressing seas. Due to heavy accumulations of these sediments, the newly developed coastal plain experienced down-to-the coast or en echelon normal faulting (Burgess, 1966). At this time, known as the Miocene Epoch, the Balcones Fault Zone was formed along the old Ouachita hingeland. The faulting due to crustal extension and the subsidence of the Gulf of Mexico caused the Edwards limestones to become raised in the north and west relative to sea level. The combination of faulting and the creation of an escarpment caused gulfward-flowing streams to downcut into the Edwards, creating discharge points which resulted in the circulation of ground water (Sheldon, 1982). The circulation of nonsaline ground waters in the limestone formations created the extensive secondary porosity (caverns, vugs, etc.) present today (Maclay and Small, 1983).

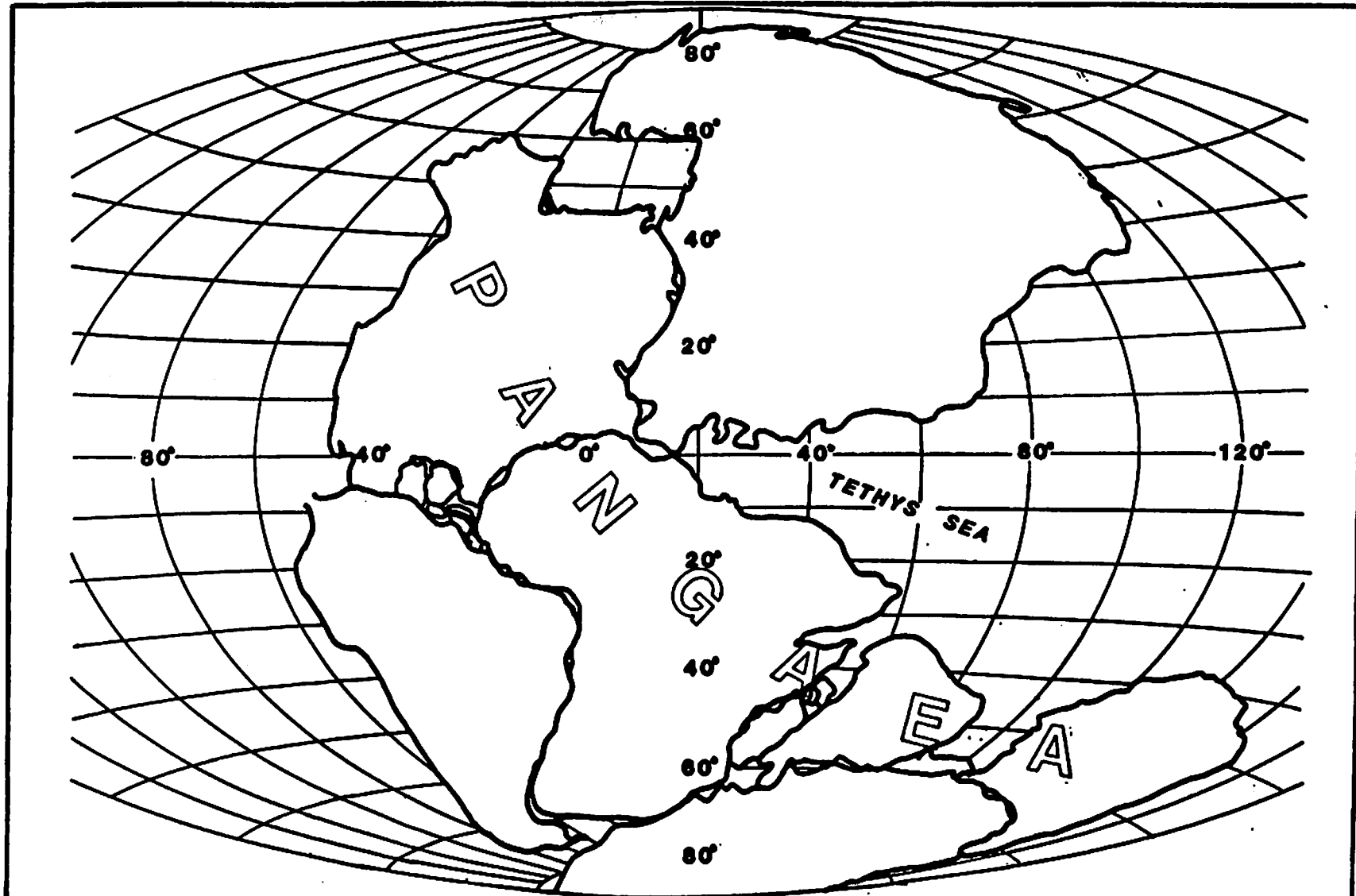


**FIGURE NO. 2-6. Universal Land Mass Pangaea (200 million years ago).
(Modified from Dietz and Holden, 1970)**

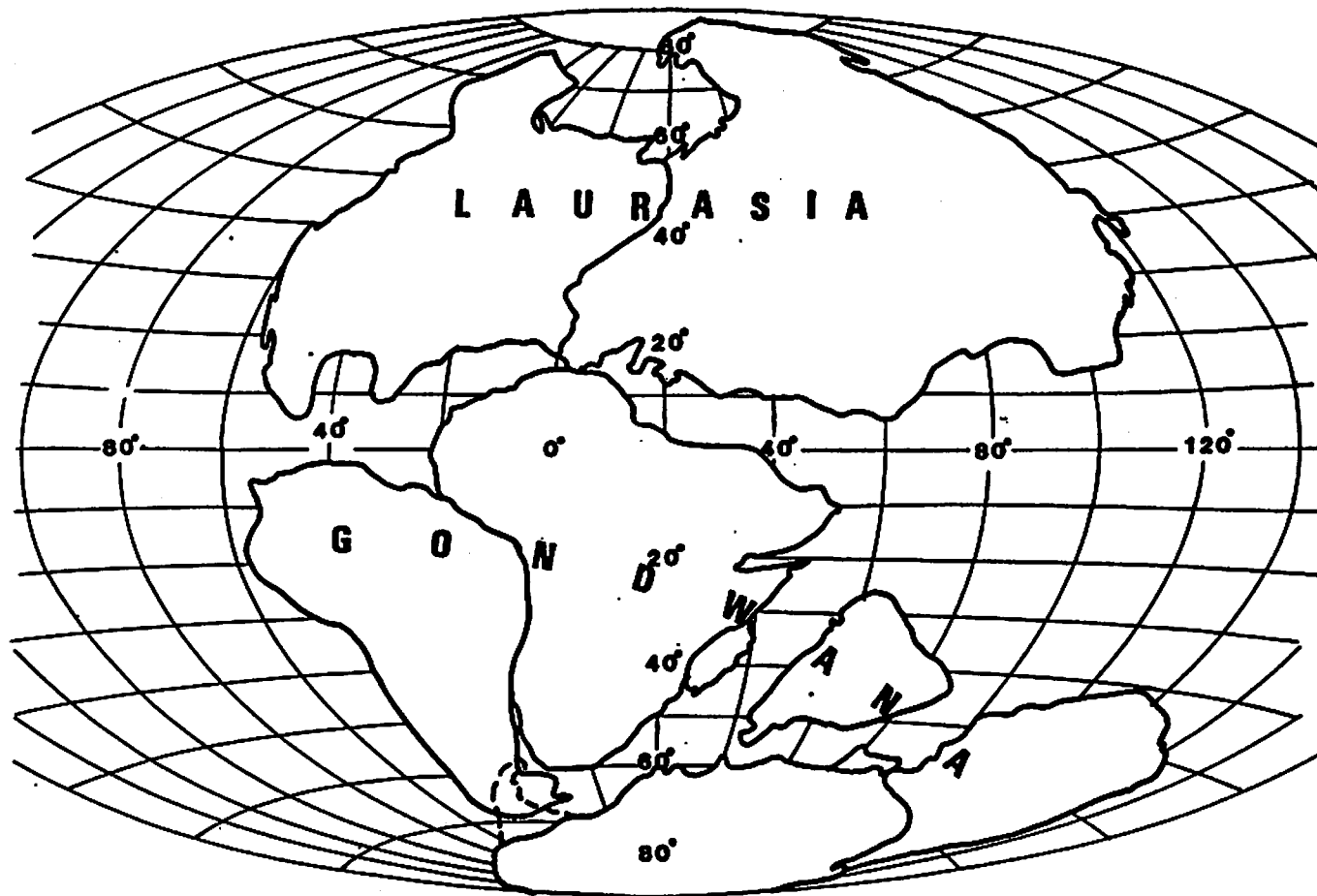


**FIGURE NO. 2-7. Break-up of Pangea after 20 million years.
(modified from Dietz and Holden 1970)**

Section 3

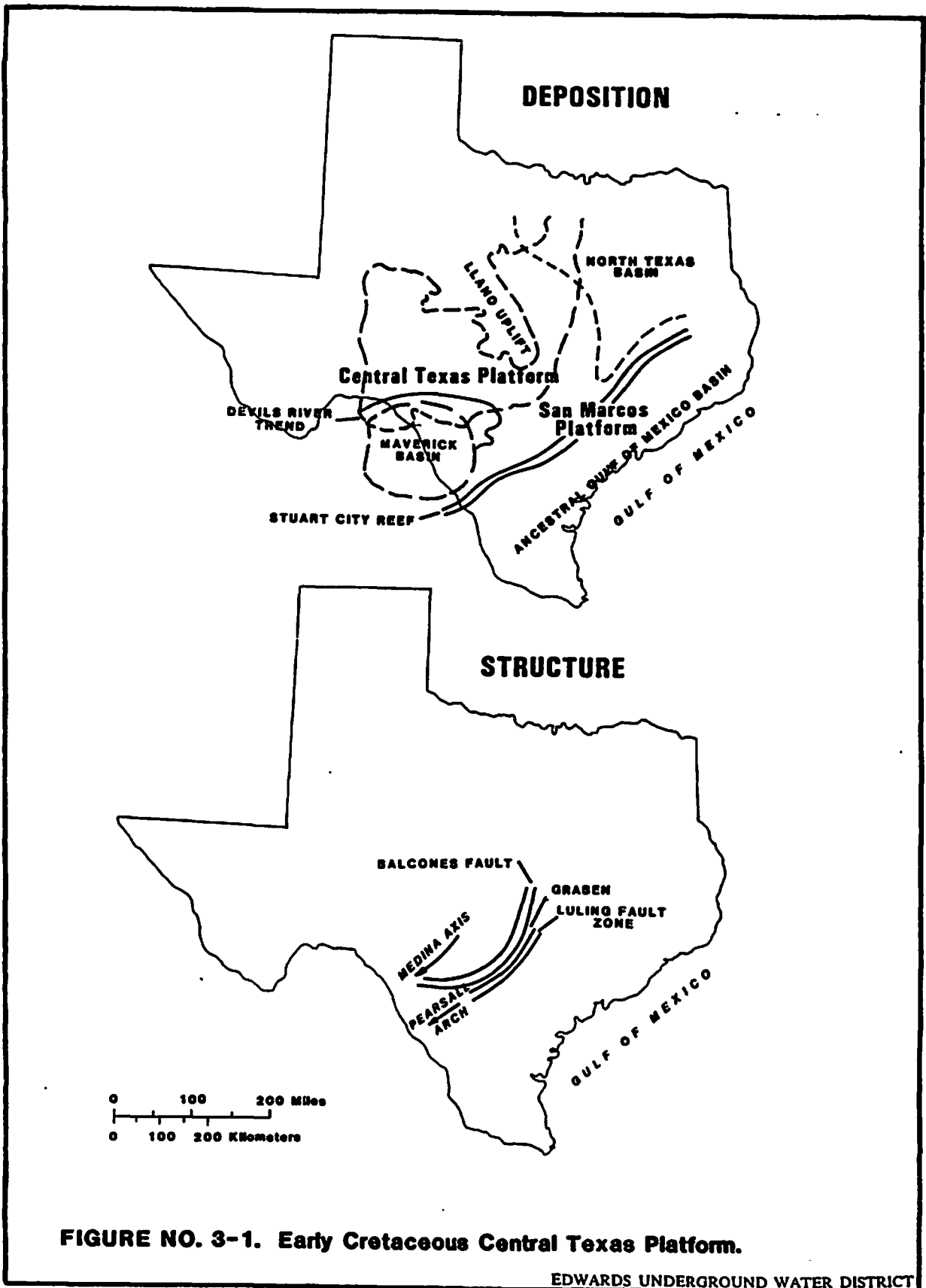
SECTION 3.0 REGIONAL GEOLOGY

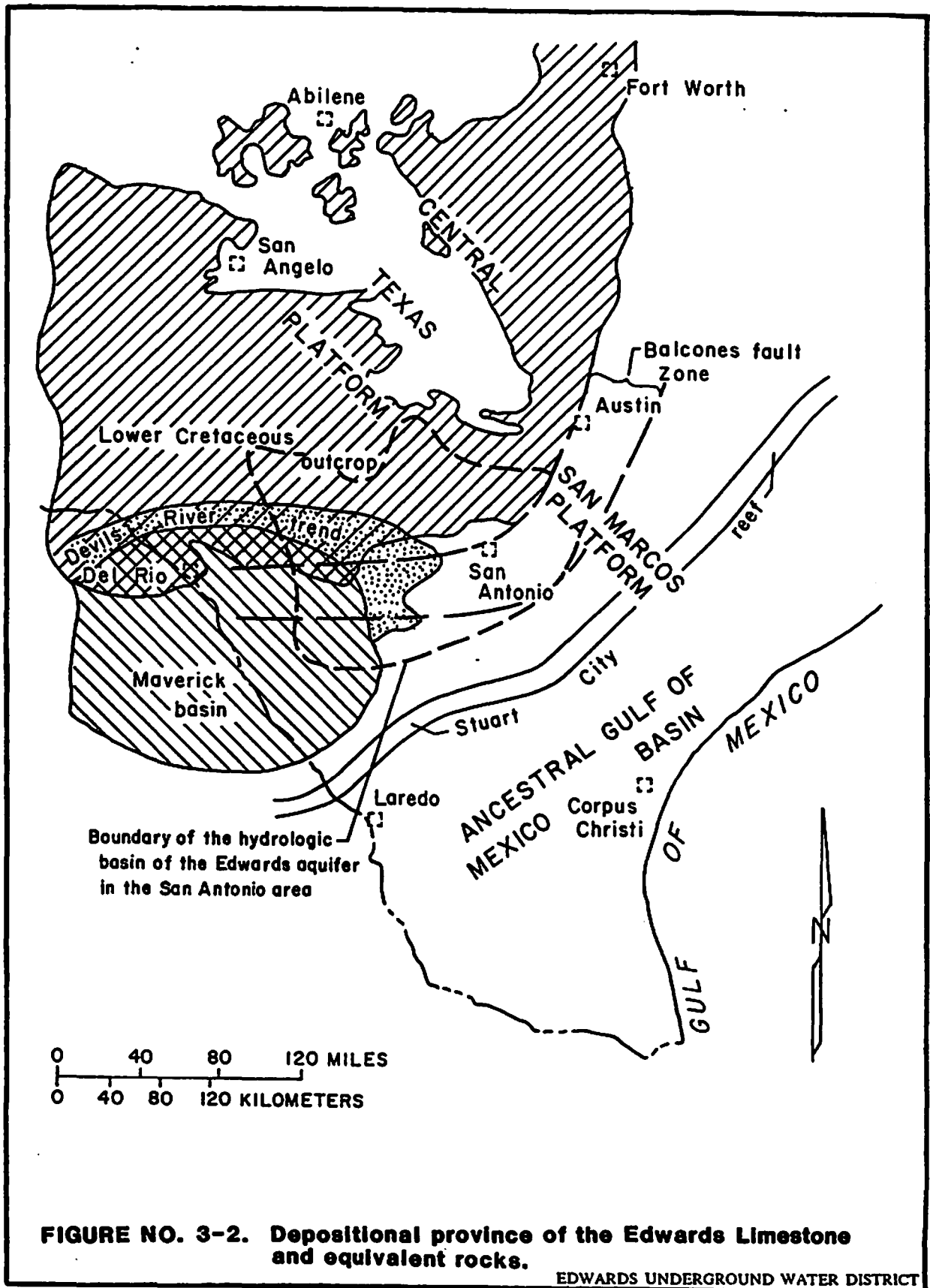
3.1 GEOLOGIC SETTING

The sediments that formed the rocks of the Edwards Limestone (the Edwards Group as designated by Rose, 1978), and its stratigraphic equivalents were deposited on the margin of the Central Texas platform, a low-lying carbonate surface that was traversed by transgressing and regressing Early Cretaceous seas (Figure No. 3-1). Some of the sediments deposited on the platform were partially removed when the platform was subaerially exposed during several occurrences within Early Cretaceous time. The platform was extensively eroded just prior to the transgression of the Georgetown sea across the platform during Middle Cretaceous time (Rose, 1972).

On Figure No. 3-2, the outline of the Edwards Aquifer in the San Antonio region is superimposed upon the major Cretaceous depositional provinces where the aquifer was formed. These major depositional regions, consisting of different water depths, affected the energy conditions under which sediments were deposited. Gulfward from the San Antonio region, the now deeply buried Stuart City reef, a rudistid barrier reef, formed the offshore margin of the Central Texas platform. The Devils River trend, another rudistid barrier reef, developed around the Maverick basin during a later period of deposition. This reef lies partly within the San Antonio region and its rocks form part of the Edwards Aquifer. The Maverick basin was a site of continuing marine deposition (without periods of subaerial erosion) during most of Edwards time. These varied depositional environments are reflected in the lithologies of the carbonate rocks within the Edwards Group. In general, most of the rocks are dense, micritic, mainly mudstones and wackestone, reflecting the low to moderate energy of the deeper-water environments. Some of the lithologies contain zones of honeycombed porosity that were developed in shallow water environments. More porous and permeable rocks occur within the area affected by depositional conditions (open marine to arid supratidal flats) that existed on the San Marcos platform.

The Cretaceous and Tertiary homoclinally-dipping beds in south-central Texas are disrupted by synthetic and antithetic systems of en echelon normal faults which are part of four major structural systems (Figure No. 3-1) called: the Karnes Trough, Astascosa Trough, Luling and Balcones Fault systems. The internal flow system of the Edwards Aquifer is directly affected by the Balcones Fault Zone.





The dominant structural feature of the Balcones Fault Zone is a series of parallel, northeastward-trending high-angle normal faults. Small grabens and horsts have formed that now exert control on ground-water circulation. Locations of the major faults are shown in Figure No. 3-3. Tectonic fractures associated with faulting have been observed in core samples extracted from test holes penetrating entire thickness of the Edwards Aquifer (Small and Maclay, 1982). These fractures, generally ranging in widths from a few to more than 100 millimeters, occur at irregular intervals throughout the entire thickness of the aquifer; however, the frequency of their occurrence within core samples was greater in the upper 300 feet of the aquifer. Most observed fractures occurred in hard dense limestone.

3.2 DIAGENESIS OF THE EDWARDS AQUIFER

Diagenesis is defined as all chemical, physical, and biological changes, modifications, or transformations undergone by sediments after their initial deposition. Knowledge of the process and products of carbonate diagenesis in the varied lithofacies in the Edwards Aquifer is essential for the prediction or interpretation of the distribution of porosity and permeability within the aquifer. Dissolution of certain lithofacies in the fresh-water zone of the aquifer resulted in an increase of the capacity of the aquifer to transmit water along interconnected secondary openings. Simultaneously, recrystallization resulted in cementation of the rock matrix, and thereby reduced the total porosity within the fresh-water zone.

The rocks in the fresh-water and saline-water zones of the Edwards Aquifer were deposited in similar environments and underwent similar early diagenetic processes, including dolomitization, micritization, and selective leaching of soluble minerals contained within certain fossils. However, because of late diagenetic processes associated with the uplift and faulting of the Edwards Limestone and the consequent opportunity for ground water to circulate relatively rapidly within the Balcones Fault Zone, a distinct change in the rock texture and mineralogic composition occurred that differentiated the rocks of the existing two water quality zones separated at the fresh/saline water interface.

The rocks in the saline-water zone are mostly dolomitic, medium to dark gray or brown, and contain un-oxidized organic material, including petroleum and accessory minerals such as pyrite, gypsum, and celestite. The matrix of the rocks in the saline-water zone is more porous than that in the stratigraphically equivalent rocks in the fresh-water zone. However, the pores are predominantly small interparticle and intercrystalline. The permeability of these rocks is relatively

EXPLANATION

- BOUNDARY OF FRESHWATER PART OF EDWARDS AQUIFER
- - - LINE SEPARATING UNCONFINED ZONE TO THE NORTH FROM THE CONFINED ZONE TO THE SOUTH, JULY 1974
- U
D --- FAULT—U, upthrown; D, downthrown. Dashed where inferred

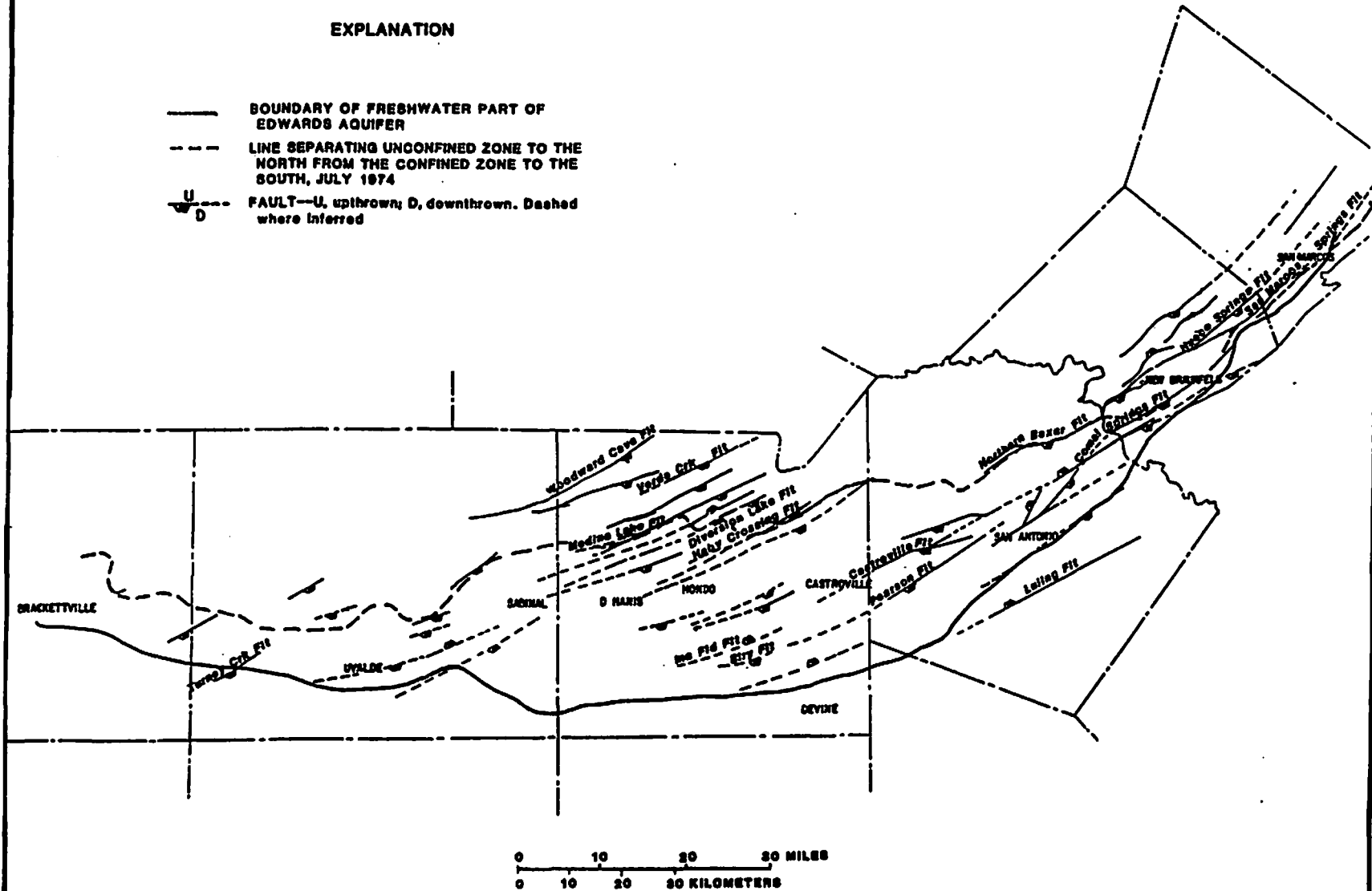


FIGURE NO. 3-3. Major Faults

EDWARDS UNDERGROUND WATER DISTRICT

low compared to that of stratigraphically equivalent rocks within the fresh-water zone. This occurs because of the very restrictive shape and size of the pore throats that interconnect the voids that form the pores.

Vugs and other larger dissolution openings occurring within the saline-water zone were formed by diagenetic processes during early Cretaceous time before the deposition of the Georgetown Limestone. These vugs and enlarged dissolution openings enhanced permeability within the saline-water zone, but to a far lesser degree than in the fresh-water zone. The difference is probably due to more restricted interconnections between the larger vugs and caverns.

The permeability of the rocks in the saline-water zone has not significantly increased during later geologic time. The restrictive size and shape of interconnections between voids results in greatly reduced movement of circulating ground water within this zone. The associated dissolution action of circulating water is minimal in interconnected openings along the flowpath.

Because water tends to move along a path of least resistance, the ground-water flow will preferentially remain, through time, with rocks of greater permeability. In turn, less flow is diverted to the saline-water zone and consequently less opportunity for dissolution. The capacity of the aquifer to transmit water in the fresh-water zone continues to increase with time along its natural flowpath, whereas, the permeability of the aquifer within the saline-water zone remains nearly unchanged. This condition remains the same until some later geologic event occurs that results in a breakout of an artesian spring downdip within the saline-water zone. The consequent diversion of flux and associated dissolution increases the permeability along the new flowpath.

The rocks in the fresh-water zone are calcitic, light buff or gray to white, strongly recrystallized, and dense. These rocks contain little pyrite and no gypsum. Dolomite has been extensively replaced by calcite. In small parts of the aquifer isolated from actively circulating ground water, the rocks are dolomitic and resemble those of the saline-water zone. These isolated parts of the aquifer occur mostly within the basal stratigraphic unit.

Dissolution along bedding planes can be observed in the cores and at the outcrop of the Edwards Limestones. Some bedding planes show evidence of ground-water circulation. Dissolution related to buried erosional surfaces is difficult to document in the subsurface; however, travertine and "cave popcorn", which is evidence of a vadose environment (within the unsaturated

zone above a water table), have been observed in cores from test holes penetrating the confined aquifer.

A summary of diagenetic stages and associated processes which contributed to the origin of the Edwards Aquifer is given in Table No. 3-1.

3.3 HYDROGEOLOGIC FRAMEWORK OF THE EDWARDS AQUIFER

3.3-1 LITHOFACIES

The Edwards Aquifer in the San Antonio region consists of 400 to 600 feet of thin- to massive-bedded carbonate rocks. These rocks contain several stratigraphic zones that possess permeable, well-developed vuggy porosity. They are separated by beds of dense to chalky limestone of very low to moderate permeability.

Lithologies and their associated porosities of the Edwards Aquifer consist mostly of recrystallized calcitic mudstone and wackestones with lesser amounts of grainstones (Table No. 3-2). Lithofacies that contain permeable strata include: (1) Tidal, burrowed mudstone and wackestone; (2) Supratidal, evaporitic breccias were formed by leaching of bedded gypsum; and (3) Reefal, rudite grainstones that have been fractured and leached. The Edwards Aquifer within the San Marcos platform contains more strata having these lithofacies than the stratigraphically equivalent rocks in the Devils River trend or the Maverick basin (Table No. 3-2).

Fractures are common within the aquifer. Open fractures commonly cross several layers of strata, but many fractures are discontinuous or closed within dense mudstones of the middle and lower parts of the aquifer. The walls of the fractures are commonly stained orange by iron and some are covered or filled with dogtooth sparry calcite. Some of the open fractures may hydraulically interconnect the permeable strata and solution openings along bedding planes.

Unconformities are common. A hydrologically significant unconformity exists at the contact between the Georgetown Formation and the Edwards Limestone. The cavernous porosity in the Edwards was formed below the contact by karstic dissolution within part of the San Marcos Platform. The karstic rocks provide an inherent zone of enhanced permeability within the aquifer that predates the fracturing and dissolution of rocks associated with structural development in the Balcones Fault Zone. Voids (open pore space) within the Edwards Aquifer

TABLE NO. 3-1 SUMMARY OF GEOLOGIC PROCESSES IN THE DEVELOPMENT OF ROCKS IN THE EDWARDS AQUIFER

TIME	STAGE OR EVENT	GEOLOGIC PROCESSES	RESULT
Early Cretaceous	Depositional - Accumulation of carbonate sediments mostly in shallow marine and tidal environments.	Shallow burial and intermittent periods of subaerial exposure. Cementation of some sediments.	Formation of lithofacies. Selective dissolution of shells containing aragonite or high magnesium calcite. Dissolution of evaporites. Formation of some collapse breccias.
Early Cretaceous	Erosional - Recession of the sea and uplift on the San Marcos platform.	Erosion and prolonged dissolution under subaerial conditions. Extensive removal of sediments in the eastern part of the San Antonio area.	Formation of a cavernous porosity system. Cementation of some grainstone by fresh water that is saturated with respect to calcite. Preferential leaching of some reefal rocks and dolomitized, burrowed tidal limestone.
Middle to Late Cretaceous	Deep burial - Transgressions of continental seas across the Edwards outcrop.	Deep burial of the Edwards Limestone by clay, limestone, sandstone of Late Cretaceous age. Very slow circulation or near stagnant conditions. Saline water in the deeply buried deposits. High pressures resulted in many stylolites. Some compaction of some sediments.	Dormant stage of aquifer development. Formation of stylolites. Compaction is indicated by "squashed" intraclasts and alloclasts in a few strata.
Late Cretaceous and Early Tertiary	Exhumation - Differential uplift and erosion of the area that presently constitutes the Edwards Plateau.	Stripping of Upper Cretaceous sediments by streams that emptied into ancestral Gulf of Mexico. Formation of karstic plain where Edwards becomes exposed.	Dormant stage of aquifer development except where Edwards became exposed subaerially. In these areas, cavernous porosity began to develop in plains adjacent to major streams.
Miocene	Tensional stresses developed in rocks of Balcones fault zone resulting from subsidence in the Gulf of Mexico.	Normal, steep-angle faulting. Most intensive faulting occurs in eastern part of the San Antonio area.	A system of nearly vertical fractures is developed throughout the Balcones fault zone. Major displacements along major faults abut permeable strata of Edwards against relatively impermeable strata. Incision of streams flowing normal to trend of major faults produces regional topographic lows near the Balcones fault escarpment.
Miocene to Present	Tensional stresses continue but are attenuating.	Periodic movement along faults in the Balcones fault zone. Dissolution and cementation occurring simultaneously in the freshwater zone of the confined Edwards aquifer.	Establishment of the regional confined aquifer in the Balcones fault zone. Major artesian springs emerge at topographic low points in the eastern part of the San Antonio area. Drainages of ancestral springs are captured by a dominant spring. Internal boundaries, formed by faults, divert ground-water flow eastward. When a lower spring outlet forms in the valley of an incising stream, cavernous openings of former solution channels are drained and then exposed as caves at higher levels on the valley walls.

EDWARDS UNDERGROUND WATER DISTRICT

TABLE NO. 3-2 SUMMARY OF THE LITHOLOGY AND HYDROSTRATIGRAPHY OF THE SAN MARCOS PLATFORM IN THE BALCONES FAULT ZONE

SYSTEM	PROVINCIAL SERIES	GROUP	FORMATION	FUNCTION	MEMBER OR INFORMAL UNIT	FUNCTION	THICKNESS (FEET)	LITHOLOGY	HYDROSTRATIGRAPHY	
Quaternary			Alluvium	AQ			45	Silt, sand, gravel.	Flood plain; aquifers in hydraulic connection with streams.	
			Terrace deposits	Not saturated			30	Coarse gravel, sand, and silt.	High terrace bordering streams and surficial deposits on high interstream areas in Balcones fault zone.	
Tertiary	Eocene	Claiborne	Reklaw	CB			200	Sand, sandstone, and clay; lignitic, friable to highly indurated sandstone.	Deltaic and swamp deposits. Leaky confining bed confining the Carrizo aquifer below.	
			Carrizo Sand	AQ			200-800	Sandstone, medium to very coarse, friable, thick bedded, few clay beds, ferruginous.	Very permeable aquifer formed by deltaic and shoreline deposits.	
			Eocene and Paleocene	Wilcox and Midway	CB		CB	500-1,000	Clay, siltstone, and fine grained sandstone; lignitic, iron-bearing.	Leaky confining bed formed by deltaic and marine shoreline.
Cretaceous	Gulfian	Navarro			Villis Pt.	CB	500	Clay and sand.		
			Taylor	Pagan Gap	CB		300-500	Marl, clay, and sand in upper part; chalky limestone and marl in lower part.	Deeper water marine deposits. Major barrier to vertical cross-formational flow separating Cretaceous aquifer from Tertiary aquifers.	
				Anacacho Limestone						
			Austin	Undivided	AQ			200-350	Chalk, marl, and hard limestone. Chalk is largely a carbonate mudstone.	Minor aquifer that is locally interconnected with the Edwards aquifer by openings along some faults.
			Eagle Ford	Undivided	CB			50	Shale, siltstone, and limestone; flaggy limestone and shale in upper part; siltstone and very fine sandstone in lower part.	Barrier to verticle crossformational flow.
Comanchean	Washita		Buda	CB			100-200	Dense, hard, nodular limestone in the upper part and clay in lower part. Thickens to the west.	Fractured limestone in the Buda is locally yielding and supplies small quantities of water to wells. Del Rio Clay has negligible permeability.	
				Del Rio Clay						

EDWARDS UNDERGROUND WATER DISTRICT

TABLE NO. 3-2 SUMMARY OF THE LITHOLOGY AND HYDROSTRATIGRAPHY OF THE SAN MARCOS PLATFORM IN THE BALCONES FAULT ZONE
(Continued)

SYSTEM	PROVINCIAL SERIES	GROUP	FORMATION	FUNC-TION	MEMBER OR INFORMAL UNIT	FUNC-TION	THICK-NESS (FEET)	LITHOLOGY	HYDROSTRATIGRAPHY
			George-town Limestone (unit is within the Edwards aquifer)	CB			20-60	Dense, argillaceous limestone; contains pyrite.	Deep water limestone with negligible porosity and little permeability.
	Edwards Group		Person (Edwards aquifer)	AQ	Marine	AQ	90-150	Limestone and dolomite; honeycombed limestone interbedded with chalky, porous limestone and massive, recrystallized limestone.	Reefal limestone and carbonates deposit under normal open marine conditions. Zones with significant porosity and permeability are laterally extensive. Karstified unit.
			Leached and collapsed members	AQ			60-90	Limestone and dolomite. Recrystallized limestone occurs predominantly in the fresh water zone of the Edwards aquifer. Dolomite occurs in the saline zone.	Tidal and supratidal deposits, conforming porous beds of collapse breccias and burrowed biomicrites. Zones of honeycombed porosity are laterally extensive.
			Regional dense bed	CB			20-30	Dense, argillaceous limestone.	Deep water limestone. Negligible permeability and porosity. Laterally extensive bed that is a barrier vertical flow in the Edwards aquifer.
			Kainer (Edwards aquifer)	AQ	Grainstone	AQ	50-60	Limestone, hard, micritic grainstone with associated beds of marly mudstones and wackestones.	Shallow water, lagoonal sediments deposited in a moderately high energy environment. A cavernous, honeycombed layer commonly occurs near the middle of the subdivision. Interparticle porosity is locally significant.

EDWARDS UNDERGROUND WATER DISTRICT

TABLE NO. 3-2 SUMMARY OF THE LITHOLOGY AND HYDROSTRATIGRAPHY OF THE SAN MARCOS PLATFORM IN THE BALCONES FAULT ZONE
(Continued)

SYSTEM	PROVINCIAL SERIES	GROUP	FORMATION	FUNC-TION	MEMBER OR INFORMAL UNIT	FUNC-TION	THICK-NESS (FEET)	LITHOLOGY	HYDROSTRATIGRAPHY
					Dolomitic includes Kirschberg evaporite)	AQ	150-200	Limestone, calcified dolomite, and Leached, evaporitic rocks with breccias toward top. Dolomite occurs principally in the saline zone of the aquifer.	Supratidal deposits toward top. Mostly tidal to subtidal deposits below. Very porous and permeable zones formed by boxwork porosity in breccias or by burrowed zones.
					Basal Nodular Bed	CB	40-70	Limestone, dense, nodular, stylitic.	Subtidal deposits. Negligible porosity and permeability.

EDWARDS UNDERGROUND WATER DISTRICT

range widely in size, shape, and degree of interconnection depending upon the texture and diagenetic history of the rock.

The total porosity (the percentage volume of open pore space per unit volume of rock) of rocks comprising the aquifer consist mostly of small voids between particles or texturally related features of the rock matrix. A large portion of these small voids are isolated and do not contribute to the hydraulic conductivity (permeability) or storativity (the capacity to contain circulating ground water). However, a large portion of the total porosity occurs within the rock matrix. This portion is interconnected by pore throats that allow for slow drainage of water to larger, secondary openings of much greater permeability. Because the rock matrix constitutes most of the bulk of the aquifer, the interconnected porosity within the rock matrix essentially provides the storage capacity of the aquifer, while providing very little to its transmissivity.

Within the Edwards Aquifer, the bulk volume of large, secondary openings is much less than that of the rock matrix. However, they contribute the most to the great capacity of the aquifer to transmit water. Most of the secondary openings have developed by dissolution and dedolomitization processes. These processes have been and are occurring below a thick cover of overlying, confining rocks. They have been accelerated by intermittent movement along faults within the Balcones fault zone. This movement has increased the opportunity for contact between unaltered permeable, sucrosic dolomites, and aggressive ground water that has a large ratio of dissolved calcium to magnesium concentrations.

The pores and pore systems of the Edwards Aquifer are physically and genetically complex. The porosity of typical lithofacies in the Edwards Aquifer is summarized in Table No. 3-3.

3.3-2 HYDROSTRATIGRAPHIC UNITS

3.3-2.1 CONFINING FORMATIONS

The confining units of the Edwards Aquifer in the San Antonio region consist of the overlying Del Rio Clay and the underlying upper part of the Glen Rose Formation. They are extremely low permeability clays, marls, and dense carbonates. The confining units are cut by faults that extend vertically up from subjacent and superjacent geologic units; however, because of the plasticity of the rocks of the confining units, fractures tend to be tight. The thickness of the Del Rio Clay ranges from about 30 feet on the San Marcos Platform to more than 120 feet in the Maverick Basin. The thickness of the upper part of the Glen Rose Formation is about 500 feet.

TABLE NO. 3-3 POROSITY OF TYPICAL LITHOFACIES OF ROCKS IN THE EDWARDS AQUIFER

CARBONATE FACIES	SEDIMENTARY STRUCTURES AND DEPOSITIONAL ENVIRONMENT	ALLOCKENS OR CRYSTALS	MATRIX	DIAGENESIS	POROSITY
MUDSTONE					
Dense non-fossiliferous.	Mudcracks, irregular lamination, stromatolitic, brecciated; supratidal.	Lithoclasts and algal fragments. Grains are isolated in mud matrix.	Carbonate mud is greater than 90 percent of the rock.	Commonly partly to completely dolomitized.	Little effective porosity except for some zones of leached collapse breccias. Porosity consists almost entirely of micropores that are poorly interconnected.
Pelletoidal, whole fossil, and shaly.	Laminated, burrowed, churned, nodular, and dolomitized; tidal flat to lagoonal.	Whole fossil and algal fragments. Grains are isolated in mud matrix.	Carbonate mud, may be pelleted.	Commonly partly dolomitized. May be chalky.	Effective porosity is dependent on leaching. Honeycombed rock is developed in some leached, mottled and burrowed zones. Modular and pelleted zones generally are dense and nonporous. Large voids commonly are molds after megafossils. Porosity in chalks is due to micropores.
MACKSTONE					
Fossil fragment, rudistid, and whole fossil.	Burrowed and churned; lagoonal.	Whole mollusk, miliolid, intraclasts. Algal grains are isolated in mud matrix.	Carbonate mud-- may be pelleted, may be converted to microsper. Comprises more than one-half of the rock constituents.	Commonly partly dolomitized. May be chalky.	Effective porosity is dependent on the leaching of grains and the conversion of a significant part of the mud to large, euhedral dolomite rhombs. Pore types include molds, intercrystalline voids, and pinpoint vugs.
PACKSTONE					
Fossil and fossil fragment, intra-elastic.	Moderately disturbed; lagoonal to open marine.	Fossils and intraclasts. Larger grains are touching.	Carbonate mud, generally comprises less than one-half of the rock constituents.	Commonly leached and dolomitized.	Effective porosity is significant where leaching and dolomitization has occurred. Pore types are vugs, interparticle, and moldic.
GRAINSTONE					
Miliolid and fossil fragment.	Cross bedded; shallow marine.	Miliolids and fossil talus. Grains are touching.	Spar.	Commonly tightly cemented.	Effective porosity is variable. Very porous where well leached. Some grainstones are leached to chalk, a very porous rock that will drain slowly.

EDWARDS UNDERGROUND WATER DISTRICT

TABLE NO. 3-3 POROSITY OF TYPICAL LITNOFACIES OF ROCKS IN THE EDWARDS AQUIFER
(Continued)

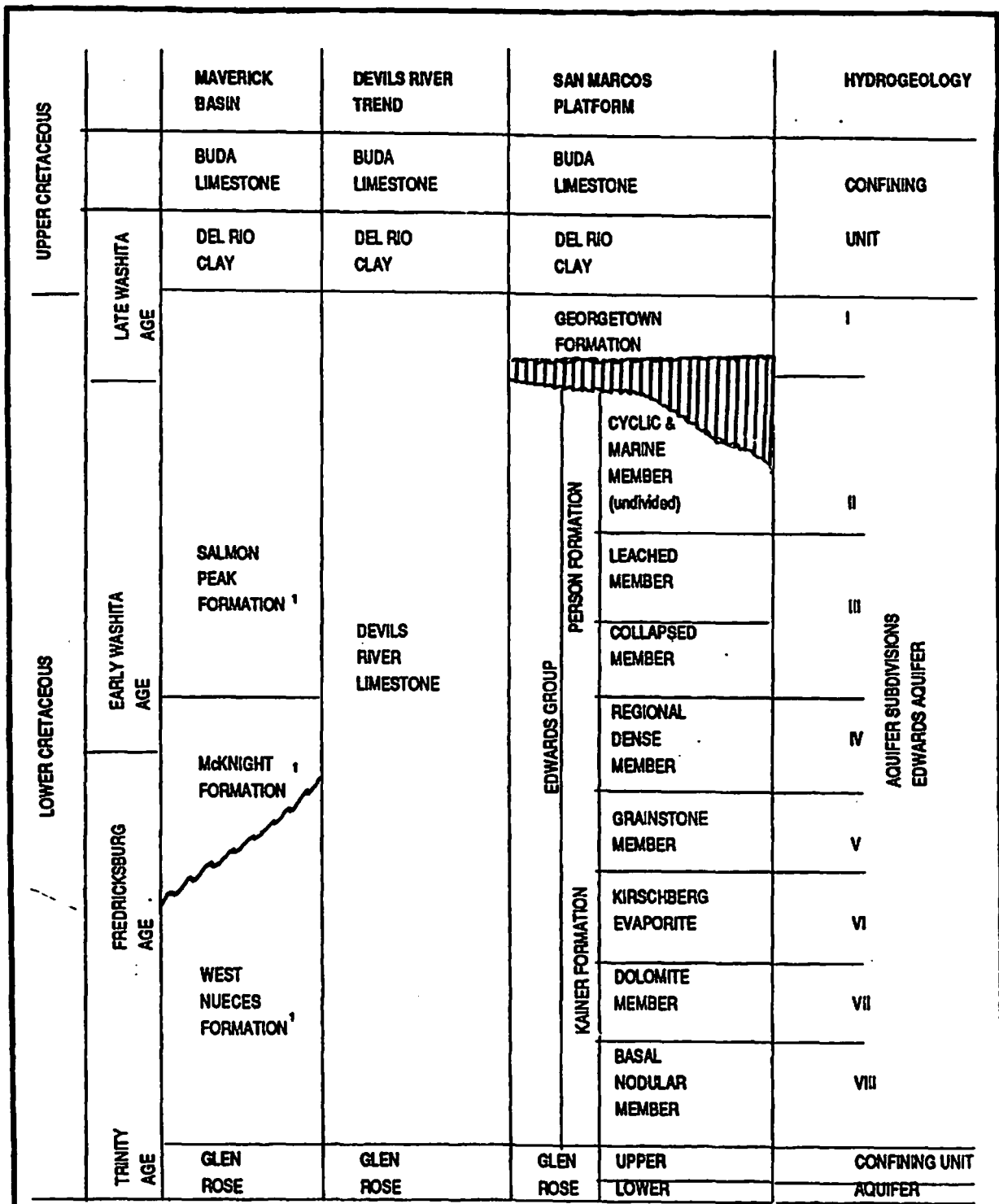
CARBONATE FACIES	SEDIMENTARY STRUCTURES AND DEPOSITIONAL ENVIRONMENT	ALLOCHENS OR CRYSTALS	MATRIX	DIAGENESIS	POROSITY
BOUNDSTONE					
	Algal and Sedimentary structure reefal. Indicates growth position of organisms; patch reefs to algal flats.	Whole mollusk fossils, commonly large rudists, algal mats.	Carbonate mud.	Algal zones commonly dolomitized.	Variable effective porosity. Leached rudistid beds have little to moderate porosity, but significant permeability.
DOLOMITE					
	No trace of original texture when dolomitization is complete.	Dolomite rhombs, ranging from very fine-grained sub-hedral to coarsely crystalline euhedral.	--	Some dolomites are extensively leached.	Generally, the coarsely sucrose dolomites have the greatest effective porosity. Porosity is increased by vugs. The fine grained dolomites have little effective porosity. These rocks occur principally in the saline zone of the aquifer.
CRYSTALLIZED LIMESTONE					
	No trace of original texture in matrix.	--	Spar.	--	Matrix has no effective porosity, but secondary vugs may be large and well connected. Boxwork porosity is developed in some evaporitic zones. These rocks occur in the fresh water zone of the Edwards aquifer.

3.3-2.2 INTERNAL STRATIGRAPHIC UNITS

The Edwards Aquifer in the San Antonio region is contained within the stratigraphic units of the Edwards Group (Rose, 1972), the Georgetown and the Devils River Limestones, and the Salmon Peak, the McKnight, and the West Nueces Formations of Lozo and Smith (1964). The correlations of the stratigraphy of the Lower Cretaceous Series in South Texas are shown in Figure No. 3-4.

The basal stratigraphic formation of the Edwards Group on the San Marcos Platform is the Kainer Formation (Rose, 1972). It is about 250 feet thick (Table No. 3-4). This formation consists of three members. The Basal Nodular Member is a marine deposit consisting of massive, nodular wackestones. This member has relatively low permeability. The middle dolomitic member consists mostly of intertidal and tidal burrowed and dolomitized wackestones with significant permeability. The upper part of the dolomitic member contains leached evaporitic deposits called by Rose "the Kirschberg Evaporite." The Kirschberg Evaporite is highly leached and contains well-developed secondary porosity that resembles boxwork. It contains permeable, cavernous rocks. The uppermost member of the Kainer Formation is the Grainstone member, which is a shallow marine deposit that marks the beginning of another cycle of sedimentation started by a transgressing sea. This member consists of well-cemented, miliolid grainstones with lesser quantities of mudstone. Commonly, some of the grainstones are leached producing a chalky rock of high porosity but of relatively low permeability.

The upper stratigraphic unit of the Edwards Group on the San Marcos Platform is the Person Formation (Rose, 1972). It is about 180 feet thick. Rose (1972) identified five informal members in the subsurface of south Texas (Figure No. 3-4). The basal member of the Person Formation is a laterally extensive marine deposit consisting of dense, shaly mudstone known as the Regional Dense Member. This member is nearly impermeable; no large solution openings occur within rocks of this member and fractures are tight. The Regional Dense Member is easily recognized in cores by its characteristic lithology and on geophysical logs by distinct shifts in the log traces. The overlying members, the Collapsed Member and Leached Member, consist of intertidal and supratidal deposits. These members contain permeable units that are formed by collapse breccias and by leached, burrowed wackestones. The uppermost member that was identified in test-hole cores in the San Antonio region (Small and Maclay, 1982) is the Marine Member, which consists of rudist-bearing wackestone and packstone and shell-fragment grainstone. This member commonly contains cavernous openings associated with bedding planes,



¹ Of Lozo and Smith (1964).

Modified from Rosa, 1972.

EDWARDS UNDERGROUND WATER DISTRICT

FIGURE NO. 3-4. Stratigraphic Correlations

TABLE NO. 3-4 POROSITY, PERMEABILITY, AND LITHOLOGY OF THE HYDROLOGIC SUBDIVISIONS OF THE EDWARDS AQUIFER IN BEXAR COUNTY

SUBDIVISION 1)	THICKNESS (feet)	TOTAL POROSITY (%) 2)	RELATIVE MATRIX PERMEABILITY 3)	FRACTURES	DESCRIPTION OF CARBONATE FACIES AND PORE TYPES
1	20-40	5	Negligible	Few, closed	Dense, shaly limestone; mudstone and wackestone; isolated fossil molds.
2	80-100	5-15	Little	Many, open	Hard, dense, recrystallized limestone; mudstone; rudistid biomicrite; some moldic porosity.
3	60-90	5-20	Little to large	Many, open	Recrystallized, leached limestone; burrowed mudstone and wackestone, highly leached in places; solution breccias, vuggy, honeycombed.
4	20-24	5	Negligible	Closed	Dense, shaly to wispy limestone; mudstone; no open fractures.
5	50-60	5-15	Little to moderate	Few, open	Limestone; chalky to hard well cemented miliolid grainstone with associated beds of mudstones and wackestones; locally honeycombed in burrowed beds.
6	50-70	5-25	Little to very large	Underdetermined	Limestone and leached evaporitic rocks with boxwork porosity; most porous subdivision.
7	110-150	5-20	Little to large	Many, open	Limestone, recrystallized from dolomite, honeycombed in a few burrowed beds; more cavernous in upper part.
8	40-60	10	Little	Few, open	Dense, hard limestone; clayey mudstone to wackestone, nodular, wispy, stylolitic, mottled; isolated molds.

1) Correlation with stratigraphic units shown in figure 12.

2) Based on visual examination of cores.

3) Matrix permeability refers to permeability related to smaller interstices, which is the bulk of the rock, and not to be larger cavernous openings.

faults, and an erosional surface. This member is a permeable unit and many very productive water wells in the San Antonio area produce from this member. The uppermost member in the Person Formation is the cyclic member. It was identified by Rose (1972) in the deep subsurface in oil fields downdip and gulfward from the San Antonio region. The cyclic member could not be identified from cores in the San Antonio region by Small and Maclay (1982). It may have been removed on the San Marcos platform by erosion during Cretaceous time.

The uppermost stratigraphic unit of the Edwards Aquifer is the Georgetown Formation. It immediately underlies the Del Rio Clay, and is relatively impermeable. Most of the wells tapping the Edwards Aquifer are cased and cemented in the Georgetown Formation. Open (uncased) holes are then drilled into the Edwards Group.

The Devils River Limestone of the Devils River trend is about 450 feet thick. It is a complex of reefal and inter-reefal deposits in the upper part and marine to supratidal deposits in the lower part. The lithofacies grade upward from about 70 feet of nodular, dense shaly dolomite and limestone above the contact with the Glen Rose Formation, to about 180 feet of tidal and marine wackestone and mudstones containing beds of burrowed, honeycombed rock. The basal 70 feet of rock has very low permeability. Above the basal 70 feet of rock are about 40 feet of mudstones and permeable collapse breccias. The upper 160 feet contain shallow marine deposits consisting of biohermal rudist mounds, talus grainstones, and inter-reefal wackestones. The upper unit contains cavernous openings and wells completed in these rocks commonly have high yields.

In the Maverick basin, the formations stratigraphically equivalent to the Edwards Group of Rose (1972) are, in ascending order, the West Nueces, McKnight, and Salmon Peak Formations (Lozo and Smith, 1964) (Figure No. 3-4). The West Nueces Formation in Uvalde County consists of nodular, shaly limestone and is divided into a lower and upper section. In the lower section, it is approximately 60 feet thick, and consists of pelleted, shell-fragmented wackestones. In the upper section, it is approximately 80 feet thick, and consists of grainstones containing beds of dolomitized, burrowed wackestones that are leached and honeycombed. The West Nueces Formation has low to moderate permeability, with most of it associated with the honeycombed rock.

The McKnight Formation consists of an upper and a lower thin-bedded limestone separated by a black, clayey, lime mudstone about 25 feet thick. The lower limestone unit, about 70 feet thick, consists of relatively impermeable fecal-pellet mudstones and shell fragment

grainstones containing zones of permeable, collapse breccias. The upper limestone, which is about 55 feet thick, is predominantly thin-bedded mudstones and associated evaporites.

The Salmon Peak formation consists of about 300 feet of dense, cherty, massive mudstones in the lower part, and in the upper part, about 75 feet of permeable grainstones that are stratified to cross-bedded, and have rounded shell fragments.

3.4 STRUCTURAL GEOMETRY

The Edwards Group and equivalent stratigraphic units occur at the surface in an irregular band along the southern edge of the Balcones Escarpment. They dip toward the southeast and thus older rocks are exposed north of the band and younger rocks south of the band. The Edwards Group has undergone extensive faulting, as shown in Figure No. 3-5. The faults generally are downthrown to the south and southeast, and trend east-northeast. They form a complex system of fault blocks that are differentially rotated and rise toward the San Marcos platform. Along the strike of some major faults, the displacement across the fault plane is sufficient to vertically offset the full thickness of the Edwards Group. Cross faults commonly intersect at acute angles at many locations.

3.5 BARRIER FAULTS

Major restrictions or barriers to lateral ground-water flow in the Edwards Aquifer occur along segments of faults where the vertical displacements are sufficient to juxtapose permeable strata opposite relatively impermeable strata. Thus, water movement is blocked in the direction normal to the fault plane and is diverted in a direction approximately parallel to the strike of the fault. Along segments of some major faults, the full thickness of the aquifer is vertically displaced, so that lateral continuity is completely disrupted in the direction perpendicular to the fault.

A series of hydrogeologic sections through the Edwards Aquifer were drawn to map the locations of internal barriers (Maclay and Small, 1984). Locations of the major internal barriers with their respective displacement values in the confined fresh-water zone of the Edwards Aquifer are shown in Figure No. 3-5 (Maclay and Small, 1984). A major barrier is designated as a section of the fault with greater than 50 percent vertical displacement of the aquifer. Vertical displacement of 50 percent or greater will place the most permeable stratigraphic subdivisions on one side of the fault plane against relatively impermeable strata on the other side.

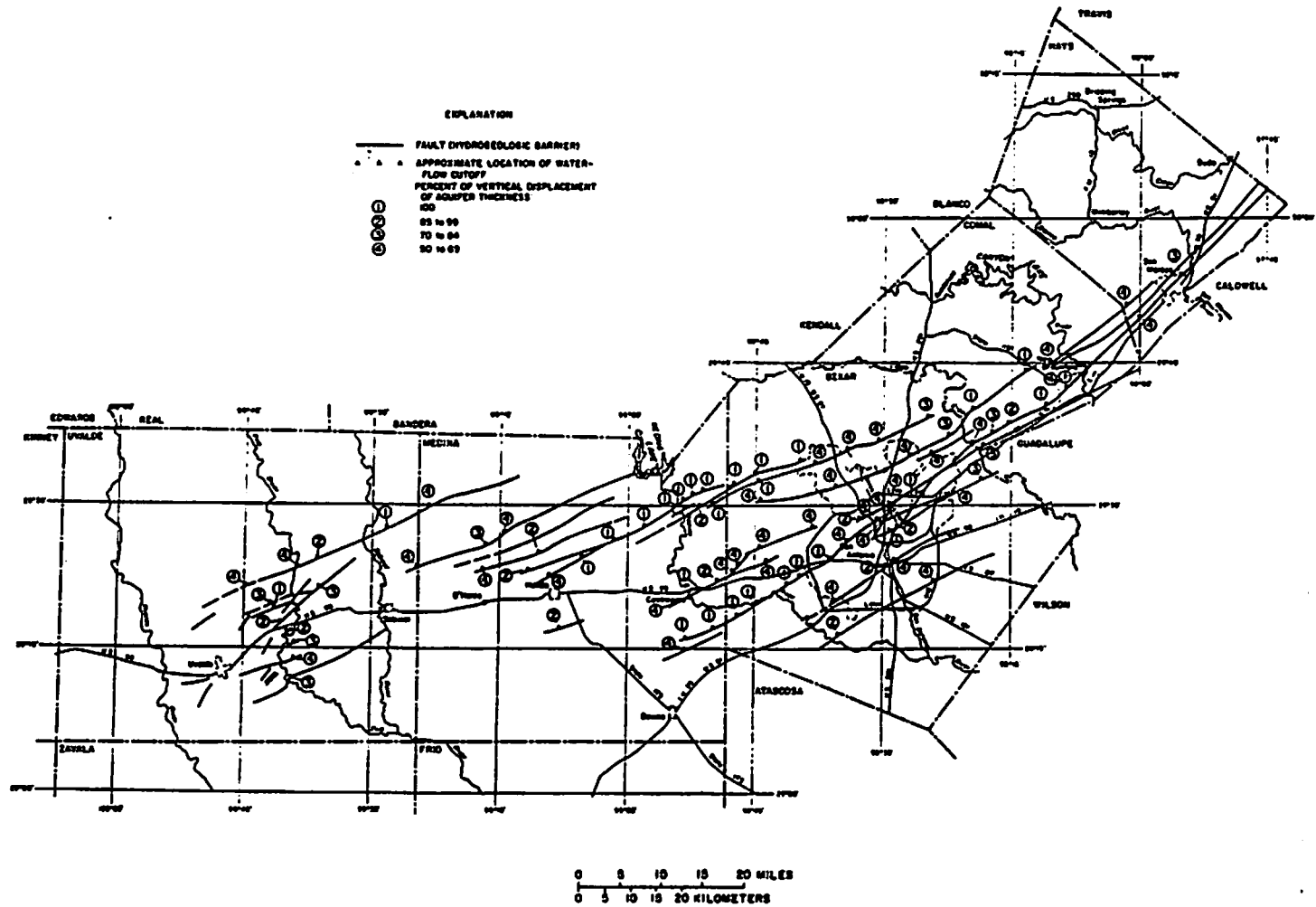


FIGURE NO. 3-5. Displacements of the Major Faults

EDWARDS UNDERGROUND WATER DISTRICT

3.6 HYDRAULIC CHARACTERIZATION

The Edwards Aquifer is hydraulically classified as heterogeneous and anisotropic. The permeability of the aquifer is dependent on the position of permeable rocks in relation to nonpermeable rocks in the aquifer. Discontinuous heterogeneity occurs in the Edwards Aquifer where faults place rocks of significantly different permeabilities in laterally adjacent positions. Therefore, heterogeneity of the Edwards Aquifer may be categorized into layered, discontinuous, and trending.

Layered heterogeneity consists of individual beds or units that have different average permeabilities. However, each bed may have variable porosity. The Edwards Aquifer of the San Marcos platform consists of eight hydrostratigraphic subdivisions (Table 3-4 and Figure No. 3-6). Very permeable zones are distributed erratically throughout subdivision 2 and 7. The most permeable zones in these subdivisions occur in honeycombed rocks formed by large rudist molds, by irregular openings developed in burrowed tidal wackestones, and by moldic porosity developed in collapse breccias. The most porous rocks are leached or incompletely cemented grainstones that occur mostly in subdivisions 3, 5, and 6. These rocks have significant storage capacity but relatively little capacity to transmit water. The lithofacies of subdivisions 1, 4, and 8 are nearly impermeable and have very low storage capacity .

The layered heterogeneity of the Edwards Aquifer within the Maverick Basin is shown by the geophysical logs of test hole YP-69-42-709 northwest of Uvalde (Figure No. 3-7). The aquifer in the Maverick Basin consists of three hydrostratigraphic subdivisions. The upper subdivision (Salmon Peak Formation) is the most permeable. Cavernous porosity is indicated by increased hole diameter as detected by the caliper log in the upper part of subdivision 1. The Edwards Aquifer is separated into an upper and a lower zone by subdivision 2 (the McKnight Formation) in the Maverick Basin and by subdivision 4 (the Regional Dense Member) on the San Marcos Platform. These subdivisions have negligible permeability and lack open fractures.

The Sabinal test hole (YP-69-37-402) entirely penetrated the Devils River Formation. The geophysical logs and core-hole data did not indicate that the Devils River Formation could be readily divided into layered hydrogeologic units (Figure No. 3-8). However, the caliper log indicated cavernous porosity in the upper part of the formation.

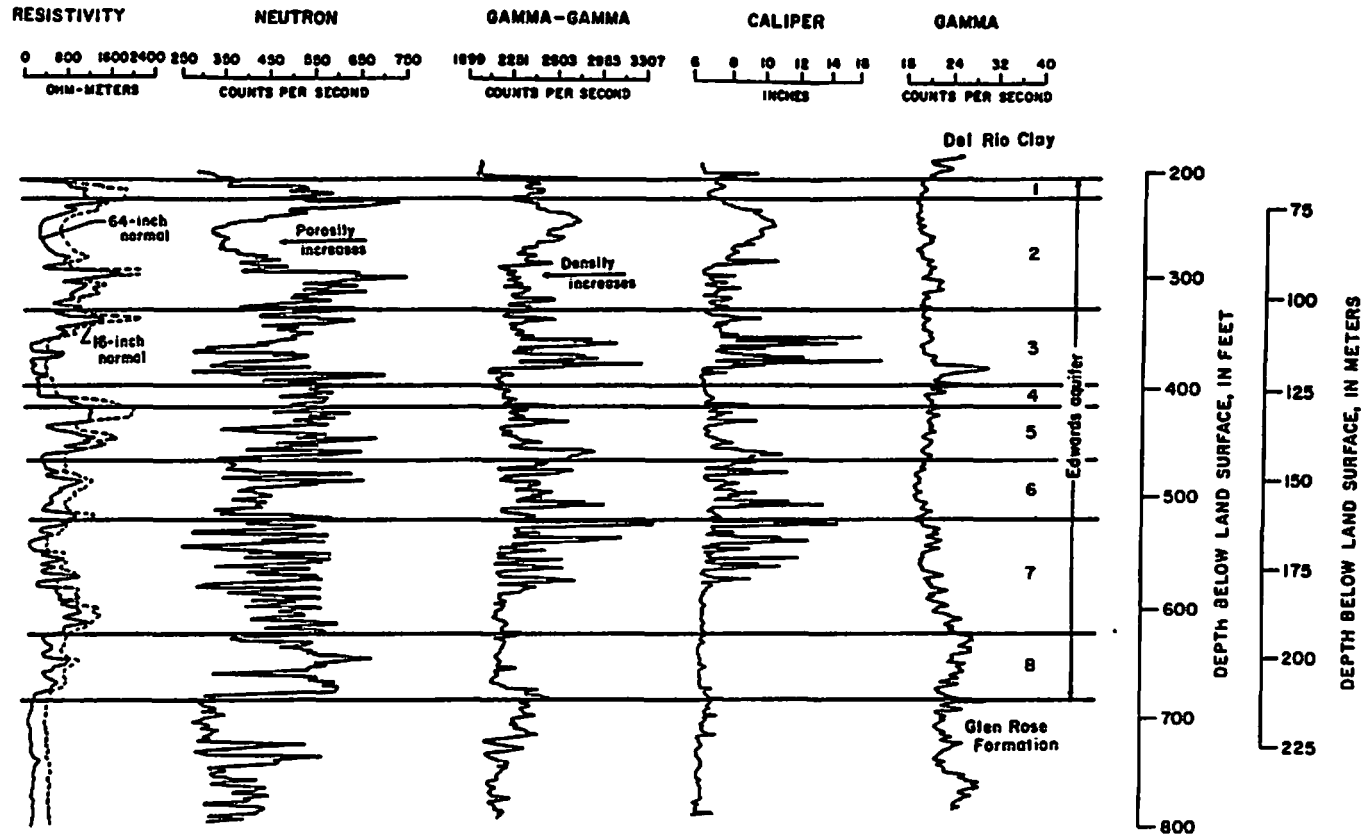


FIGURE NO. 3-6. Layered heterogeneity of the Edwards Aquifer on the San Marcos platform, Castle Hills test hole (AY-68-28-910)

EDWARDS UNDERGROUND WATER DISTRICT

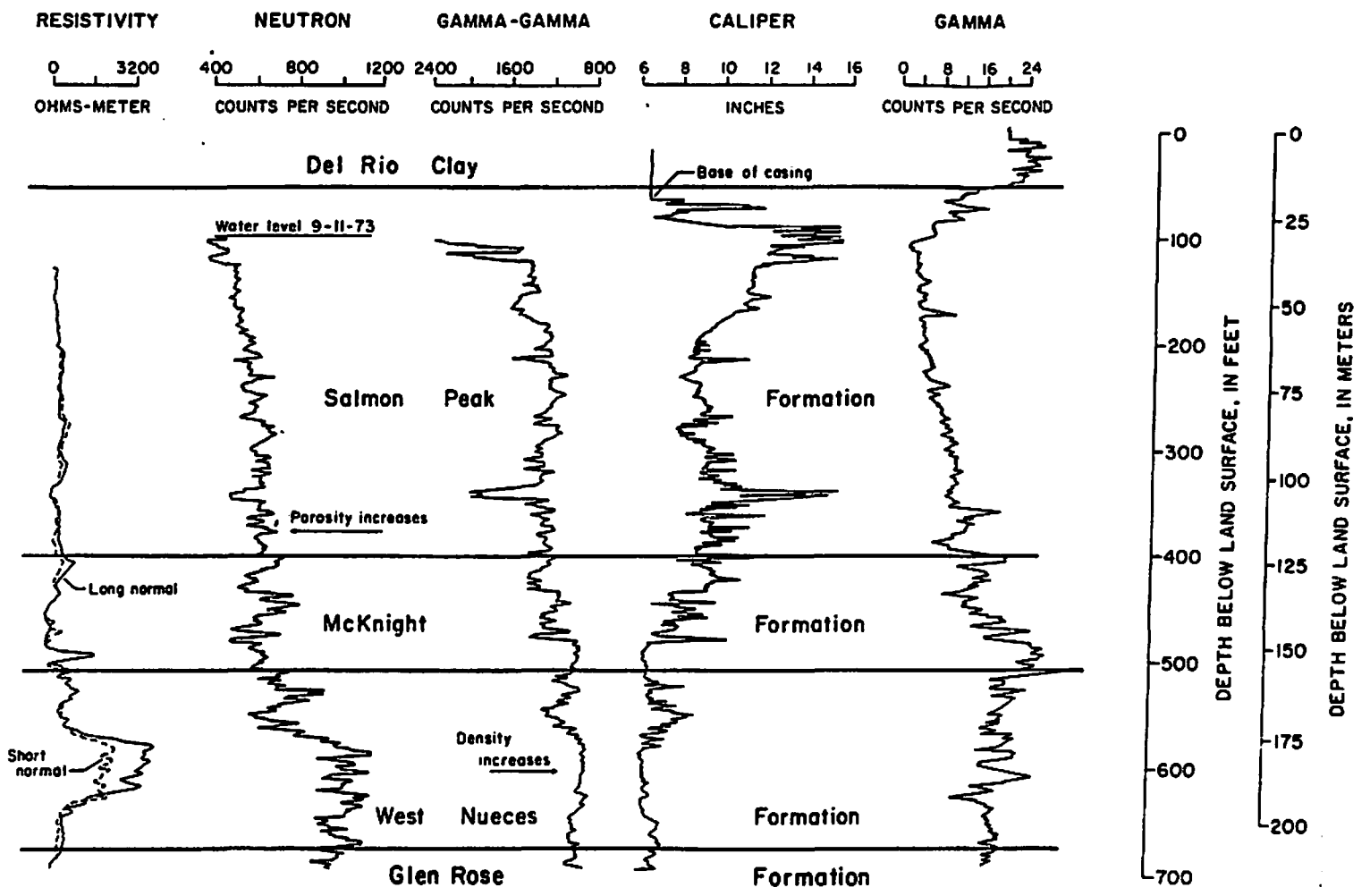


FIGURE NO. 3-7. Layered heterogeneity of the Edwards Aquifer within the Maverick Basin, Uvalde test hole (YP-69-42-709)

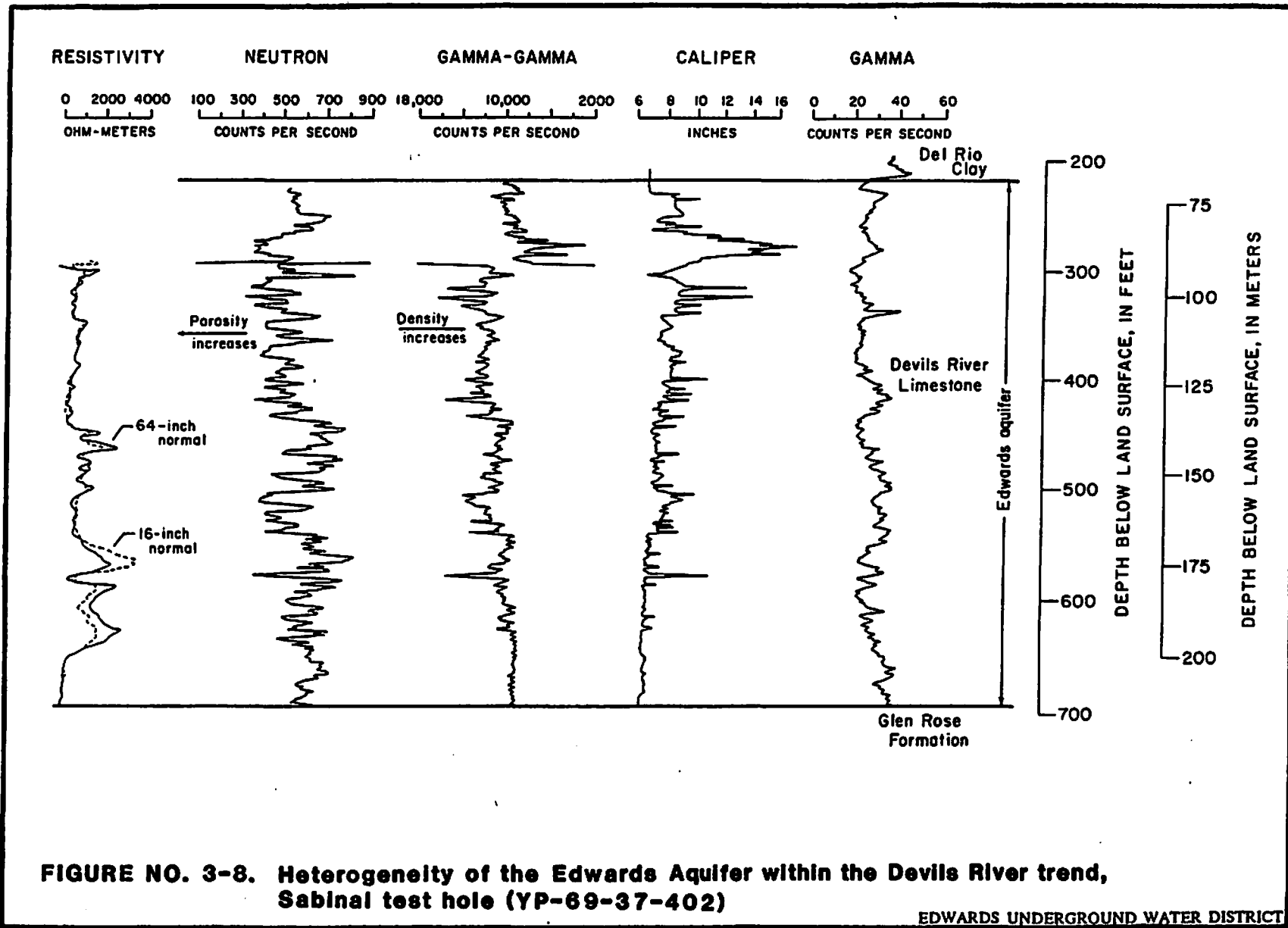


FIGURE NO. 3-8. Heterogeneity of the Edwards Aquifer within the Devils River trend, Sabinal test hole (YP-69-37-402)

EDWARDS UNDERGROUND WATER DISTRICT

Trending heterogeneity is caused by a gradational and regional change in the permeability of the Edwards Aquifer. Trending heterogeneity occurs in the aquifer because of regional changes in depositional environments that affected lithologies; the occurrence of paleokarst on the San Marcos platform; and the distribution and intensity of fractures. Carbonate rocks deposited on the San Marcos platform and in the Devils River trend contain a much greater abundance of sedimentary and diagenetic features that contribute to the development of large secondary opening than the rocks in the Maverick basin. Paleokarst is extensively dissolved carbonate rocks that are buried by later sediments. Karst is a terrain, generally underlain by limestone in which the topography, formed chiefly by dissolving rock, is characterized by closed depressions, subterranean drainage, and caves.

Anisotropy of an aquifer occurs when the permeability shows variations with direction at any given point in a geologic formation. Therefore, an anisotropic aquifer will have a dominant permeability in one or more directions depending upon geologic and hydrologic conditions. Anisotropic properties need to be accurately quantified to solve local problems at the scale of a well field. For problems at a regional scale, documentation of the anisotropy of a carbonate aquifer is very difficult and must be estimated from geologic knowledge.

The hydrogeologic conditions that contribute to or affect the development of anisotropy in the Edwards Aquifer in the San Antonio region are:

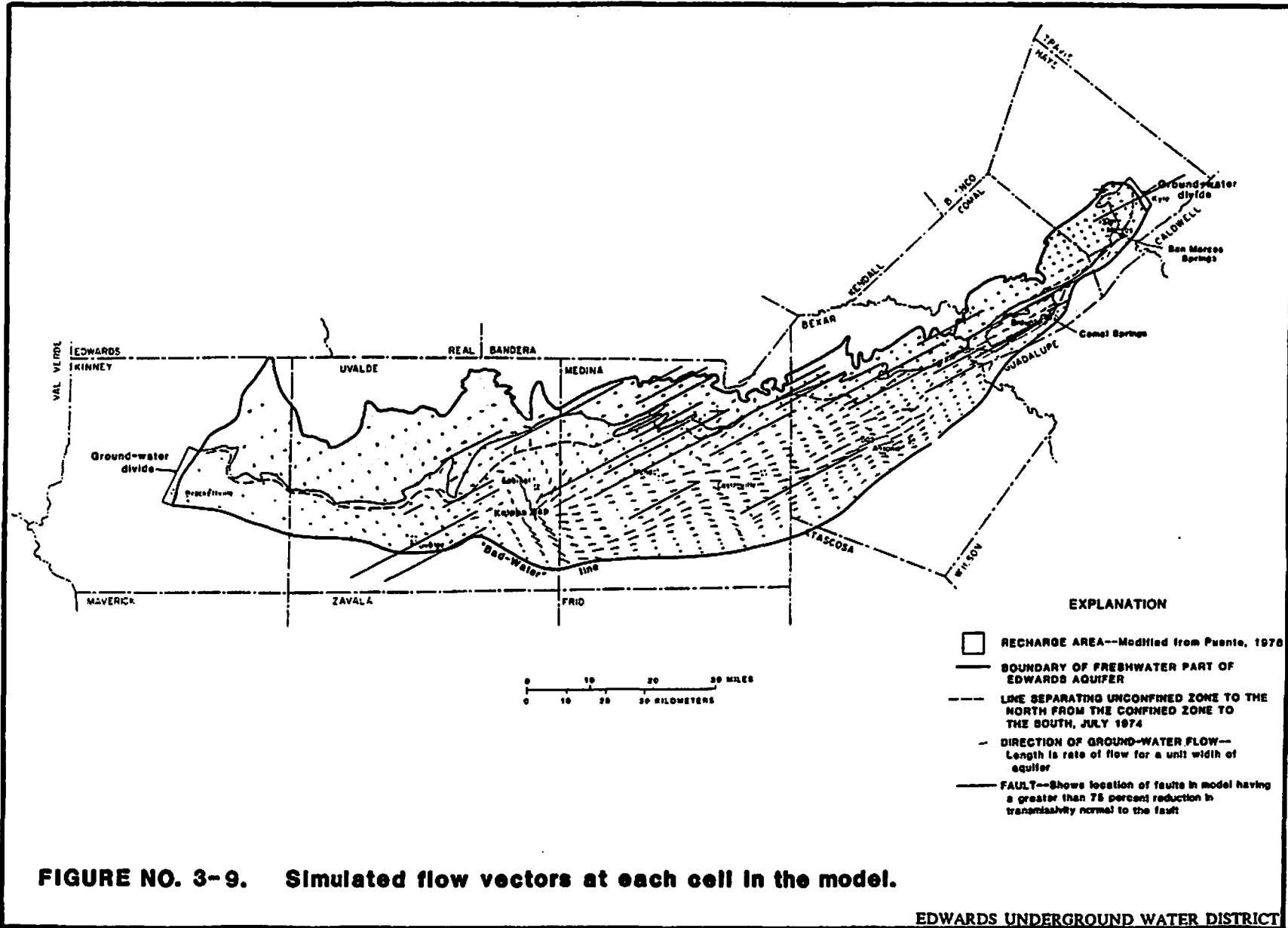
1. Tubular openings or solution channels that are associated with paleokarst;
2. The occurrence of faults that vertically separate the aquifer;
3. The possibility that solution channels may be oriented parallel to the stream courses of certain recharging streams;
4. Vadose and phreatic solution channels are well developed within the recharge area; and
5. The distribution and orientation of open fractures.

3.7 REGIONAL GROUND-WATER FLOW

3.7-1 WATER LEVELS AND GROUND-WATER FLOW

The altitude of the water level within a well tapping an aquifer, called the potentiometric head or head, is a measure of the potential energy of the contained fluid at the location of the well. Water within the saturated ground-water reservoir or the phreatic zone moves under the force of gravity from a position of higher head or higher energy toward a position of lower head. The circulating waters within the phreatic zone move down the energy or hydraulic gradient which reflects the path of least resistance.

To investigate flow within aquifers, heads are determined throughout the aquifer during a short time that is representative of current hydrologic conditions. The heads are then used to prepared a contoured or potentiometric map. Ground water movement follows the hydraulic gradient which is drawn perpendicular to the contours of equal head. Commonly, sufficient head data are not available to determine local and subregional details in some parts of the area under investigation. A knowledge of the geologic framework and the location of hydrologic boundary conditions provide information that can be used in conjunction with head data to interpret local or subregional complexities of the potentiometric surface and the ground-water flow lines. This is the situation within the recharge area of the Edwards Aquifer. Few head observations are available but geologic data show the locations of faults that affect the direction of ground-water flow (Figure No. 3-9).



Section 4

SECTION 4.0 DATA COLLECTION

Records of all activities were maintained during the projects. Daily accounts were recorded for drilling operations and measurements obtained during testing procedures. Separate records were maintained on the cutting descriptions, water quality data, and pump tests. Records were also kept on the drilling operations to account for work performed in accordance with bid documents. Borehole geophysical wireline logs were run by the EUWD, the TWDB, Beeline Services, Comprobe, and Schlumberger. All documents are maintained at the EUWD.

The drilling of the wells in New Braunfels was contracted to Texas Water Wells while the drilling of the wells in San Marcos was contracted to Layne Texas, a division of Layne-Western Company, Inc.

The limestones of the Edwards Aquifer (which includes the Georgetown Formation and the Edwards Group which consists of the Person and Kainer Formations) lies approximately 400 to 800 feet beneath the surface at both the New Braunfels and San Marcos sites. To isolate the shallow alluvial aquifers, a 16-inch inside diameter conductor casing was set inside a 24-inch diameter boring. A 7-7/8-inch diameter pilot hole was then drilled to the top of the Edwards Aquifer (or Georgetown Formation) using mud rotary drilling equipment. The 7-7/8-inch diameter pilot hole was then reamed to a 16-inch nominal diameter, and a 10-inch surface casing was set. A 7-7/8-inch hole from the top of the Edwards Aquifer to near the top of the Glen Rose Formation was drilled using reverse circulation-air lift method (see Figure No. 4-1).

Table No. 4-1 shows the depths of the stratigraphic units encountered above the Edwards Group, while Table No. 4-2 shows the depths of the formations and members within the Edwards Group. All depths are based on interpretations from the various wireline logs which were run in each well. In Table No. 4-2, only one well at each transect was drilled through the Basal Nodular Member to the Glen Rose. After drilling the A-1 well in New Braunfels and the C-1 well in San Marcos and calculating production of the formations, the determination was made that the Basal Nodular was not a producing zone. This conclusion is also supported by both the petrographic and petrophysical analyses.

In drilling through the Edwards Aquifer in the San Antonio transect, reverse circulation-air lift method was used. This method provided several advantages, and thus, it was used at both New Braunfels and San Marcos. The advantages are related to the drilling process.

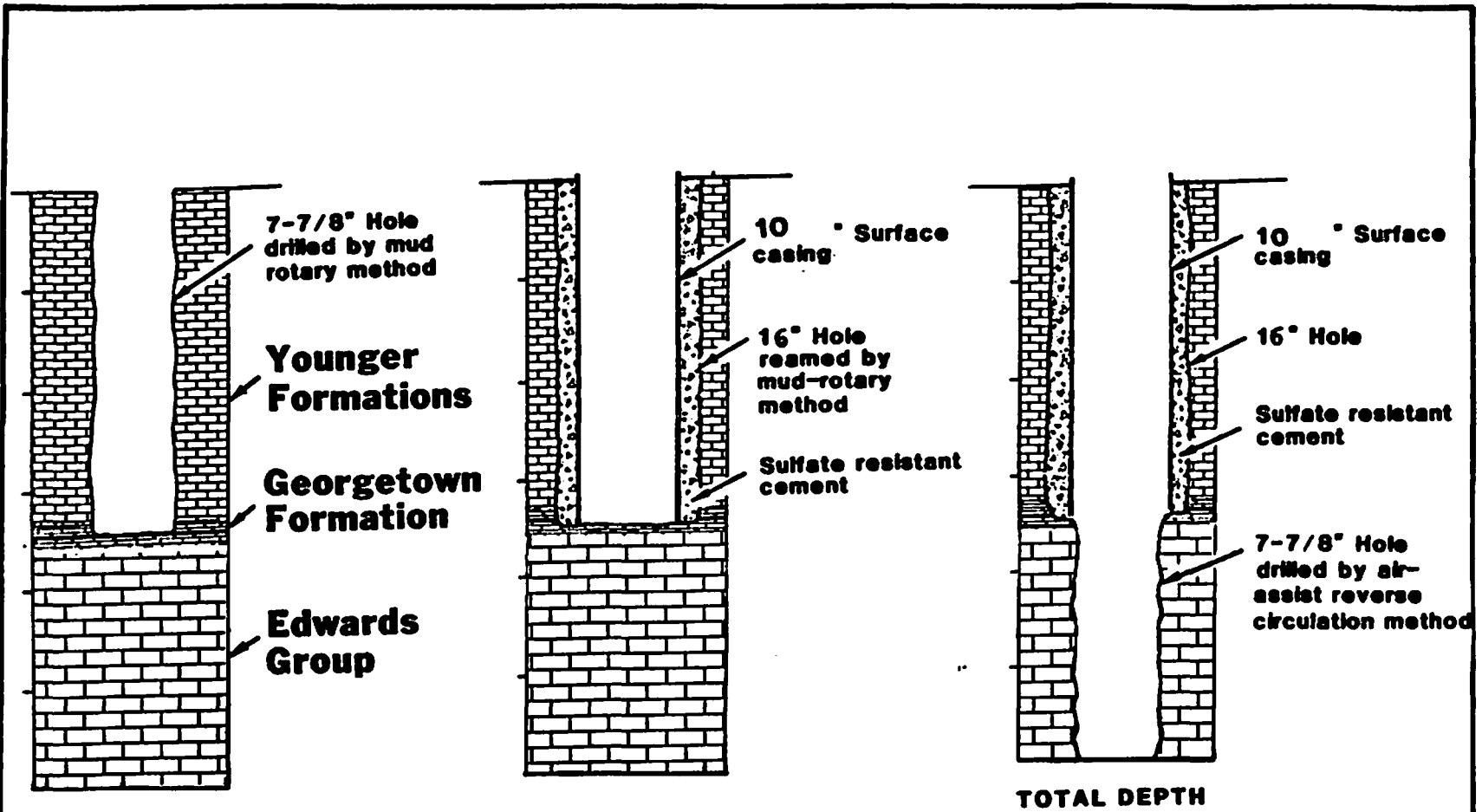


FIGURE NO. 4-1. Drilling Procedure

As shown in Figure No. 4-2 (Guyton, 1986), compressed air is fed into the drill pipe through an air-line which draws water and cuttings from outside the drill stem back up the drill pipe. The drill cuttings and water are discharged at the surface into a sample collection box and holding tank(s). Therefore, no cuttings are lost through void spaces and cavities, and the cuttings are clean enough to be examined when discharged. Water quality samples can also be collected, which provide depth-specific samples as the hole is being drilled.

During the drilling process, the cuttings were collected at 10-foot intervals with the lithologic descriptions accomplished by an EUWD staff geologist. The cuttings were bagged and marked for each 10-foot interval within the Edwards. The cutting descriptions were later reviewed with a binocular scope at the EUWD offices. Representative samples from each bag from each well were made into thin sections for petrographic (microscopic) examination.

Air-lift pump tests were performed at 50-foot intervals. Submersible pump tests with expandable packers were also performed at three separate settings in the openhole section of the Edwards. The packer tests were performed for different producing zones of the aquifer: one in the Person Formation, above the Regional Dense Member; and two in the Kainer Formation. Once total depth had been reached, but before completion of the holes as monitoring wells, a 9-hour pump test at New Braunfels and a 7-hour pump test at San Marcos were performed using submersible pumps. A 9-hour pump test was later performed at San Marcos once the D well had been drilled. Water level measurements collected during the 50-foot air lift tests, packer-interval pump tests, and full thickness pump tests were performed utilizing a combination of air lines, E-lines, and continuous recording devices.

Water quality samples for common ion analysis were collected after every pump test. Conductivity and temperature readings were made during all pump test and when samples were collected for analysis. Samples collected for analysis were filtered, titrated for alkalinity, measured for pH, and acidized at the site. The samples were delivered to the USGS for laboratory analysis. Selected duplicate samples were also sent to the TWDB.

As stated above, formation waters were discharged at the surface into two holding tanks. The water at both sites, but particularly at San Marcos, was high in total dissolved solids and had to be disposed of carefully. After receiving approval from appropriate city departments, the water discharged from the wells was pumped-off to the city sewer where the conductivity values and discharge rates were monitored. City water was added to the system when the

TABLE NO. 4-1 STRATIGRAPHIC UNITS ENCOUNTERED ABOVE THE EDWARDS GROUP AT THE NEW BRAUNFELS AND SAN MARCOS TRANSECTS

Stratigraphic Unit	NB-A1			NB-B1			NB-C1			SM-B			SM-C			SM-D		
	Depth to top (ft.)	Depth to bottom (ft.)	Thickness (ft.)	Depth to top (ft.)	Depth to bottom (ft.)	Thickness (ft.)	Depth to top (ft.)	Depth to bottom (ft.)	Thickness (ft.)	Depth to top (ft.)	Depth to bottom (ft.)	Thickness (ft.)	Depth to top (ft.)	Depth to bottom (ft.)	Thickness (ft.)	Depth to top (ft.)	Depth to bottom (ft.)	Thickness (ft.)
Quaternary Alluvium	0	39	39	0	42	42	0	44	44	0	30	30	0	30	30	0	30	30
Pecan Gap	39	176	137	42	207	165	44	248	204	30	80	50	30	96	66	30	114	84
Austin Chalk	176	313	137	207	343	136	248	386	138	80	260	180	96	271	175	114	306	192
Eagle Ford	313	341	28	343	372	29	386	414	28	260	293	33	271	304	33	306	340	34
Buda	341	389	48	372	406	34	414	462	48	293	342	49	304	352	48	340	394	54
Del Rio	389	433	44	406	462	56	462	506	44	342	391	49	352	401	49	394	440	46
Georgetown Formation	433	464	31	462	494	32	506	540	34	391	426	35	401	432	31	440	473	33

* Contacts determined from EUWD Logs

TABLE NO. 4-2 STRATIGRAPHIC UNITS ENCOUNTERED WITHIN THE EDWARDS GROUP AT THE NEW BRAUNFELS AND SAN MARCOS TRANSECTS

Stratigraphic Unit	NB-A1			NB-B1			NB-C1			SM-B			SM-C			SM-D		
	Depth to top (ft.)	Depth to bottom (ft.)	Thickness (ft.)	Depth to top (ft.)	Depth to bottom (ft.)	Thickness (ft.)	Depth to top (ft.)	Depth to bottom (ft.)	Thickness (ft.)	Depth to top (ft.)	Depth to bottom (ft.)	Thickness (ft.)	Depth to top (ft.)	Depth to bottom (ft.)	Thickness (ft.)	Depth to top (ft.)	Depth to bottom (ft.)	Thickness (ft.)
Edwards Group	464	910	446	494	916*	422*	540	959*	419*	426	891*	465*	432	907	475	473	774*	301
Person Formation	464	646	182	494	674	180	540	724	184	426	580	158	432	591	159	473	603	130
Cyclic, Marine, Collapsed, & Leached Members Combined	464	626	162	494	656	162	540	702	162	426	566	140	432	574	142	473	588	115
Regional Dense Member	626	646	20	656	674	18	702	724	22	566	580	15	574	587	13	588	603	15
Kainer Formation	646	910	264	674	916*	242*	724	959*	235*	580	891*	311*	587	907	320	603	774*	171
Grainstone Member	646	706	60	674	730	56	724	772	48	580	644	63	587	660	73	603	661	58
Kirschberg & Dolomitic Members (combined)	706	874	168	730	900	170	772	940	168	644	850	206	660	853	213	661	744*	83*
Basal Nodular Member	874	910	36	900	---	---	940	---	---	850	---	---	853	911	38	---	---	---
Glen Rose Formation	910	---	---	---	---	---	---	---	---	---	---	---	911	---	---	---	---	---
Total Depth of Well	935			916			959			891			911			774		

* Contacts determined from Schlumberger Logs

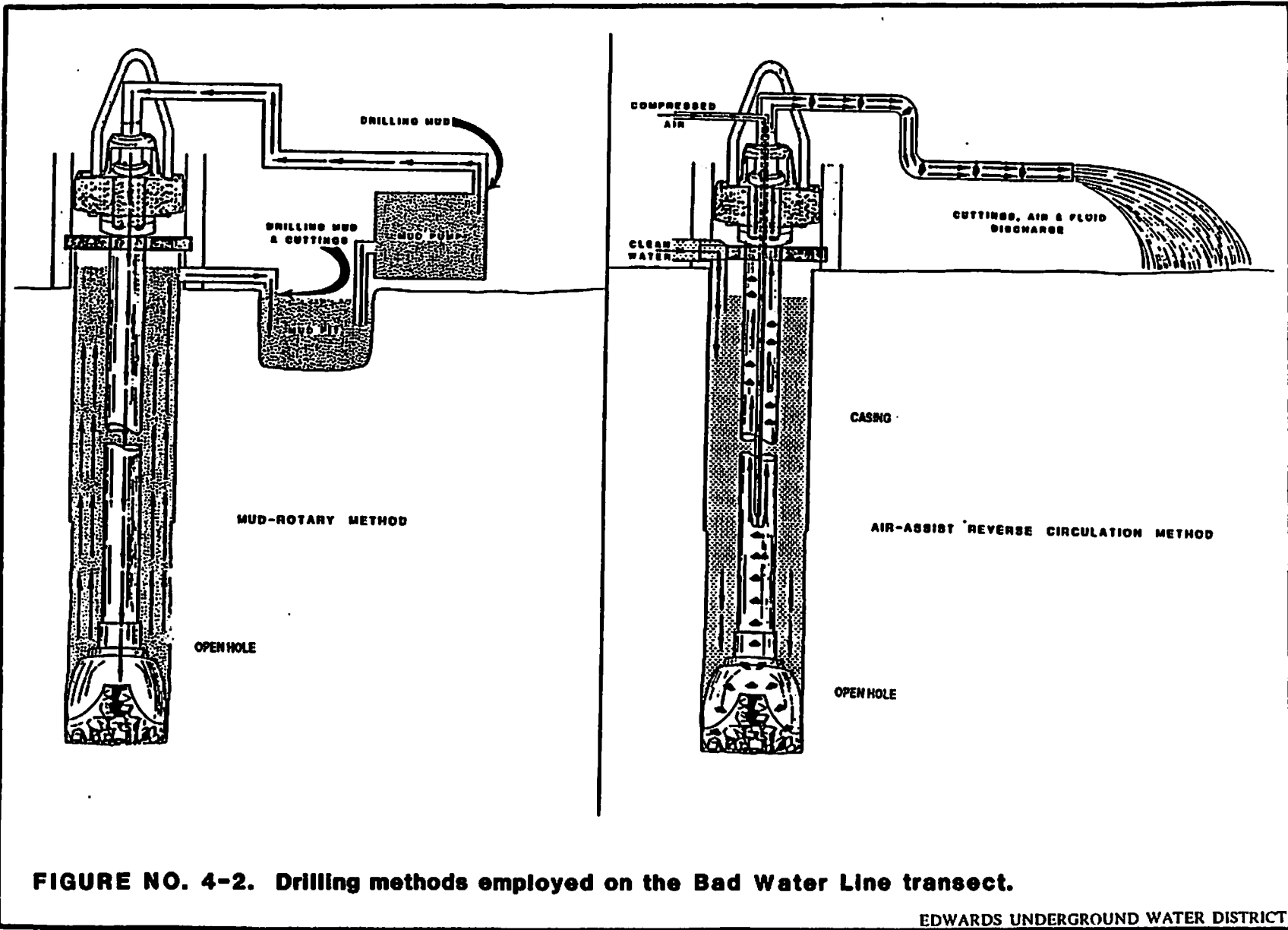


FIGURE NO. 4-2. Drilling methods employed on the Bad Water Line transect.

EDWARDS UNDERGROUND WATER DISTRICT

conductivity values were between 3000 and 7000 $\mu\text{S}/\text{cm}$. Reports of all discharge events were submitted to the city wastewater departments .

The holes were then completed above and/or below the Regional Dense Member. Figures No. 4-3 shows how the wells were completed. Note that wells B-1 and B-2 in New Braunfels and B in San Marcos contain one well screen per borehole, while wells A-1 and C-1 in New Braunfels, and C and D in San Marcos contain 2 well screens per borehole. The PVC screens are 40 feet long and gravel packed. For more details about the completions, refer to the bid documents for the projects at the EUWD.

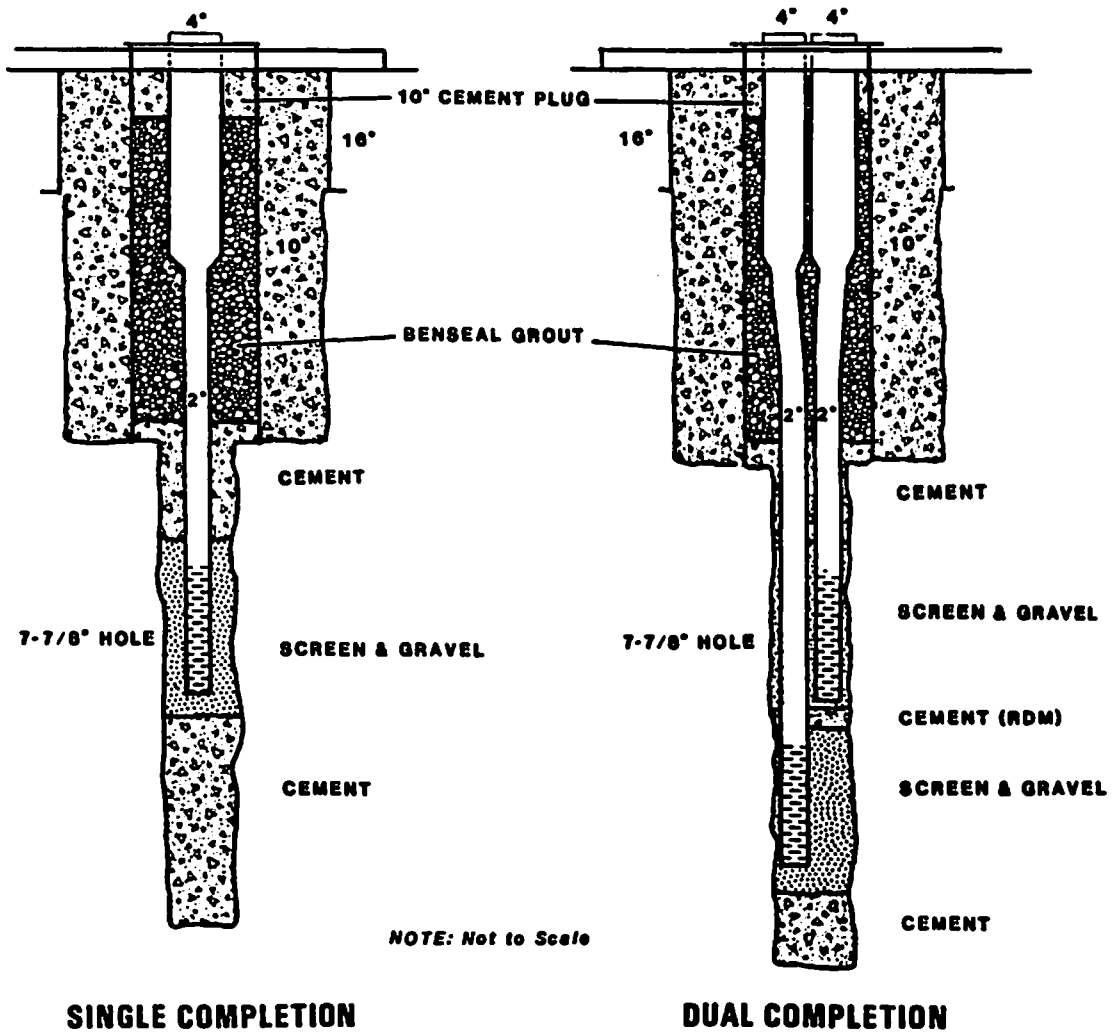


FIGURE NO. 4-3. Completion Procedure

EDWARDS UNDERGROUND WATER DISTRICT

Section 5

SECTION 5.0 PUMP TESTS, WATER QUALITY DATA, AND CUTTING DESCRIPTIONS

5.1 PUMP TESTS RESULTS

As mentioned in Section 4.0, at approximately fifty-foot intervals, pump tests were performed using the air-lift system of the reverse circulation drilling system. Pump tests in packer isolated intervals (packer tests) utilizing submersible pumps were also performed. Because the discharge rates were highly variable, recovery-test methods were used to analyze the pump tests and calculate aquifer transmissivity. Storage coefficients could not be calculated using this method. However, at each site after the total depth of each well had been reached, one submersible-pump pumping test was performed using observation wells. This allowed the Theis Equation to be used to calculate both transmissivity and the storage coefficient of the Edwards Aquifer.

5.1-1 RECOVERY TESTS PERFORMED AT VARIOUS DEPTH INTERVALS

Water levels were measured after the pump or air was turned off until the water level returned to or near the static level. The water level measurements collected for these tests are in Appendix I. The test intervals, thicknesses, resultant transmissivities, water conductivities, and water temperatures are in Table Nos. 5-1 and 5-2.

The rise of the water level is referred to as the recovery of ground-water levels (Todd, 1976). The difference between the water-level measurements collected during the recovery period and the static water level are called the residual drawdowns. The residual drawdowns (s) are plotted on the y-axis against t/t' on the x-axis on semilogarithmic paper. If the storage component of the aquifer remains constant over the testing interval, the data will plot approximately a straight line (Figure No. 5-1). However, in carbonate aquifers, storage can vary due to changes in boundary conditions: boundaries between less permeable layers and greater permeable layers may be encountered; or in the case of leaky aquifer conditions, leakage from overlying or underlying semipermeable layers may be encountered (Hammond, 1984). Hammond (1984) explains further:

With continuing lowering of the pumping level in the well, the cone of depression in the potentiometric surface could intersect the upper boundary of the confined aquifer, resulting in an unconfined system.

TABLE NO. 5-1 PUMP/RECOVERY TEST RESULTS - NEW BRAUNFELS WELLS

Date/Time	Sample Number (If Collected)	Test Interval (Feet)	Thickness (Feet)	Q-Average Discharge Rate (GPM)	T-Transmissivity (GPD/feet)	Specific Conductance (µs/cm)	Temperature C°
Well A-1							
89/09/06 17:00	1	444-506	72.00	47.00	283	2,413	28.8
89/09/07 11:35	-	444-556	112.00	62.30	2,961	2,885*	25.5
89/09/08 07:10	-	444-606	162.00	50.70	1,858	2,672*	25.6
89/09/12 07:22	2	534.5-634	99.50	74.00	4,717	3,095	25.5
89/09/13 12:23	-	444-686.5	262.50	70.50	2,716	2,830*	25.2
89/09/13 16:40	-	444-736.5	292.50	69.70	2,283	2,550*	25.5
89/09/14 13:15	3	638-781.5	143.50	67.40	3,586	2,440	26.0
89/09/15 13:42	4	444-836.5	392.50	85.00	5,145	3,370	26.1
89/09/18 10:45	5	444-886.5	442.50	78.60	4,458	4,070	26.3
89/09/19 07:57	6	799-936.5	137.50	86.00	6,401	5,540	27.0
Well B-1							
89/10/10 10:45	7	472-529.7	57.20	28.00	302	595	25.0
89/10/11 07:25	8	472-564.2	91.70	58.50	634	557	25.4
89/10/12 08:45	-	472-616.7	144.20	54.00	598	668*	25.2
89/10/14 09:10	9	561-661.7	100.70	26.00	738	1,100	25.5
89/10/16 15:00	-	472-726.7	254.20	63.70	1,932	704*	25.7
89/10/17 15:58	10	670-781.7	111.70	54.00	3,756	578	25.7
89/10/18 14:00	11	472-831.7	341.20	80.00	7,902	990	25.7
89/10/19 07:35	12	472-881	409.20	80.10	9,260	1,850	25.9
89/10/20 07:10	13	773-916.5	143.50	58.00	4,172	3,750	26.3
Well C-1							
90/01/22 13:45	-	518-576.5	58.50	29.60	35	508*	24.2
90/01/23 07:20	17	518-612.6	94.60	66.70	623	498	25.0
90/01/23 16:20	-	518-661.33	143.33	68.52	856	512.4*	25.3
90/01/24 11:00	-	518-706.33	188.33	61.50	2,231	513	25.2
90/01/25 14:00	18	618-706.33	88.33	36.60	1,844	578	26.0
90/01/29 10:53	-	518-776.34	25.34	70.68	6,823	527*	25.6
90/01/29 17:20	19	715-826.94	111.94	60.00	8,046	565	26.5
90/01/30 11:45	-	518-826.94	309.44	84.03	10,395	545*	26.0
90/01/31 16:45	20	518-876.55	359.15	82.06	7,934	1,050	26.0
90/02/01 10:35	-	518-928.09	410.09	83.78	10,969	1,911*	26.0
90/02/01 16:15	21	518-959.35	441.35	86.01	9,265	2,180	26.0
90/02/02 11:08	22	821-959.35	138.35	68.75	7,939	4,190	27.0

Note: N882 was not analyzed - data in appendix
 * = not corrected according to conductivity meter calibrations

TABLE NO. 5-2 PUMP/RECOVERY TEST RESULTS - SAN MARCOS WELL

Date/Time	Sample Number (If Collected)	Test Interval (Feet)	Thickness (Feet)	Q-Average Discharge Rate (GPM)	T-Transmissivity (GPD/feet)	Specific Conductance (µs/cm)	Temperature C°
Well B							
90/06/22 13:44	-	403-476.9	73.90	12.70	31	13,440*	29.0
90/06/23 13:29	1	403-508.8	105.80	33.00	263	13,000	27.0
90/06/24 08:20	-	403-566.39	163.39	39.50	267	12,420*	28.0
90/06/25 14:25	2	509-566	57.00	21.00	257	14,400	26.0
90/06/27 09:20	-	403-668.69	265.69	75.00	335	14,370*	25.0
90/06/28 07:00	4	573-707	134.00	20.50	578	14,680	26.0
90/06/29 09:20	-	403-727	323.75	75.00	573	14,580*	25.0
90/06/29 16:00	-	403-770	367.00	75.00	727	14,580*	25.0
90/06/30 10:00	-	403-833.4	430.40	74.00	1,622	14,410*	26.0
90/07/01 09:20	5	403-890.5	487.50	31.00	3,671	14,400	27.0
90/07/02 07:51	6	694-890	196.50	20.00	2,581	14,500	26.8
Well C							
90/07/19 23:05	-	416.4-489.22	72.82	12.76	21	13,090*	24.8
90/07/20 05:00	7	416.4-520.31	103.91	21.00	66	13,000	24.7
90/07/20 13:30	-	416.4-583.69	167.29	27.10	112	13,300*	26.5
90/07/21 04:20	8	520-583.69	63.69	11.00	44	14,300	26.5
90/07/21 22:45	-	416.4-632.59	216.19	52.70	229	14,020*	26.5
90/07/21 17:25	-	416.4-676.44	260.40	84.60	432	14,020*	25.8
90/07/23 01:15	-	416.4-739.51	323.11	96.00	2,393	14,400*	25.5
90/07/23 09:30	-	416.4-791.48	375.08	70.50	1,958	14,400*	26.0
90/07/23 15:00	-	416.4-844.29	427.89	98.70	9,402	14,380*	26.0
90/07/24 13:20	10	746-920	174.00	20.50	1,659	14,710	26.5
90/07/24 03:55	-	416.4-920	504.10	93.06	3,009	14,400*	26.5
90/07/26 13:30	11	416.4-920	504.10	70.00	4,669	14,500	26.5
Well D							
92/02/20 16:30	14	462-556.07	94.07	78.26	453	16,405	25.8
92/02/25 08:10	15	549-601	52.00	20.5	153	14,080	25.3
92/02/27 10:30	16	598.3-658	59.70	20.5	176	12,356	25.5
92/02/28 13:15	-	462-711	249.00	132.00	8,150	11,230	25.5
92/02/29 14:00	17	658-774	53.00	28.00	8,298	13,438	26.0
92/03/02 11:00	18	462-774	32.00	70.00	7,672	12,687	25.5

Note: #3 or #13 samples were not analyzed
 * not corrected according to conductivity meter calibrations

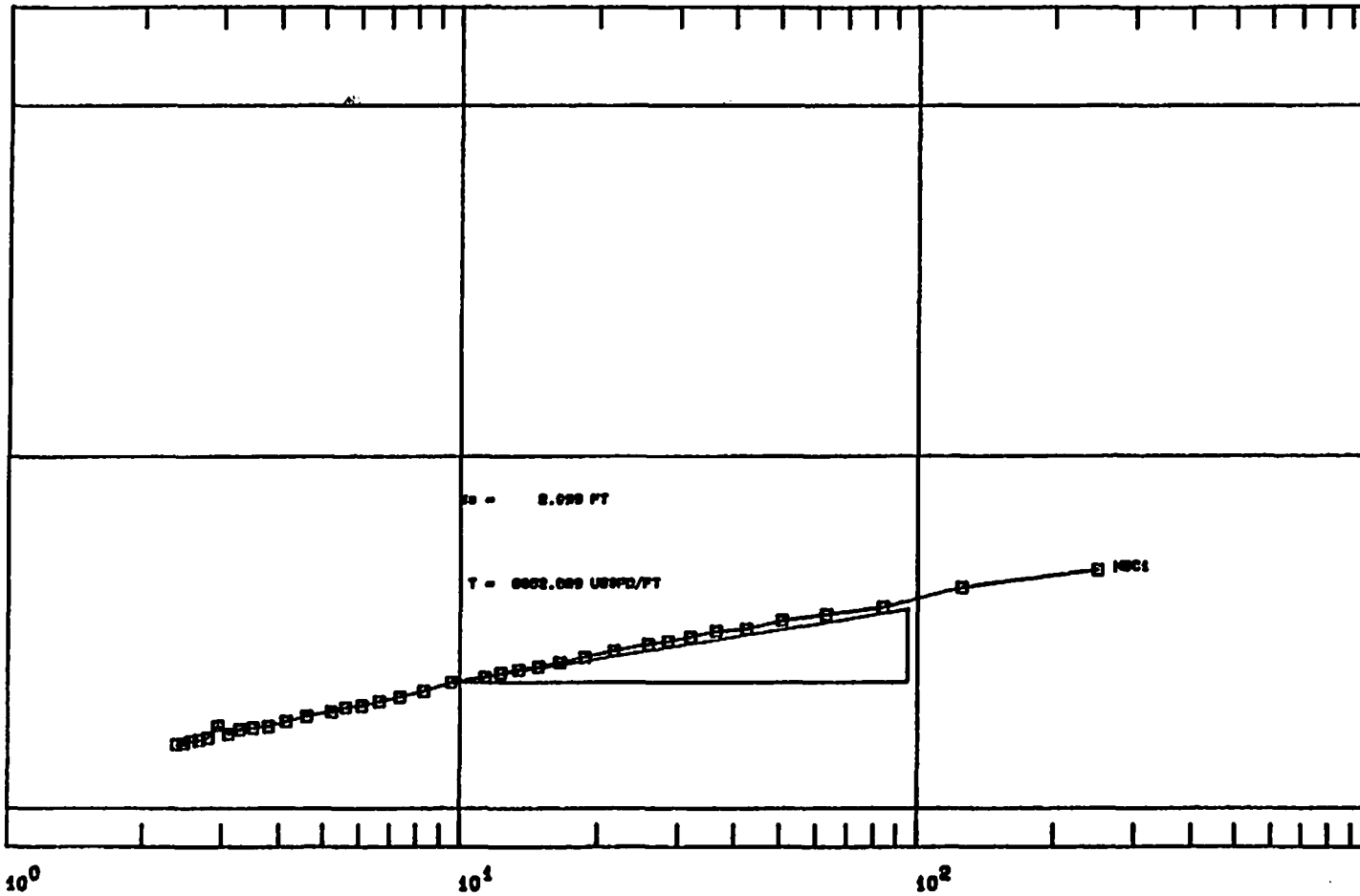
PUMPING TEST ANALYSIS Recovery

Ratio t/t'

20

10

0



(ft) Residual Drawdown (FT)

New Braunfels Well No. C-1
TD = 938.35 feet

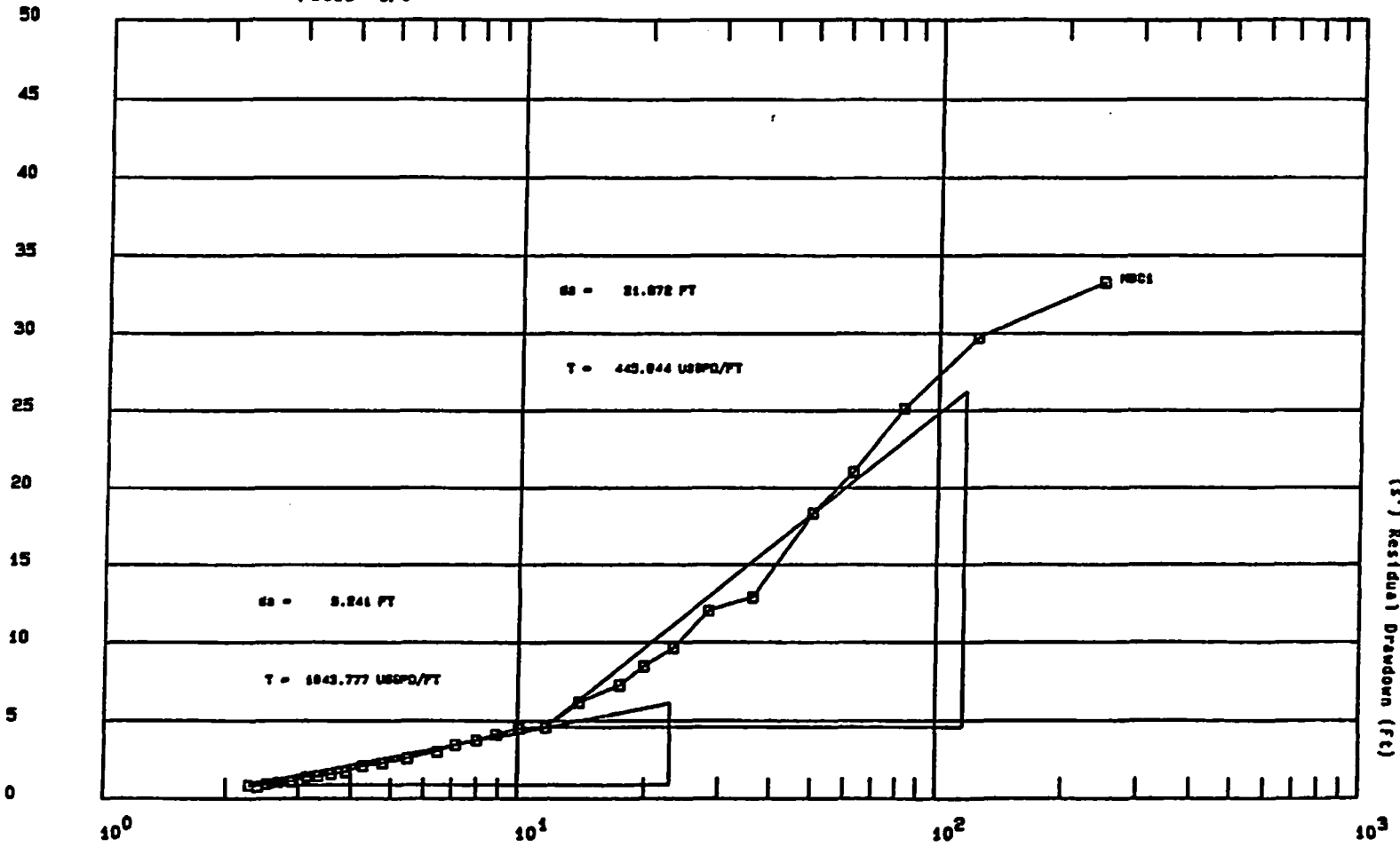
Pecker Test/Interval = 821-889.35 feet

EDWARDS UNDERGROUND WATER DISTRICT

Figure : 5-1

PUMPING TEST ANALYSIS Recovery

Ratio t/t'



New Braunfels Well No. C
TD = 708.33 feet

Packer Test/Interval = 818-708.33 feet

On Figure Nos. 5-3 and 5-4, a straight vertical line indicates the test interval within the Edwards Aquifer where a recovery test was performed. Each line is placed on the graph so as to correspond to the most "representative" transmissivity value for that recovery test. The most representative transmissivity value for each test interval was determined by: 1) the analyzed segment of the residual drawdown curve which was longest or contained the most data points; and 2) the resultant values which were most reasonable (ie. a test interval transmissivity value which was less than transmissivity value of the whole aquifer thickness would be used rather than one which was greater).

In New Braunfels, the transmissivity values varied between 35 and 10,969 gallons per day/foot, with A-1 and B-1 wells having the lower values, and C-1 well having the higher values (see Table No. 5-1). In all cases, the transmissivities increased below the Regional Dense Member.

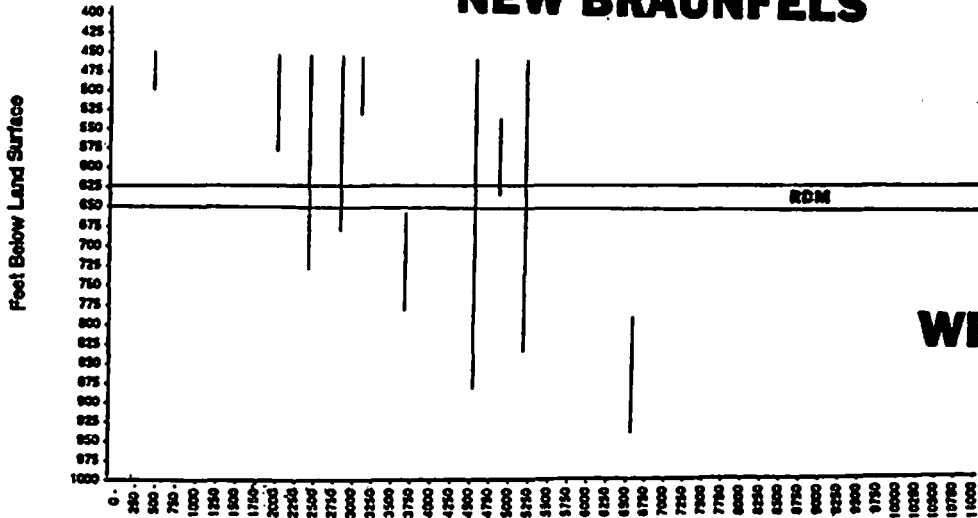
In San Marcos, the transmissivity values varied between 21 and 8298 gallons per day/foot (see Table No. 5-2). The wells were very similar in their transmissivity values and both had increasing transmissivity values below the Regional Dense Member, and as the distance between the well and the San Marcos Springs Fault decreased.

A comparison between the two sites indicates that the New Braunfels wells had higher ranges in transmissivity values than the San Marcos site. All wells appeared to have an increase in transmissivity below the Regional Dense Member, and as the distance decreased between the well and the major fault for that site.

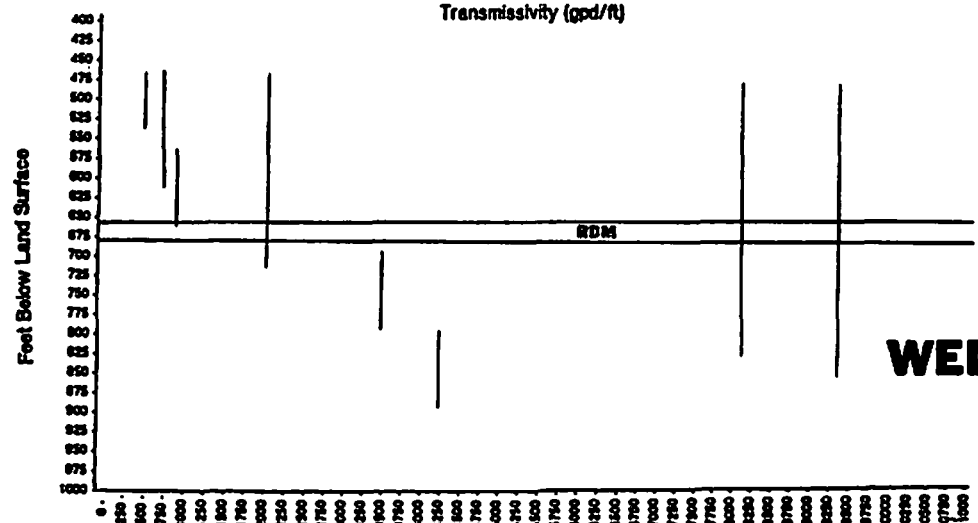
5.1-2 PUMP TESTS PERFORMED WITH OBSERVATION WELLS AT TOTAL DEPTH

In New Braunfels, a 9-hour pumping and a 9-hour recovery test was performed with well B-1 as the production well, and with wells A-1, B-2, and C-1 as the observation wells. In San Marcos, a 7-hour pumping and a 7-hour recovery test was performed with well C as the production well and with well B as the observation well. The resultant transmissivity and storage coefficient values are in Table 5-3. A 9-hour pump test and a 9-recovery test were also performed at the San Marcos D well after the total depth of 744 feet was reached. Appendix No. II has the results to this test. The observation wells, SMB, SMC/upper zone, and SMC/lower zone, were not affected by the pumping occurring in the D well for this test. Thus, no storage or hydraulic conductivity values could be ascertained.

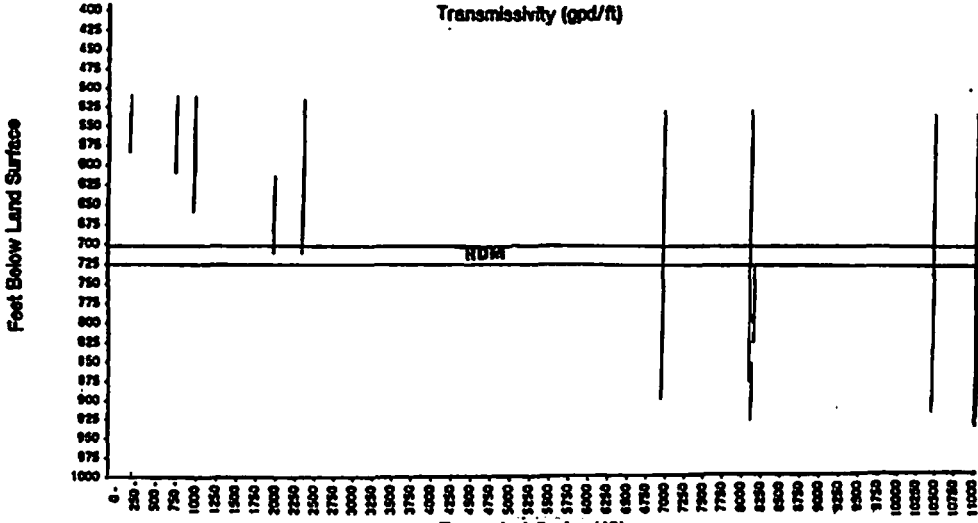
NEW BRAUNFELS



WELL "A"



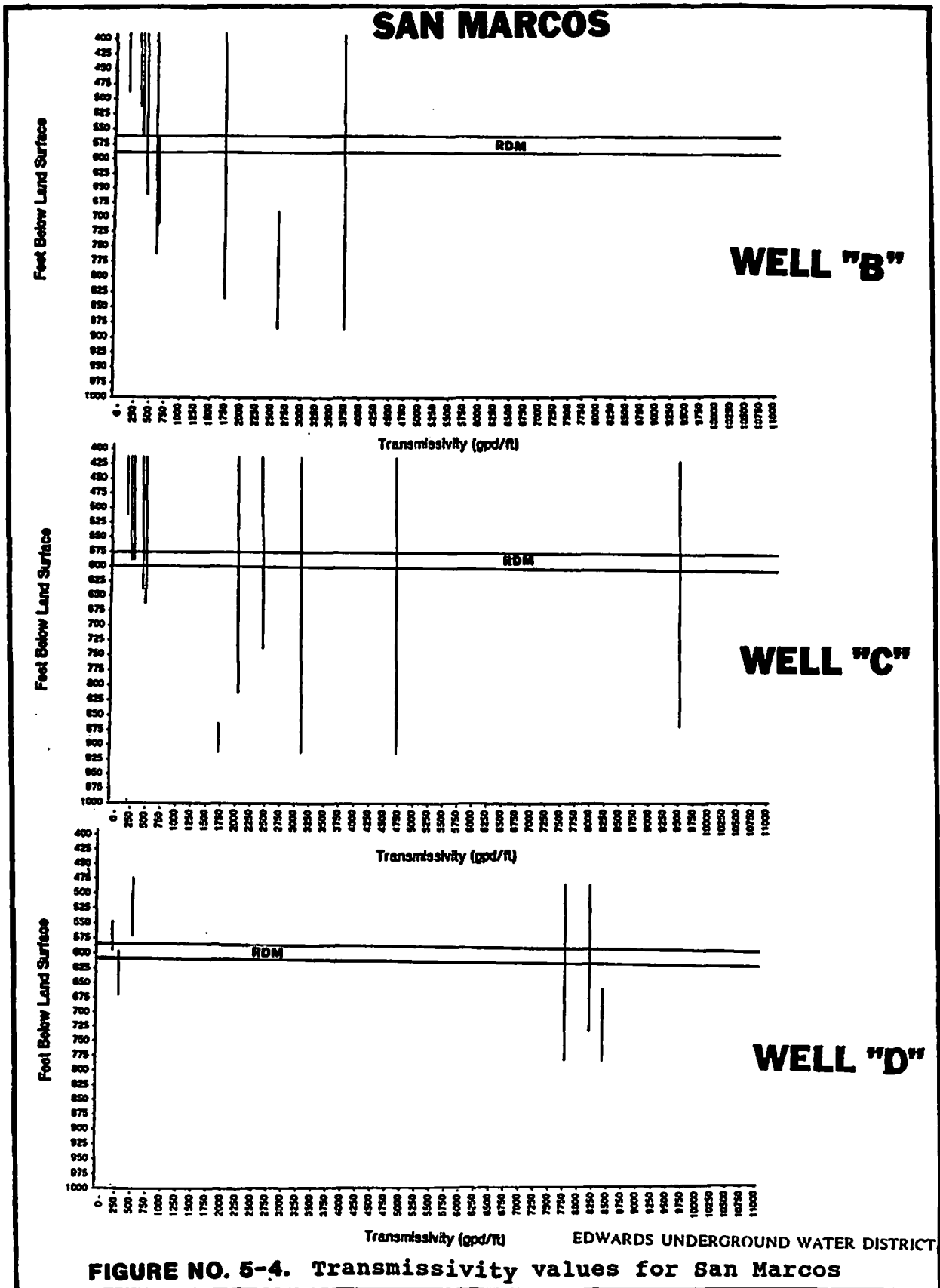
WELL "B"



WELL "C"

EDWARDS UNDERGROUND WATER DISTRICT

FIGURE NO. 5-3 Transmissivity values for New Braunfels



In New Braunfels, the highest transmissivity value was in well C-1. A-1 had a lower transmissivity, and B-2 was a slightly lower value. The lower value in B-2 was probably due to fact that the well did not fully penetrate the aquifer. The C-1 well has mostly fresh water while the others have more mineralized water. The San Marcos well B, which contains highly mineralized water, had a transmissivity value between that of the New Braunfels A-1 and B-2 wells.

In New Braunfels, the storage coefficient values were highest in the B-2 well, with A-1 next, and C-1 lowest. The C-1 well was in the fresh-water zone, which tends to have more zones of porosity lost to cementation due to diagenetic processes. In the San Marcos wells, the storage coefficient was much lower than any of the New Braunfels wells which is indicative of porosity either having been reduced by diagenesis or having never been present.

In New Braunfels, the hydraulic conductivity was highest in the C-1 well, with A-1 next, and B-2 last. In San Marcos, the hydraulic conductivity was slightly lower than the B-2 well in New Braunfels. These values are reflective of the higher permeability in fresh water zones compared to the saline zone.

The values in Table No. 5-3 were determined through the "Theis Method." The drawdown values are plotted against time on logarithmic scaled paper (Figure No.5-5). The resultant curve is then matched with the "Theis Curve" for a confined aquifer (Figure No. 5-6), also graphed on logarithmic scaled paper (from GEOBASE). Appendix II contains the water level measurements and resultant graphs plotted for using this method for the respective pump tests performed at each site.

The "Theis Curve" is graphically formed by plotting "W(u)" (the well function or conventional symbol form for the exponential integral from the "Theis or Nonequilibrium Equation") values against "u" (the lower limit of this integral). The Theis Equation was first derived from the differential equation for unsteady radial flow in a confined aquifer. A simplified version of the "Theis Equation" is:

$$s = (Q/4\pi T) W(u) \quad (\text{Eq. 5-2})$$

where: s = drawdown
 Q = constant well discharge rate
 T = Transmissivity

TABLE NO. 5-3 THEIS CURVE MATCHING DATA

PARAMETER	OBSERVATION WELLS				PUMPED WELLS	
	NB A-1	NB B2	NB C-1	SM B	NB C-1	SM C
(T) Transmissivity (Ft ² /DAY)	793.3	617.1	1207.3	772.0	1278.8	429.0
(GPD/Ft)	5935.0	4616.1	9031.5	5775.8	9566.2	3209.0
(S) Storage Coefficient	0.000092	0.001598	0.000064	0.000198	*	*
(K) Hydraulic Conductivity (GPD/Ft ²)	16.11	12.9	25.3	11.5	6.4	27.0
(Q) Discharge Rate (GPM)	95.4	95.4	95.4	70.0	95.4	70.0
(r) Distance from pumped well (Ft)	711.0	65.5	757.0	403.0	0	0
(b) Aquifer thickness (Ft)	357.3	357.3	357.3	503.6	357.3	503.6
<u>MATCH POINT:</u>						
w(u)	1.9	1.9	1.9	1.8	3.5	6
1/u	10.0	10.0	10.0	10.0	50	1000.0
s (drawdown-ft)	3.5	4.5	2.3	2.5	4	15
t (time-minutes)	210.0	40.0	110.0	150.0	100	100

Note: * no "r," well contained pump
NB=New Braunfels and SM=San Marcos

SMD had no other aquifer parameter values determined, other than (T) Transmissivity, when pumped for 9 hours (see Table 5-2).

The observation wells, SMB, SMC/Upper Zone and SMC/Lower Zone, showed no effect during this 9 hour pump test (see Appendix No. 11 for pump test results).

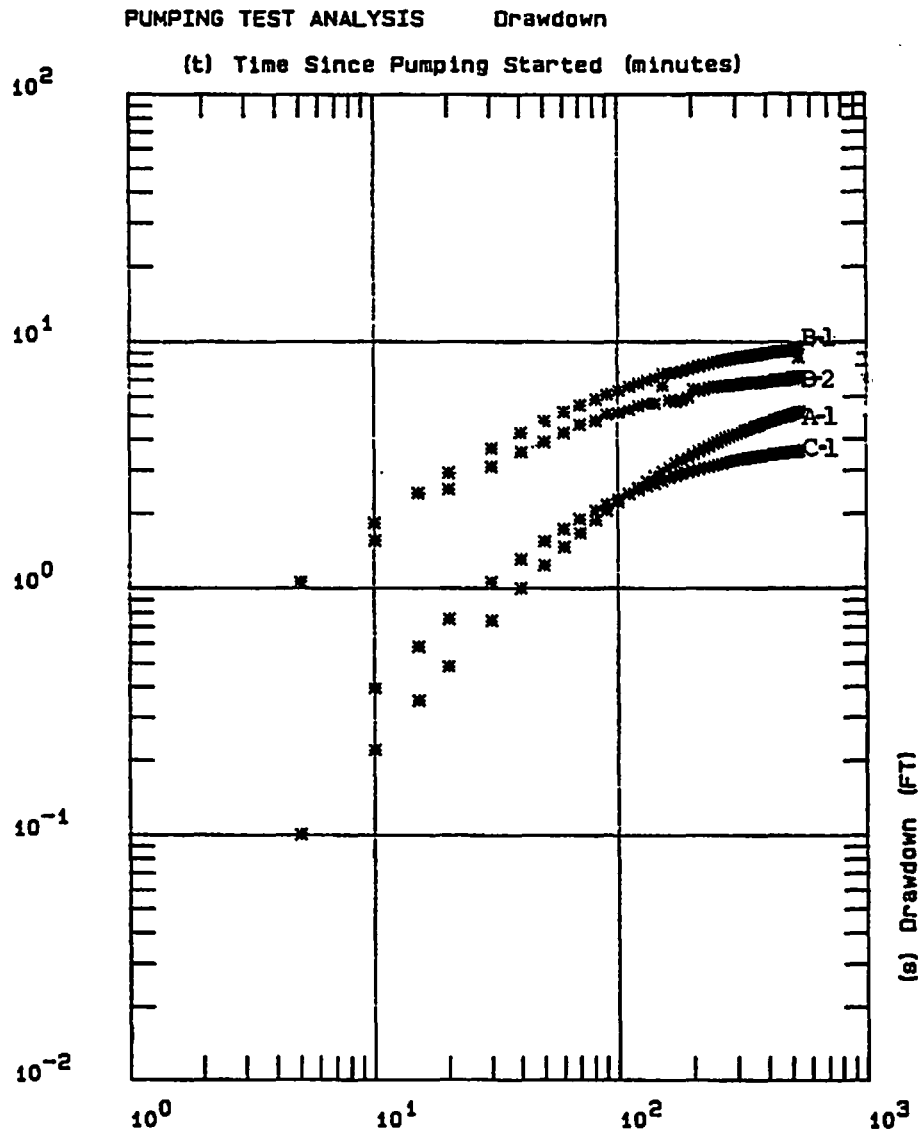
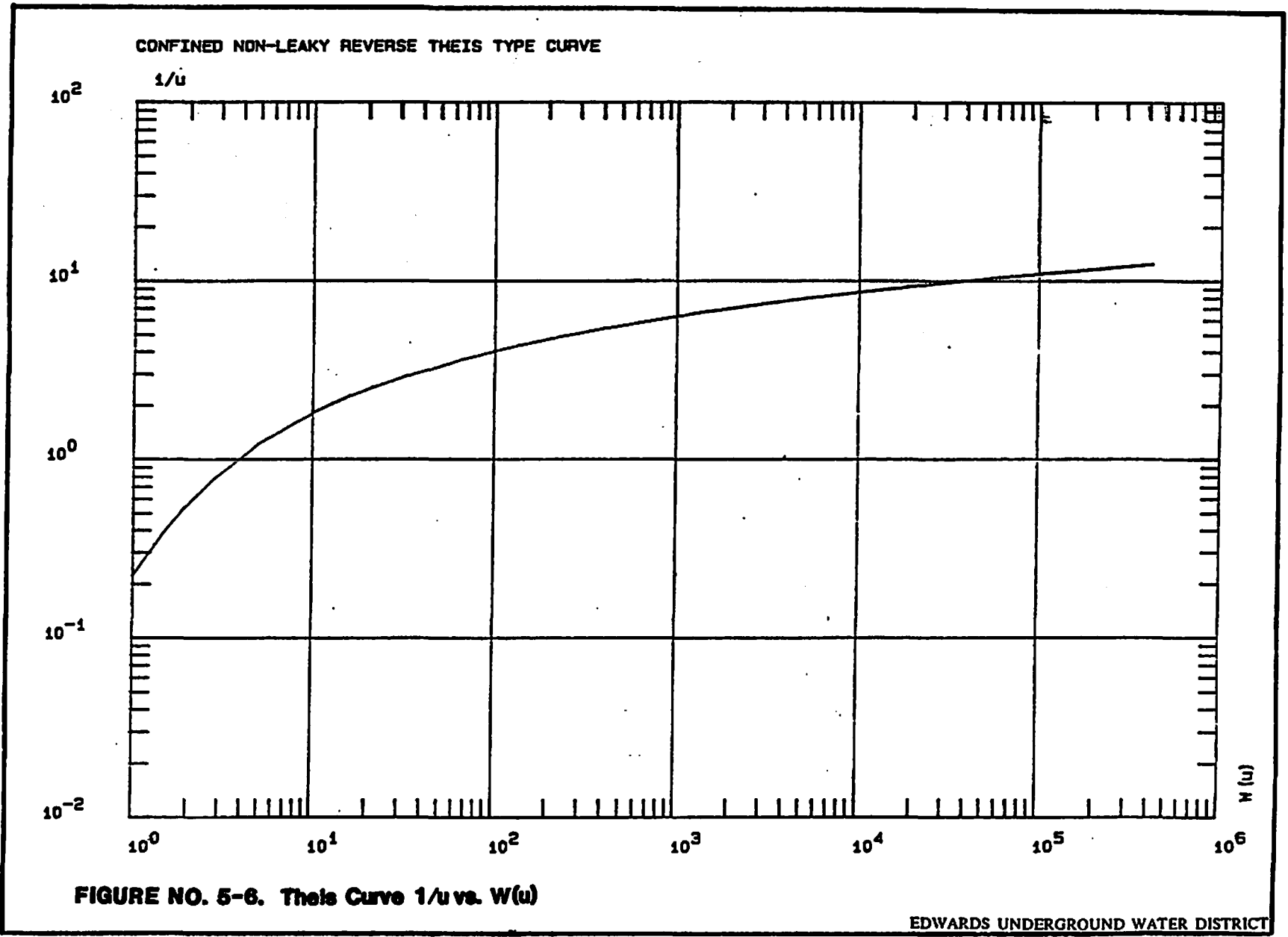


FIGURE NO. 5-5. Drawdown vs. Time for the New Braunfels seven hour pump test.

EDWARDS UNDERGROUND WATER DISTRICT



$$\text{and } u = r^2S/4Tt \quad (\text{Eq. 5-3})$$

$$\text{or } r^2/t = (4T/S)u \quad (\text{Eq. 5-4})$$

where: **S** = storage coefficient
 t = time since beginning of pumping
 r = radial distance from pumping well

This determined that the log s and log r^2/t were comparable with log $W(u)$ and log u because the terms in the parentheses in Equations 5-2 and 5-4 were constant. Due to these relationships, This developed the above method of graphically comparing the two lines and solving for T and S . Hydraulic conductivity can be obtained by using Equation 5-6, derived from the following relationship in Equation 5-5, once T is found:

$$T = Kb \quad (\text{Eq. 5-5})$$

$$\text{or: } K = T/b \quad (\text{Eq. 5-6})$$

where: **T** = transmissivity
 K = hydraulic conductivity
 b = aquifer thickness

5.2 INORGANIC WATER SAMPLE RESULTS

Table Nos. 5-4 and 5-5 show the water analysis results for the New Braunfels and San Marcos wells, respectively. The values for specific conductance, temperature, pH, alkalinity (as CaCO_3), 4 cations, 4 anions, and 6 saturation indices were compared from sample to sample, from well to well, and then from study site to study site. Various types of graphics and graphics software programs were used for these tasks.

5.2-1 SPECIFIC CONDUCTANCE

Specific conductance is the measured ability of water to conduct an electrical current. The units used to expressed specific conductance are microsiemens per centimeter or " $\mu\text{S}/\text{cm}$." Specific conductance can be related to the ion concentration in a solution and can be used for approximating dissolved-solids concentration in water. Water with a total dissolved solids concentration (TDS) of 1000 mg/l or less is considered fresh, while water containing TDS values over 1000 mg/l and up to 3000 mg/l are considered slightly saline. The approximate specific

TABLE NO. 5-4 WATER QUALITY DATA - NEW BRAUNFELS WELLS

Sample No.	Date	Depth of top of water-bearing zone (ft.)	Depth of bottom of water-bearing zone (ft.)	Temperature (°C)	Specific conductance (µS/cm)	pH (Standard units)	Alkalinity (as CaCO ₃) (mg/L as CaCO ₃)	Calcium dissolved (mg/L as Ca)	Magnesium dissolved (mg/L as Mg)	Sodium dissolved (mg/L as Na)	Potassium dissolved (mg/L as K)	Chloride dissolved (mg/L as Cl)	Sulfate dissolved (mg/L as SO ₄)	Fluoride dissolved (mg/L as F)	Silica dissolved (mg/L as SiO ₂)	Solids, sum of dissolved constituents (mg/L)	Calcite saturation	Dolomite saturation	Gypsum saturation	Anhydrite saturation	Celestite saturation	Halite saturation
A Well																						
1	09-06-89	444.0	506.0	25.8	2,460	7.9	255.9	140	84	250	17	370	440	0.1	10	1,460	+0.8	+1.7	-1.0	-1.2	-1.9	-5.7
2	09-12-89	534.5	634.0	25.5	3,170	8.0	283.7	180	110	320	23	350	600	2.9	13	1,970	+1.0	+2.2	-0.8	-1.0	-1.5	-5.4
3	09-16-89	638.0	781.5	26.0	2,440	7.8	248.0	150	88	250	16	400	460	3.4	13	1,330	+0.7	+1.6	-0.9	-1.1	-1.9	-5.6
4	09-15-89	444.0	836.5	26.1	3,370	7.7	269.0	210	120	380	23	370	690	3.3	13	2,170	+0.7	+1.5	-0.7	-0.9	-2.0	-5.3
5	09-18-89	444.0	836.5	26.3	4,070	7.5	277.2	250	140	430	26	750	830	3.0	13	2,610	+0.6	+1.3	-0.6	+0.8	-2.4	-5.2
6	09-19-89	799.0	936.5	27.9	5,540	8.0	298.6	340	180	590	35	1,000	1,100	3.4	13	3,640	+1.2	+2.4	-0.4	-0.6	-1.3	-4.9
B-1 Well																						
7	10-10-89	472.0	529.7	25.0	595	8.0	203.4	49	28	32	3.3	34	36	1.6	12	338	+0.5	+1.1	-2.0	-2.2	-1.9	-7.3
8	10-11-89	472.0	564.0	25.4	537	7.2	218.2	51	30	25	2.3	27	46	2.0	13	375	-0.2	-0.3	-2.1	-2.3	-3.5	-7.8
9	10-16-89	561.0	661.7	25.5	1,100	7.6	221.5	76	47	84	3.2	130	160	2.7	13	650	+0.3	+0.7	-1.5	-1.7	-2.5	-6.6
10	10-17-89	670.0	781.7	25.7	578	7.6	226.4	61	27	11	1.3	18	36	1.3	12	321	+0.3	+0.5	-1.9	-2.1	-2.7	-8.3
11	10-18-89	472.0	831.7	25.7	990	7.4	226.7	73	40	62	4.6	100	140	1.9	12	570	+0.1	+0.3	-1.5	-1.7	-3.0	-6.8
12	10-19-89	472.0	881.7	25.9	1,850	7.9	242.0	120	69	180	11.0	310	340	2.2	12	1,190	+0.7	+1.6	-1.1	-1.3	-1.8	-5.9
13	10-20-89	773.0	916.5	26.3	3,750	7.7	267.4	210	130	420	24.0	680	750	3.1	13	2,390	+0.7	+1.3	-0.7	-0.9	-2.0	-5.2
B-2 Well																						
14	01-11-90	472.0	560.2	24.6	556	7.3	209.2	50	29	21	2.2	30	47	2.0	13	320	-0.2	-0.2	-2.0	-2.3	-3.3	-7.8
15	01-12-90	472.0	660.0	24.9	732	7.3	212.6	59	35	41	3.3	67	85	2.3	13	433	+0.1	+0.3	-1.8	-2.0	-2.8	-7.7
C Well																						
17	01-23-90	518.0	612.6	25.0	498	6.9	213.3	52	28	13	1.5	17	36	1.3	13	290	+0.3	+1.0	-2.1	-2.4	-4.1	-8.2
18	01-25-90	618.0	706.33	26.0	578	7.1	210.0	53	32	19	1.8	28	37	2.6	13	319	-0.3	-0.3	-2.0	-2.2	-3.6	-7.9
19	01-30-90	715.0	826.94	26.5	565	6.4	216.5	60	27	12	1.3	18	36	1.8	13	380	-0.9	-1.9	-1.9	-2.1	-5.0	-8.2
20	01-31-90	518.0	876.65	26.0	1,050	6.5	228.8	79	42	70	4.6	120	130	1.8	13	618	-0.8	-1.3	-1.3	-1.7	-4.7	-8.7
21	02-01-90	518.0	939.35	26.0	2,180	6.8	242.0	140	78	210	19.0	390	400	2.2	13	1,390	-0.3	-0.3	-1.0	-1.2	-4.0	-9.7
22	02-02-90	821.5	939.35	27.0	4,190	6.7	288.7	240	150	470	5.1	820	870	3.1	14	2,750	-0.2	-0.3	-0.6	-0.8	-3.9	-9.1

(no #16)

DRP/mar

drp064

TABLE NO. 5-5 WATER QUALITY DATA - SAN MARCOS WELLS

Sample No.	Date	Depth of top of water-bearing zone (ft.)	Depth of bottom of water-bearing zone (ft.)	Temp-erature (°C)	Specific conduc-tance (µS/cm)	pH (Standard Units)	Alkalinity (M, Fe, P, mg/L as CaCO ₃)	Calcium dissolved (mg/L as Ca)	Magnesium dissolved (mg/L as Mg)	Sodium dissolved (mg/L as Na)	Potassium dissolved (mg/L as K)	Chloride dissolved (mg/L as Cl)	Sulfate dissolved (mg/L as SO ₄)	Fluoride dissolved (mg/L as F)	Silica dissolved (mg/L as SiO ₂)	Solids, sum of dissolved constituents (mg/L)	Celestite saturation	Dolomite saturation	Gypsum saturation	Anhydrite saturation	Celestite saturation	Malite saturation
B Well																						
1	06-23-90	403	508.0	27.0	13,000	7.9	362.5	780	420	1,800	80	3,000	2,500	0.9	13	8,800	+1.3	+2.7	-0.0	-0.3	-1.3	-4.0
2	06-25-90	509	566.0	26.5	14,400	6.6	390.4	870	450	1,900	83	3,800	2,700	6.8	14	10,100	+0.1	+0.3	-0.0	-0.2	-3.8	-3.9
4	06-28-90	573	707.0	26.0	14,400	6.6	388.8	870	450	1,900	84	4,000	2,800	2.1	14	10,400	+0.1	+0.2	+0.0	-0.2	-3.9	-3.9
5	07-01-90	403	890.5	27.0	14,400	6.7	405.2	860	440	1,900	83	3,500	2,700	2.3	14	9,700	+0.2	+0.5	+0.0	-0.2	-3.6	-4.0
6	07-02-90	696	890.5	26.8	14,500	6.6	387.1	860	450	2,000	85	4,000	3,000	2.3	14	10,600	+0.1	+0.3	+0.0	-0.2	-3.8	-3.9
C Well																						
7	07-20-90	416	520.3	24.7	14,000	7.5	375.6	860	420	1,800	83	3,200	2,300	1.4	14	8,900	+1.0	+2.0	-0.0	-0.2	-2.1	-4.0
8	07-21-90	520	583.7	26.3	14,300	6.5	393.7	920	420	2,000	84	3,800	2,700	2.1	14	10,200	+0.1	+0.2	+0.0	-0.2	-4.0	-3.9
10	07-24-90	744	920.0	26.5	14,500	6.5	395.6	900	430	1,800	79	3,800	2,600	2.4	14	9,900	+0.1	+0.3	+0.0	-0.2	-3.9	-3.9
11	07-26-90	416	920.5	26.5	14,400	6.6	392.0	950	450	1,800	84	3,900	2,600	2.3	14	10,000	+0.1	+0.4	+0.0	-0.2	-3.8	-3.9
12	08-10-90	490	564.0	25.0	13,900	6.9	386.3	790	390	1,800	85	3,700	2,500	0.8	14	..	+0.4	+0.8	-0.1	-0.3	-3.3	-3.9
13	08-10-90	630	699.0	25.7	13,900	6.6	395.3	850	440	1,900	88	3,800	2,400	2.7	18	..	+0.1	+0.3	+0.0	-0.2	-3.7	-3.9
D Well																						
14	02-20-92	465	556	26.0	16,000	6.6	400.0	870	450	1,800	8.8	3,700	2,600	2.8	14	9,900	+0.1	+0.3	+0.0	-0.2	-3.8	-3.9
15	02-25-92	548	602	25.5	16,000	6.7	420.0	900	450	1,800	9.1	4,500	2,600	2.9	14	10,500	+0.2	+0.6	+0.0	-0.2	-3.6	-3.9
16	02-27-92	600	650	26.0	12,600	7.1	370.0	880	430	1,900	9.1	3,500	2,200	2.3	13	9,160	+0.6	+1.3	+0.0	-0.2	-2.8	-3.9
17	02-29-92	656	774	26.0	13,400	6.6	390.0	870	430	1,900	9.1	3,700	2,600	3.1	14	9,760	+0.1	+0.3	+0.0	-0.2	-3.8	-3.9
18	03-02-92	465	774	25.0	12,700	6.7	400.0	840	400	1,900	8.7	3,800	2,400	2.8	13	9,600	+0.2	+0.5	-0.0	-0.2	-3.7	-3.9

(see #s 3 & 9)

CRP/mar

dry065

conductance value corresponding to 1000 mg/l would be 650 $\mu\text{S}/\text{cm}$. Other varying degrees of salinity have also been established: over 3000 mg/l would be moderately saline while over 10,000 mg/l would be very saline. For these TDS values, the approximate corresponding values in specific conductance based on the sample analysis from the New Braunfels and San Marcos transect wells would be approximately 5000 $\mu\text{S}/\text{cm}$ for 3000 mg/l and 14,400 $\mu\text{S}/\text{cm}$ for 10,000 mg/l.

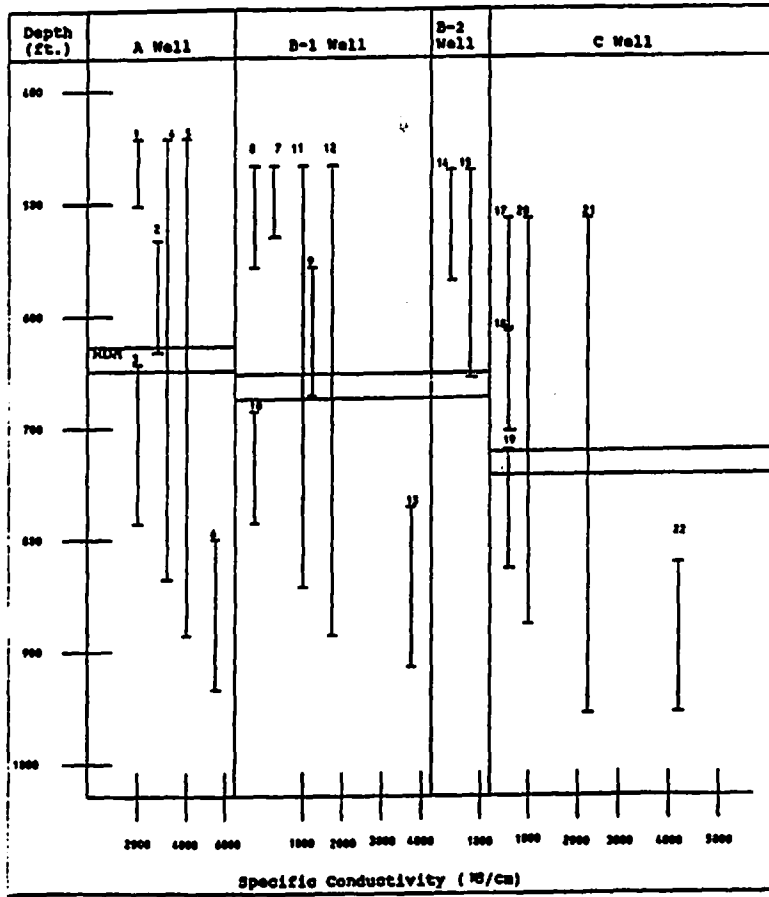
5.2-1.1 VALUES RECORDED AT THE END OF EACH PUMP OR AIR-LIFT TEST

Figure No. 5-7 shows how the specific conductivity values varied. For New Braunfels, specific conductance values collected after each pump or air-lift test ranged from values found in fresh to moderately saline waters (498 to 4,190 $\mu\text{S}/\text{cm}$ or a total dissolved solids range of 290 to 3640 mg/l). For well A-1, all samples were between 2,440 and 4,000 $\mu\text{S}/\text{cm}$, except for the bottom sample, with a sample interval of 800 to 920 feet, which was nearer to the 5,000 to 6,000 $\mu\text{S}/\text{cm}$ range. Wells B-1 and C-1 had specific conductance values ranging from 578 to 1,850 $\mu\text{S}/\text{cm}$, with the bottom zones being approximately 3,750 $\mu\text{S}/\text{cm}$, which is approximately 2000 $\mu\text{S}/\text{cm}$ higher than the rest of the well. Therefore, vertically, the specific conductance varied from high values at the bottom of the well to low at the top. A slight decrease in conductance was noted in the zone just below the Regional Dense Member in all the wells. Horizontally, the highest values were in the A-1 well and the lowest in the C-1, the latter being nearest the fresh-water zone.

In San Marcos, most all the specific conductivity values were between 14,000 and 16,405 $\mu\text{S}/\text{cm}$, except for one sample above the Regional Dense Member, SMB-1, which was 13,000 $\mu\text{S}/\text{cm}$. The corresponding ranges in total dissolved solids was 8,800 to 10,500 mg/l. Thus, the conductivity values did not vary significantly from well to well nor vertically within a well.

In comparing the specific conductance values between the two sites, the San Marcos site appears to have a much greater specific conductance values than New Braunfels. Both wells at the San Marcos site had very high and similar conductance values of 13,000 to 16,405 $\mu\text{S}/\text{cm}$ or a total dissolved solids range of 8,800 to 10,500 mg/l, while the values from the New Braunfels wells varied and ranged from 498 to 5,540 $\mu\text{S}/\text{cm}$ or a total dissolved solids range of 290 to 3,640 mg/l.

NEW BRAUNFELS WELLS



SAN MARCOS WELLS

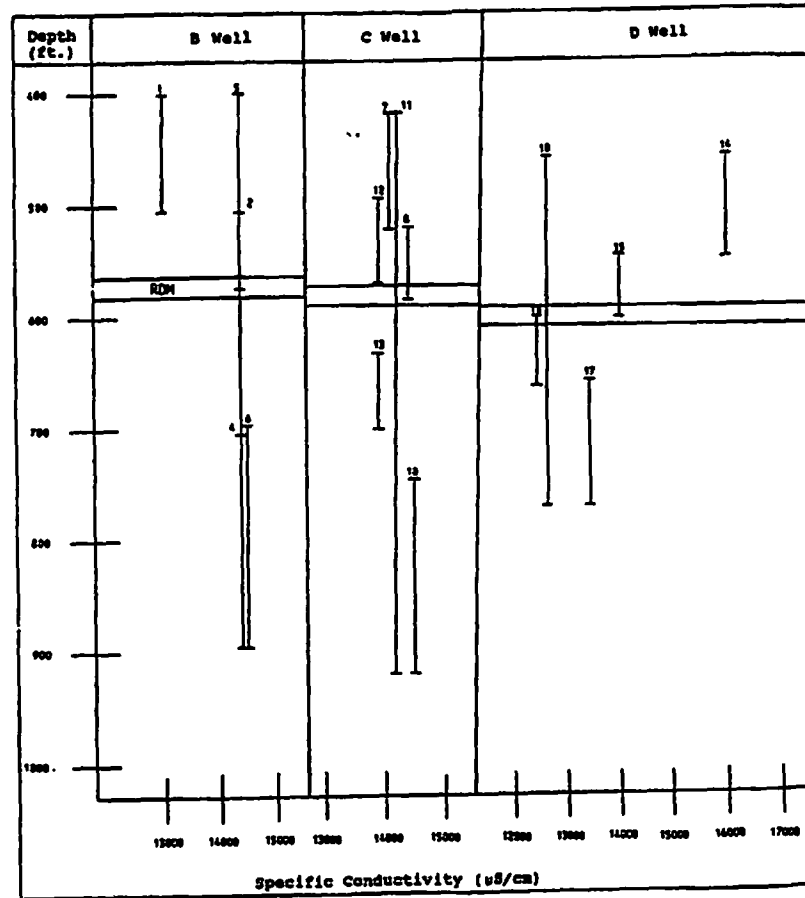


FIGURE NO. 5-7. Conductance vs. Depth

EDWARDS UNDERGROUND WATER DISTRICT

5.2-1.2 VALUES RECORDED DURING PUMP OR AIR-LIFT TESTING

The changes in specific conductivity values collected during pump/air-lift tests were plotted against time and can be examined in Appendix I and II, with the other pump and recovery test information. At both sites, the values either remained constant, increased over time and then leveled off, or continued to increase over time. Out of a total of approximately 59 tests for both sites, 36 showed no change in conductivity over time, regardless of the depth interval.

In New Braunfels, a total of 12 tests increased in conductivity and then leveled off: the A-1 well had 4 tests in the middle to upper zone; the B-1 well had 6 tests spanning all intervals; and the C-1 well had 2 tests, 1 in the lower zone and 1 in the middle zone of the well. These initial increases can be partly explained by the introduction of fresh water from the surface during the first 100 feet of drilling into the Edwards because of a lack of formation water to circulate the cuttings properly, and partly due to fresher formation water present near the well bore in the middle to upper zones of wells B-1 and C-1.

The 9-hour pump test performed in the New Braunfels wells showed a continued increase in specific conductance from 1000 to 2000 $\mu\text{S}/\text{cm}$ in the B-1 well. Due to a flat potentiometric surface, the flow lines to the pumping well would be nearly flat lying, and thus, could be drawing both saline water from the A-1 well and fresh water from the C-1 well. The rationale for this conclusion is that after 9 hours of pumping, the specific conductance should have reached the high values in the A-1 well at 3000 $\mu\text{S}/\text{cm}$ and greater, if it were only receiving saline water found in the A-1 well direction. However, since the last readings recorded were approximately 2000 $\mu\text{S}/\text{cm}$, the conclusions which may be reached are: 1) formation water that had a specific conduction of 2000 $\mu\text{S}/\text{cm}$ was being drawn to the pumping well at the end of the test; 2) that mixing of fresh water found in the C-1 well and saline water found in the A-1 well was occurring; or 3) only saline water was being drawn to the pumping well. Monitoring of the specific conductance in the observations wells during a similar pump test may aid in reaching further supporting conclusions.

In San Marcos, the measurements of specific conductance collected over time from 6 tests in the upper to middle zones of the Edwards in both the B and C wells increased and then leveled off. During 4 tests in the upper portion of the Edwards in the B well, the specific conductance continued to increase over time. In the D well, conductivity decreased over time in 4 tests in the middle to lower zone. During the 9-hour pump test at the B well site, the specific

conductance first increased and then leveled off by the end of the test. However, during the 9-hour pump test at D well site, the conductivity improved over time.

5.2-2 TEMPERATURE

The temperature values varied slightly from 25.0 °C to 27.5 °C at both sites. The New Braunfels wells showed a pattern of increasing temperature from top to bottom and decreasing from well C-1 to A-1, which may be related to the changes in water salinity as measured by water specific conductance. The temperature values for San Marcos did not vary significantly which may also reflect the lack of variation in water salinity as measured by specific conductance in the transect wells.

5.2-3 IONIC CONCENTRATIONS

Stiff, Scheoller, and Piper diagrams were used for the cation and anion graphical presentations and GEOBASE software was used to calculate the milliequivalents per liter (meq/l) for each ion and for actual drafting of the charts.

The purpose of using meq/l is that cations and anions combine and disassociate in definite weight ratios (Todd, 1959). Thus, in order to change from milligrams per liter (mg/l) to meq/l, the formula weight of an ion is divided by its charge and then multiplied by the concentration in mg/l. The formula weight divided by the charge of the ion is known as the conversion factor, and can be found in published lists or calculated as mentioned above.

In application, therefore, the sum of the meq/l of the cations should be equal to the sum of the meq/l of the anions, and the total dissolved solids in the ground-water sample is balanced. If a difference arises from this balance there is either some other undetermined constituent(s) present or an error has been made in the analysis.

In Table No. 5-6, the balance error for all the samples are listed in ascending order. The standard deviation was 2.98 and the mean was 1.82. Those above 2.0 may be considered questionable and not valid. However, only those that were in the higher concentrations of total dissolved solids were affected, and thus, some consistency exists. At any rate, these sample results have been included in the graphic presentations which follow.

TABLE NO. 5-6 BALANCE ERROR

Mean = 1.815

Standard Deviation = 2.983

<u>Well/Sample I.D.</u>	<u>Value</u>
SMD/15	-7.88
SMB/4	-3.574
SMB/6	-3.567
SMD/14	-2.400
SMC/10	-2.187
SMC/12	-2.122
SMD/18	-1.870
SMC/11	-1.692
SMB/2	-1.367
NBC1/22	-1.191
NBC1/21	-0.807
SMD/17	-0.980
NBA1/2	-0.177
SMC/8	-0.052
NBB1/12	-0.033
SMC/13	-0.032
NBA1/5	+0.446
SMB/5	+0.712
NBB1/13	+1.111
NBC1/20	+1.450
NBA1/6	+2.042
NBA1/3	+2.129
NBB1/11	+2.225
NBA1/1	+2.888
NBA1/4	+3.619
NBB1/9	+3.702
SMD/16	+3.71
NBB2/15	+3.742
SMB/1	+3.785
NBB1/10	+4.082
SMC/7	+4.500
NBC1/19	+4.984
NBB2/14	+5.372
NBC1/18	+6.317
NBB1/7	+6.596
NBB1/8	+6.827
NBC1/17	+7.593

EDWARDS UNDERGROUND WATER DISTRICT

5.2-3.1 STIFF DIAGRAMS

Stiff diagrams were made because they can graphically show the vertical changes in the concentrations of ions from one sample to another. Stiff diagrams use four horizontal parallel axes, with the cations plotted on the left and anions on the right from an axis extended vertically from the horizontal axis zero point. The points are then connected to form an irregular polygonal pattern. Each pattern represents one sample and each chart represents one well. It is to be noted that waters of a similar quality define a distinctive shape.

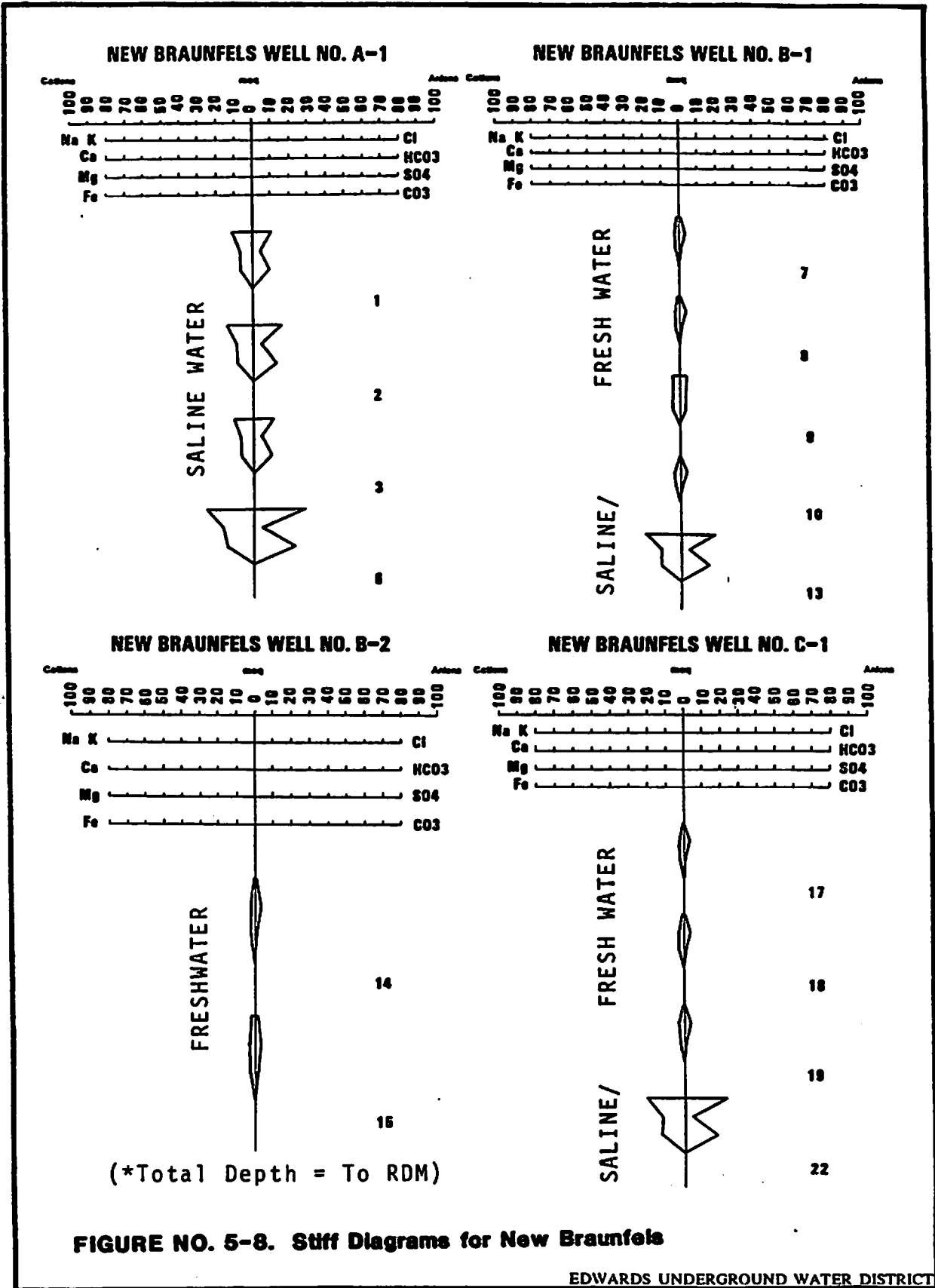
The Stiff diagrams varied in the New Braunfels wells both vertically within a well and horizontally between the wells. In Figure No. 5-8, the A-1 well samples are shown in the top diagram on the left. All the sample results have the same pattern: relatively high ionic concentrations. The next Stiff diagram in the same figure demonstrates that for the B-1 well samples, the first four, taken above the Regional Dense Member, have a different pattern (less ionic concentrations) than A-1, while the sample taken below the Regional Dense Member was similar to the patterns in A-1. The next diagram in Figure No. 5-8 shows that B-2 (all samples taken above the Regional Dense Member) has patterns similar to the first four in B-1. The diagram on the far right shows that the C-1 samples all resemble the B-1 samples.

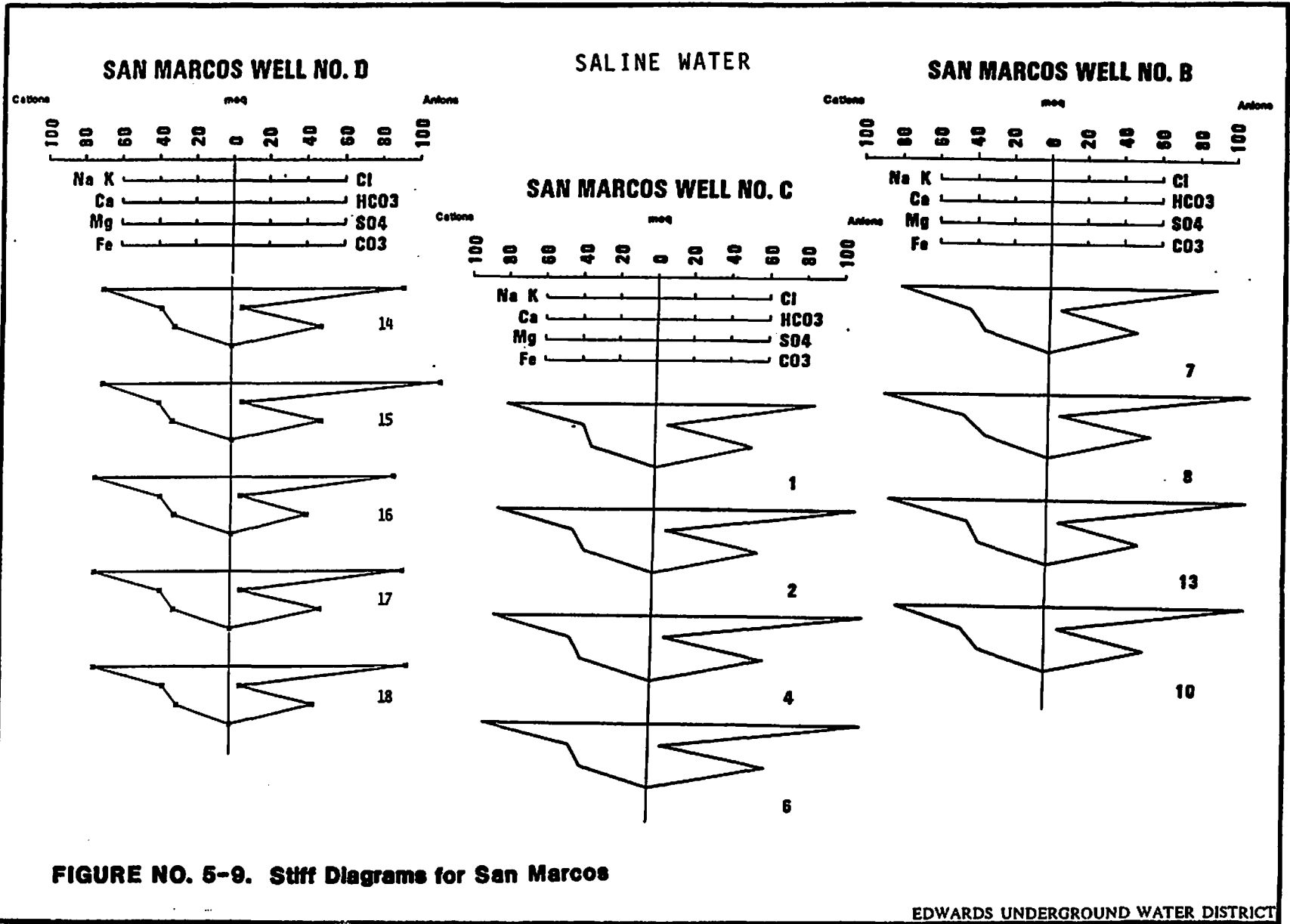
The San Marcos Stiff diagrams on Figure No. 5-9 are all very similar and show a pattern of relatively high ionic concentrations, similar to the New Braunfels A-1.

5.2-3.2 SCHOELLER DIAGRAMS

The diagrams developed by Schoeller are another widely employed method of comparing ground-water analyses. The ionic concentrations are plotted on six equally spaced logarithmic scales. Once the points are plotted, they are connected by lines. This type of graph exhibits both the ion value and the concentration of each analysis. One line on a chart represents one sample analysis while one diagram represents one well. These diagrams were made so that the analyses for these wells could be compared to the work done by Clement (1989).

Clement (1989) described several hydrochemical facies of the saline zone in the Edwards Aquifer. Comal and Hays Counties are within what she described as the Na-Cl facies mixed with Na-SO₄-Cl which have Schoeller diagrams with the pattern that "arcs up" as shown in Figure No. 5-10. Also in this figure, a pattern of "arcing down" is representative of a the fresh-water





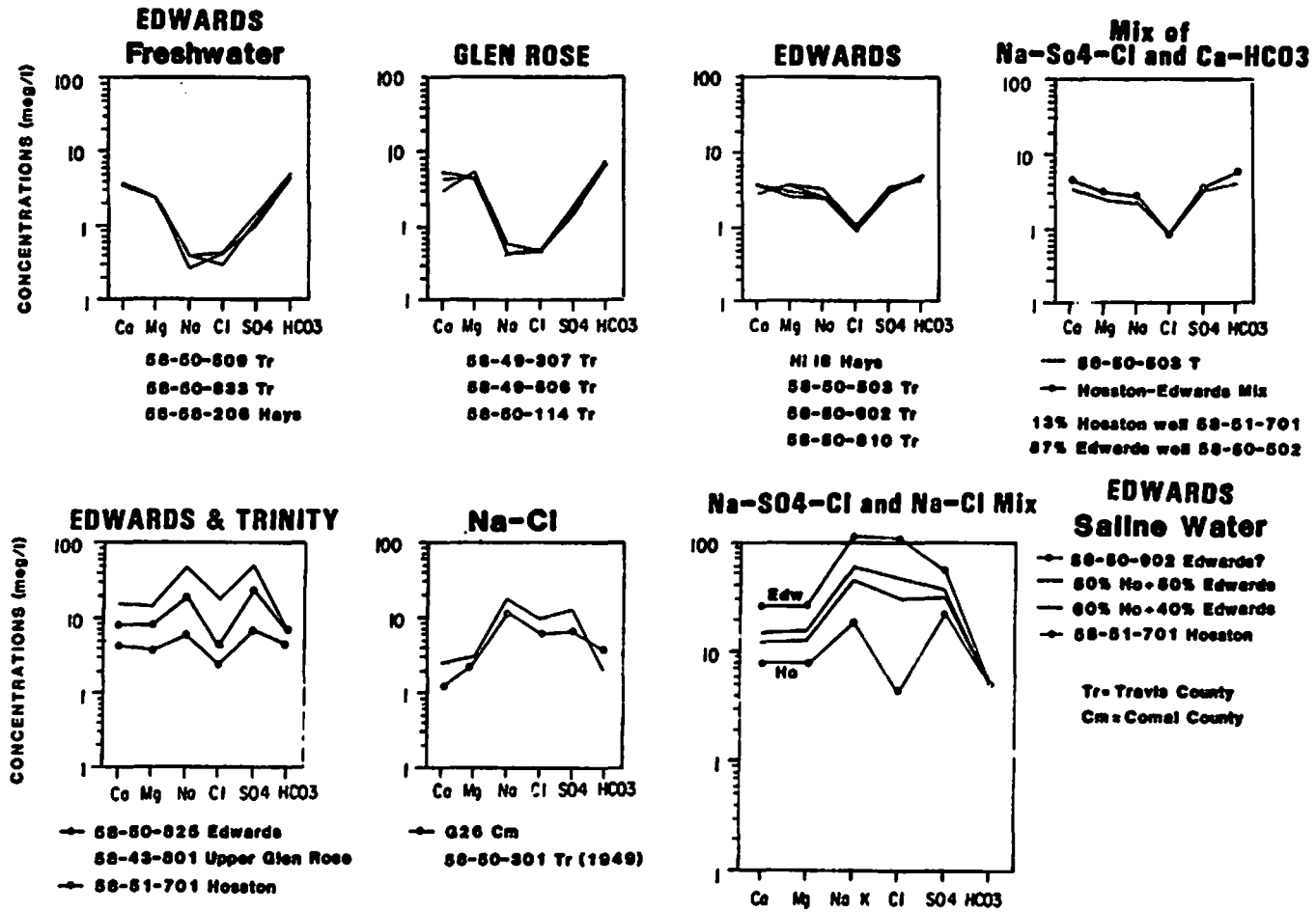


FIGURE NO. 5-10. Comparison of "Edwards" fresh and saline water with analyses from the Trinity Group with Edwards-Trinity mixtures. (Clements, 1989)

zone in the same counties. Any pattern in between these two is considered a mixture of the two water types.

The New Braunfels Schoeller diagram for the A-1 well is in Figure No. 5-11 on the top left. It demonstrates an arcing upward pattern for all the samples. The next Schoeller diagram in this figure is for the B-1 well and it shows more variability: the sample for the bottom interval has an arc-up, while the others arc down or lie almost flat. The next diagram represents the results of the B-2 samples which are all arcing downward (all samples are above the Regional Dense Member). The Schoeller diagram for the C-1 well on the bottom right exhibits a downward arc for all samples above the Regional Dense Member or combined intervals. The bottom sample interval is the only exception, for it arcs up.

Thus, for all the New Braunfels Schoeller diagrams, as with the Stiff diagrams, three zones of chemical similarity exist: a bottom saline zone persists throughout all the wells, and in the B-1, B-2, and C-1 wells, a fresh-water zone above the Regional Dense Member, and a third, a mixed zone, just below the Regional Dense Member.

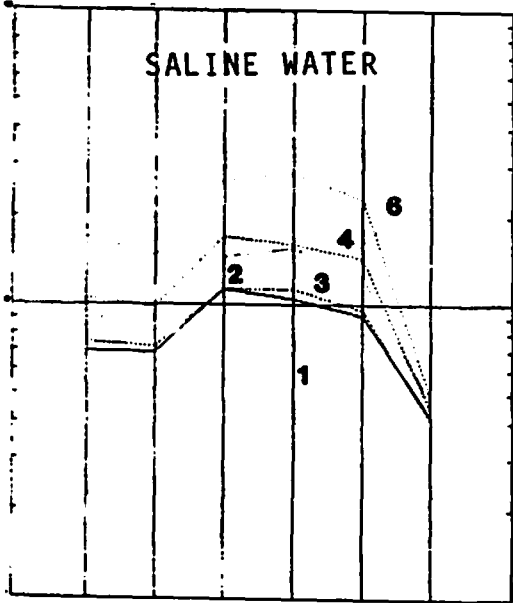
The Schoeller diagrams in Figure No. 5-12 exhibit the arcing upward pattern, indicative of the saline zone, for all the San Marcos samples, which is similar to the New Braunfels A-1 well and the bottom zone in the A-1, B-1, and C-1 wells.

5.2-3.3 PIPER DIAGRAMS

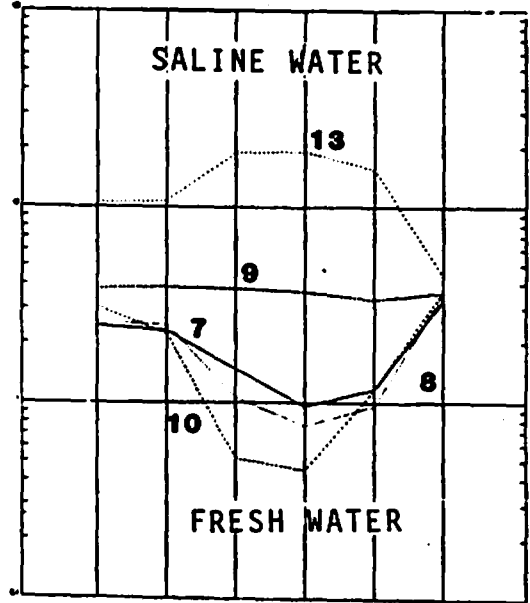
The trilinear diagram by Piper is considered one of the most useful for graphic representation of chemical analyses. The USGS has used these diagrams to show the differences in ionic concentrations between the saline and the fresh zones (Figure No. 5-13). Thus, trilinear diagrams were made so that comparisons could be made with the USGS data.

Expressed in percentages of total cations or anions in meq/l, the cations are plotted as a single point on the bottom left triangle while the anions are plotted on the bottom right triangle. These two points are then projected into one point in the central diamond-shaped area. The total ionic concentration can be represented by a circle around this point. The radius of this circle is then proportional to the total dissolved solids of that sample. Similar samples plot together while different ones plot separately. A mixture of two waters will plot on a line between the two end members.

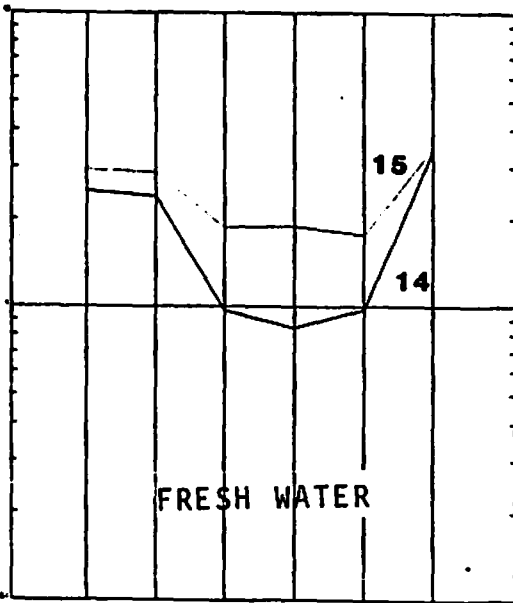
NEW BRAUNFELS WELL NO. A-1



NEW BRAUNFELS WELL NO. B-1



NEW BRAUNFELS WELL NO. B-2



NEW BRAUNFELS WELL NO. C-1

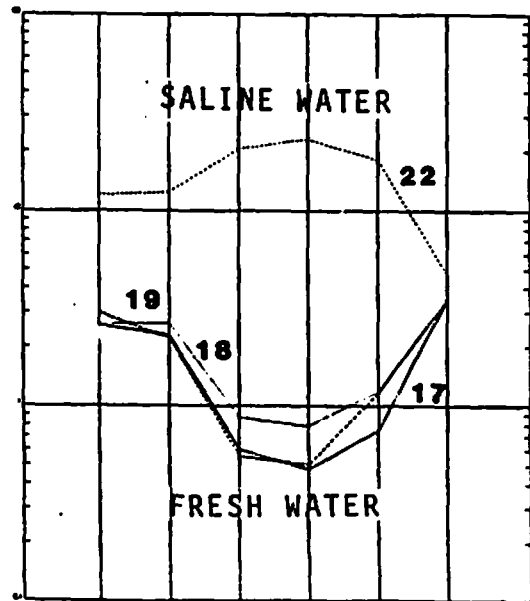
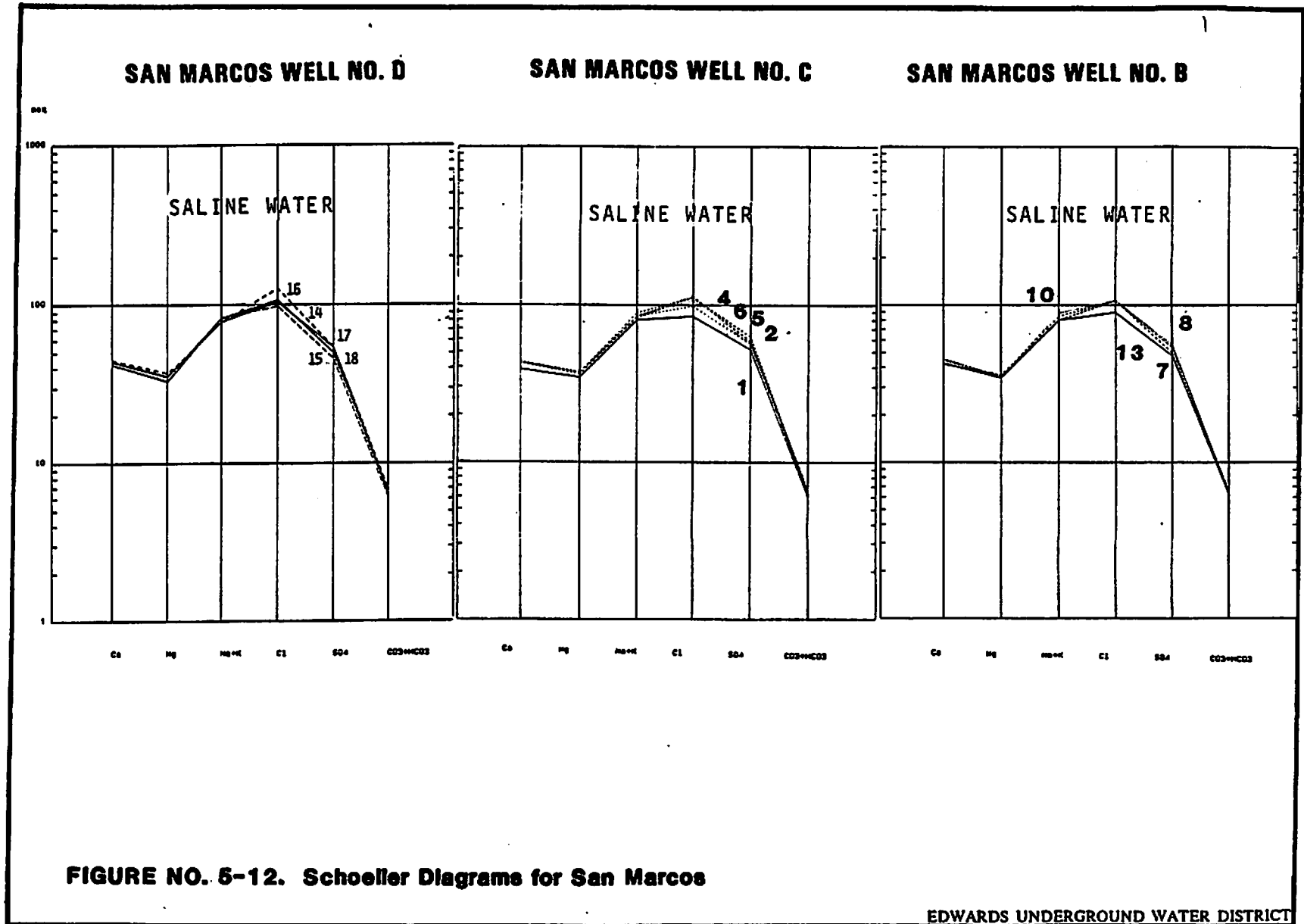
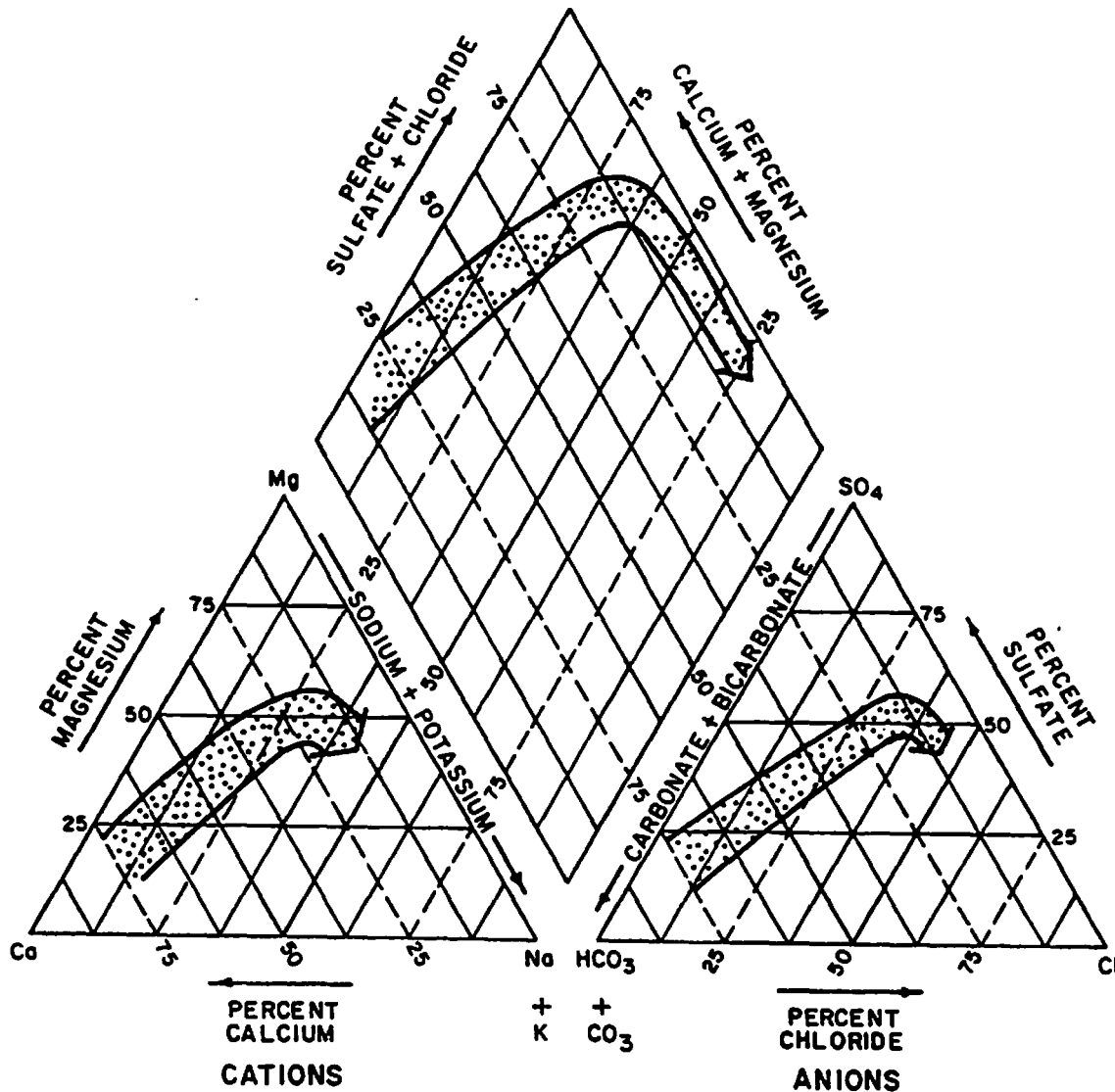


FIGURE NO. 5-11. Schoeller Diagrams for New Braunfels

EDWARDS UNDERGROUND WATER DISTRICT





**FIGURE NO. 5-13. USGS Piper Diagram
(Maclay, Small, and Retiman, 1980)**

EDWARDS UNDERGROUND WATER DISTRICT

Each diagram represents one well, while each point in a central diamond zone on a diagram is one sample result while one diagram represents one well. The diagrams in Figure No. 5-6, from Maclay, Small, and Rettman (1980) were made from samples collected from many wells across the Edwards Aquifer region. The right diagram has both a typical fresh-water sample labelled #1, and a typical saline-water sample labelled #2. On the left diagram, the normal sequence of the hydrochemical facies from fresh water to saline water in the Edwards Aquifer is shown.

The diagram on the top left in Figure No. 5-14, for the New Braunfels A-1 well exhibits that which is typical for saline water. The B-1 and C-1 wells show a combination of fresh (samples from above the Regional Dense Member or just below), and saline waters (samples from a bottom zone), and B-2 exhibits fresh water. Thus, the same pattern as shown previously from the Stiff and Schoeller diagrams persist.

The diagrams for the San Marcos wells on Figure No. 5-15 are representative of saline waters.

5.2-4 SATURATION INDICES

A saturation index is a unitless value which indicates how saturated or unsaturated a solution is with respect to a mineral. "Unsaturated" is represented by negative numbers and "saturated" is designated by positive numbers. The last 6 columns in both Table Nos. 5-4 and 5-3, represent saturation indices for calcite, dolomite, gypsum, anhydrite, celestite, and halite. A computer program was used to calculate these indices. The program is called PCWATEQ developed and released in 1989 by a company called Shadow Ware, and is adapted for personal computer use from WATEQ developed by Truesdell and Jones in 1974, and later revised by Truesdell, Plummer, and Jones in 1984. A program called WQXFER by John Fogarty was used to transfer the original chemical data from a LOTUS spreadsheet to PCWATEQ.

In order to understand how this program calculates the saturation indices, several terms and concepts need to be discussed, which are:

Ionic activity. Interionic attractions make a solution behave as though its ion concentrations were less than they actually are, thus, activity is defined as the "effective concentration of the ion" (Mortimer, 1975); and

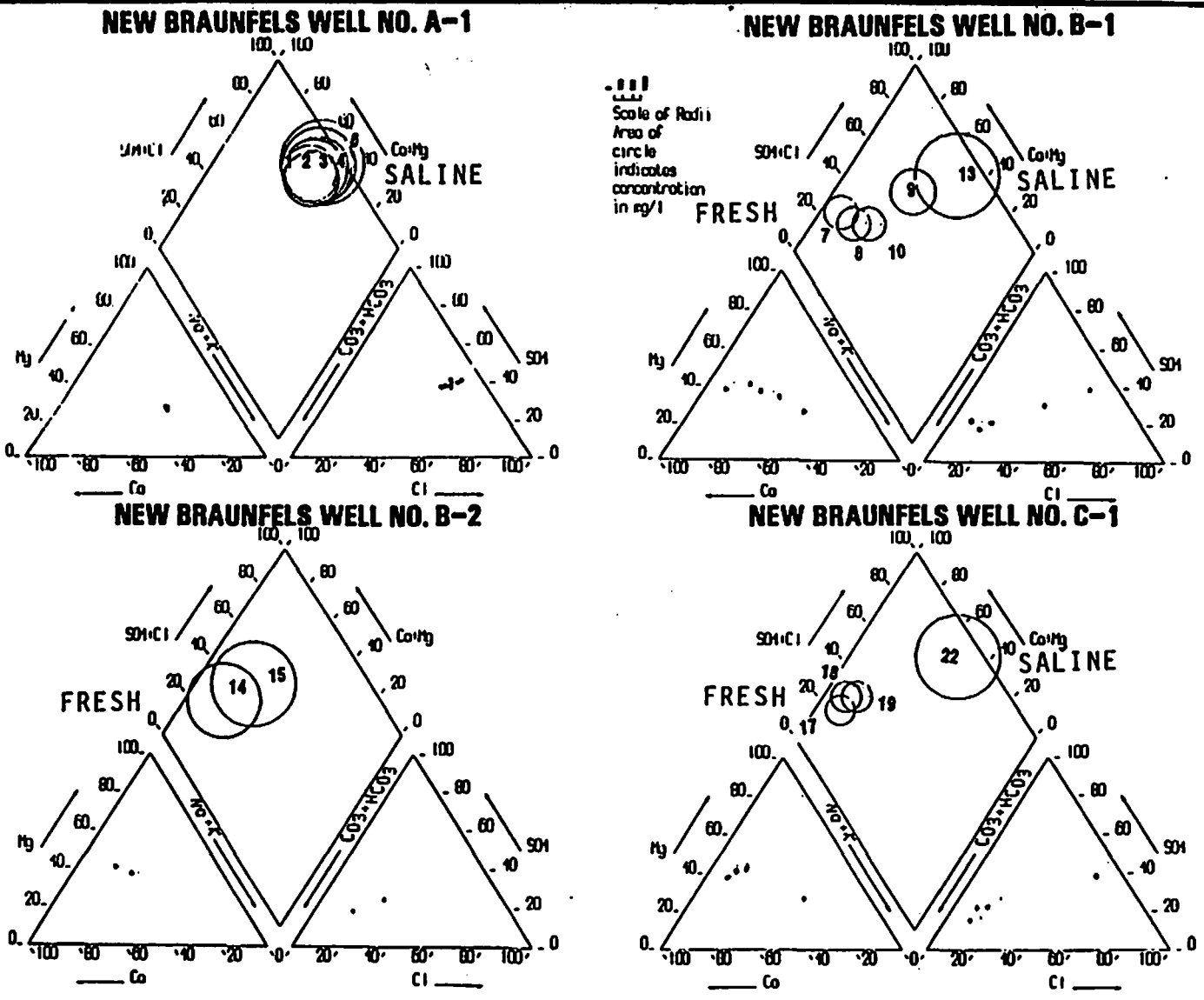


FIGURE NO. 5-14 Piper Diagrams - New Braunfels

Equilibrium constant. The law of mass action ($B+C=D+E$) expresses the relationship between the reactants and the products when the reaction is at equilibrium: $K = \frac{[D][E]}{[B][C]}$ where K is known as the stability constant or theoretical equilibrium constant (Freeze and Cherry 1979).

The equilibrium distribution of dissolved minerals is computed by PCWATEQ. PCWATEQ makes its calculations under the same principles as WATEQ. The program compares the "ionic activity products" of the assorted combinations of dissolved minerals species with their "theoretical equilibrium constant" applicable with the solid-mineral equilibrium which is being studied. Calcium and carbonate are minerals found in limestone aquifers such as the Edwards. To calculate the saturation index (Si) for calcite in contact with ground water, the equation would be:

$$\log Si = \frac{[Ca][CO_3]}{K_{cal}}$$

If the Si is greater than 1, the reaction proceeds to the left: the water has excessive amounts of the ionic constituents, and thus, precipitation must occur. If the Si value is less than 1, the reaction proceeds to the right, and the mineral dissolves. Zero denotes the equilibrium condition.

In New Braunfels, all saturation indices increased from top to bottom and decreased from the A-1 well to the C-1 well. The A-1 well was slightly saturated with respect to both calcite and dolomite while the C-1 was slightly undersaturated. All the B-1 and B-2 samples were saturated to respect of calcite and dolomite, with the bottom sample having higher indices values. With respect to gypsum, anhydrite, celestite, and halite, all the samples were undersaturated, with the values becoming less negative from top to bottom within a well, and less negative from well A-1 to C-1.

The San Marcos wells were saturated with respect to calcite and dolomite but undersaturated with respect to gypsum, anhydrite, celestite, and halite. The saturation of calcite and dolomite increased above the Regional Dense Member, while the saturation indices for celestite decreased.

In comparing the two sites, the San Marcos wells had slightly more positive values of saturation indices for calcite and dolomite while the negative values for gypsum, anhydrite, celestite, and halite were very similar.

5.3 CUTTING AND THIN SECTION DESCRIPTIONS

All the cutting descriptions, Plate Nos. 5-1, through 5-6, and the thin section descriptions for New Braunfels wells A-1, B-1, C-1 and San Marcos wells C and D in Appendix IV, for both sites show the same general trends in the basic lithology and color. However, for texture, porosity, minor mineral and fossil content, the cutting descriptions proved to be very different from what was revealed by the petrographic microscope. Thus, in order to characterize the rock within the saline/fresh-water interface, the petrographic descriptions will be discussed further rather than the cutting descriptions. The latter can best be used for those are interested in a guideline when examining cuttings from wells being drilled in the areas of these drill sites. The terms and symbols used in the Plates Nos. 5-1 through 5-5 are defined as follows:

Formation. Formations refers to the formations within the Edwards Group, for example: GT = Georgetown; P = Person; and K = Kainer.

Member. Members refers to the members within the Person and Kainer Formations, such as: C, M, L, & C = Cyclic, Marine, Leached, and Collapsed Members; RD = Regional Dense Member; K & D = Kirschberg and Dolomitic Members; and BN = Basal Nodular Member.

Depth (feet). The feet below land surface is indicated by a scale 2.5 inches equal 100 feet.

Lithology. The lithologic column refers to the rock type, such as the following: limestone = blue with brick pattern; dolomite = purple with a "slanted" brick pattern; mixture of dolomite and limestone = light blue/green brick pattern with a slash in the bottom corner of each brick;

Texture. This column refers to Dunham's (1962) classification system of: mudstone (m); wackestone (w); packstone (p); and grainstone (g). If two lithology were present, such as dolomite and limestone, and thus, two types of textures were present in an interval, then a ";" separates them (c;m). A "/" means that the texture ranges from one rock type to another: a mudstone to a packstone would be designated as "m/p."

Minor Minerals and Structures. The observed accessory minerals were, for example, pyrite or "BRB's" which stands for black round bodies or unidentifiable opaque minerals. The only observed structures were stylolites. Stylolites is sometimes abbreviated as "stylol" and celestite as "celest."

Fossil Content. Very few fossils were specifically classified. Miliolids were the only fossil identified, everything else was identified as either a fossil or an allochem.

Porosity. Porosity was characterized in four ways: n = none visible; l = low, m = medium, and h = high. See "texture" above for explanations on the use of ";" versus "%."

Porosity Type. Two types of porosity were identified: m = moldic; and bp = between particles.

Color. The color of the cuttings were abbreviated to the following: br = brown; g = gray; bl = black; and w = white. Light, medium, or dark were used as adjectives and were abbreviated to: lt, m, and dk, respectively. See "texture" above for explanations on the use of ";" versus "%."

The general lithologic composition of all the wells is presented in Table No. 5-7 (based more on thin section descriptions than on the cutting descriptions). In summary, the dolomites varied in porosity from very low to very high with vuggy and moldic pore types. Most of the limestones had little to no porosity. The significant changes in the wells in New Braunfels were an increase in dolomoldic porosity and an increase in cementation, including quartz, dolomite, and sparry calcite, occurring from the A-1 well to the C-1 well, above and below the Regional Dense Member. In San Marcos, the significant changes in the wells were that the D well had much less dolomitization than the C or B wells, the latter being more like New Braunfels.

Section 6 further details the lithologic composition, texture, permeability, and porosity characteristics. In addition, comparisons between these characteristics and the well log data are made. Note that the cutting descriptions compared very well with the lithology-porosity logs in Plate Nos. 6-3 to 6-7. The dolomite (pink) and limestone (blue) in track 1 of the lithology-porosity column on the logs match the appearance of dolomite (purple) and limestone (blue) in the cutting descriptions (Plate Nos. 5-1 to 5-5). The appearance of both limestone and dolomite on the

TABLE NO. 5.7 GENERAL WELL LITHOLOGIC COMPOSITION

Georgetown Formation:

LIMESTONE: Shaly, Fossiliferous Wacke/Packstone
Low to No Porosity

Edwards Group

Person Formation

Cyclic, Marine, Leached, & Collapsed Members Combined

VERY FINE DOLOMITE: Wacke/Packstone
PLUS DOLOMITIC CHERT
Low to Medium Porosity
Dolomoldic Porosity and Sparry Calcite Cement

Regional Dense Member

LIMESTONE: Shaly Fossiliferous Mud/Wacke/Packstone
No Porosity

Kainer Formation

Grainstone Member

DOLOMITIC LIMESTONE: Peloidal/Miliolid/Fossiliferous Pack/Grainstone
Low/Medium/High Porosity
Dolomoldic Porosity and Sparry Calcite Cement

Kirschberg & Dolomitic Members Combined

Alternating Sequences of:

VERY FINE DOLOMITE:
DOLOMITIC LIMESTONE: Miliolid/Peloidal Packstone
PLUS DOLOMITIC CHERT
Low/Medium/High Porosity
Dolomoldic Porosity and Sparry Calcite Cement

Basal Nodular Member

Alternating Sequences of:

VERY FINE/FINE DOLOMITE:
DOLOMITIC LIMESTONE: Miliolid/Peloidal Packstone
Low/Medium/High Porosity
Dolomoldic Porosity

EDWARDS UNDERGROUND WATER DISTRICT

logs corresponds to the green areas on the cutting descriptions. This would indicate that the EUWD geologist reliably distinguished lithologies from the rock cuttings.

Section 6

SECTION 6.0 PETROPHYSICAL AND PETROGRAPHIC ANALYSIS

This chapter is a petrophysical and petrographical analysis of the New Braunfels A-1, B-1, and C-1 and the San Marcos B, C, and D wells. The New Braunfels B-2 well was not studied because it was too shallow (total depth of 660.15 feet) and it was not logged with the same suite of wireline logs ran in the other wells.

Considerable work has been done on the petrography of the Edwards Aquifer. Pertinent references include Rose (1972), Maclay and Small (1984), and Ellis (1985).

Many hydrogeological reports on the Edwards Aquifer include wireline logs (e.g. Guyton and Associates, Inc., 1986, and Pavlicek, et al., 1987). However, there is usually very little discussion of the logs. Only two studies have concentrated on log analysis of the Edwards Aquifer (MacCary, 1978 and Maclay, et al., 1981). Both of them only dealt with wells in Bexar and Uvalde counties. The New Braunfels and San Marcos wells provided an opportunity to conduct a petrophysical analysis of the eastern part of the Edwards.

6.1 PETROGRAPHIC ANALYSIS OF THE CUTTINGS

While the wells were being drilled, an EUWD geologist collected samples of the cuttings. Most of the samples were collected at 10-foot intervals. The geologist described the cuttings macroscopically and with a binocular microscope. At the EUWD offices, a geologist standardized and edited the descriptions and added the lithology columns (Plate Nos. 5-1 through 5-6). The descriptions were drafted at a scale of 2.5 inches equals 100 feet, the same scale at which the wireline logs were plotted.

6.1-1 METHODOLOGY

Thin sections were made of the drill cuttings from each sample interval for the New Braunfels A-1, B-1, and C-1 wells, and the San Marcos C and D wells. Thin sections were not made for the San Marcos B well, since it is very similar to the San Marcos C well.

Each thin section was impregnated with blue epoxy, which gives the pores a blue color and facilitates identification of the pore spaces. Each thin section was treated with an alizarin red-potassium ferricyanide solution. With this mixture calcite stains red, dolomite takes no stain, ferroan dolomite stains deep turquoise, and ferroan calcite stains very pale pink-red and pale to dark blue.

The descriptions of the thin sections are contained in Appendix IV. Eight characteristics of each thin section were described:

%. A visual estimation of the percent of limestone and/or dolomite in the thin section. A grab-sample of the cuttings was used to make most of the thin section. Grab-samples provided as representative a sample of each interval as could be obtained. For a few of the intervals large cuttings were selected for the thin sections, so an S (designating a selected sample) is present in the column.

Lithology. Lithology of the cuttings (limestone or dolomite), plus crystal size of the dolomite. In some cases the limestone and/or the dolomite component was divided into subgroups. Subgrouping was done when there was significant variation in the characteristics of a single lithology.

Major Constituents. The most abundant carbonate and noncarbonate constituents in the cuttings: fossils, shale, chert, peloids, pellets, etc.

Texture. Dunham's carbonate rock classification.

ϕ . A visual estimation of the amount of porosity.

Pore Type. The major pore types classified according to Choquette and Pray (1970).

Dolomoldic ϕ . Porosity created by the dissolution or partial dissolution of dolomite crystals.

K. A visual estimation of the amount of permeability.

Comments. Any minor constituents or additional characteristics of the sample that were deemed important.

6.1-2 PETROGRAPHIC ANALYSIS

In order to quantify and compare the aquifer quality (i.e. porosity and permeability) of the various rock units, the cuttings in each thin section were classified according to aquifer types. The classification is qualitative and general. It is based on a visual comparison of the pore diameters and the amount, type, and distribution of porosity. Four rock types were recognized. This rock classification is used in the following descriptions of the formations and members of the Edwards Group and associated limestones. They are defined as follows:

- Type 1.** These rocks have virtually no visible porosity when the thin section is viewed at a magnification of 100x (Figure Nos. 6-1 and 6-2). Log porosities are 5 to 15 percent. These rocks have almost no permeability. If the bed is laterally extensive, it will serve as a confining unit. The Regional Dense member, the Georgetown Formation at New Braunfels, most cherts in the Edwards Group, some dolomites in the Basal Nodular Member, and some limestones scattered throughout other portions of the Edwards Group are Type 1 rocks.
- Type 2.** These rocks have very low visible porosity when viewed at a magnification of 100x (Figure Nos. 6-3 and 6-4). Actual porosities are less than 15 percent. The most common pore types are moldic, interparticle, and intercrystalline. The combination of low porosity, isolated pores, and small pore diameters makes the permeability very low. If the bed is laterally extensive, it will serve as a confining or a semi-confining unit. The Georgetown Formation at San Marcos, some cherts, and some limestones and dolomites scattered throughout all members of the Edwards Group except the Regional Dense Member are Type 2 rocks.
- Type 3.** These rocks have low to medium porosity (approximately 15 to 25 percent log porosity). Pore types are predominantly moldic, interparticle, intercrystalline, and vuggy (Figure Nos. 6-5 to 6-8).

TYPE 1: No visible porosity

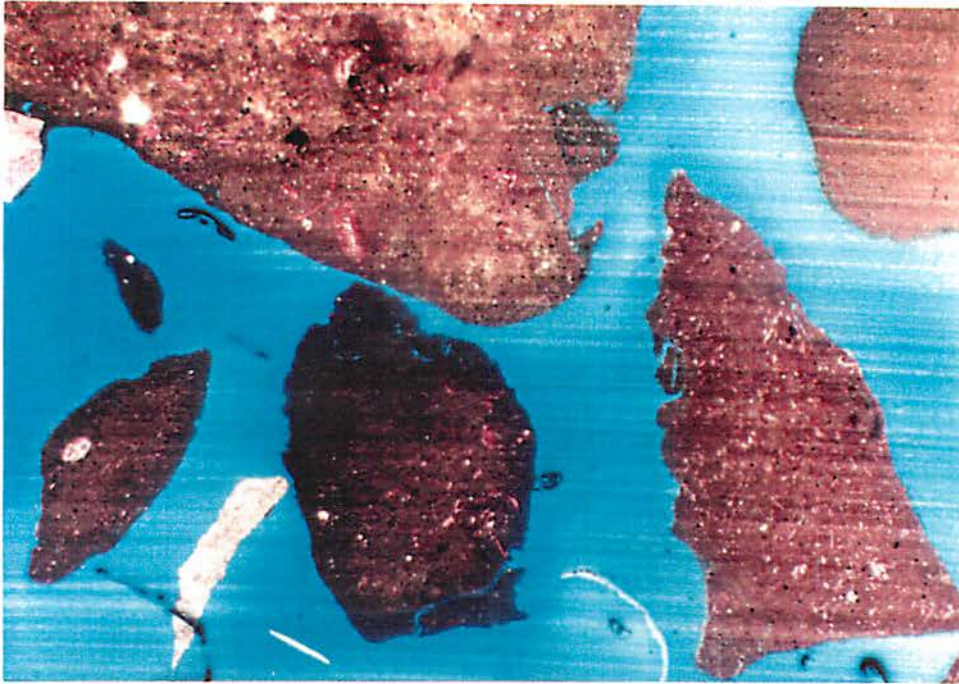


Figure No. 6-1. NBA-1, 626-31 The limestone is a shaly, fossiliferous wackestone. There is no visible porosity. The rock is from the Regional Dense Member. 20x



Figure No. 6-2. NBC-1, 561.7-71.7 The rock is a dolomitic chert with no visible porosity. The rock is from the Person Formation above the Regional Dense Member. 20x

TYPE 2: Very little visible porosity; very low permeability

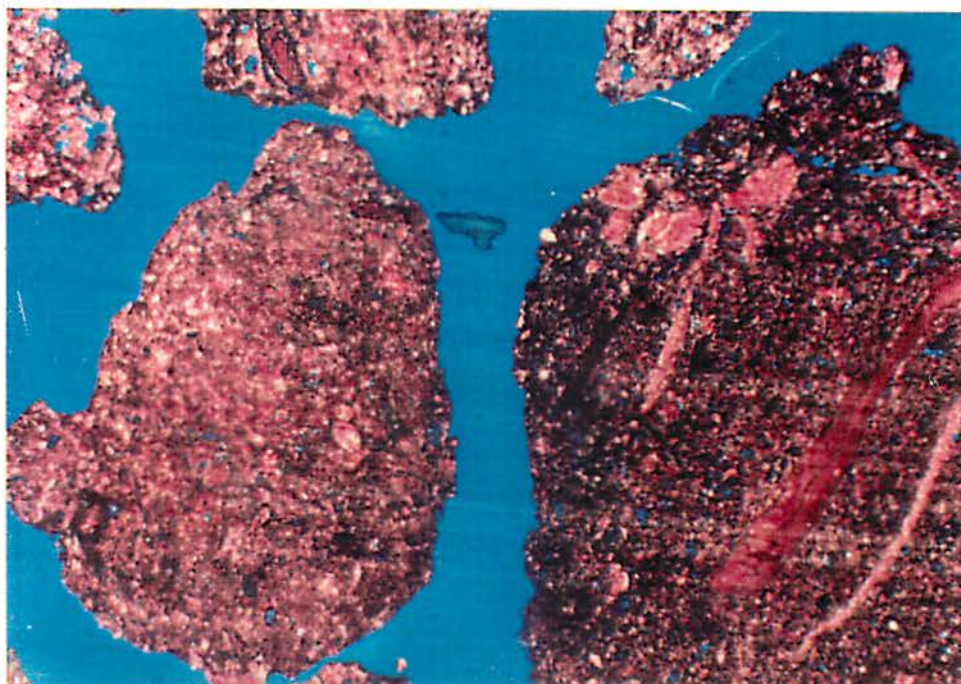


Figure No. 6-3. NBC-1, 540.7-51.7 The limestone is a shaly, fossiliferous packstone. Isolated, moldic porosity is scattered throughout the cuttings. Permeability is very low. The rock is from the very top of the Person Formation. 20x

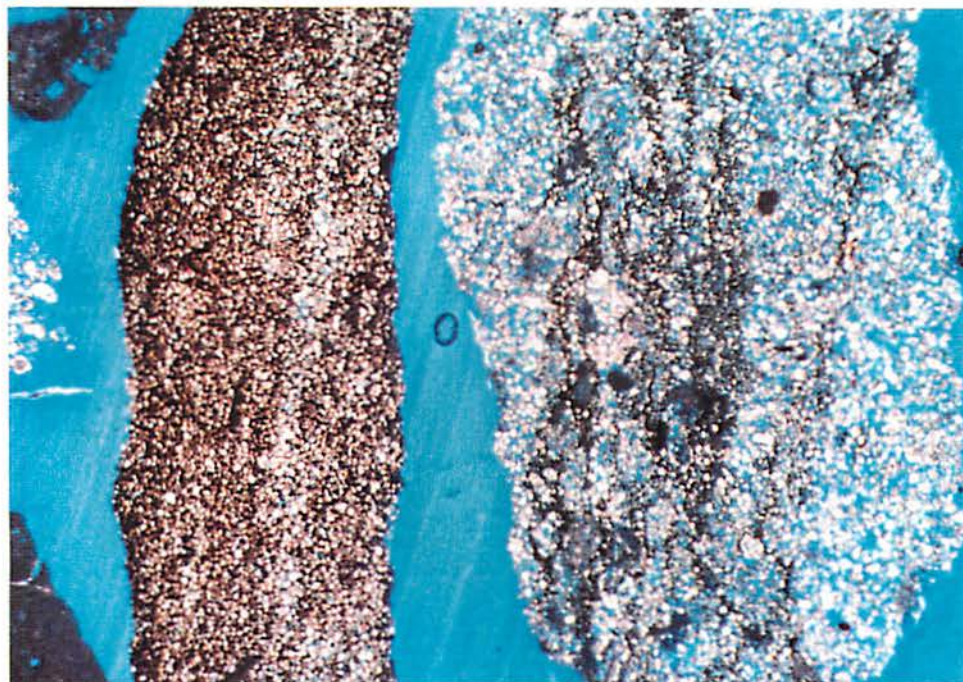


Figure No. 6-4. NBA-1, 516.2-26.2 The shaly, very fine dolomite on the left side of the photomicrograph has little visible porosity. Shale greatly reduces intercrystalline porosity. The cutting on the right half of the photo is Type 4 rock. The cuttings are from the Person Formation above the Regional Dense Member. 40x

TYPE 3 Low to medium porosity and permeability

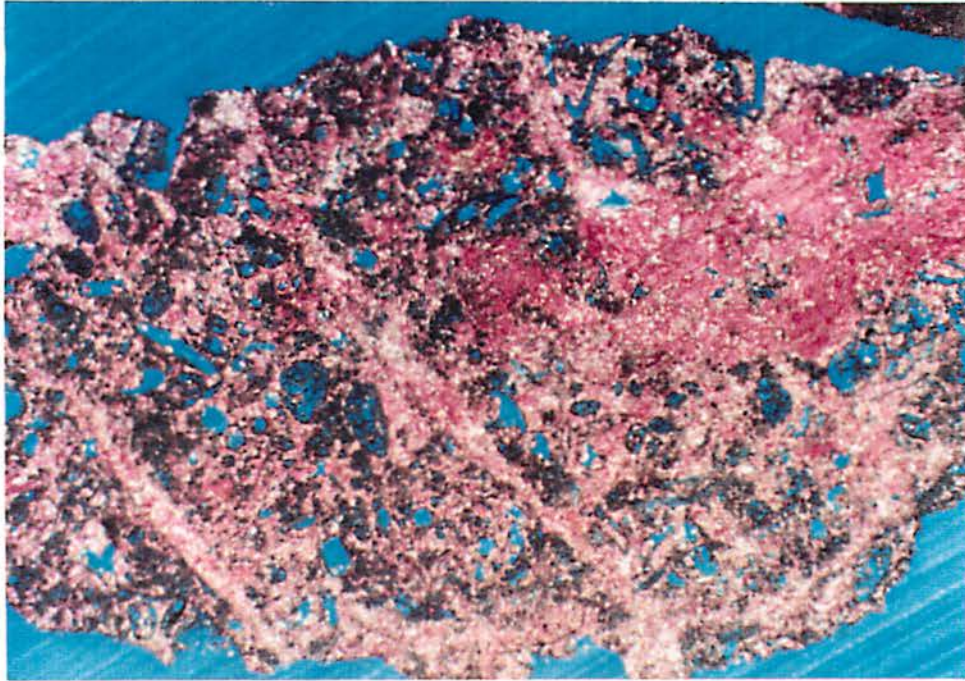


Figure No. 6-5. NBC-1, 540.7-51.7 The limestone is a fossiliferous packstone. Most of the porosity is moldic. Porosity is medium, but it does not appear to be well connected. The rock is from the top of the Person Formation. 40x

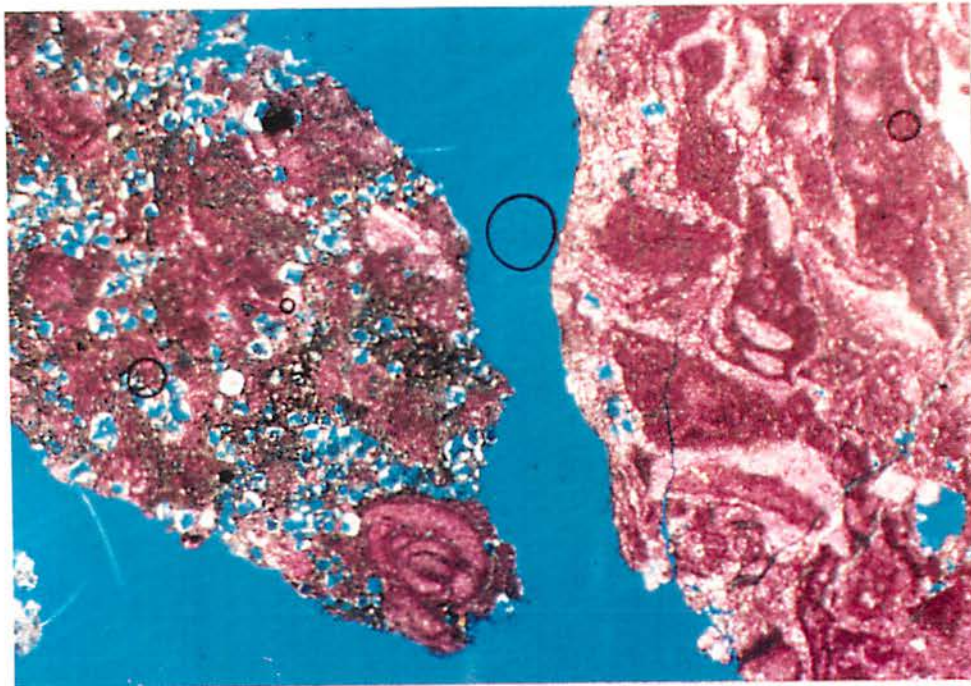


Figure No. 6-6. NBC-1, 581.7-91.5 Most of the porosity in the limestone on the left side of the photomicrograph is from partially dissolved dolomite rhombs (dolomoldic porosity). The limestone on the right is Type 2 rock. The rock is from the top of the Person Formation. 40x

TYPE 3 Low to medium porosity and permeability (continued)



Figure No. 6-7. NBA-1, 586-96 The very fine dolomite on the left side of the photomicrograph has medium porosity. Pore types are intercrystalline and vuggy. However, the pore diameters are so small that the permeability is very low. The rest of the cuttings are Type 1 and 2 limestones. The rock is from the Person Formation above the Regional Dense Member. 20x

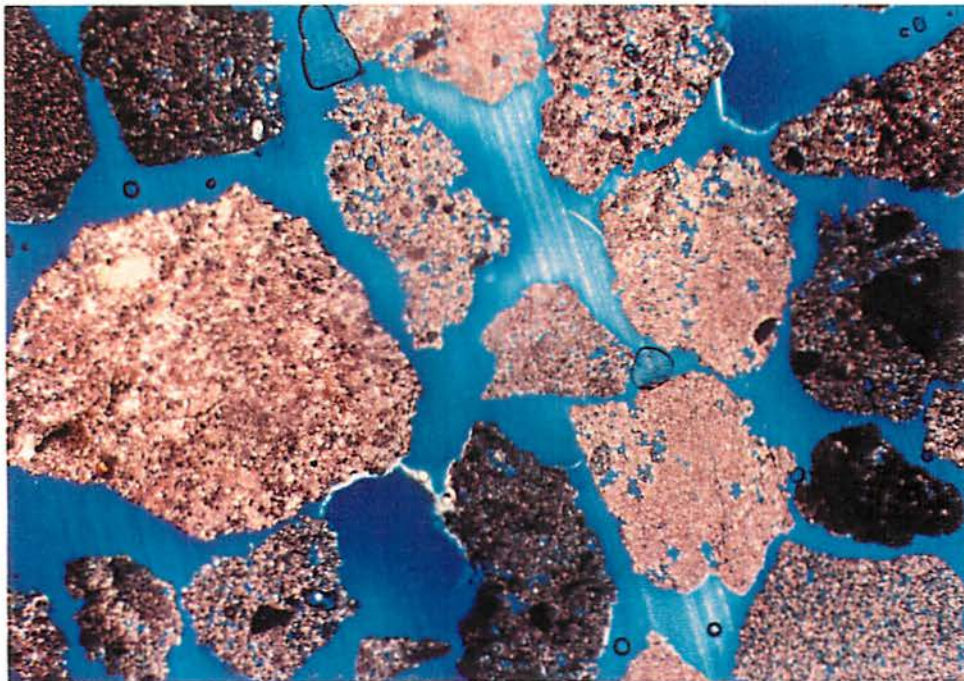


Figure No.6-8. NBC-1, 756-66 All of the cuttings are dolomite and most of them are low porosity Type 3 rocks. Moldic and vuggy porosity predominate. The large cutting on the left is Type 2. The rock is from the Grainstone Member. 20x

Permeabilities of these rocks is low to medium. Some limestones and dolomites with medium porosity have low permeability due to intercrystalline pores with small diameters. Most limestones and some dolomites scattered throughout both the Person Formation (excluding the Regional Dense Member) and the Kainer Formation are Type 3 rock.

Type 4. These rocks have high porosity (30 to 45 percent). Pores are large and well connected (Figure Nos. 6-9 to 6-14). The most common pore types are moldic, vuggy, and intercrystalline. Some of the dolomites and a few of the limestones scattered throughout the Person Formation (excluding the Regional Dense Member) and the Kainer Formation (excluding the limestones in the Basal Nodular Member) are Type 4.

6.1-2.1 GEORGETOWN FORMATION

New Braunfels

At this site the formation is limestone. It is a shaly, fossiliferous wackestone and packstone. Accessory minerals include glauconite and opaques (pyrite?). Opaques are common. Basalt is present in the A-1 well. There is no visible porosity. Log porosity averages 10 percent although it reaches 14 percent in the A-1 well. Permeability is so low that the rock is a confining unit. The rock is Type 1. Refer to Figure Nos. 6-15 to 6-18.

San Marcos

The formation is limestone. It is a shaly, fossiliferous packstone with glauconite and opaques (pyrite?) as accessory minerals. Quartz silt is abundant. Visible porosity, consisting of interparticle and moldic pore types, is very low. Log porosity is 14 to 18 percent. Pore diameters are 0.01 mm. or less. Permeability is very low and is poorly connected. The rock is a semi-confining unit. The rock is Type 2. Refer to Figure Nos. 6-15 to 6-18.

TYPE 4 High porosity and permeability

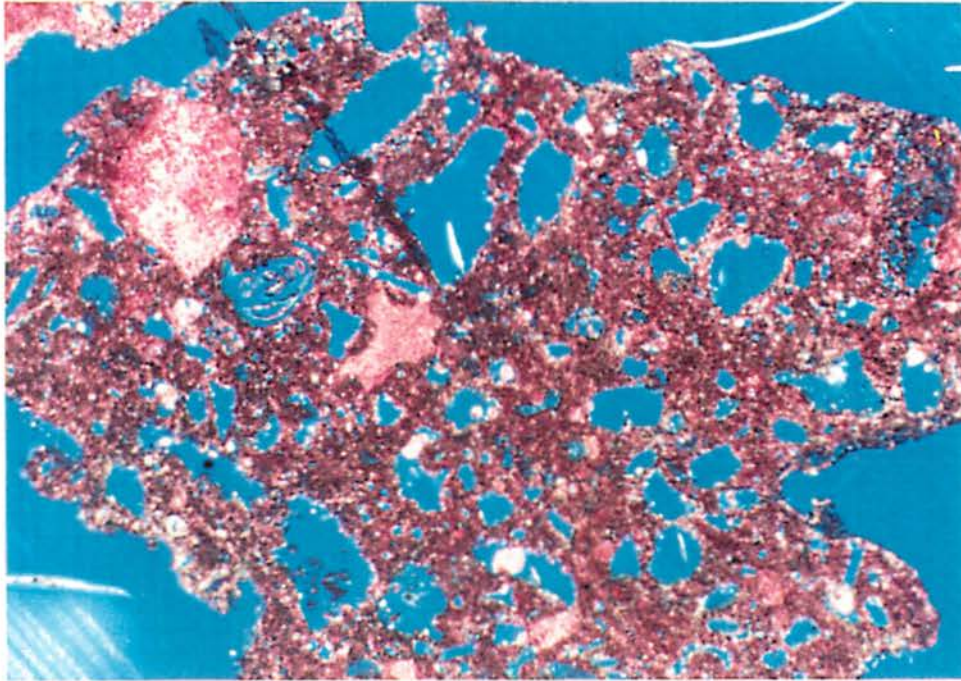


Figure No. 6-9. NBC-1, 591.5-601.5 The limestone has high moldic porosity. Permeability may be somewhat reduced if the molds are not well connected. The rock is from the Person Formation above the Regional Dense Member. 40x

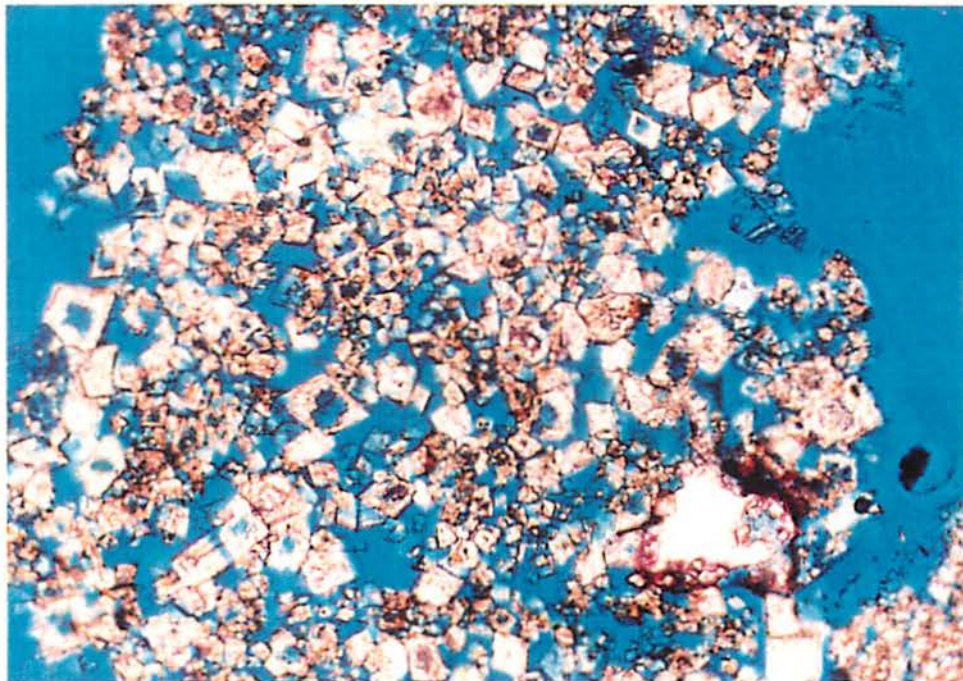


Figure No. 6-10. NBC-1, 571.7-81.7 The very fine dolomite has high porosity. Pore types are intercrystalline and moldic. Dolomoldic porosity is present. Pores are well connected. The rock is from the Person Formation above the Regional Dense Member. 100x

TYPE 4 High porosity and permeability (continued)

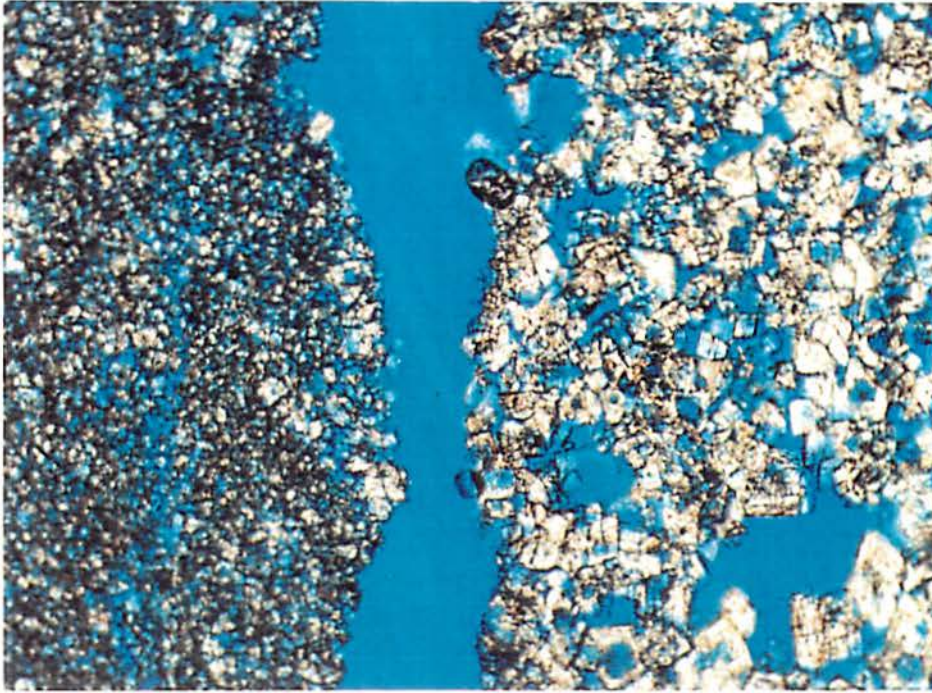


Figure No. 6-11. SMD, 668-79.5 The very fine dolomite on the left side has abundant intercrystalline porosity. The very fine to fine dolomite cutting on the right has abundant moldic intercrystalline and vuggy porosity. The cuttings are from the Kirschberg Evaporite and Dolomitic Members of the Kainer Formation. 100x

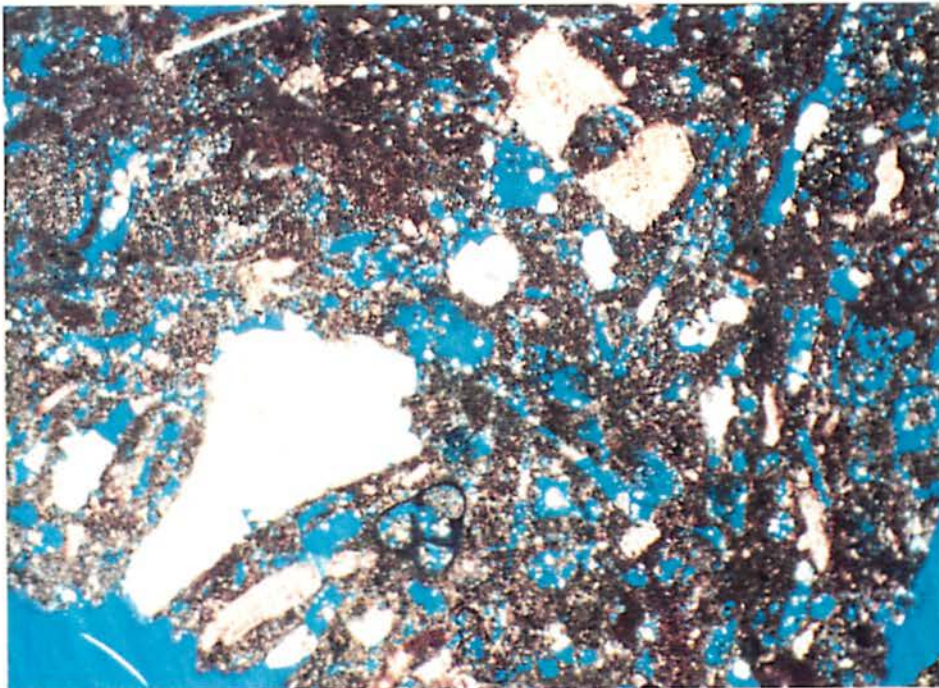


Figure No. 6-12. SMD, 482-96 The rock is a fossiliferous packstone with high moldic and vuggy porosity. The cutting is from the top of the Person Formation. 40x

TYPE 4 High porosity and permeability (continued)

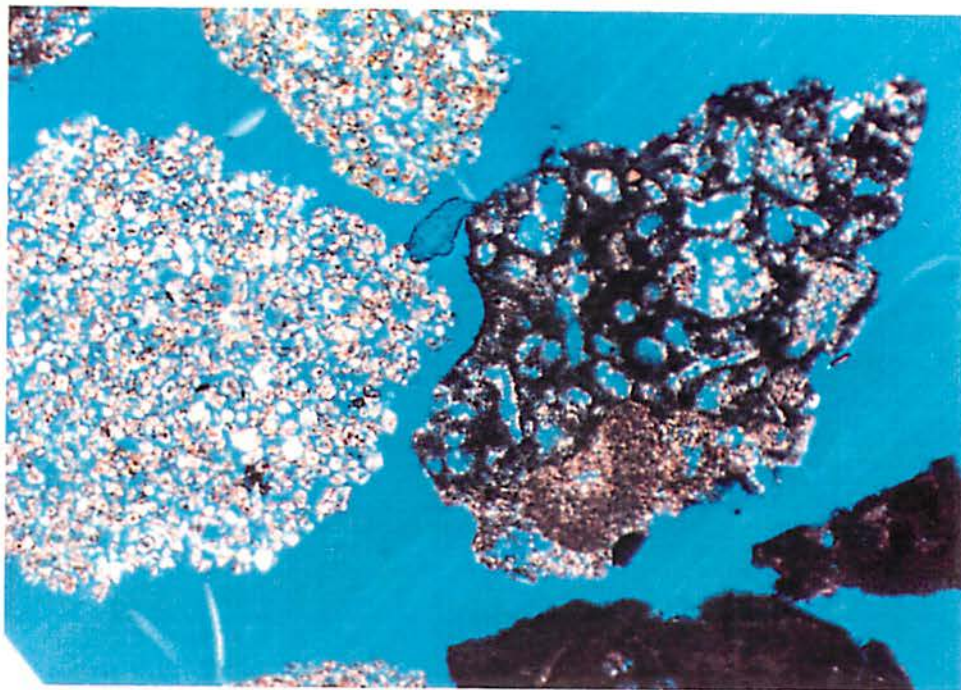


Figure No. 6-13. NBA-1, 516.2-26.2 The very fine dolomite on the left side of the photomicrograph has abundant intercrystalline and moldic porosity. The large dolomite cutting on the right has high moldic porosity, but the pores are not well connected. It may be Type 3 rock. The cuttings are from the Person Formation above the Regional Dense Member. 40x

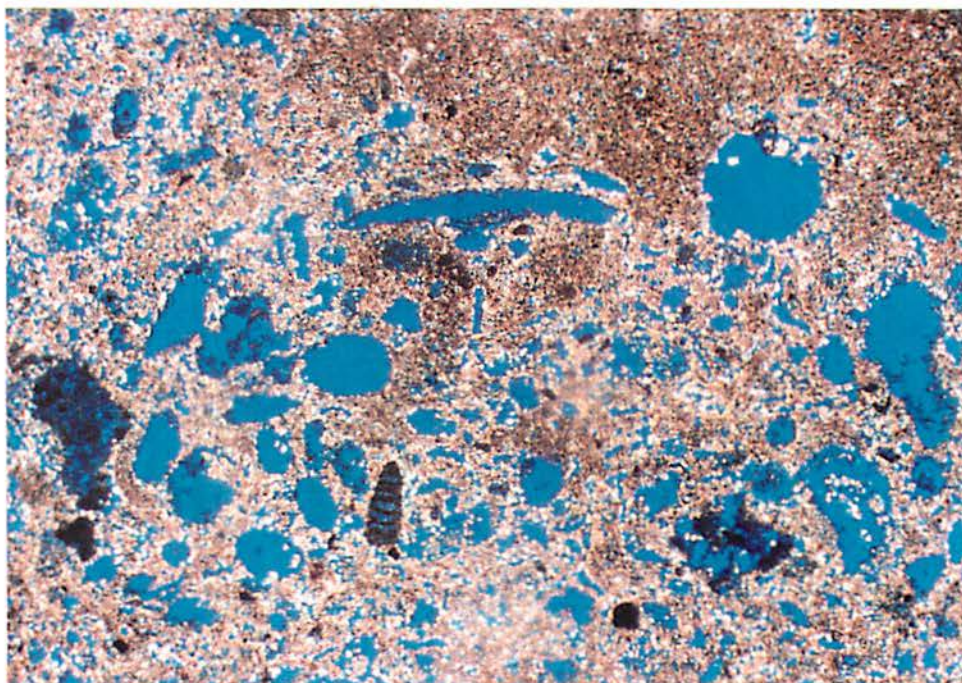


Figure No. 6-14. NBA-1, 476.2-86.2 The very fine dolomite has high porosity. Pore types are moldic, intercrystalline and vuggy. Permeability is high but not as high as the dolomites in Figures 6-10 and 6-11. The rock is from the top of the Person Formation. 20x

GEORGETOWN FORMATION



Figure No. 6-15. SMC-1, 425-35 The rock is a shaly, fossiliferous packstone. Quartz silt (white grains) and an opaque mineral (pyrite?) are present. Porosity is predominantly moldic and very low. Type 2 rock. 40x

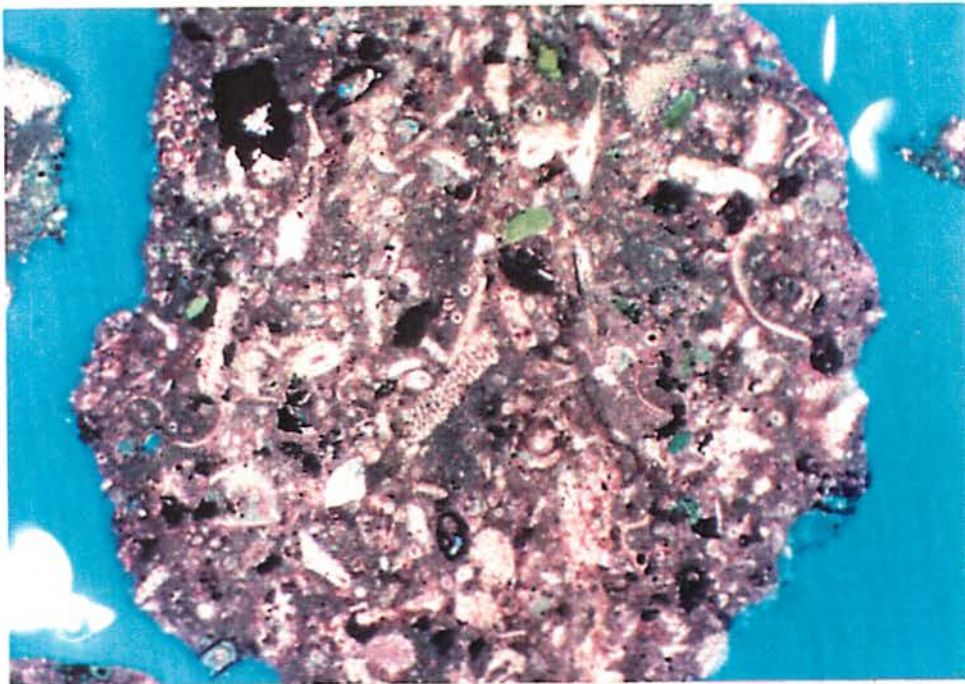


Figure No. 6-16. NBA-1, 446.2-47.2 The rock is a fossiliferous packstone. Glauconite (green grains) and an opaque mineral (pyrite?) are present. Porosity is intercrystalline and very low. Type 2 rock. 40x

GEORGETOWN FORMATION (continued)

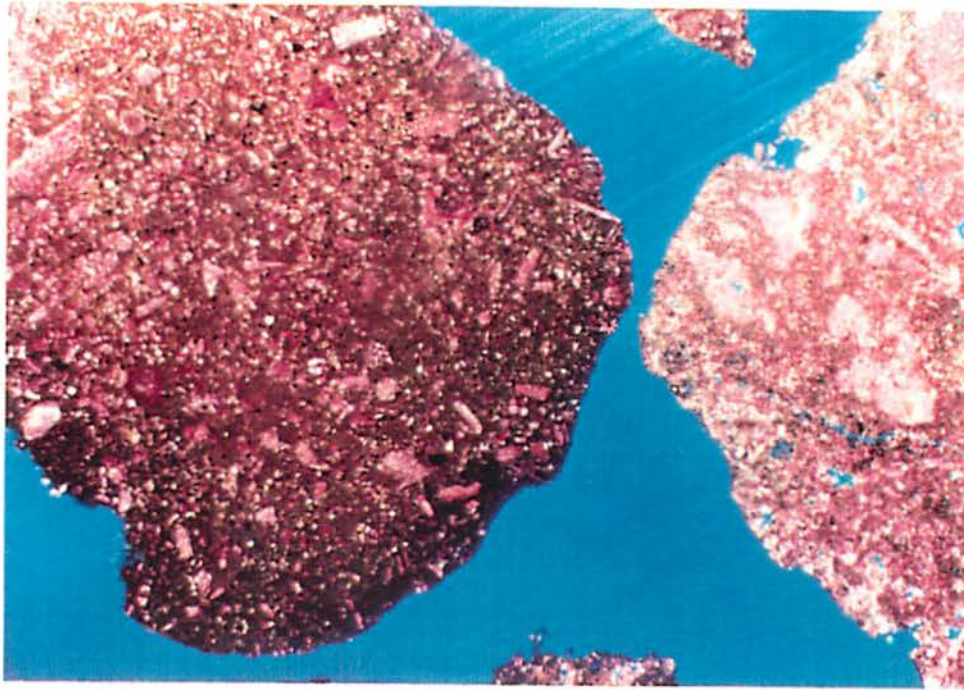


Figure No. 6-17. NBC-1, 530.7-40.7 The rock is a shaly, fossiliferous packstone. Opaques are present. No porosity is visible in the large cutting. Type 1 rock. 20x

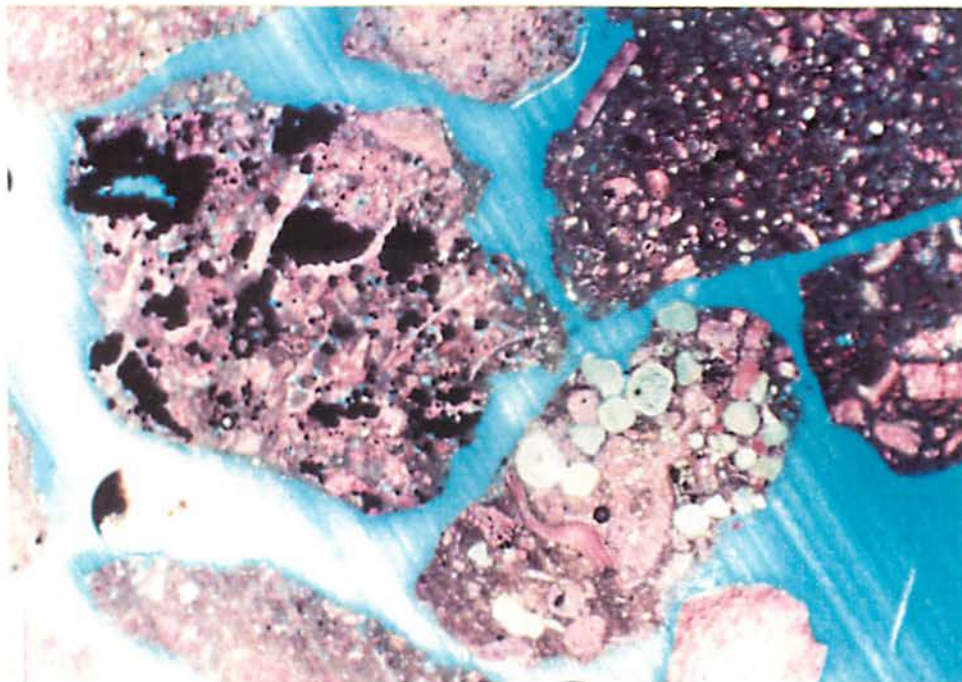


Figure No. 6-18. SMC, 419-25 The rock is a shaly, fossiliferous packstone. Opaques (pyrite?) and glauconite (green) are visible. Type 2 rock. 40x

6.1-2.2 PERSON FORMATION

6.1-2.2-1 Cyclic, Marine, Leached, and Collapsed Members (Undifferentiated)

New Braunfels

This section of the Person Formation is predominantly a very fine dolomite. A wackestone or packstone texture is visible in some cuttings. Shaliness increases from the fresh (C-1) to the saline water (A-1). There is a wide variety in the aquifer quality of the dolomite. Types 4, 3, and 2 are present. The amount of porosity decreases slightly toward the base of the section, thus increasing the amount of low permeability Type 3 rock. Refer to Figure Nos. 6-19 to 6-26.

Dedolomitization is evidenced by partially dissolved dolomite rhombs and sparry calcite cement filling intercrystalline and dolomoldic porosity. The degree of dedolomitization correlates strongly with present-day water salinity:

1. The degree to which dolomite rhombs are dissolved greatly increases from the saline (well A-1) to the fresh water (well C-1).
2. The amount of sparry calcite cement filling intercrystalline and dolomoldic porosity significantly increases from the saline to the fresh water well.
3. The amount of sparry calcite cement increases up the section, which is the direction of the decrease in salinity.
4. The degree to which dolomite rhombs are dissolved greatly increases up the section.
 - a. In the A-1 well dolomoldic porosity in dolomites only occurs within the top 40 feet of the formation. This may indicate that at one time fresh water filled the pores in this interval.
 - b. In the B-1 well dolomoldic porosity in dolomites does not occur below the limestone bed at 557 to 564 feet. This may indicate that the Person Formation below 564 feet has never been

PERSON FORMATION
CYCLIC, MARINE, LEACHED, AND COLLAPSED MEMBERS (UNDIFFERENTIATED)

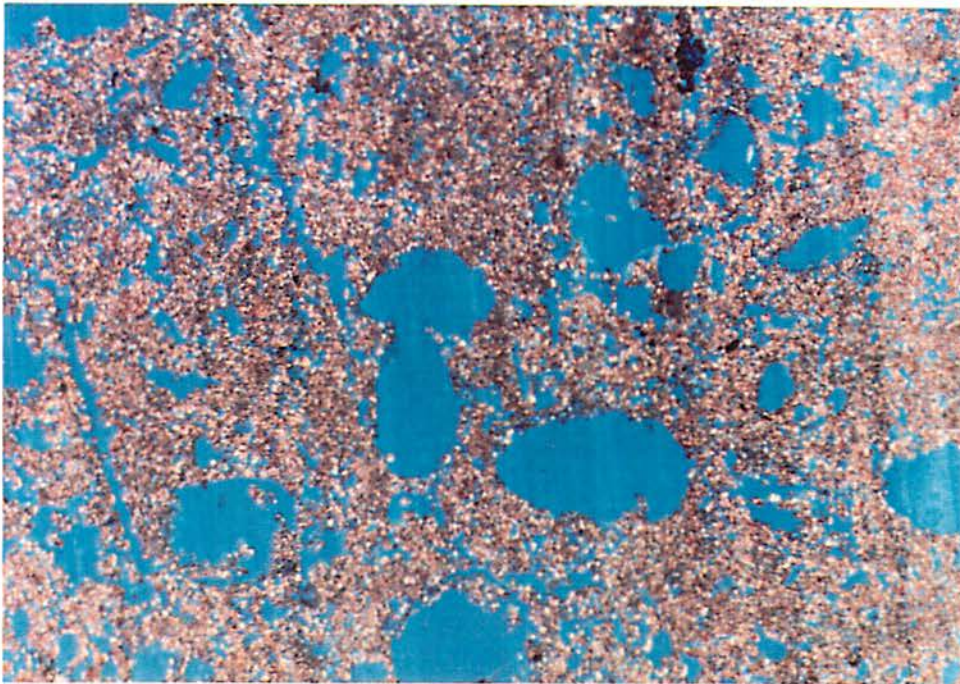


Figure No. 6-19. NBC-1 551.7-61.7 The rock is a shaly, very fine dolomite. Porosity is very high. Pore types are moldic, vuggy, and intercrystalline. Type 4 rock. 40x

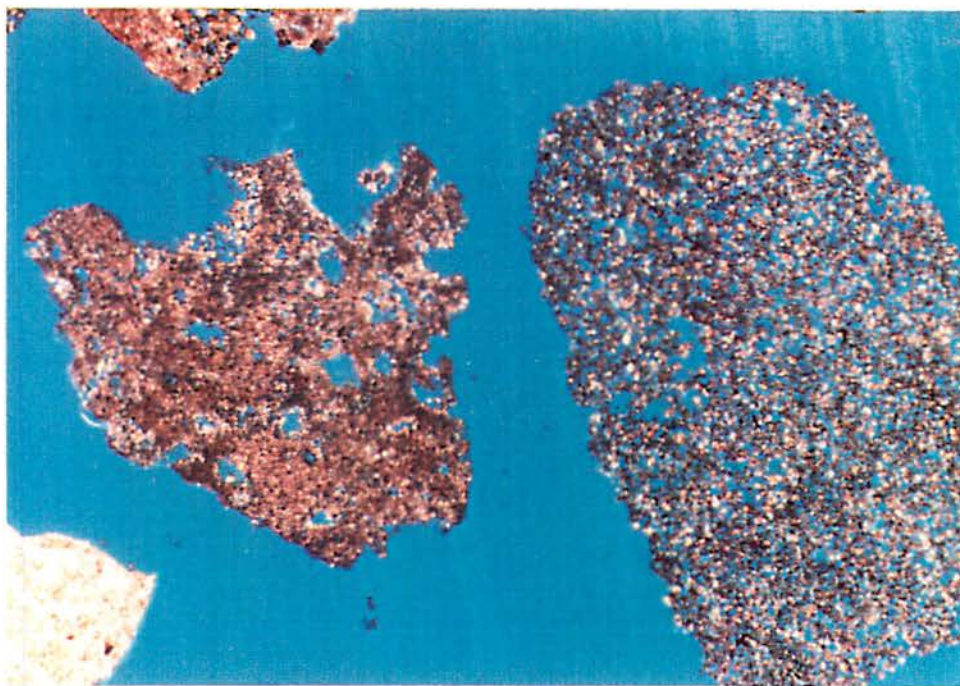


Figure No. 6-20. NBC-1, 561.7-71.7 The rock is a shaly, very fine dolomite. The small cutting at the lower left is dolomitic chert with no porosity. The dolomite cutting at the left of the picture has mainly vuggy/moldic porosity and is Type 3 rock. The cutting at the right is Type 4 rock. 40x

PERSON FORMATION (continued)
CYCLIC, MARINE, LEACHED, AND COLLAPSED MEMBERS (UNDIFFERENTIATED)

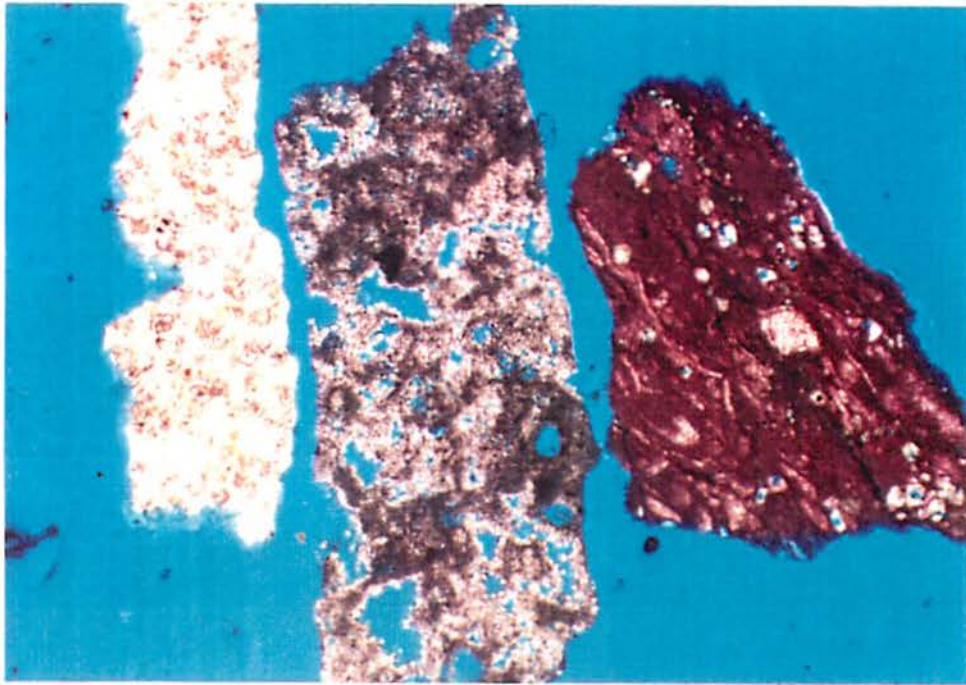


Figure No. 6-21. NBA-1, 506.2-16.2 A dolomitic chert cutting with no porosity is on the far left of the picture. A very fine dolomite with vuggy porosity is in the middle. The rock is Type 3. A shaly, fossiliferous wackestone is on the far right. The rock is Type 2. The only porosity is in partially dissolved very fine dolomite rhombs. 40x



Figure No. 6-22. NBA-1, 516.2-26.2 A shaly, Type 2, very fine dolomite is on the far left. Type 4 dolomite (middle bottom), Type 2 peloidal, packstone dolomite (top right), and dolomitic chert (right) are also pictured. 40x

PERSON FORMATION (continued)
CYCLIC, MARINE, LEACHED, AND COLLAPSED MEMBERS (UNDIFFERENTIATED)

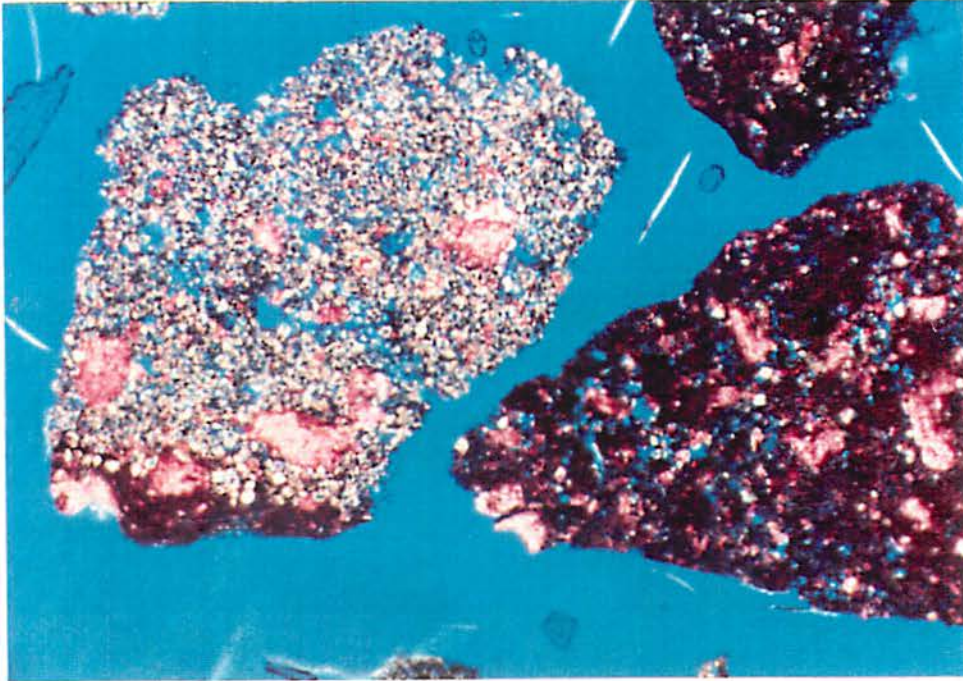


Figure No. 6-23. SMC, 477-89 The cutting at the left of the photomicrograph is very fine dolomite with sparry calcite cement and dolomoldic porosity. Type 4 rock. The cuttings at the right are dolomitic, peloidal packstones. 40x

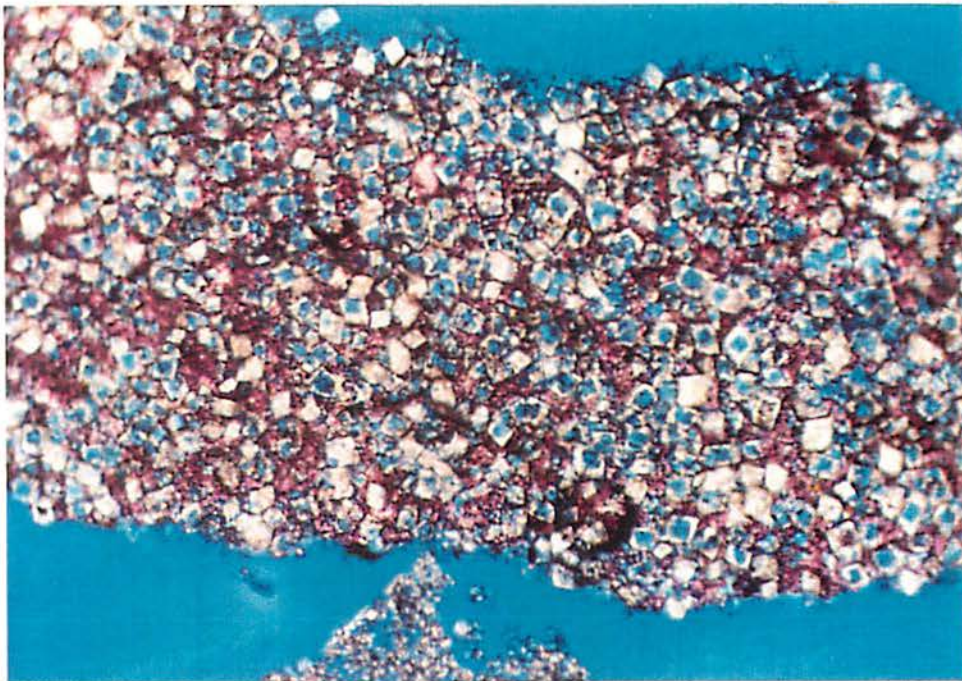


Figure No. 6-24. SMC, 457-67 The rock is very fine dolomite with abundant dolomoldic porosity and sparry calcite cement. Type 3 rock. 100x

PERSON FORMATION (continued)
CYCLIC, MARINE, LEACHED, AND COLLAPSED MEMBERS (UNDIFFERENTIATED)

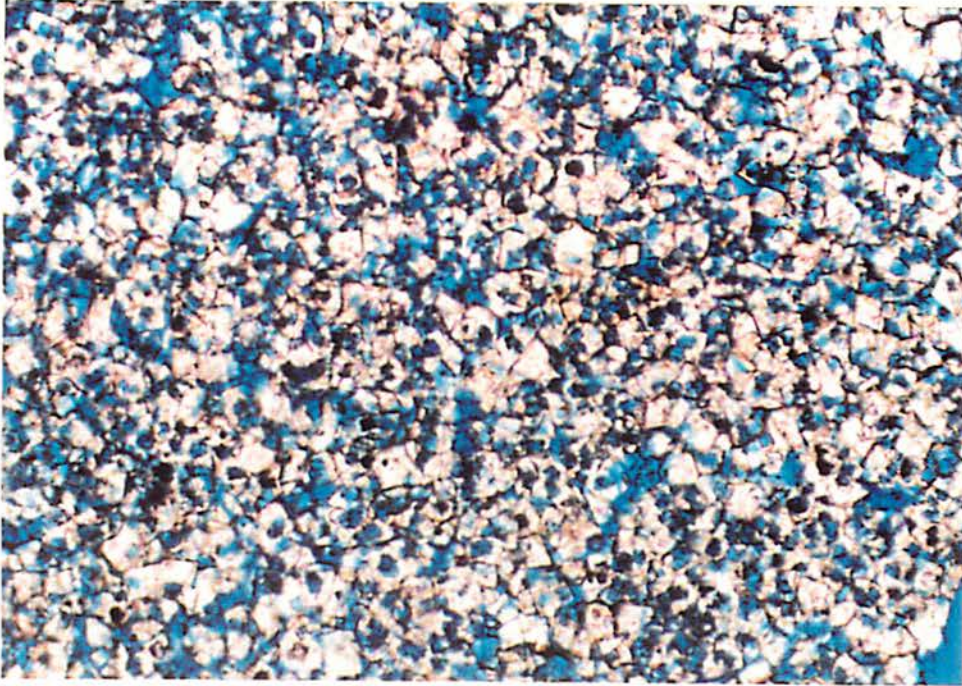


Figure No. 6-25. NBB-1, 551.7-61.7 The rock is very fine dolomite. Dolomoldic porosity is abundant. Intercrystalline porosity is common. The rock has medium porosity and is Type 3. 100x

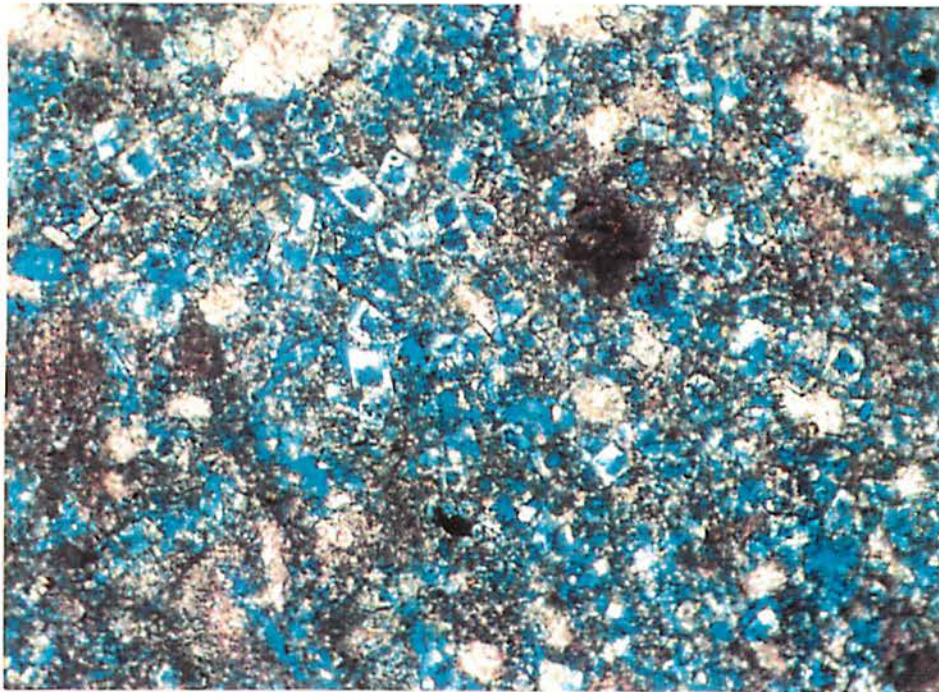


Figure No. 6-26. SMD, 506-16 The rock is a high porosity dolomitic limestone. Dolomoldic and intercrystalline porosities are abundant. Type 4 rock. 100x

exposed to fresh water, at least not long enough to initiate dedolomitization.

- c. In the C-1 well dolomoldic porosity in dolomites occurs throughout the section but it is more abundant above the limestone bed at 604 to 612 feet. This may indicate that the Person Formation above 604 feet has been exposed to fresh water for a much longer period of time than the rest of the formation.

Limestone beds are scattered throughout the section. Most of the beds consist of shaly, dolomitic, fossiliferous wackestones and packstones. These beds are Types 1 and 2 rocks. Some of the limestones are fossiliferous packstones with low to medium porosity. Permeability is low to medium. These beds are Type 3 rocks. Dolomoldic porosity is present in some of these cuttings. Dolomitic chert is scattered throughout the formation, but it is more abundant in the upper part. The chert is Type 1 rock.

San Marcos

The section at the C-site is predominantly a very fine dolomite, while at the D-site, limestone is more abundant than dolomite. A wackestone or packstone texture is visible in some dolomite cuttings. There is a wide variety in the aquifer quality of the dolomite at both wells. Types 4, 3, and 2 are present. Porosity decreases slightly toward the base of the section, thus increasing the amount of low permeability Type 3 rock. Refer to Figure Nos. 6-19 to 6-26.

Partially dissolved dolomite rhombs and sparry calcite elements occur throughout the section. They are as common here as they are in the fresh water well C-1 at New Braunfels, but they are more abundant at the C-site than at the D-site. This seems to indicate that the San Marcos section was at one time exposed to fresh water long enough for dedolomitization to significantly alter the rock at both sites. More extensive dedolomitization occurred at the C-site because of: 1) longer exposure to fresh water; or 2) fresh-water diagenesis had less an effect on the rock because the rock was more calcitic to begin with. Petrographic evidence exists for the latter explanation. There is really no way to verify the former.

Limestone beds are scattered throughout the section. They are very similar to the limestones in the New Braunfels section, but more abundant. The D-site is predominantly limestone. Most of it is fossiliferous or peloidal packstone and much of the limestone has been

partially dolomitized. At the D-site, dolomoldic porosity generally occurs in the dolomitic limestones rather than in the dolomites. At the C-site, it commonly occurs in both.

6.1-2.2-2 REGIONAL DENSE MEMBER

New Braunfels

This section is a limestone. It is a shaly, fossiliferous mudstone and wackestone. Opaques (pyrite?) and quartz silt are accessory minerals. Dolomite rhombs are scattered throughout the B-1 and C-1 wells. There is virtually no visible porosity. Log porosity is 5 to 10 percent with porosity increasing toward the base of the section. Permeability is low enough for the rock to be a confining unit. The rock is Type 1. Refer to Figure No. 6-27.

San Marcos

The section at this site is a limestone. It is a shaly, fossiliferous wackestone and packstone. Opaques (pyrite?) and quartz silt are accessory minerals. At the C-site quartz silt is less common than in the New Braunfels wells. At the D-site, quartz silt is common. There is virtually no visible porosity. Log porosity averages about 7 to 9 percent. Permeability is low enough for the rock to be a confining unit. The rock is Type 1. Refer to Figure 6-27.

6.1-2.3 KAINER FORMATION

6.1-2.3-1 GRAINSTONE MEMBER

New Braunfels

The section is predominantly limestone. Rock types include a miliolid grainstone with extensive sparry calcite cementation and a peloidal and/or fossiliferous packstone. Rock Types 2 and 3 predominate, with some grainstones in lower part of the section approaching Type 4. Refer to Figure Nos. 6-28 to 6-31.

A very fine dolomite occurs in the lower one-half of the section. Rock types are 2, 3, and 4. Dolomoldic porosity is abundant. Sparry calcite fills some of the pores.

PERSON FORMATION (continued)
REGIONAL DENSE MEMBER

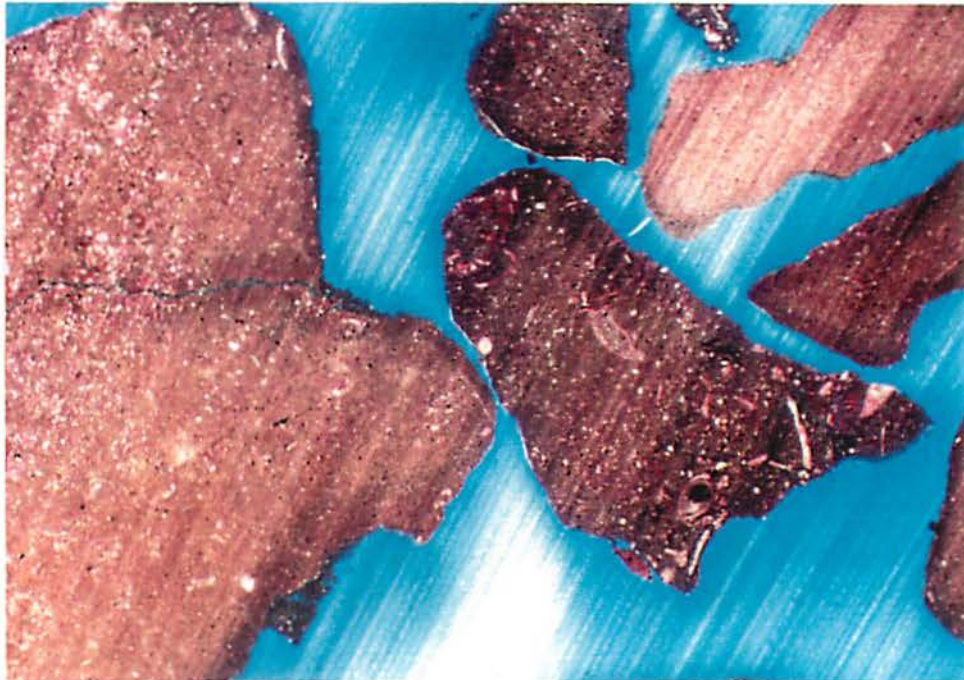


Figure No. 6-27. NBC-1, 706.5-16.3 The rock is a shaly, fossiliferous wackestone. Opaques (pyrite?) are present. Type 1 rock. 40x

KAINER FORMATION
GRAINSTONE MEMBER

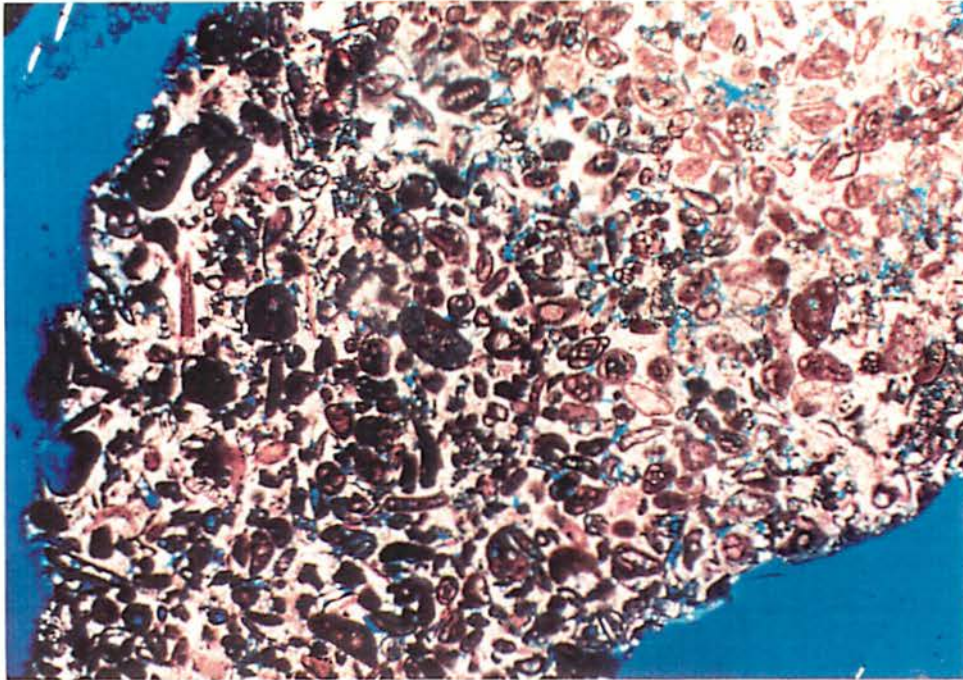


Figure No. 6-28. NBA-1, 646.5-56.8 The rock is a miliolid grainstone. Sparry calcite has occluded most of the porosity. The rock has low porosity and low permeability. Type 2 rock. 40x

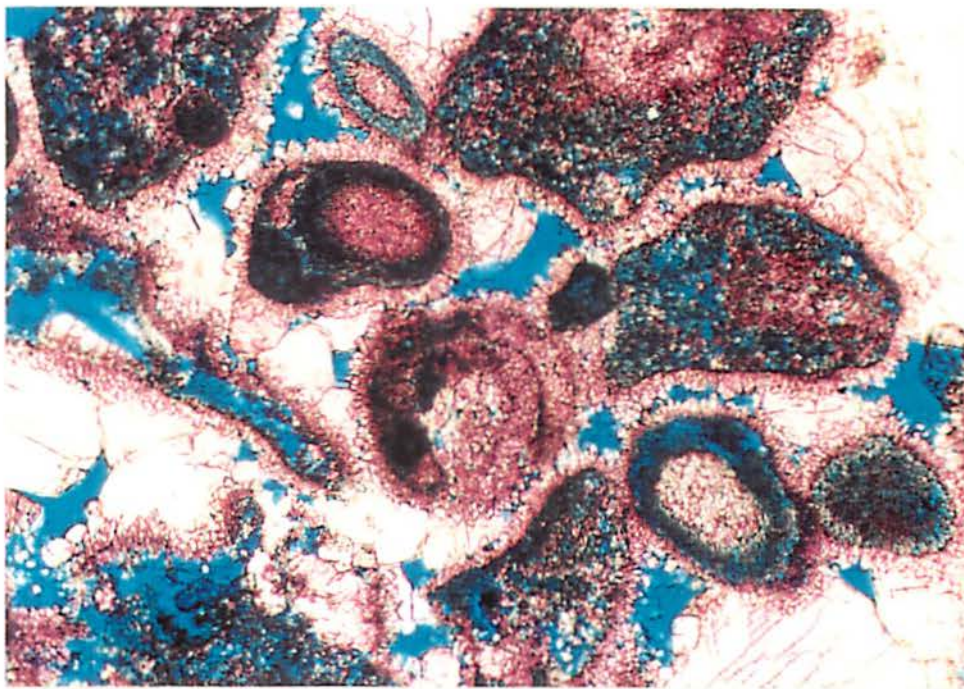


Figure No. 6-29. NBC-1, 726.3-36.3 Two generations of calcite cement are visible: isopachous cement rims the grains and a later equant spar fills most of the pores. Porosity is intergranular and moldic. Type 3 rock. 100x

KAINER FORMATION (continued)
GRAINSTONE MEMBER



Figure No. 6-30. NBB-1, 706.7-11.4 Type 3 dolomite with intercrystalline, moldic, and vuggy porosity. Porosity is high but the pore diameters are small. 40x

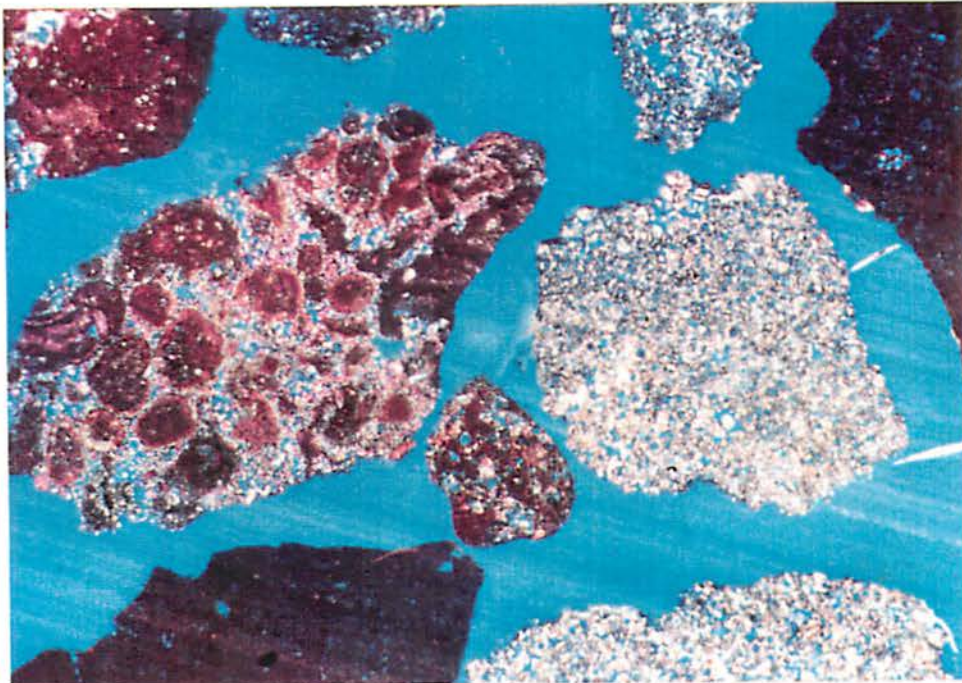


Figure No. 6-31. SMC, 622.6-32.6 A dolomitic packstone with dolomoldic and interparticle porosity is on the left side of the photomicrograph. Three cuttings that are very fine dolomite with dolomoldic porosity are present in the right part of the photograph. Both rocks are Type 3. 40x

The dolomites have higher porosities than the limestones. Porosity increases toward the base of the section with the dolomites developing more moldic, vuggy, and intercrystalline porosity and the limestone developing more interparticle and moldic porosity.

Dolomitic chert also occurs in the section.

San Marcos

This section is very similar at both sites. It has less dolomite than the New Braunfels wells. Otherwise, the intervals are very similar, including the presence of dolomoldic porosity and sparry calcite in the dolomite. Porosity in the limestone increases toward the base of the C and D wells, as it does at New Braunfels. Refer to Figure Nos. 6-28 to 6-31.

6.1-2.3-2 KIRSCHBERG AND DOLOMITIC MEMBERS (UNDIFFERENTIATED)

New Braunfels

This section consists of alternating limestone and dolomite, with dolomitic chert scattered throughout. Dolomite is the dominant rock type, but 30 to 40 percent of the interval is limestone. Refer to Figure Nos. 6-32 to 6-37.

The dolomites have a crystal size of very fine to fine. Some are shaly. Rock Types 2, 3, and 4 are present with low permeability rocks predominating (Types 2 and 3). The limestones are dolomitic miliolid and peloidal packstones. Rock Types 2 and 3 are most common. Dolomoldic porosity is common throughout the section in both the limestones and the dolomites.

Sparry calcite cement fills some pores in the Type 4 dolomite in the lower 40 feet of the B-1 well and throughout the section in the C-1 well. The calcite fills moldic, vuggy and intercrystalline porosity, in some cases significantly reducing the porosity. This type of sparry calcite is not found in the A-1 well, perhaps indicating that in the A-1 well the section has not been exposed to fresh water.

KAINER FORMATION (continued)
KIRSCHBERG AND DOLOMITIC MEMBERS (UNDIFFERENTIATED)

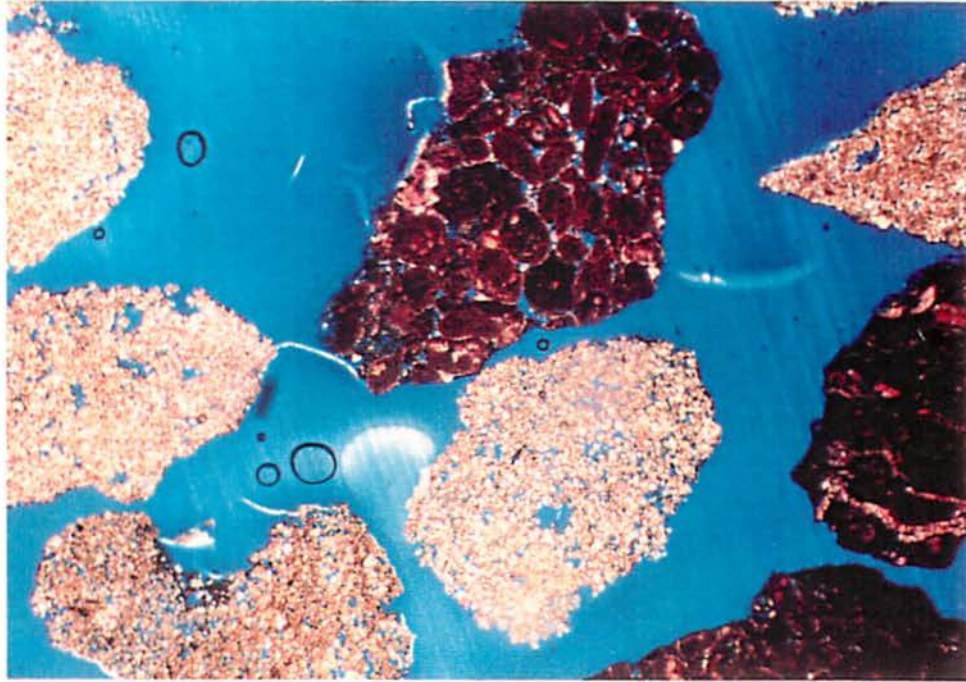


Figure No. 6-32. NBC-1, 939.1-49.1 The fine to very fine dolomite is Types 2 and 3. A shaly dolomite cutting is in the lower left corner. The miliolid grainstone (upper center) has low porosity and is Type 3. The shaly limestones at the lower right are Type 1. 20x

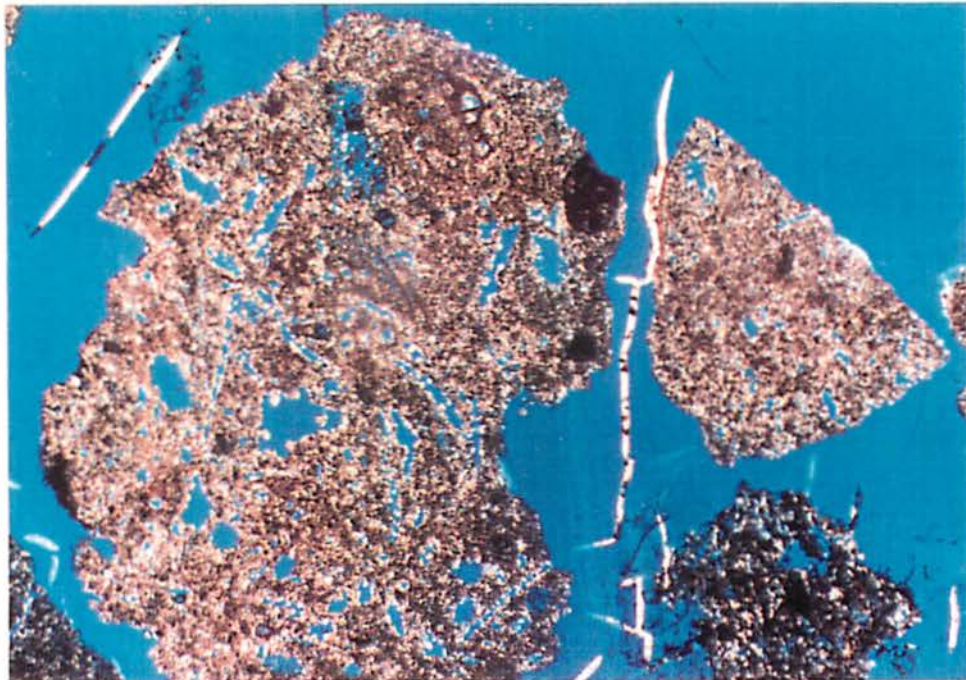


Figure No. 6-33. NBA-1, 706.5-16.3 The cuttings are very fine dolomite with predominantly moldic and vuggy porosity. Type 3. 20x

KAINER FORMATION (continued)
KIRSCHBERG AND DOLOMITIC MEMBERS (UNDIFFERENTIATED)

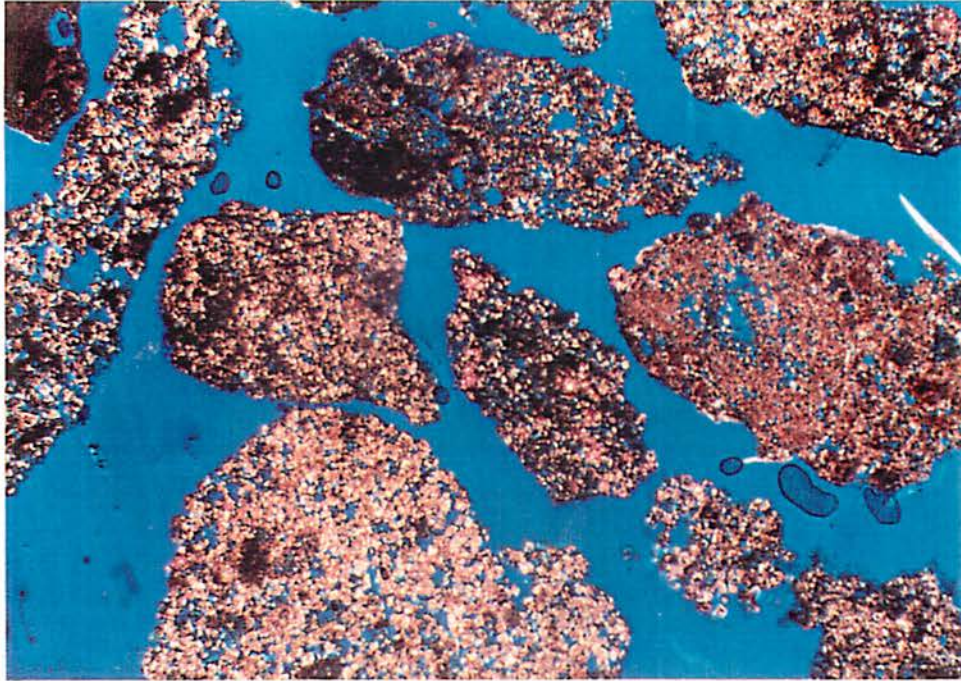


Figure No. 6-34. NBA-1, 746.5-56.5 The cuttings are very fine to fine dolomite with moldic, vuggy, and intercrystalline porosity. Type 3. 20x

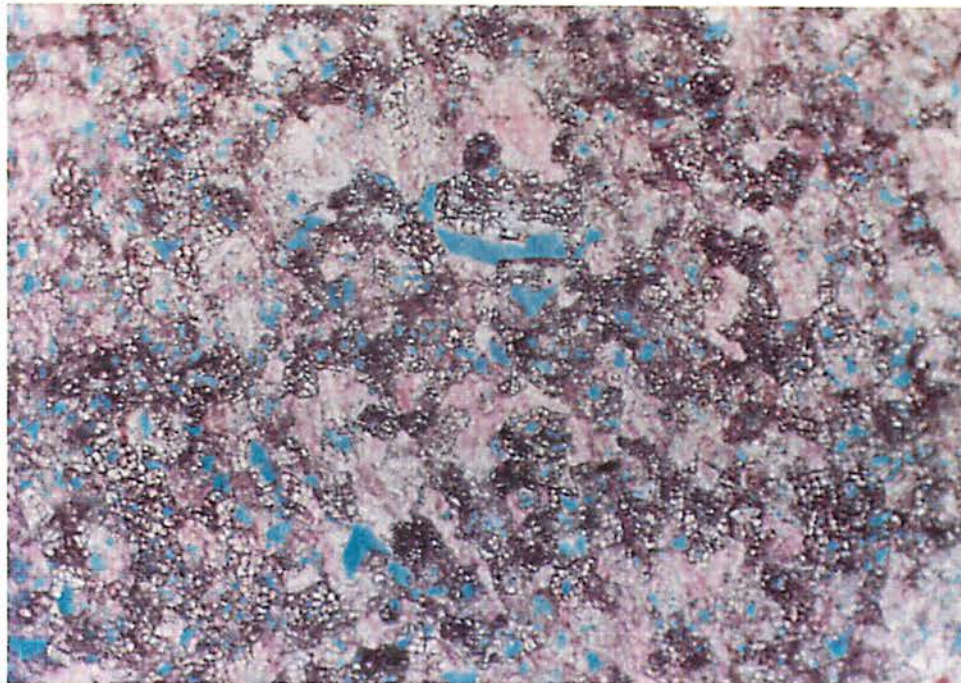


Figure No. 6-35. NBC-1, 918.1-28.1 Sparry calcite (light pink) has occluded much of the porosity in what would otherwise be a very high porosity and high permeability dolomite. Type 3 rock. 100x

Porosity is lower in this interval than in the Grainstone Member or the Person Formation (excluding the Regional Dense Member). This section has less chert than the Person Formation above the Regional Dense Member.

San Marcos

The section at San Marcos also consists of alternating limestone and dolomite. At least 50 percent of the rock is limestone. Dolomoldic porosity and sparry calcite are common throughout the section; more so at the C-site. The same rock and aquifer types occur at both San Marcos and New Braunfels, but the percentages vary (refer to Figure Nos. 6-32 to 6-37):

1. The San Marcos section has more limestone.
2. Dolomoldic porosity is more abundant at San Marcos.
3. Sparry calcite cement is more abundant at San Marcos.
4. The limestone at San Marcos has higher porosity, with a greater abundance of Types 3 and 4 rocks.

If the presence of abundant dolomoldic porosity and sparry calcite is a reliable indicator of fresh water diagenesis, then the San Marcos C and D wells have been exposed to fresh water for a considerable period of time. The C-site has been more extensively altered.

6.1-2.3-3 BASAL NODULAR MEMBER

New Braunfels and San Marcos

This section consists of alternating limestone and dolomite. The limestones are predominantly miliolid and peloid packstones. Rock types 2 and 3 are most common, with a minor amount of Type 4. Refer to Figure Nos. 6-38 and 6-39.

The fine to very fine dolomites are Types 1, 2, 3 and 4. Types 2 and 3 predominate. Dolomoldic porosity is scattered throughout the section in all the wells.

KAINER FORMATION (continued)
KIRSCHBERG AND DOLOMITIC MEMBERS (UNDIFFERENTIATED)

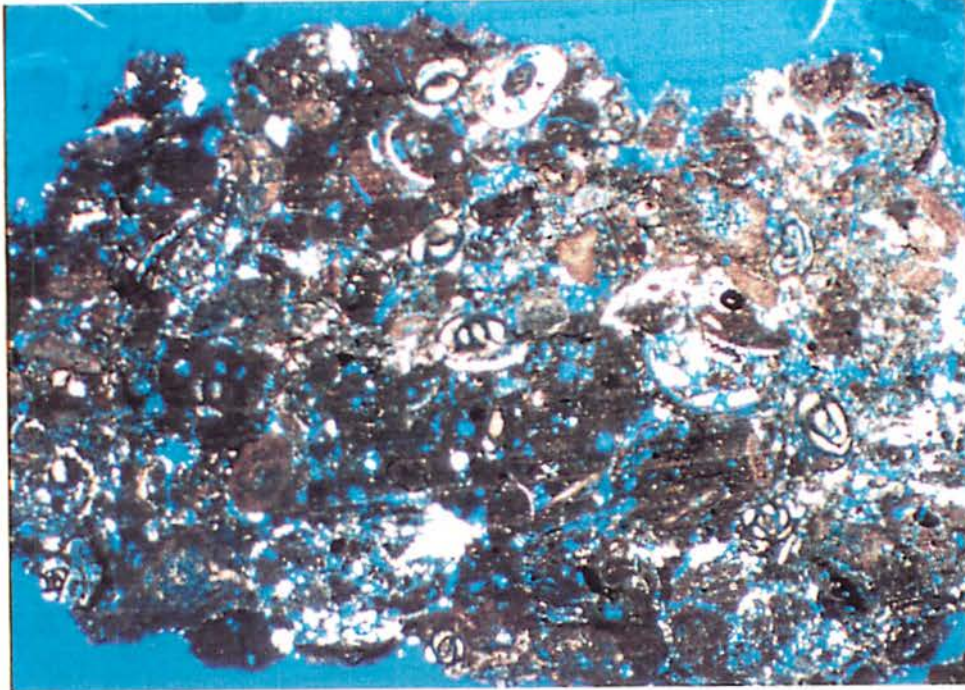


Figure No. 6-36. SMD, 763-74.6 The rock is a medium porosity (Type 3) miliolid packstone. Pores are intergranular, moldic, and intraparticle. 20x

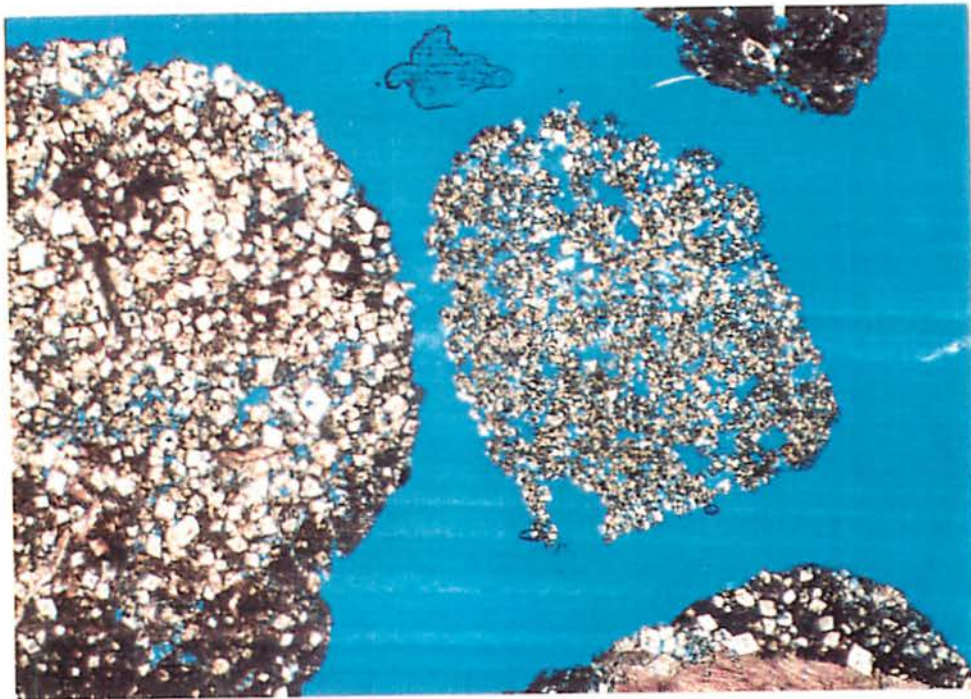


Figure No. 6-37. SMD, 731-43.1 The cuttings on the left and bottom right of the photomicrograph are shaly, very fine dolomitic limestone. Porosity is very low. The cutting on the right is a high porosity, very fine dolomite. Porosity is intercrystalline, moldic, and vuggy. 40x

KAINER FORMATION (continued)
BASAL NODULAR MEMBER



Figure No. 6-38. NBC-1, 949.1-59.1 Most of the cuttings are Types 2 or 3. All of the cutting are fine to very fine dolomite, except the dolomitic, miliolid packstone at the bottom left. 20x



Figure No. 6-39. SMC, 886.4-97 The rock is dolomitic wackestone. Type 1 rock. 40x

Only two wells (San Marcos C and New Braunfels A-1) penetrated the entire section. Differences between the Basal Nodular Member at the two sites are as follows:

1. The New Braunfels section is largely dolomite, while the San Marcos section is largely limestone.
2. The limestones at San Marcos have lower porosities than those at New Braunfels.
3. The San Marcos section has more dolomoldic porosity.
4. The New Braunfels section has too much porosity and permeability to be confining unit. The San Marcos section has low enough porosity and permeability to be a confining unit.

6.2 ANALYSIS OF THE BOREHOLE GEOPHYSICAL LOGS

Extensive suites of slimhole and conventional (petroleum-type) logging tools were run in each of the five wells (Table No. 6-1). The logging was conducted in conjunction with Texas Water Development Board research project 8-483-511, which was a study to evaluate the application of borehole geophysical techniques to ground-water aquifers in Texas.

6.2-1 METHODOLOGY

This report utilized only those logging curves germane to this study: caliper, gamma ray, compensated neutron, compensated density, photoelectric, and fluid resistivity. These curves, along with a few others which were added for the sake of completeness, are contained herein. For ease in handling, the logs were reproduced as plates and are located in a pocket at the back of this volume. The rest of the logs are on file at the EUWD office.

The logs were normalized and plotted using Terrasciences' TerraStation log analysis software. The logs were plotted from the base of surface casing to total depth (T.D.). The logs from each well were plotted using the same format (if the appropriate logs were available) and the same scale (2.5 inches equals 100 feet). The neutron porosity and the density-neutron crossplot porosity curves from the San Marcos B well are not included because the neutron porosity curve is incorrect and Schlumberger has been unable to correct it.

TABLE NO. 6-1 BOREHOLE GEOPHYSICAL LOGS RAN IN EACH WELL

NEW BRAUNFELS A-1

Schlumberger
 Dual Induction-SFL
 Phasor Induction-SFL
 Dual Laterolog-MSFL
 Compensated Neutron-Lithodensity
 Long Spacing Sonic with Waveforms
 Electromagnetic Propagation
EUWD
 Short and Long Normal
 Gamma Ray
 Caliper
 Fluid Resistivity
 Temperature

NEW BRAUNFELS B-1

Schlumberger
 Dual Induction-SFL
 Phasor Induction-SFL
 Dual Laterolog-MSFL
 Compensated Neutron-Lithodensity
 Long Spacing Sonic with Waveforms
 Electromagnetic Propagation
EUWD
 Short Normal
 Gamma Ray
 Caliper
 Fluid Resistivity
 Temperature

NEW BRAUNFELS C-1

Schlumberger
 Dual Induction-SFL
 Compensated Neutron-Lithodensity
 Borehole Compensated Sonic
 Formation Microscanner
EUWD
 Short and Long Normal
 Gamma Ray
 Caliper
 Fluid Resistivity
 Temperature

SAN MARCOS B

Schlumberger
 Dual Induction-SFL
 Phasor Induction-SFL
 Array Induction-MSFL
 Dual Laterolog
 Compensated Neutron-Lithodensity
 Long Spacing Sonic with Waveforms
EUWD
 Short and Long Normal
 Fluid Resistivity
 Temperature

SAN MARCOS C

Schlumberger
 Dual Induction-SFL
 Phasor Induction-SFL
 Array Induction-MSFL
 Dual Laterolog
 Long Spacing Sonic with Waveforms
 Compensated Neutron-Lithodensity
 Hi-Resolution Compensated
 Neutron-Lithodensity
EUWD
 Short and Long Normal
 Fluid Resistivity
 Temperature

SAN MARCOS D

Halliburton
 Dual Induction-Gard
 Compensated Spectral
 Natural Gamma Ray Log
 Spectral Density
 Dual Spaced Neutron II
 Dual Spaced Epithermal Neutron
EUWD
 Short and Long Normal
 Gamma Ray
 Caliper
 Fluid Resistivity
 Temperature

EDWARDS UNDERGROUND WATER DISTRICT

Environmental corrections were only applied to the gamma ray logs. They were not necessary for other logs because:

1. The bit size is 7 7/8 inches.
2. Most of the washouts were less than 2 inches in the New Braunfels wells. Although washouts of up to 5 inches are present in the San Marcos wells, the borehole diameter is usually less than 12 inches.
3. There was very little filtrate invasion since the wells were drilled by reverse air rotary.
4. The ratio of formation resistivity to borehole fluid resistivity is low.

The TerraStation software was used to analyze the log data:

1. A density-neutron crossplot porosity curve was calculated for each well except the San Marcos B well. The curve is located in Track 3 of Plate Nos. 6-3 to 6-7. This crossplot technique yields accurate porosity values that have been corrected for the effect of lithology.
2. Apparent grain density curves were calculated from a crossplot of the density and neutron logs.
3. Relative proportions of limestone, dolomite, shale, and porosity were calculated using the Petra Lithologic Analysis program. The lithology plots are in Track 1 of Plate Nos. 6-3 to 6-7. The program used the overdetermined case relationship:

where:

$$N + 1 > M$$

N = the number of log curves

M = the number of lithology and porosity equations solved for in the program

The log curves used in the calculations were gamma ray, bulk density, photoelectric, and neutron porosity. The lithologic log-response constants utilized in the calculations are listed in Table No. 6-2. This combination of inputs was deemed to provide the most accurate answers, based upon a comparison of calculations utilizing various values for the constants, various combinations of input logs, and various lithologies. However, a spectral gamma ray ran in the last well (San Marcos D) revealed that much the gamma ray response was from uranium, not shale. The gamma ray response of clean shale was determined to be 25 API units, rather than the 15 API units listed in Table No. 6-2. If this finding is valid for the other wells, then the shale volume displayed on the lithology plots is too high (see Figure No. 6-58). Quartz (chert) was not included in the lithology plots because the program grossly overestimated the percentage of quartz. A plot was not made of the San Marcos B well because an accurate neutron log was not available.

4. In order to facilitate comparisons of log responses between wells, overlays were made of the gamma ray, photoelectric, and density-neutron crossplot porosity curves. Overlays were constructed for the New Braunfels A-1 and C-1 wells (Plate No. 6-1) and the New Braunfels A-1 and San Marcos C wells (Plate No. 6-2). No overlay was constructed for the San Marcos C and D wells because of differences in the thicknesses of the Person Formation. For each composite the curves were correlated to the New Braunfels B-1 well and hung on the Regional Dense Member. Although the Edwards section varies somewhat in thickness from well to well, this was deemed the best way to overlay the curves.
5. Neutron porosity-bulk density, neutron porosity-gamma ray, and gamma ray-bulk density crossplots (Figure Nos. 6-40 to 6-48) were constructed to facilitate comparisons of the differences in petrophysical properties between wells and between different intervals in a single well. Crossplots were constructed for the Person Formation (excluding the Regional Dense Member), the Regional Dense Member, and the Kainer Formation

TABLE NO. 6-2 LOG-RESPONSE CONSTANTS FOR VARIOUS LITHOLOGIES

LOG CURVE	LOG-RESPONSE CONSTANTS			
	Dolomite (0% porosity; single mineralogy)	Limestone	Shale	100% Porosity (fresh water)
Gamma Ray (API units)	15	15	120	10
Bulk Density (g/cm ³)	2.87	2.71	2.91	1
Photoelectric (barns per electron)	3	5	3	4
Neutron Porosity (%)	0.07	0	0.3	1

EDWARDS UNDERGROUND WATER DISTRICT

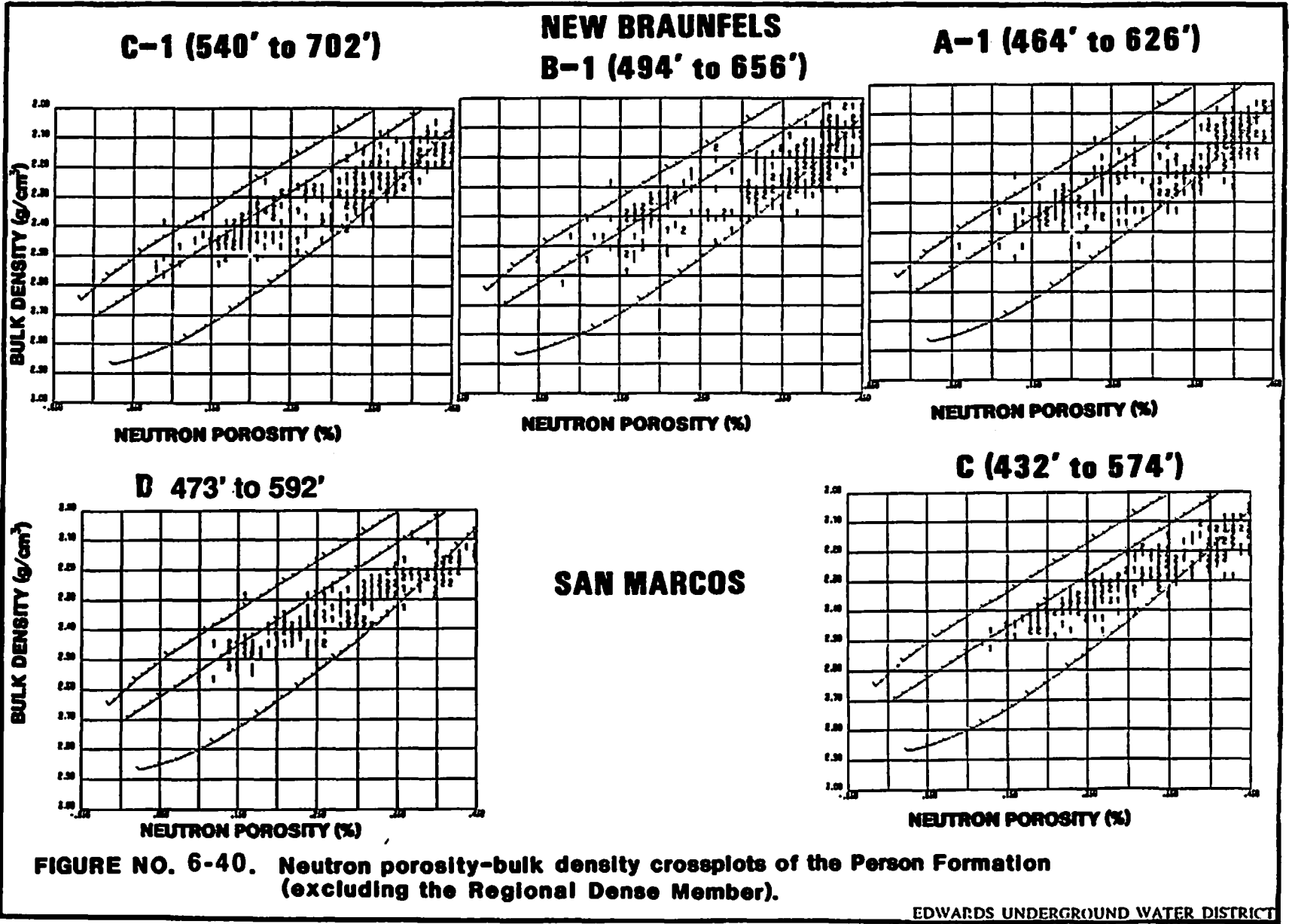
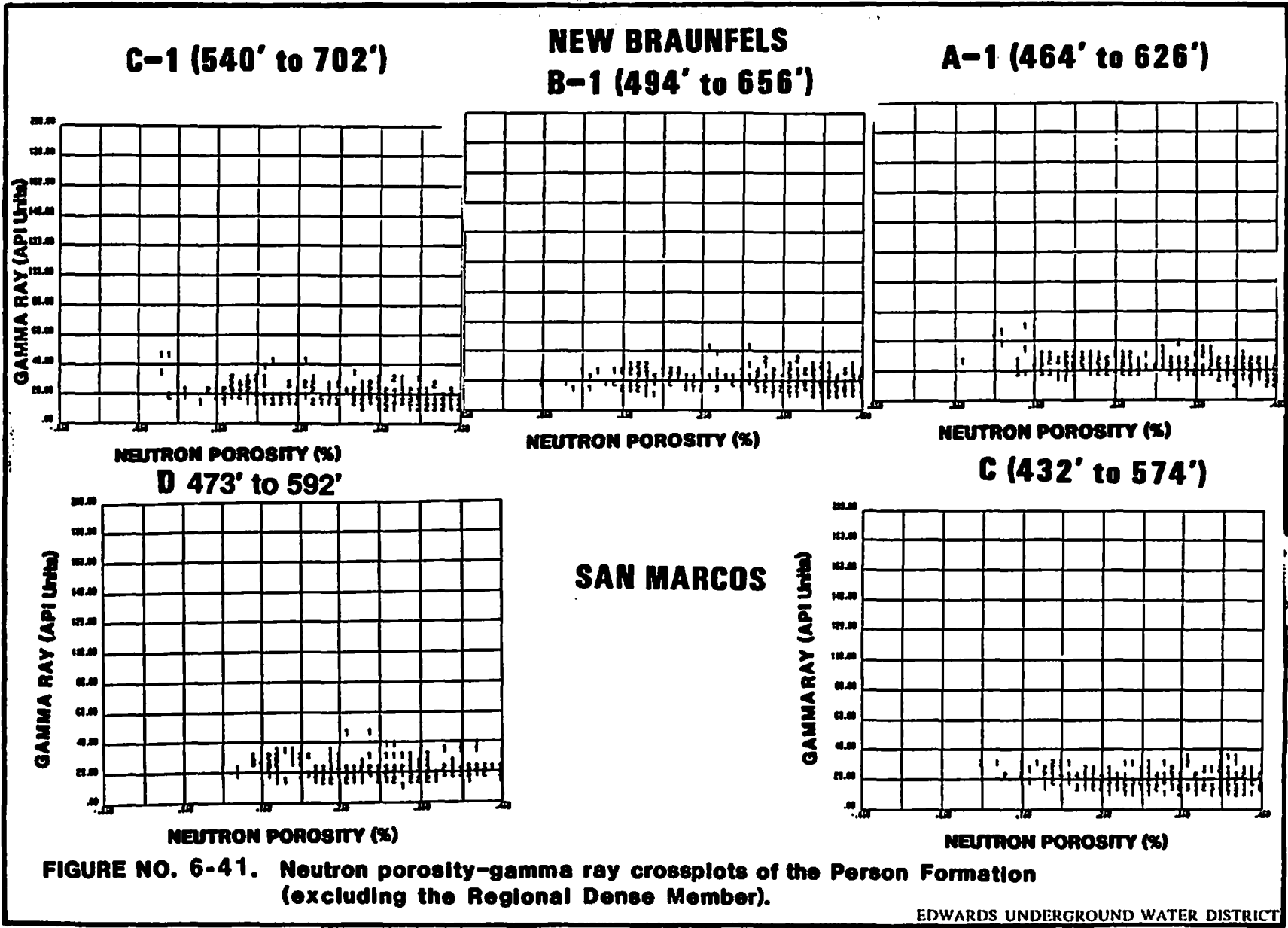
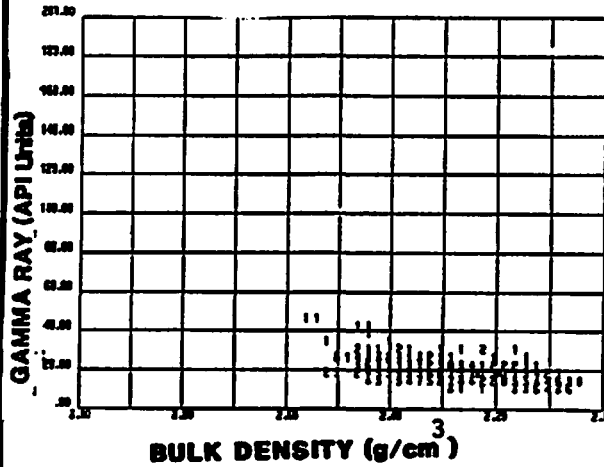


FIGURE NO. 6-40. Neutron porosity-bulk density crossplots of the Person Formation (excluding the Regional Dense Member).

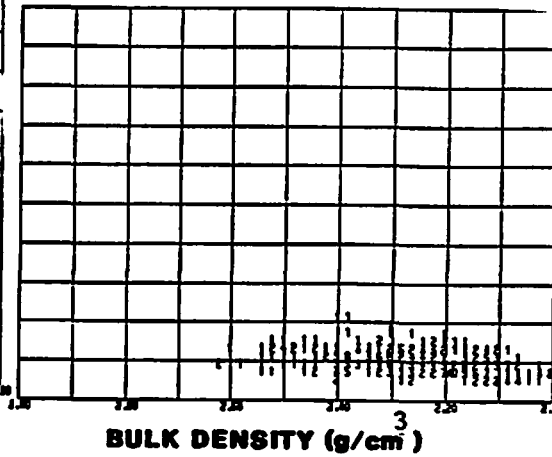
EDWARDS UNDERGROUND WATER DISTRICT



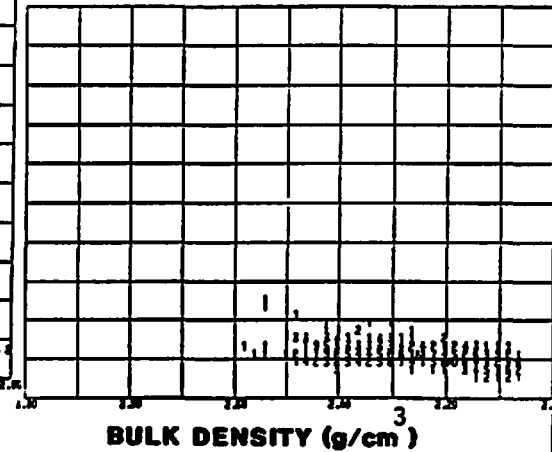
C-1 (540' to 702')



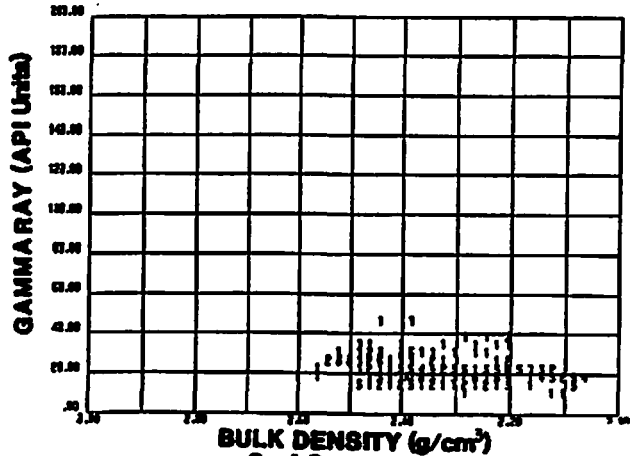
**NEW BRAUNFELS
B-1 (494' to 656')**



A-1 (464' to 626')



D 473' to 592'



SAN MARCOS

C (432' to 574')

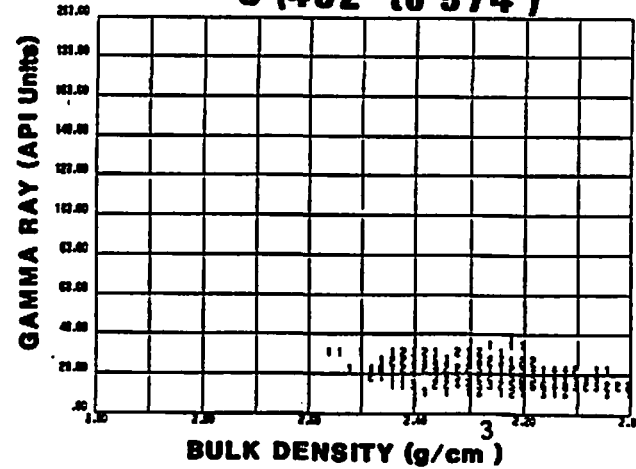


FIGURE NO. 6-42. Gamma ray-bulk density crossplots of the Person Formation (excluding the Regional Dense Member).

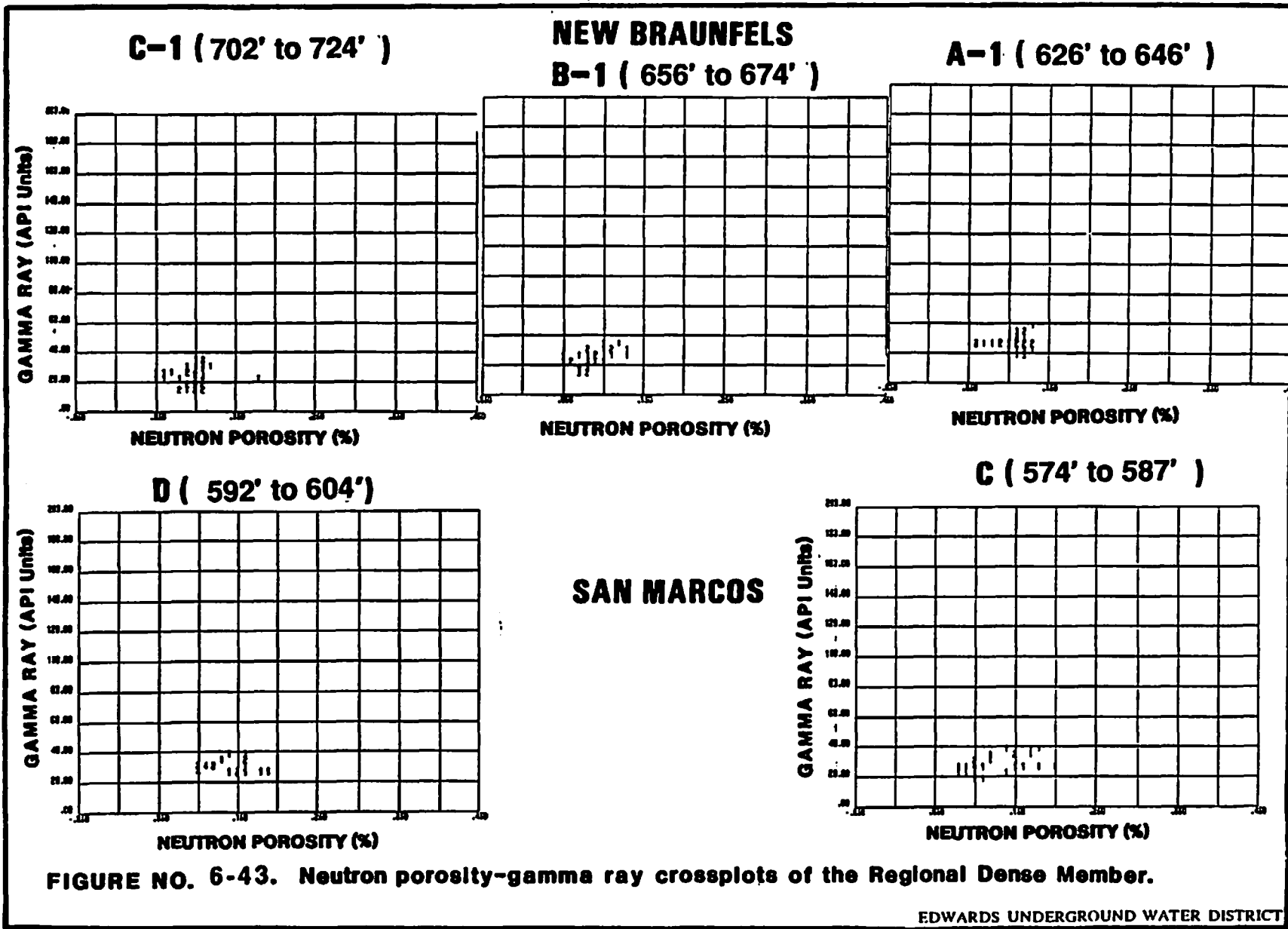
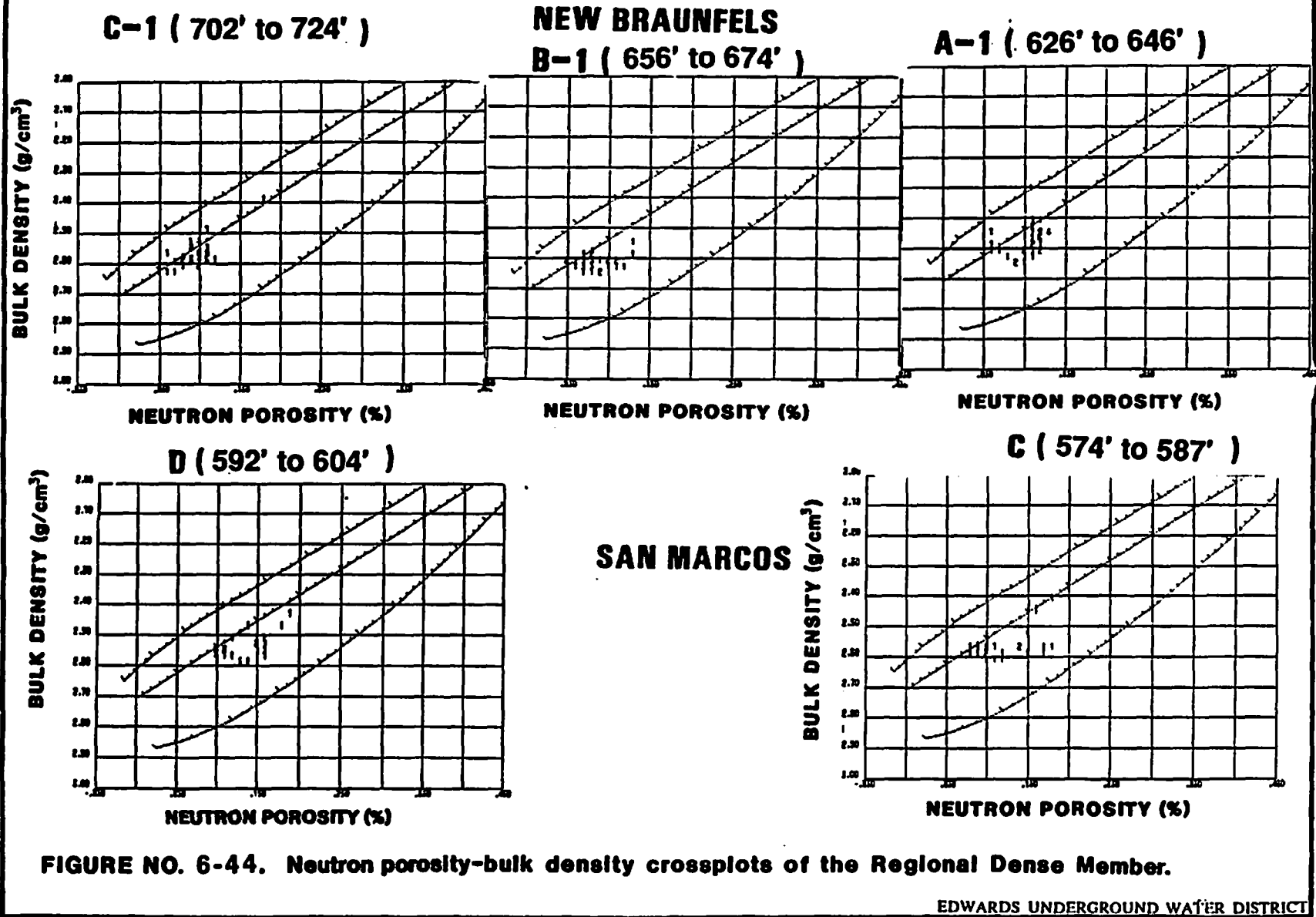


FIGURE NO. 6-43. Neutron porosity-gamma ray crossplots of the Regional Dense Member.



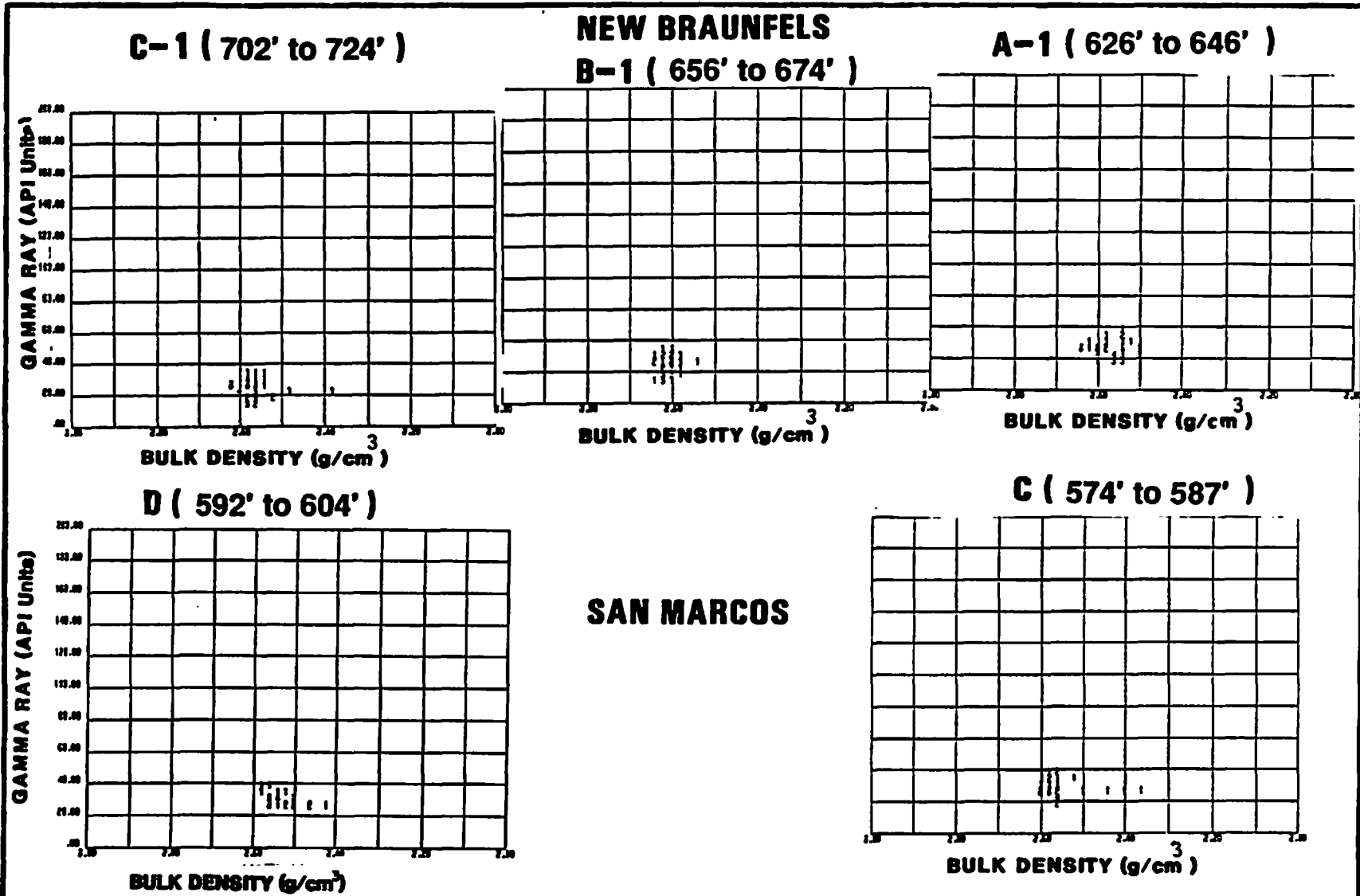


FIGURE NO. 6-45. Gamma ray-bulk density crossplot of the Regional Dense Member.

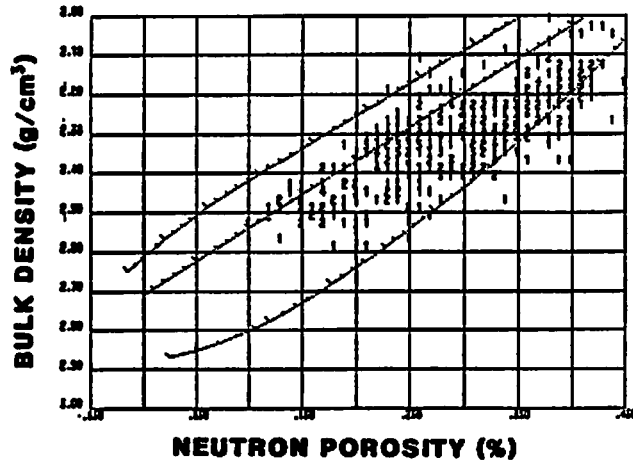
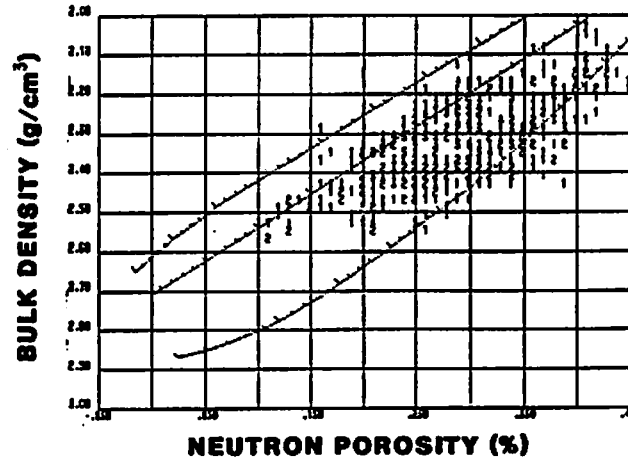
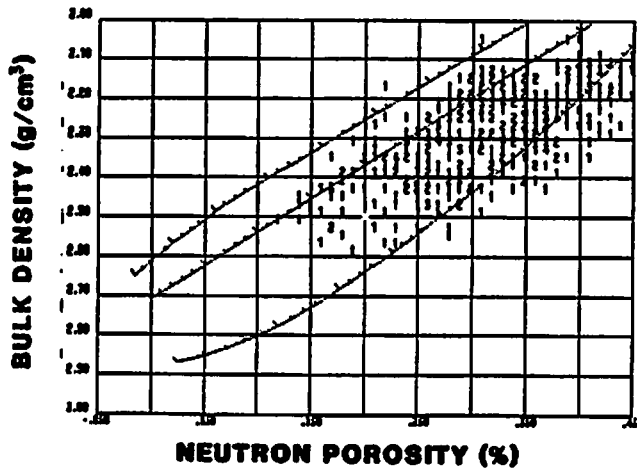
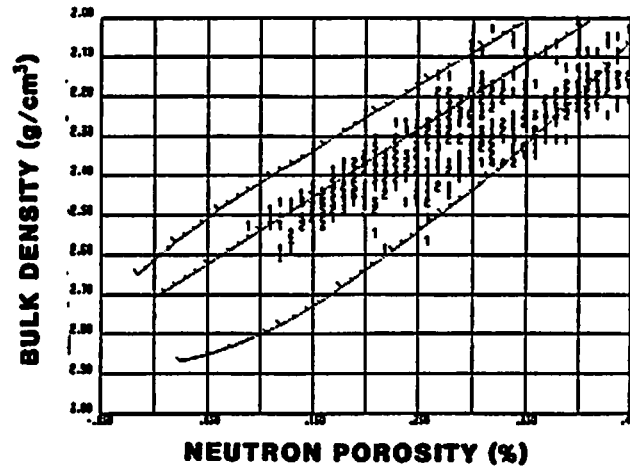
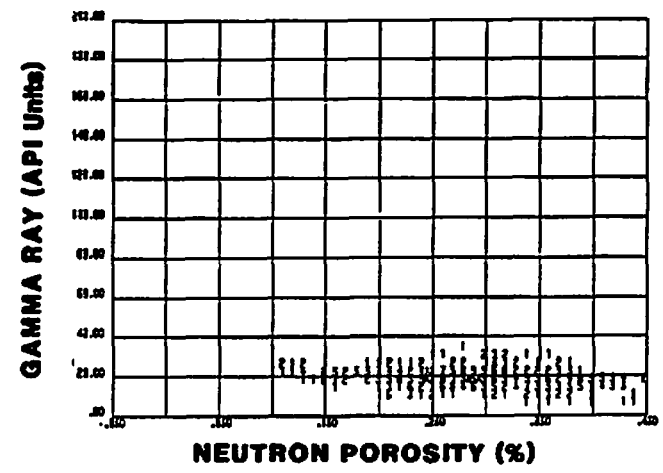
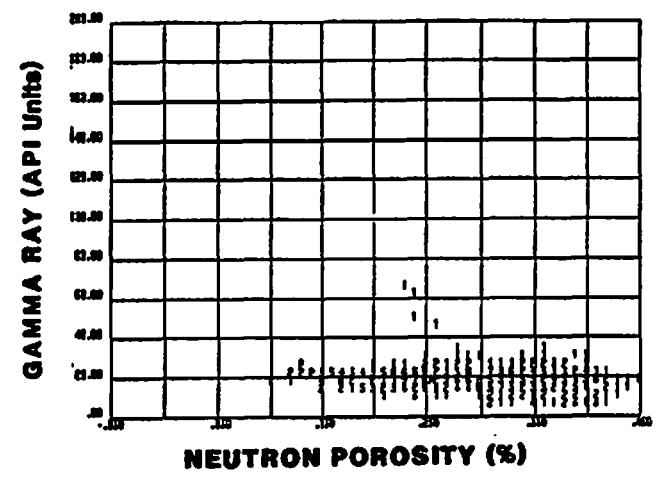
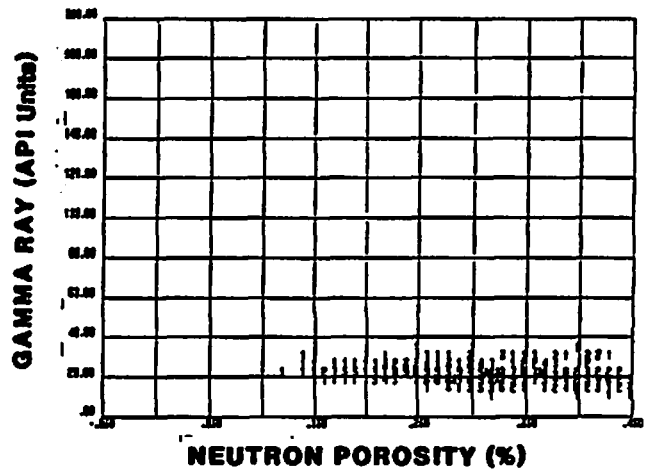
NEW BRAUNFELS C-1 (724' to 940')**NEW BRAUNFELS B-1 (674' to 900')****NEW BRAUNFELS A-1 (646' to 874')****SAN MARCOS C (587' to 853')**

FIGURE NO. 6-46. Neutron porosity-bulk density crossplots of the Kainer Formation (excluding the Basal Nodular Member).

NEW BRAUNFELS C-1 (724' to 940') NEW BRAUNFELS B-1 (674' to 900')



NEW BRAUNFELS A-1 (646' to 874')



SAN MARCOS C (587' to 853')

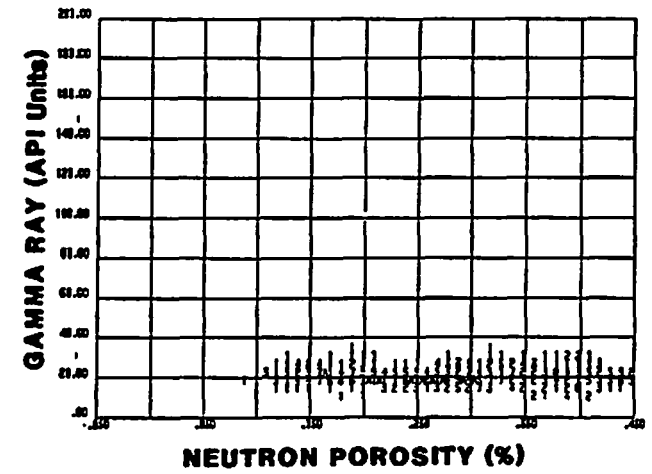
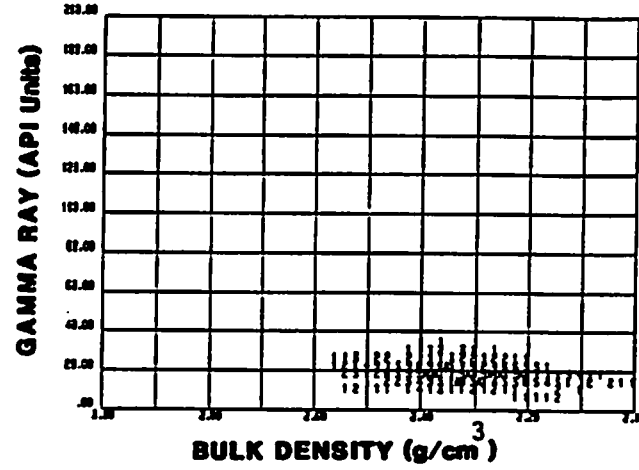
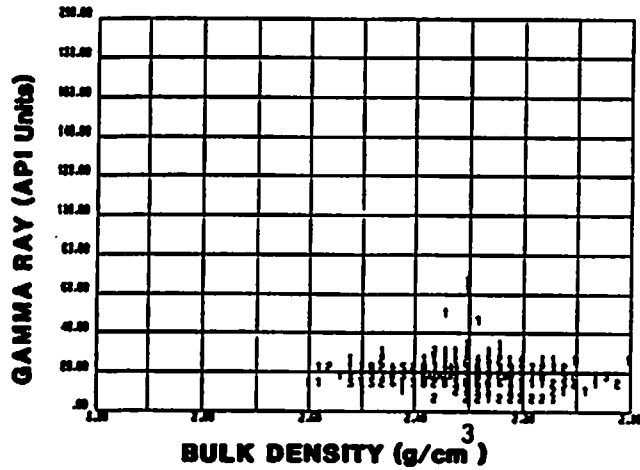


FIGURE NO. 6-47. Neutron porosity-gamma ray crossplots of the Kainer Formation (excluding the Basal Nodular Member).

NEW BRAUNFELS C-1 (724' to 940') NEW BRAUNFELS B-1 (674' to 900')



NEW BRAUNFELS A-1 (646' to 874') SAN MARCOS C (587' to 853')

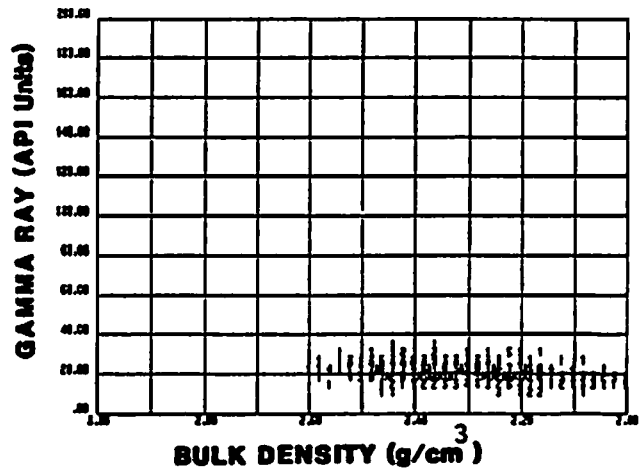
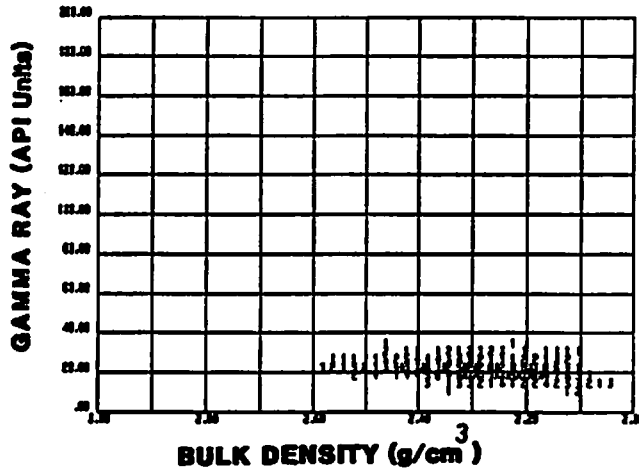


FIGURE NO. 6-48. Gamma ray-bulk density crossplots of the Kalner Formation (excluding the Basal Nodular Member).

(excluding the Basal Nodular Member). The Georgetown Formation and the Basal Nodular Member of the Kainer Formation were not included in the crossplots because varying amounts of the intervals were logged in each well. Surface casing was set part of the way through the Georgetown Formation and some wells did not penetrate all of the Basal Nodular Member. The San Marcos B well was not included. In Figure Nos. 6-40 to 6-48 the wells are arranged from left to right in order of increasing formation water salinity.

6. Normalized histograms (Figure No. 6-49 to 6-56) were constructed of four log responses (gamma ray, apparent grain density, density-neutron crossplot porosity, and photoelectric factor) in order to quantify the differences in petrophysical properties between wells and between different intervals in a single well. Overall, the histograms were more helpful than the crossplots in delineating trends. Histograms were constructed for the Person Formation (excluding the Regional Dense Member), the Regional Dense Member, the Kainer Formation (excluding the Basal Nodular Member), and the Edwards Group (excluding the Georgetown Formation and the Basal Nodular Member). The mean, median, mode, and skewness of each histogram were calculated. The software calculates the values to three decimal places, but in reality the numbers are significant to only the first decimal place. Numbers on the right side of each histogram indicate what percent of the entire sample population occurs within each log-value increment.

7. An apparent formation water resistivity (RWA) curve was calculated for each well. The following equation was used to calculate RWA:

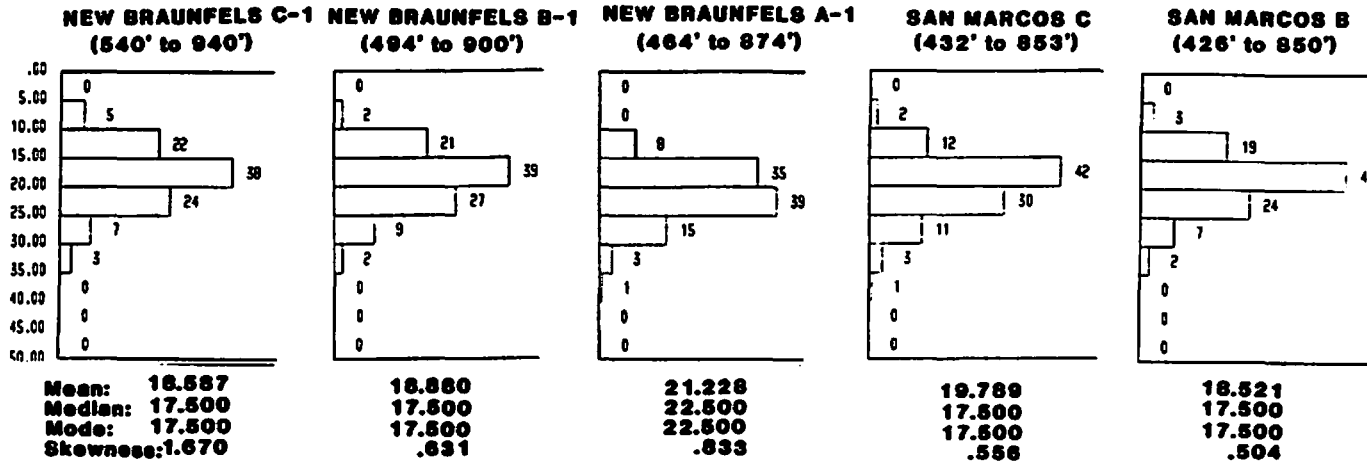
$$RWA = Rt(\text{Porosity})$$

where:

RWA = apparent formation water resistivity at formation temperature

Rt = resistivity of the formation 100 percent saturated with water

GAMMA RAY VALUES (API UNITS)



APPARENT GRAIN DENSITY VALUES (gms/cm³)

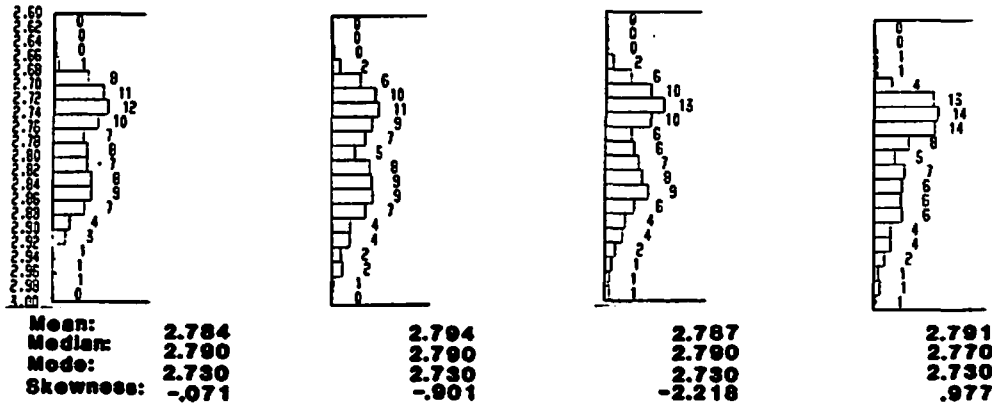
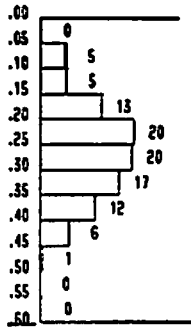


FIGURE NO. 6-49. Normalized histograms of the gamma ray and apparent grain density values of the Edwards Aquifer (excluding the Georgetown Formation and the Basal Nodular Member).

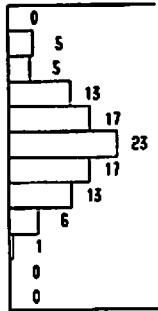
CROSSPLOT POROSITY VALUES (%)

NEW BRAUNFELS C-1
(540' to 940')



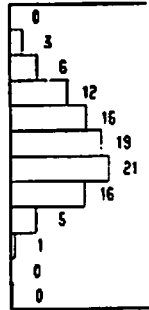
Mean: .266
Median: .275
Mode: .225
Skewness: .196

NEW BRAUNFELS B-1
(494' to 900')



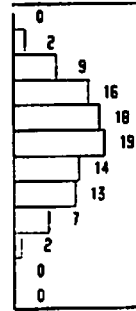
.271
.275
.275
.173

NEW BRAUNFELS A-1
(464' to 874')



.281
.275
.325
.423

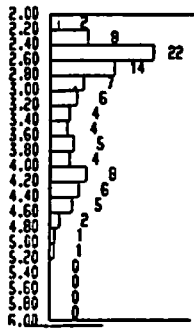
SAN MARCOS C
(432' to 853')



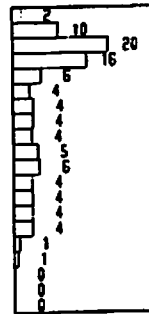
.266
.276
.275
.130

SAN MARCOS B
(426' to 850')

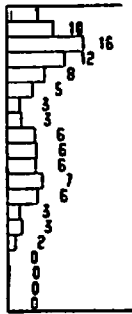
PHOTOELECTRIC FACTOR VALUES



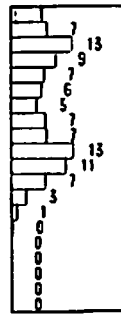
Mean: 3.186
Median: 2.900
Mode: 2.500
Skewness: .696



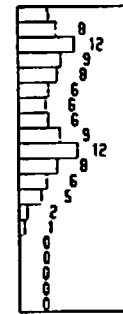
3.240
2.900
2.500
.785



3.309
3.100
2.500
.344



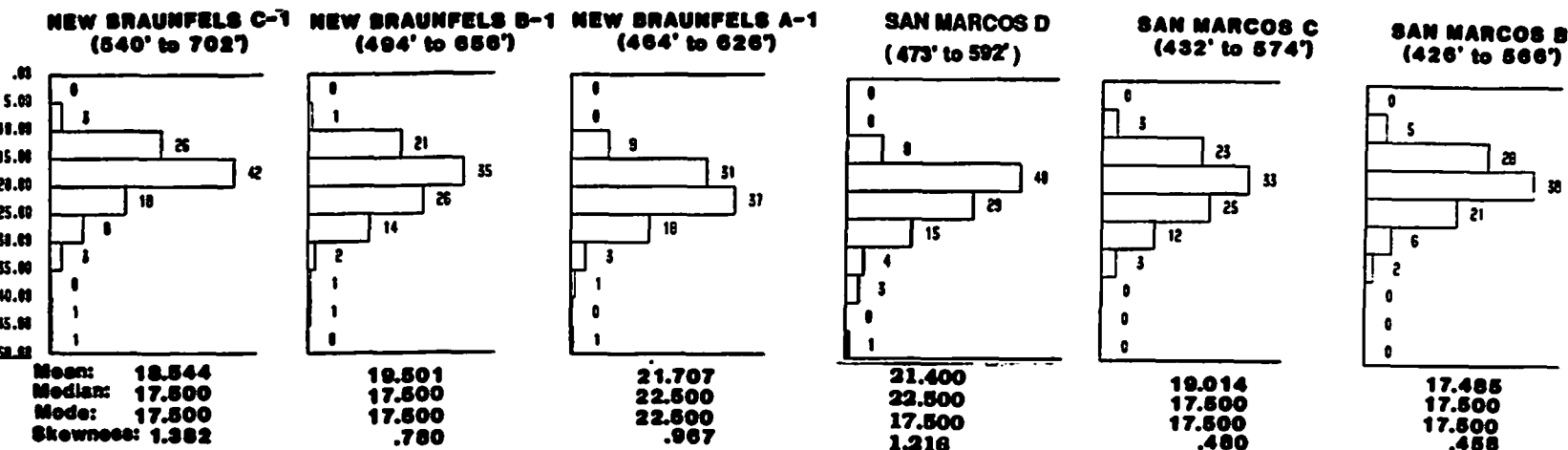
3.363
3.500
3.900
-.014



3.371
3.500
3.900
.102

FIGURE NO. 6-50. Normalized histograms of the density-neutron crossplot porosity and photoelectric factor values of the Edwards Aquifer (excluding the Georgetown Formation and the Basal Modular Member).

GAMMA RAY VALUES (API UNITS)



APPARENT GRAIN DENSITY VALUES (g/cm³)

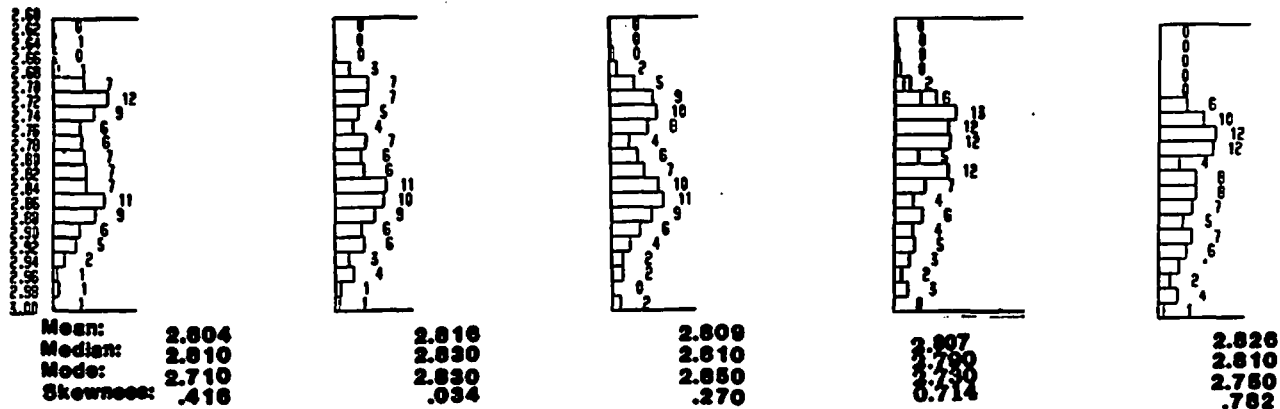
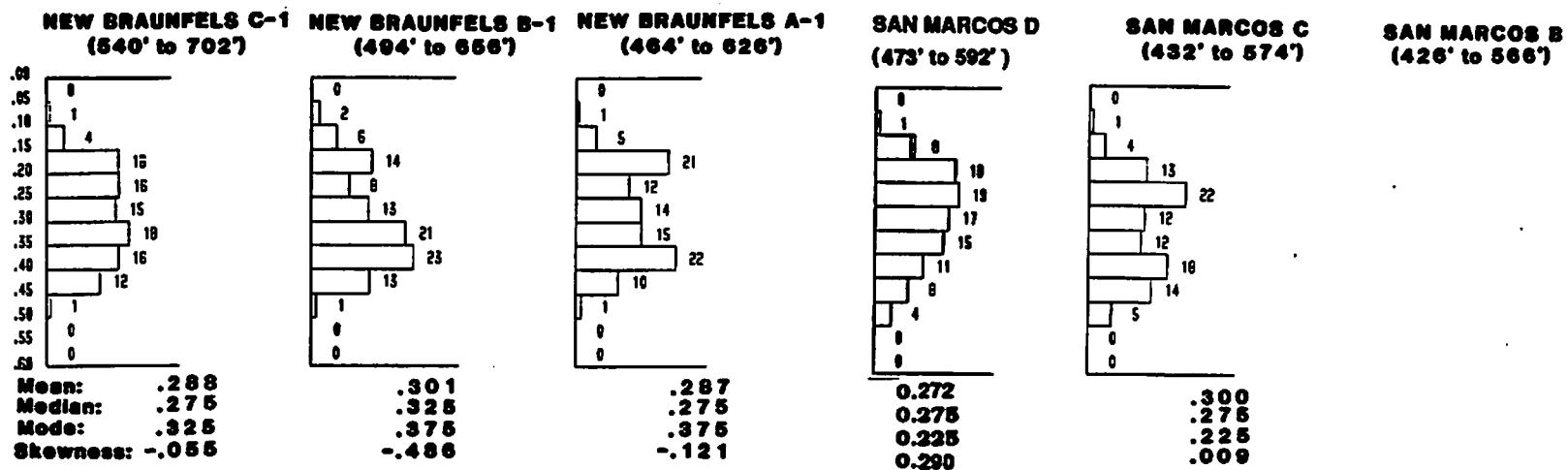


FIGURE NO. 6-51. Normalized histograms of the gamma ray and apparent grain density values of the Person Formation (excluding the Regional Dense Member).

EDWARDS UNDERGROUND WATER DISTRICT

CROSSPLOT POROSITY VALUES (%)



PHOTOELECTRIC FACTOR VALUES

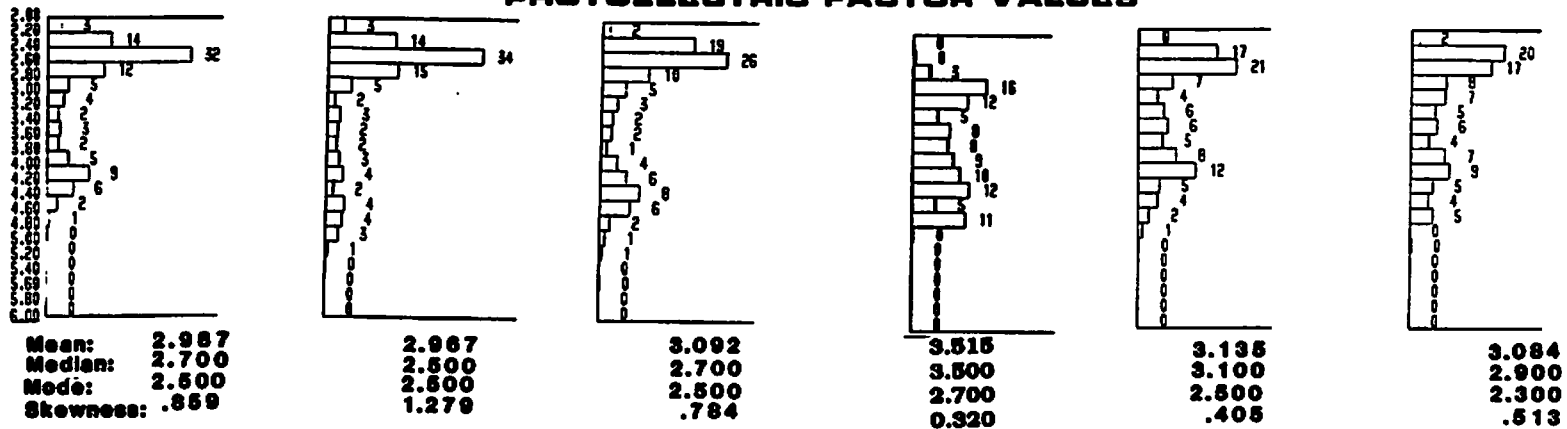
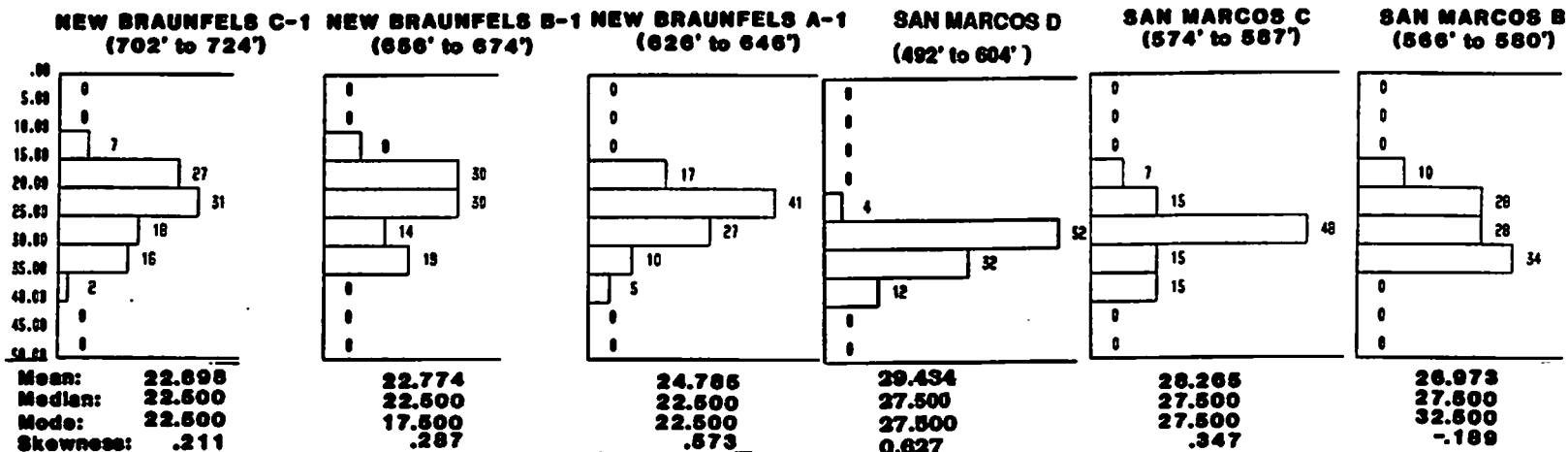


FIGURE NO. 6-52 Normalized histograms of the density-neutron cross plot porosity and photoelectric factor values of the Person Formation (excluding the Regional Dense Member).

GAMMA RAY VALUES (API UNITS)



APPARENT GRAIN DENSITY VALUES (g/cm³)

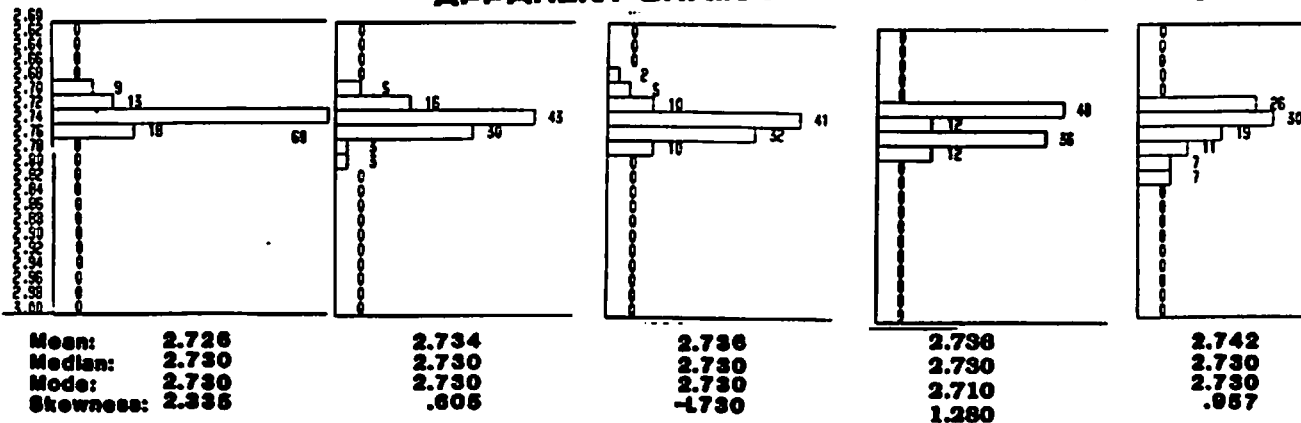
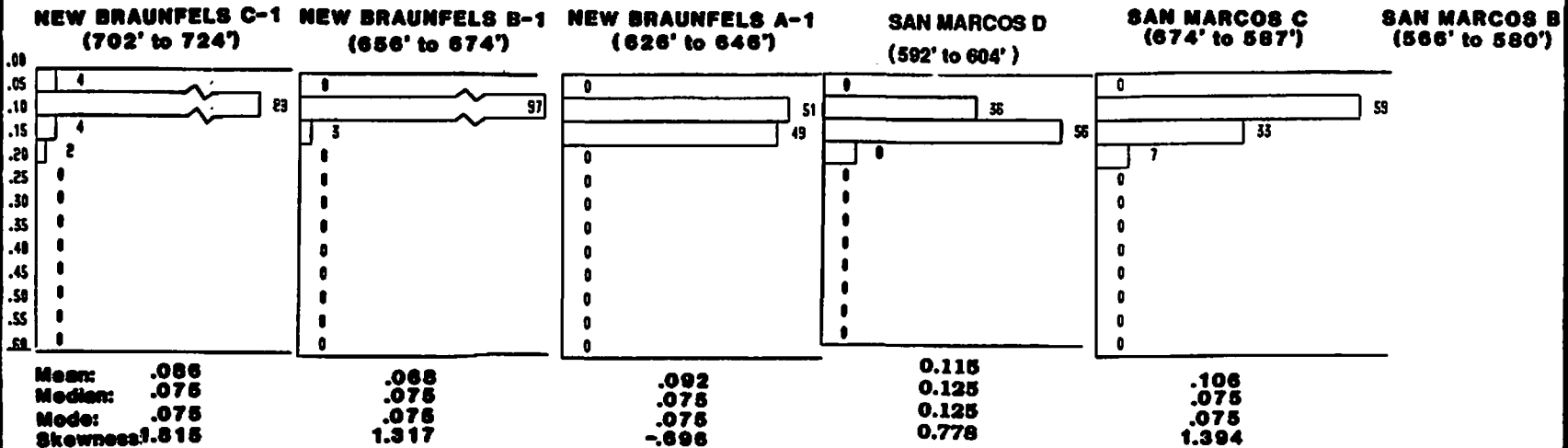


FIGURE NO. 6-53. Normalized histograms of the gamma ray and apparent grain density values of the Regional Dense Member.

CROSSPLOT POROSITY VALUES (%)



PHOTOELECTRIC FACTOR VALUES

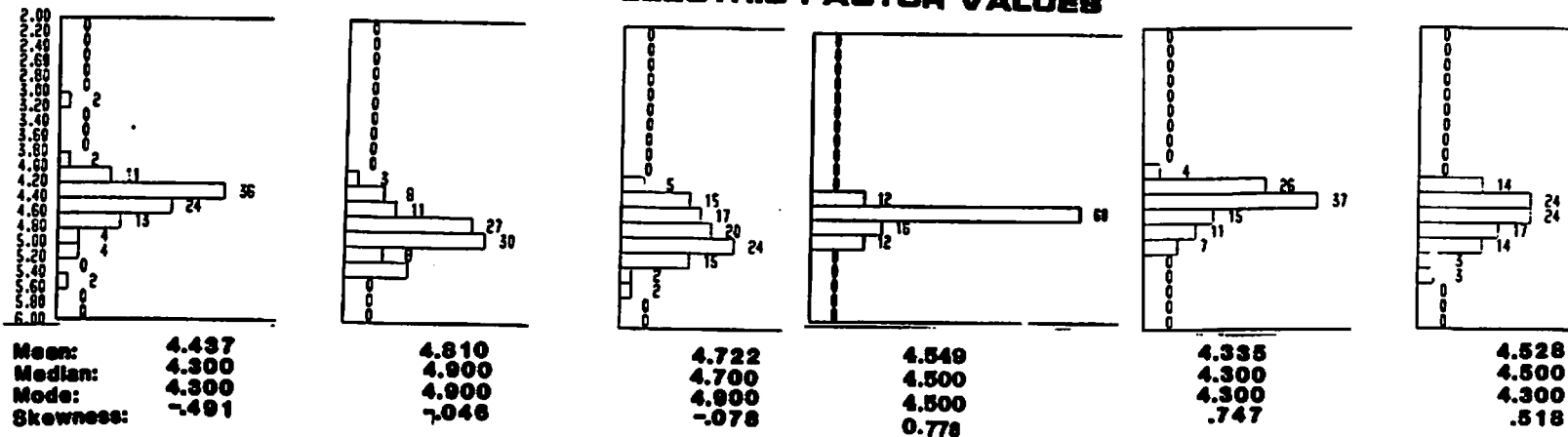
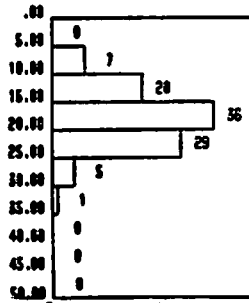


FIGURE NO. 6-54. Normalized histograms of the density-neutron crossplot porosity and photoelectric factor values of the Regional Dense Member.

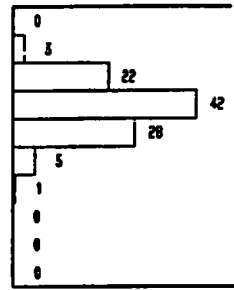
EDWARDS UNDERGROUND WATER DISTRICT

GAMMA RAY VALUES (API UNITS)

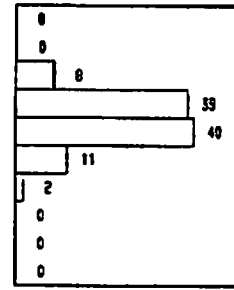
**NEW BRAUNFELS C-1
(724' to 940')**



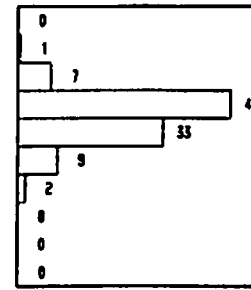
**NEW BRAUNFELS B-1
(674' to 900')**



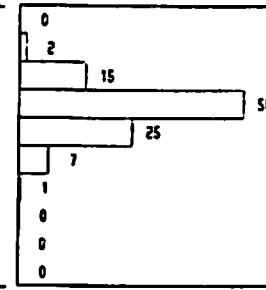
**NEW BRAUNFELS A-1
(646' to 874')**



**SAN MARCOS C
(587' to 853')**



**SAN MARCOS B
(580' to 860')**



Mean:
Median:
Mode:
Skewness:

18.178
17.500
17.500
2.072

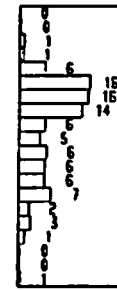
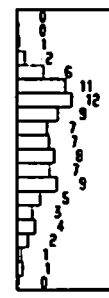
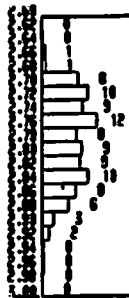
18.128
17.500
17.500
.167

20.679
22.500
22.500
.335

19.807
17.500
17.500
.445

18.625
17.500
17.500
.444

APPARENT GRAIN DENSITY VALUES (g/cm³)



Mean:
Median:
Mode:
Skewness:

2.775
2.790
2.750
-.633

2.783
2.770
2.730
-1.899

2.776
2.790
2.730
-2.699

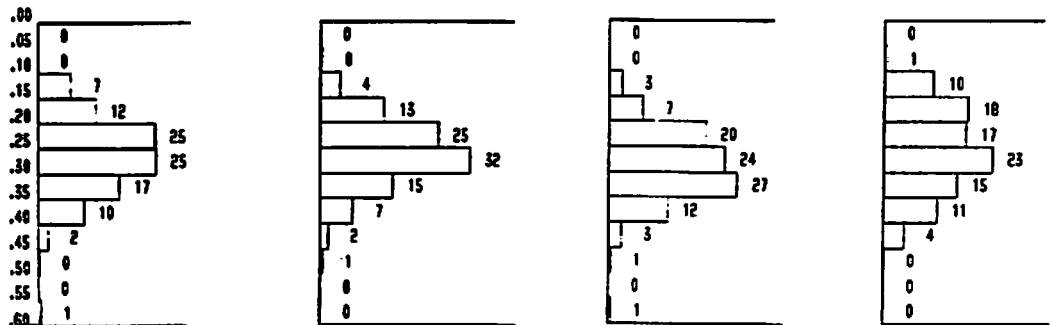
2.777
2.750
2.710
.915

FIGURE

NO. 6-55. Normalized histograms of the gamma ray and apparent grain density values of the Kainer Formation (excluding the Basal Nodular Member).

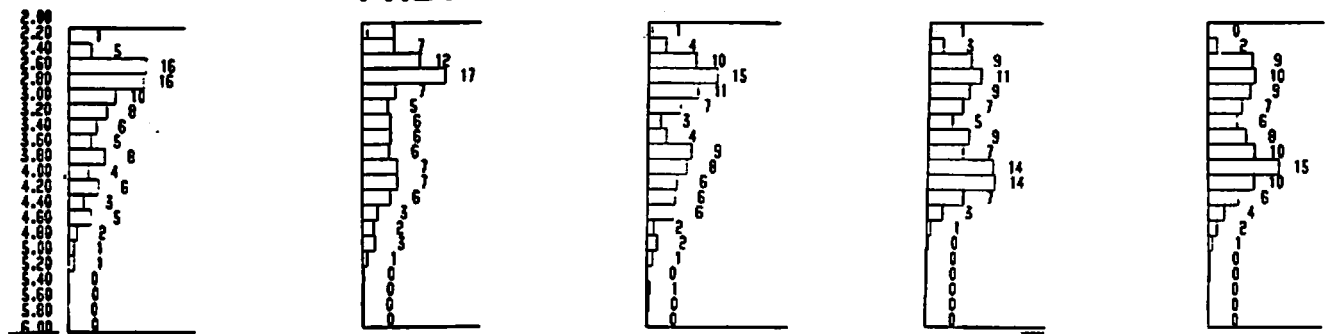
CROSSPLOT POROSITY VALUES (%)

NEW BRAUNFELS C-1 (724' to 940') **NEW BRAUNFELS B-1 (674' to 900')** **NEW BRAUNFELS A-1 (646' to 874')** **SAN MARCOS C (587' to 853')** **SAN MARCOS B (560' to 850')**



Mean:	.268	.265	.293	.257
Median:	.275	.275	.275	.275
Mode:	.275	.275	.325	.275
Skewness:	.925	1.491	1.449	.144

PHOTOELECTRIC VALUES



Mean:	3.211	3.314	3.344	3.439	3.461
Median:	3.100	3.100	3.300	3.500	3.500
Mode:	2.500	2.700	2.700	4.100	3.900
Skewness:	.636	.718	.177	-.161	-.034

FIGURE NO. 6-56. Normalized histograms of the density-neutron cross plot porosity and photoelectric factor values of the Kalmer Formation (excluding the Basal Nodular Member).

Porosity = total porosity of the rock

The SFL or Guard curve was used for Rt. The density-neutron crossplot porosity was used for Porosity.

- 8. The sonic log was not included in the crossplots and histograms because**
 - a. Digitized sonic logs were not available for the New Braunfels C-1 and San Marcos C wells.**
 - b. A sonic log was not run in the D well.**
 - c. For those wells where the sonic log was available, crossplots and histograms of the sonic data did not alter the petrophysical characterization of any of the wells.**

6.2-2 PETROPHYSICAL ANALYSIS

6.2-2.1 LITHOLOGY VARIATIONS

In the New Braunfels wells the gamma ray count increases from the fresh water (well C-1) to the saline water (well A-1). The fresh water wells (B-1 and C-1) have very similar gamma ray responses. This trend is evident on the lithology-porosity columns (Plate Nos. 6-3 to 6-7) and on the crossplots that have the gamma ray (Figure Nos. 6-41, -42, -44, -45, -47, and -48). The normalized histograms (Figure Nos. 6-49, -51, -53, and -55) quantify the trend. The San Marcos C, San Marcos D, and New Braunfels A-1 wells, all saline, have similar responses. However, the San Marcos B well, which is also saline water, has a gamma ray response more like to the New Braunfels fresh water wells. The San Marcos D well, the closest well to the springs, has a gamma ray response more akin to the New Braunfels saline wells.

As a general rule, an increase in the gamma ray count corresponds to an increase in shale (clay) content. Thin section petrography confirms this to some degree, to be the case in the wells at New Braunfels. A spectral gamma ray log would have greatly aided in quantifying the shale content, but the log was run only in the San Marcos D. At this site it confirmed that much of the gamma ray response was due to uranium, not shale (Figure No. 6-57 and 6-58).

Well Name: SAN MARCOS D

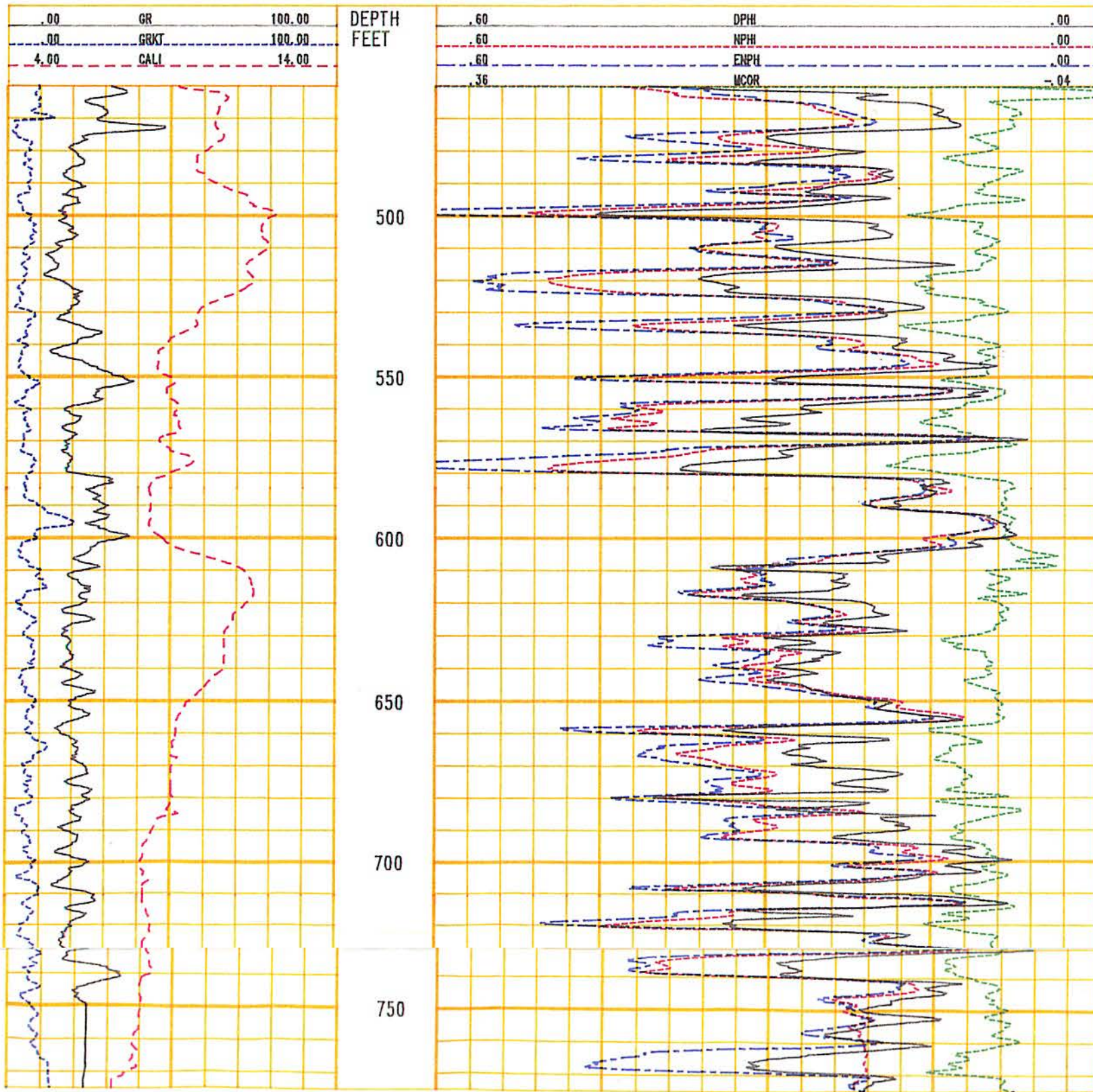


Figure No. 6-57 Track 1 contains a normal gamma ray curve (GR), a spectral gamma ray curve that does not contain the uranium count (GRKT), and a caliper curve (CALI). A comparison of the two gamma ray curves reveals that most of the gamma ray count is from uranium. This means that the section is not as shaly as the normal gamma ray curve would indicate. Tracks 2 and 3 contain three porosity curves: density (DPHI), neutron (NPHI), and epithermal neutron (ENPH). The epithermal neutron curve is reading too high a porosity over much of the log. This is because the tool is a sidewall device that is adversely affected by borehole rugosity. When the borehole is enlarged, the tool does not have good pad contact with the wall. This means that the tool is affected by pore fluid in the enlargement, as well as the formation, and measures a porosity value that is too high. The correction curve for the epithermal neutron curve (MCOR) confirms that a large correction was applied to much of the epithermal neutron curve.

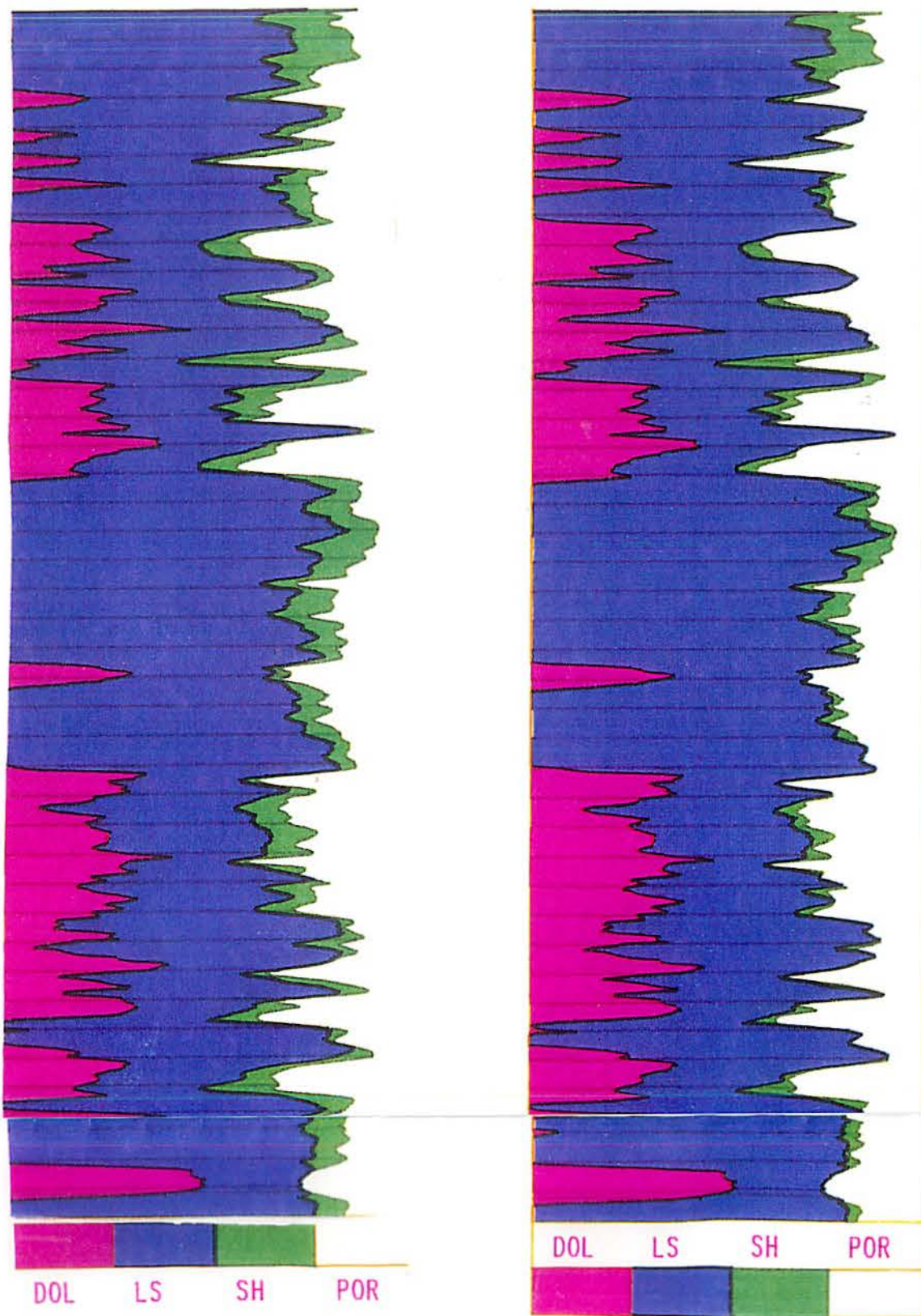


Figure No. 6-58 Lithology plots for two different gamma ray constants. Plot A was made using gamma ray constants of 15 API units for limestone and dolomite, a value obtained from examination of the normal gamma ray curve. Plot B was made using gamma ray constants of 25 API units, a value obtained by examination of the spectral gamma ray curve. The shale volume is less in Plot B and is more accurate. The well is the San Marcos D.

The trend of an increasing gamma ray count from fresh to saline water wells has been observed in other parts of the Edwards Aquifer (ie. Bexar County), and was attributed to oxidation of organic matter by fresh water with an accompanying reduction in the gamma ray count (Deike, 1990). This is also the most plausible explanation for the trend at New Braunfels and is consistent with the petrographic evidence for a greater fresh-water diagenetic imprint on the fresh water wells (B-1 and C-1). Mineralogical changes related to fresh water diagenesis may also contribute to the trend. The anomalous response of the San Marcos B and C wells is difficult to explain. In the D well, it may be because the section was never diagenetically altered as much as the C well. Drilling a fresh-water well at San Marcos may help explain the anomaly.

The Georgetown Formation, Regional Dense Member, Basal Nodular Member, and Glen Rose Formation are the shaliest intervals of the Edwards Aquifer. As a general rule, the limestones are shalier than the dolomites. Thin section petrography confirms these conclusions. The computed lithology (Plate Nos. 6-3 to 6-7) tends to overestimate the amount of shale. Only by inputting a spectral gamma ray curve could the shale volume be accurately calculated (Figure No. 6-58).

Apparent grain density histograms (Figure Nos. 6-49, -51, -53, and -55) do not show any trends among the wells. Figure Nos. 6-51 and 6-55 do show the Person Formation (excluding the Regional Dense Member) to be more dolomitic than the Kainer Formation (excluding the Basal Nodular Member). The San Marcos D well appears to be more dolomitized in the Kainer Formation, but since the entire section was not drilled, a histogram was not prepared.

The grain density of limestone (calcite) is 2.71 grams/cm³, dolomite is 2.87 grams/cm³, quartz (chert) is 2.65 grams/cm³, and shale (clay) is about 2.5 grams/cm³. When all four minerals are present, it is difficult to calculate a precise grain density from the logs. In such cases, the calculation is truly an apparent grain density. However, comparison of apparent grain densities gives at least an indication of the proportions of the dominant lithologies, limestone and dolomite.

The photoelectric factor (PEF) curve is part of the lithodensity and spectral density tools. By measuring the number of low-energy gamma rays reaching the detector, the tool calculates a PEF curve, which is a good lithology indicator. Limestone (calcite) has a photoelectric value (Pe) of 5.08, dolomite is 3.14, quartz (chert) is 1.8, and shale is about 3.4. Pe values decrease as porosity increases. For example, a dolomite with 35% porosity has a Pe value of 2.66.

The PEF histogram of the Edwards Aquifer (excluding the Georgetown Formation and the Basal Nodular Member) in Figure No. 6-50 shows a clear trend of decreasing Pe values from the saline water (well A-1) to the fresh water (well C-1) at New Braunfels. A similar trend is seen in the other PEF histograms (Figure Nos. 6-52, 6-54, and 6-56). This can be interpreted as either an increase in the percent of rock component with low Pe values (dolomite, chert, or porosity) or a decrease in shale from the A-1 to the C-1 well. The trend is best explained by a combination of an increase in the chert content and a decrease in the shale content from the A-1 to the C-1 well. Evidence for this interpretation is as follows:

1. The density-neutron crossplot porosity histograms show a decrease in porosity, just the opposite trend needed to explain the PEF response.
2. The thin section petrography (Appendix No. IV) shows a decrease in dolomite content from A-1 to C-1, just the opposite trend needed to explain the PEF response.
3. The thin section petrography shows an increase in chert content from A-1 to C-1 which could explain the PEF response.
4. The gamma ray data shows a decrease in shale content from A-1 to C-1 which could also explain the PEF response.

The PEF histograms of the San Marcos C and B wells correlate with the saline well A-1 at New Braunfels. However, the Kainer Formation is more calcitic in the San Marcos wells (Figure No. 6-56 and lithology-porosity columns in Plate Nos. 6-3 to 6-7). At San Marcos, there is an increase in the Pe values of both the Person Formation (excluding the Regional Dense Member) and the Regional Dense Member (Figure Nos. 6-52 and 6-54) from the C well to the D well. This is confirmed by the thin section petrography (see Section No. 6.1-2.2 for an explanation).

The PEF curves (Plate Nos. 6-3 to 6-7) show the Georgetown Formation, Regional Dense Member, and Grainstone Member to be virtually all limestone in all the wells. The Basal Nodular Member is virtually all limestone in the San Marcos wells, while in the New Braunfels wells it is limestone and dolomite. The Person Formation (excluding the Regional Dense Member) is

more dolomitic than the Kainer Formation above the Basal Nodular Member (Figure Nos. 6-52 and 6-56) in all the wells except San Marcos D. The apparent grain density histograms (Figure Nos. 6-51 and 6-55), the neutron porosity-bulk density crossplots (Figure Nos. 6-40 and 6-46), and a visual examination of the PEF curves (Plate Nos. 6-3 to 6-7) all confirm this.

There is a very high degree of correlation of beds from well to well at New Braunfels and for San Marcos C and B (see the Composite Plate Nos. 6-1 to 6-2). (The Person Formation is about 20 feet thinner in well D.) In the Person Formation at both sites gamma ray and PEF curves are almost identical and the density-neutron crossplot porosity curves have a high degree of correlation. At San Marcos the Kainer Formation, except for a five foot change in the thickness of the section, has virtually the same gamma ray and PEF curves in the B and C wells. There is some change in the thickness of the Kainer Formation at New Braunfels. After adjusting for these changes, the gamma ray and PEF curves have a high degree of well-to-well correlation. However, the well-to-well porosity correlation is not quite as high as it is for the San Marcos B and C wells. Overall, at New Braunfels the Person Formation has a higher degree of well-to-well correlation than does the Kainer Formation. The difference in the amount of lateral variation between the two formations may reflect slight lateral variations in the depositional facies and/or the homogenizing effect of more extensive fresh water diagenesis within the Person.

6.2-2.2 POROSITY

There is a very high correlation between lithology and porosity (Plate Nos. 6-3 to 6-7). The dolomites have the highest porosities, with some zones attaining 45 percent. Porosities less than 20 percent are almost always in the limestones. Alternating high and low porosity intervals occur within the Kainer Formation, and in the Person Formation above the Regional Dense Member due to the interbedded nature of the limestones and dolomites.

The Regional Dense Member has the lowest porosity (5 to 10 percent), followed by the Georgetown Formation with 10 to 18 percent. At New Braunfels the Basal Nodular Member has the next lowest porosity, but at San Marcos it has lower porosity than the Georgetown Formation. The Kirschberg and Dolomitic Members of the Kainer Formation have the next lowest porosity. The Grainstone Member of the Kainer Formation has slightly higher porosity than the rest of the formation, given the presence of fewer low porosity streaks in the Grainstone Member. The Person Formation above the Regional Dense Member has the highest overall porosity. (It is hard to confirm this in the San Marcos D well, since the entire Kainer Formation was not drilled.)

The low porosities of the Georgetown Formation, the Regional Dense Member, and the Basal Nodular Member in the San Marcos well, coupled with small pore throat diameters, make the intervals confining units. As such, the intervals should control down-gradient lateral movement, as well as vertical movement, of water. The Regional Dense Member is a confining bed in the New Braunfels B-1 and A-1 wells as evidenced by the fact that it separates very saline water from overlying slightly water.

The rest of the Edwards Aquifer has water-bearing quality rocks interbedded with rocks that have the extremely low porosities and permeabilities of a confining unit. The Kainer Formation has a higher percent of these poor water-bearing quality rocks than does the Person Formation (excluding the Regional Dense Member).

Within a single well a high degree of correlation exists between low porosity and high resistivity. The lithology of the low porosity zones is either limestone or chert. Therefore, in the absence of porosity logs, the resistivity logs can be used as a gross qualitative indicator of porosity and lithology:

- a. The zones with the highest resistivities have the lowest porosities (less than 20 percent).
- b. High resistivity zones less than a few feet thick are either chert or low porosity limestone.
- c. High resistivity zones more than a few feet thick are limestone, since the chert beds are less than a few feet thick.
- d. Zones with the lowest resistivities have the highest porosities (25 to 45 percent) and are almost always dolomite.

In the New Braunfels wells the histograms of the Edwards Aquifer (excluding the Georgetown Formation and the Basal Nodular Member) show a decrease in porosity from the saline water (A-1) well to the fresh water (C-1) well (Figure No. 6-50). The Regional Dense Member shows a hint of the same trend (Figure No. 6-54). The Kainer Formation (excluding the Basal Nodular Member) also shows this trend (Figure No. 6-56). The Person Formation (excluding

the Regional Dense Member) exhibits no trend (Figure No. 6-57). This is the same trend described in other studies of the Edwards Aquifer (MacCary, 1978 and Ellis, 1985).

At San Marcos, porosity decrease in the Person Formation (excluding the Regional Dense Member) from well C to D. This correlates with an increase in limestone from well C to D. The San Marcos C well correlates slightly better with the New Braunfels freshwater wells (B-1 and C-1) than with it does with the saline water well (A-1). This similarity is probably best explained by lateral variations in the depositional facies between the two sites. Only by drilling a fresh water well at San Marcos can the porosities in the B, C, and D wells be properly evaluated in terms of their relationship to the fresh-water portion of the aquifer.

6.2-2.3 WATER QUALITY

There is very good agreement between water resistivities calculated from the logs and those obtained by analysis of water samples taken during pump tests (Plate Nos. 6-13 to 6-15). A log-derived water resistivity curve (RWA curve) clearly shows the stratified nature of the water salinity within the Edwards Aquifer, as well as the transition zones between the waters of different salinity. The New Braunfels A-1 and B-1 curves clearly show the Regional Dense Member separating more saline water from underlying fresher water. Although the curve can be very spiky, averaging the extreme values makes the trends easy to recognize. This also demonstrates that water quality calculations, to be accurate, would be done over the entire aquifer, rather than at a few specific depths.

6.3 EFFECTIVENESS OF THE LOGGING PROGRAM AT THE TRANSECT SITES

An extensive variety of logging tools was run at both transect sites (see Table No. 6-1). Comparisons of the various logs provided an excellent opportunity to evaluate the effectiveness of each log. An evaluation was also made regarding the influence of the drilling program on log quality. The following conclusions, although directed specifically to the New Braunfels and San Marcos transect sites, are valid for wells throughout the Edwards Aquifer region:

1. The 7 7/8 inch borehole diameter used in these wells is the ideal size for conventional logging equipment. Slimhole logging tools, however, give their best results in a borehole 6 inches or smaller in diameter.

2. **The reverse air rotary drilling method is excellent for evaluating of the Edwards Aquifer because:**
 - a. **It provides large cuttings that are excellent for petrographic analysis.**
 - b. **Formation water is used during the drilling process, therefore foreign fluid is not introduced into the borehole and the pores of the rock. Using only formation water makes analysis of the logs easier and more accurate.**
3. **Careful attention must be paid to the effect of the drilling process on borehole enlargement. The San Marcos wells had considerably more washouts than the New Braunfels wells. This may have been due to either differences in drilling practices or differences in the competency of the rock. Drilling should be conducted in a manner so as to minimize washouts. Washouts adversely affect logging tools, especially pad-type tools.**
4. **Floppy disks of the logs should always be included in the logging program. In addition to being a good medium for data storage, floppy disks make it easy to analyze and replot the data at a later date.**
5. **The best suite of logs for evaluating the wells was a spectral gamma ray, caliper, dual induction, compensated neutron, compensated density, photoelectric, temperature, fluid resistivity, flow meter, and downhole video camera. This combination of logs permitted delineation of the formations, as well as accurate characterization of aquifer properties such as lithology, porosity, and water quality. It also did an excellent job of describing the condition of the borehole and identifying fluid movement within the borehole.**
6. **Since the Edwards section is only about 500 feet thick, repeat logging passes should be made of the entire interval rather than the standard 100 to 200 feet of borehole.**

7. Some logging tools were not useful in characterizing the Edwards in wells at the transect sites:

a. The microspherically focused log (MSFL), a pad-type tool which measures the resistivity of the flushed zone, did not work properly because the borehole was too rugose (Figure No. 6-59). In addition, the tool is not needed in boreholes drilled by air reverse rotary because there is no mud filtrate invasion and consequently no lateral variation in resistivity.

b. The electromagnetic propagation tool (EPT), a pad-type tool which can be used to calculate porosity, did not work properly because the borehole was too rugose (Figure No. 6-60). As long as other porosity tools (density, neutron, or sonic) are available there is no need to run an EPT.

c. The single-point resistance log, which is used for correlation, did not work as well as other resistivity tools. There is no reason to run the tool.

d. The dual spatial epithermal neutron (DSEN) provided porosity values that were too high (Figure No. 5-57). This was possibly because the borehole was too rugose. However, an evaluation of the accuracy of the DSEN porosity values was inconclusive because the tool was calibrated incorrectly.

8. Some logging tools provide useful data, but the same data can be obtained more effectively with other logging tools:

a. The formation microscanner (FMS) is a four-pad tool which produces an electrical image of the borehole. Features such as fractures, bedding planes, and vugs can be imaged with the tool (Figure No. 6-61). The tool is designed to provide an image of a borehole that is filled with drilling mud. In boreholes filled with

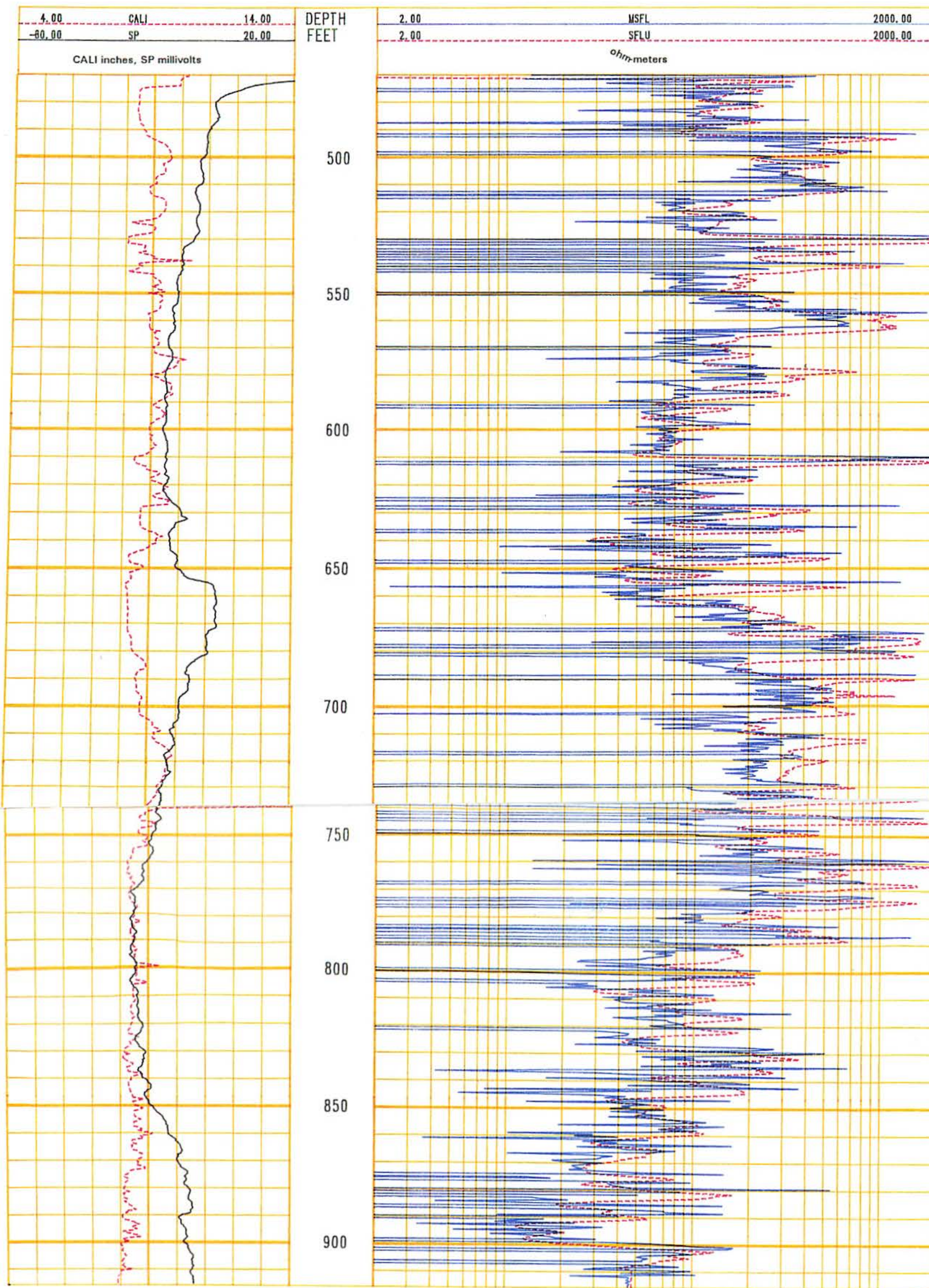


Figure 6-59. A comparison of resistivity values measured by a microspherically focused log (MSFL) and an unaveraged spherically focused log (SFLU). Low resistivity spikes on the MSFL are due to a loss of pad contact with the borehole wall. The thin bed resolution of the SFLU is comparable to that of the MSFL. There is no advantage to running an MSFL in Edwards aquifer wells drilled by reverse air rotary.

Well Name: NEW BRAUNFELS A-1

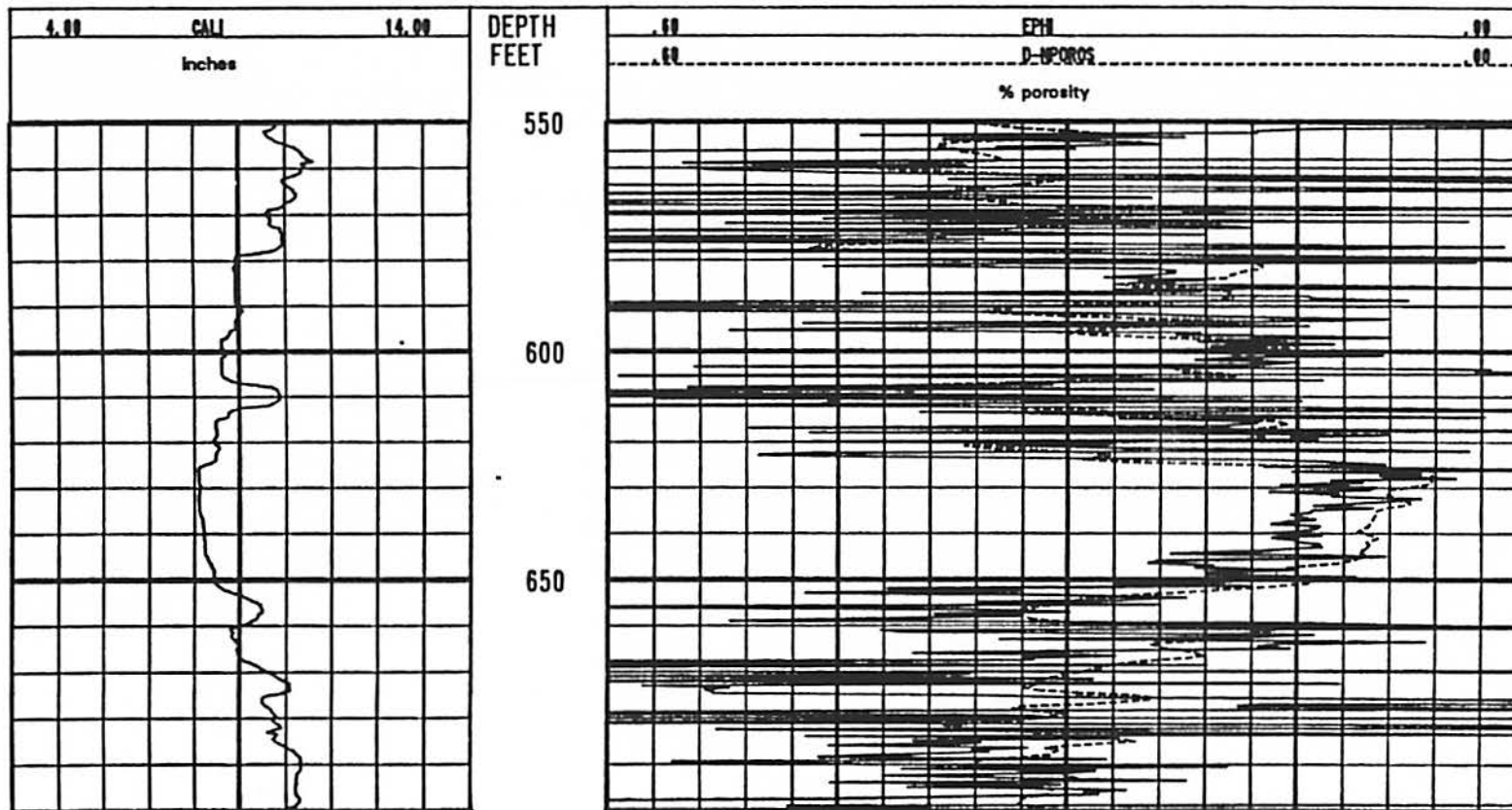


Figure 6-60 A comparison of porosity values calculated with an electromagnetic propagation tool (EPI) and a density-neutron crossplot (D-NPOROS). The EPI was calculated using a limestone matrix (t_{pi} of 9.1 ns/m). Borehole rugosity is causing the spikes on the EPI. Intervals with little borehole rugosity, such as the Regional Dense Member (626 to 646 feet), have fairly accurate EPI values. The accuracy of the EPI values in this interval could be improved by correcting for the effect of shale. However, as long as other porosity tools (density, neutron, and sonic) can be run, there is no need to run an electromagnetic propagation tool.

EDWARDS UNDERGROUND WATER DISTRICT

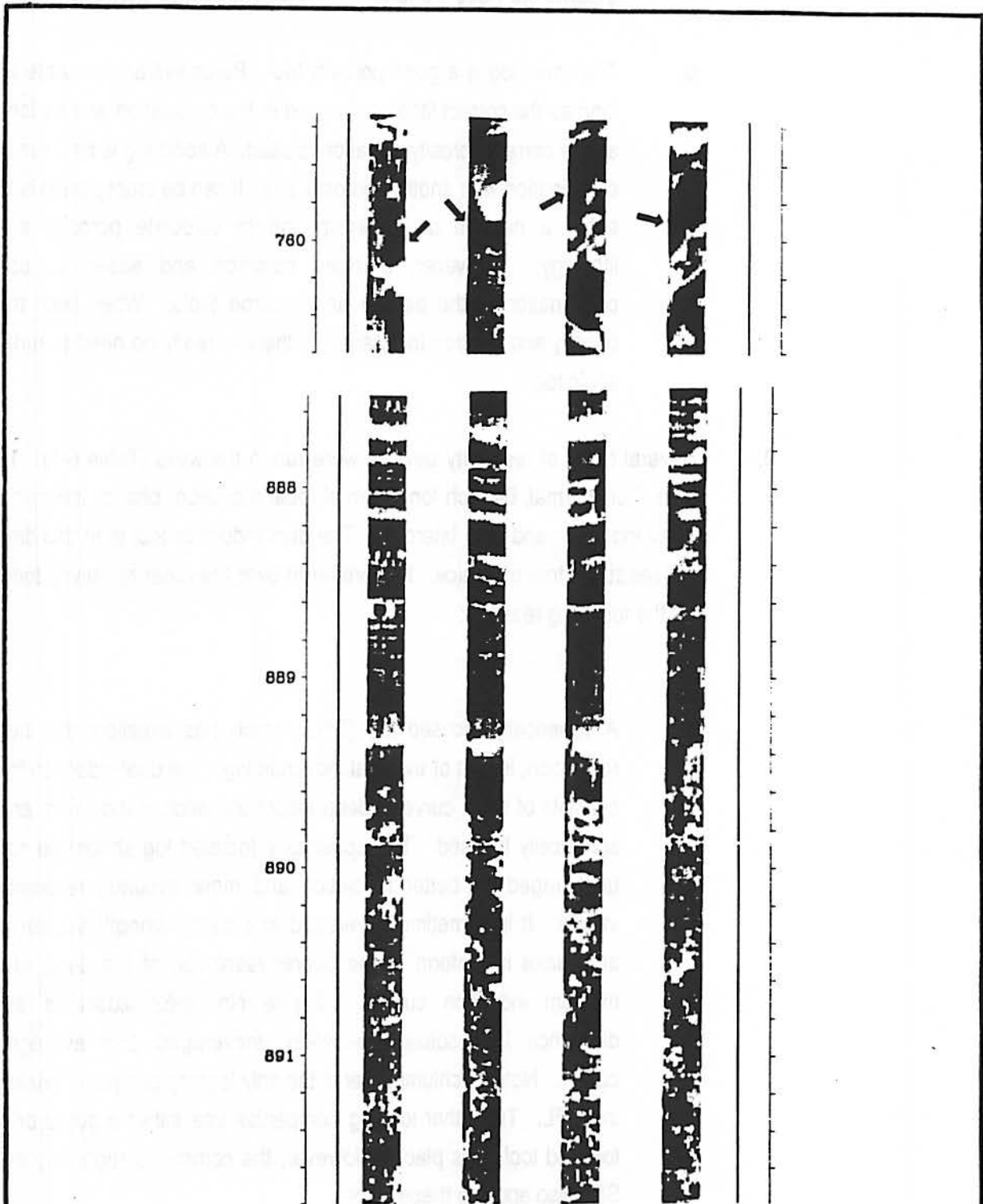


Figure 6-61 A formation microscanner (FMS) image of portions of the New Braunfels C-1 well. A fracture is located at the arrows just above 760 feet. Horizontal bedding is visible at 888 feet. Extensive vuggy porosity occurs below 890 feet.

EDWARDS UNDERGROUND WATER DISTRICT

clear formation water, such as those drilled by reverse air rotary, a downhole video camera will give a better image than the FMS.

- b. The sonic log is a good porosity tool. Porosities are accurate as long as the correct lithology is used in the calculation and as long as the correct porosity equation is used. A sonic log is best run in combination with another porosity tool. It can be crossplotted with either a neutron or a density log to calculate porosity and lithology. However, a more common and easier to use combination is the density and neutron tools. When both the density and neutron tools are run, there is really no need to run a sonic tool.
9. Several types of resistivity devices were run in the wells (Table 6-1): 16 inch short normal, 64 inch long normal, dual induction, phasor induction, array induction and dual laterolog. The dual induction tool is at this time the resistivity tool of choice. It is preferred over the other resistivity tools for the following reasons:
- a. A spherically focused log (SFL), which has excellent thin bed resolution, is part of the dual induction log. The dual induction log consists of three curves: deep induction, medium induction, and spherically focused. The spherically focused log should be run unaveraged for better resolution and more accurate resistivity values. It is sometimes averaged in order to smooth the curve and make it conform to the poorer resolution of the deep and medium induction curves. Figure No. 6-62 illustrates the difference in resolution between unaveraged and averaged curves. Note: Schlumberger is the only logging company running the SFL. The other logging companies use either a guard or a focused tool in its place. However, the comments regarding the SFL also apply to these tools.
 - b. Short and long normal tools do not have the thin bed resolution of the unaveraged spherically focused log. The short normal has

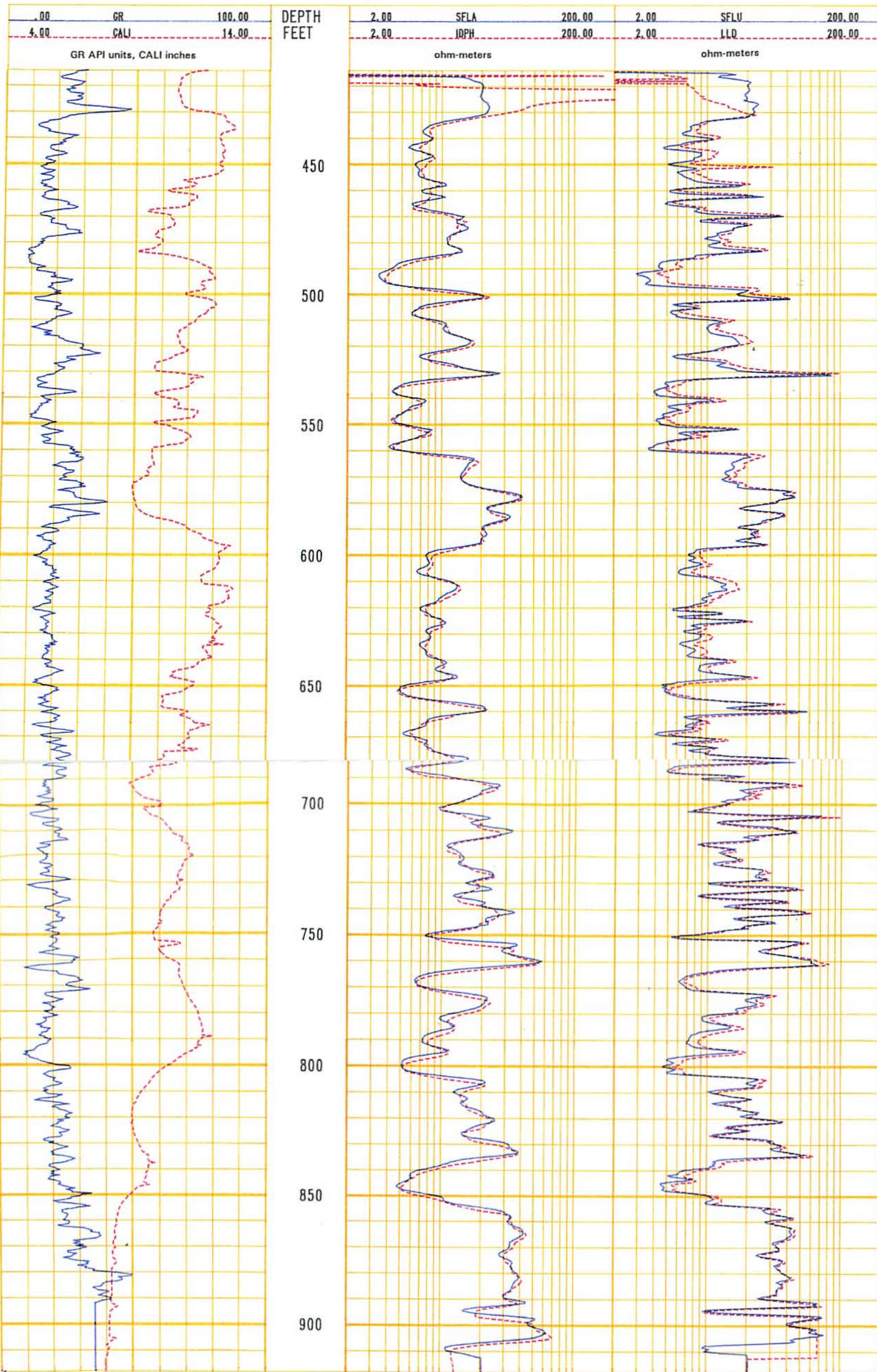


Figure 6-62. A comparison of averaged spherically focused (SFLA) and unaveraged spherically focused (SFLU) resistivity values. Track 2 contains an SFLA and a phasor deep induction (IDPH). Track 3 contains an SFLU and a deep laterolog (LLD). The spherically focused log is averaged to make it better agree with the poorer resolution of the induction log. The spherically focused log has better thin bed resolution if the curve is not averaged. The SFLU has the same resolution as a laterolog.

better resolution than the long normal, about the same resolution as the deep induction. However, the unaveraged spherically focused log has much better thin bed resolution than the short normal (Figure No. 6-63).

- c. The phasor induction is not as readily available as the dual induction and is more expensive to run. It did not perform that much better than the dual induction to warrant the extra cost (Figure No. 6-64).
 - d. The array induction is not readily available and is even more expensive to run than the phasor induction. It did not perform that much better than the dual induction to warrant the extra cost.
 - e. The dual laterolog is not readily available and many logging engineers are not adept at running the tool (Figure No. 6-65). It does have better thin bed resolution than either the dual or phasor induction tools (Figure No. 6-64). However, the thin bed resolution of the unaveraged spherically focused log is just as good as that of the dual laterolog (Figure No. 6-62). Since the spherically focused log is a standard part of a dual induction log, there is no need to run a dual laterolog.
10. The spectral gamma ray provides a much more realistic measurement of the shale content of the Edwards Aquifer than an ordinary gamma ray (Figure Nos. 6-57 and 6-58).
11. Bed boundaries are best picked by utilizing a suite of logs, rather than relying on a single curve. If available, the best logs to use are porosity (density, neutron, or sonic) and photoelectric factor. The gamma ray is sometimes useful and the caliper is usually useful in delineating the Georgetown Formation, Regional Dense Member, and Basal Nodular Member. Resistivity curves usually distinguish formation and member boundaries, as well as changes in porosity. The SP curve is not useful in distinguishing bed boundaries.

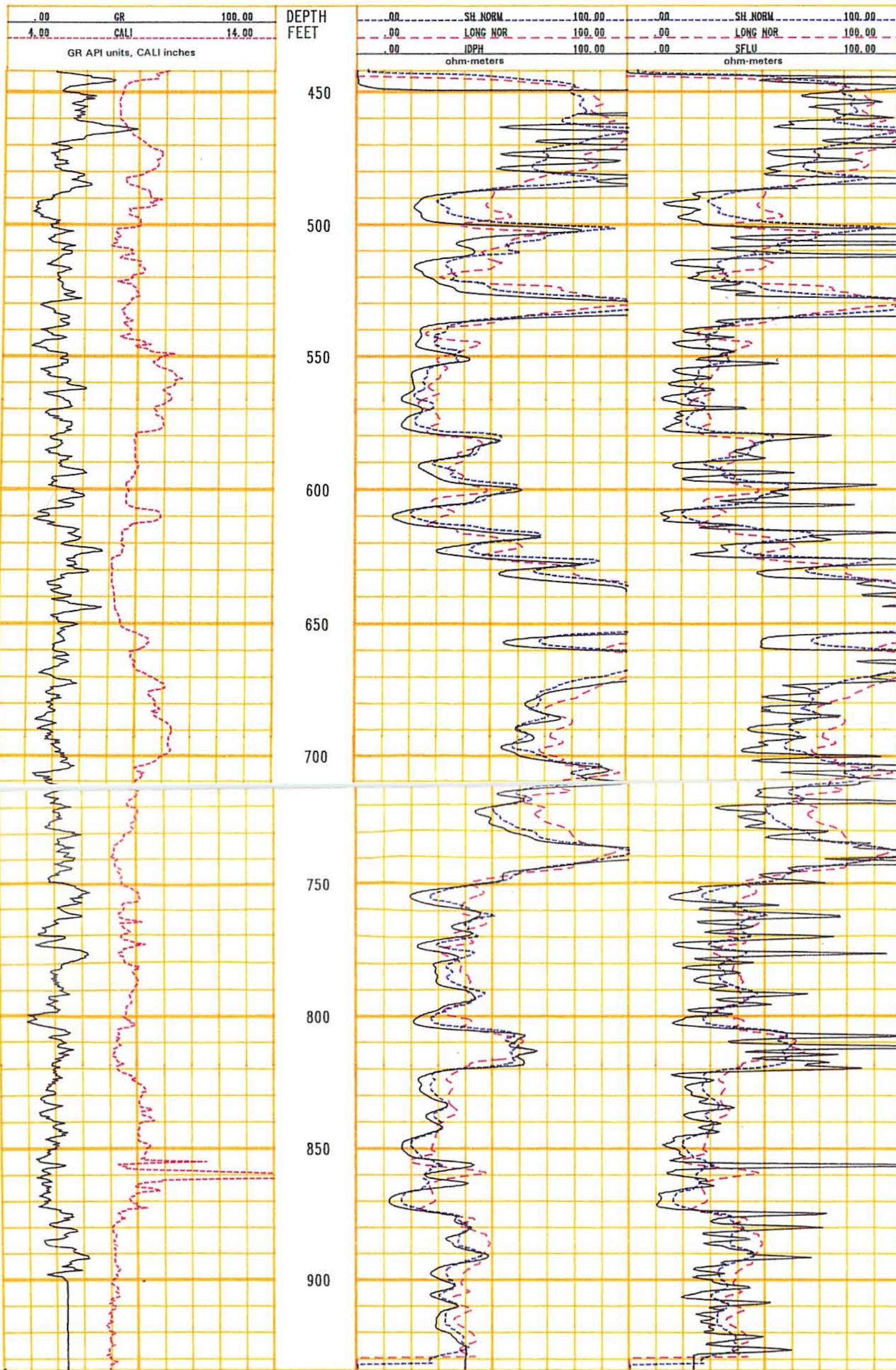


Figure 6-63 A comparison of the vertical resolution of the 16 inch short normal (SH NORM), 64 inch long normal (LONG NOR), deep phasor induction (IDPH), and unaveraged spherically focused (SFLU) curves. The long normal has the worse vertical resolution. The short normal has about the same vertical resolution as the IDPH. The SFLU has much better resolution than any of the others.

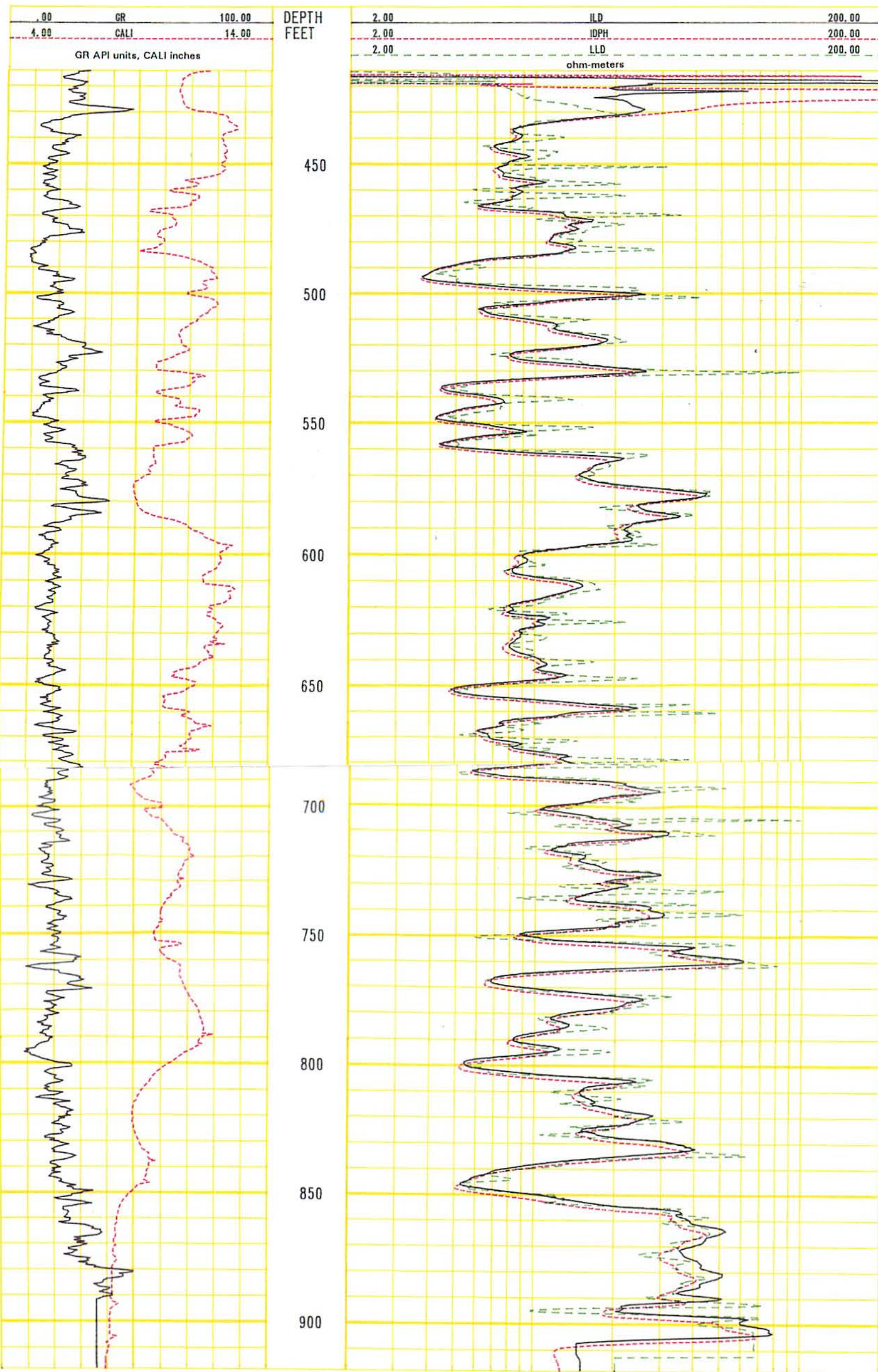


Figure 6-64 A comparison of resistivity values measured by a deep induction (ILD), a phasor deep induction (IDPH), and a deep laterolog (LLD). The LLD has the best thin bed resolution. The resolution of the IDPH is not significantly better than that of the ILD.

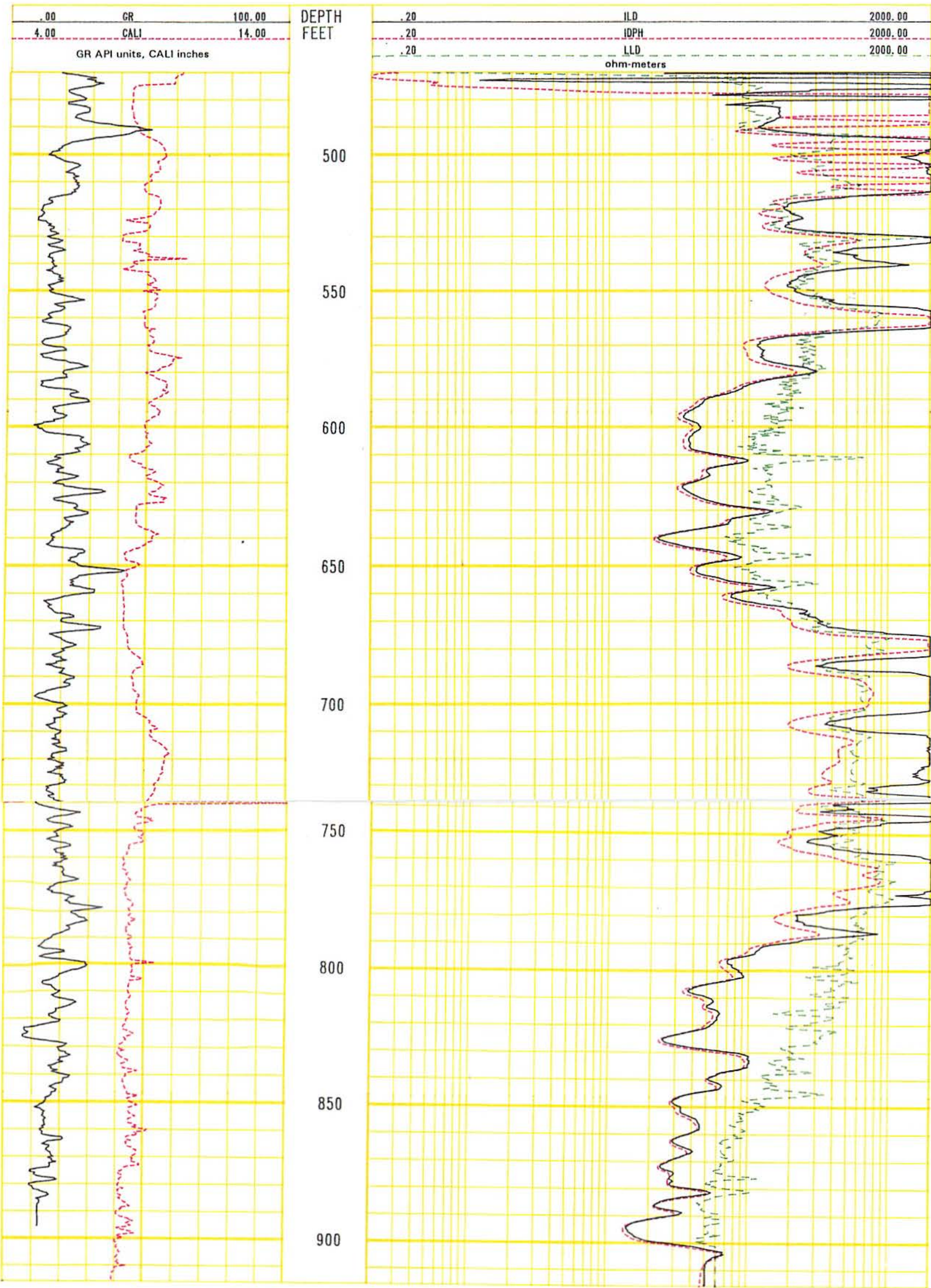


Figure 6-65. A comparison of resistivity values measured by a deep induction (ILD), a phasor deep induction (IDPH), and a deep laterolog (LLD). However, the LLD tool is not working properly. The ILD curve also has problems, above 500 ohm-meters it is recording resistivity values that are too high.

does have better thin bed resolution than either the dual or phasor induction tools (Figure No. 6-64). However, the thin bed resolution of the unaveraged spherically focused log is just as good as that of the dual laterolog (Figure No. 6-62). Since the spherically focused log is a standard part of a dual induction log, there is no need to run a dual laterolog.

10. The spectral gamma ray provides a much more realistic measurement of the shale content of the Edwards Aquifer than an ordinary gamma ray (Figure No. 6-57 and 6-58).
11. Bed boundaries are best picked by utilizing a suite of logs, rather than relying on a single curve. If available, the best logs to use are porosity density, neutron, or sonic) and photoelectric factor. The gamma ray is sometimes useful and the caliper is usually useful in delineating the Georgetown Formation, Regional Dense Member, and Basal Nodular Member. Resistivity curves usually distinguish formation and member boundaries, as well as changes in porosity. The SP curve is not useful in distinguishing bed boundaries.

Section 7

SECTION 7.0 SUMMARY AND CONCLUSIONS

7.1 SUMMARY

- 1. The drilling of a third well in San Marcos allowed for better trend development regarding the resultant data (ie. transmissivity values, lithologic trends. etc.) within the transect, as well as between the San Marcos and New Braunfels sites. The geologic data from the third well re-defined the geologic cross-section at the San Marcos site. As a result of this revised view, both transect sites proved to have increasing faulting and increasing transmissivity toward the respective major fault at their site.**

- 2. Recovery tests and pump tests were used to determined aquifer parameters such as transmissivity, storage coefficient, and hydraulic conductivity.**
 - a. In New Braunfels, the transmissivity values from the recovery tests and pump tests with observation wells in the saline zone were relatively lower than the transmissivities in the fresh zone within increasing transmissivity toward the Comal Springs Fault. In San Marcos, the transmissivity values from the recovery tests and pump tests with observation wells were, overall, relatively lower than the values for New Braunfels. All wells in San Marcos were in the saline zone, with increasing transmissivity toward the San Marcos Fault and below the Regional Dense Member. For both sites, zones below the Regional Dense Member showed increases in relative transmissivity values.**

 - b. Storage coefficients for the saline-water wells in New Braunfels were higher than for the fresh-water wells. In San Marcos, the storage coefficient was much lower than any of the values obtained in New Braunfels.**

 - c. The freshest-water well (C-1) in New Braunfels had the highest hydraulic conductivity value, while the other wells (A-1 and B-1), including the San Marcos wells (B C, and D), had hydraulic conductivity values which were similar and relatively lower.**

- 3. In New Braunfels, specific conductance values collected after each pump or air-lift test ranged from values found in fresh to moderately saline waters (498 to 4,190 $\mu\text{S}/\text{cm}$ or a**

total dissolved solids range of 290 to 3640 mg/l). In San Marcos, the values were much higher (13,000 to 16,405 $\mu\text{S}/\text{cm}$ or a total dissolved solids range of 8,800 to 10,500 mg/l) than in New Braunfels. The San Marcos values represented values found in very saline water. At New Braunfels, the specific conductance values first slightly decreased and then increased below the Regional Dense. In San Marcos, the values slightly increased below the Regional Dense Member, except in the D well where the values decreased below the Regional Dense Member and over time when pumped. Most of the specific conductance values recorded over time during the pump or air-lift tests (36 out of 59 tests) remained constant for both sites. Most significantly, during the 9-hour pump test in New Braunfels, the pumping well increased in specific conductance which represented an increase in salinity over time.

4. Temperatures did not significantly vary other than by increasing with increasing salinity.
5. Ionic Concentrations: In New Braunfels, all the graphic water quality diagrams showed the stratification of the fresh and saline zones. For San Marcos, both diagrams resembled the New Braunfels well A-1 which was indicative of the saline zone.
 - a. In New Braunfels, the Stiff diagrams demonstrated an increase in concentration for Na, Cl, K, SO_4 , and Mg, and a decrease in HCO_3 compared to the fresh zone. A definite mineralized zone persisted at the bottom of all the wells. In San Marcos, both wells had the same high concentrations of anions and cations, and the Stiff diagrams resembled those diagrams in New Braunfels for the saline zone.
 - b. The Schoeller diagrams demonstrated that the Na, and SO_4 ions had the highest concentrations in the saline zone for New Braunfels and San Marcos. This relationship is consistent with Clement's thesis (1989). The Schoeller diagrams for the fresh water zone in New Braunfels were low in Na/Cl ions. A few samples showed a mixing between the two zones in the New Braunfels wells B-1 and B-2.
 - c. The trilinear or Piper diagrams drawn for New Braunfels well A-1 and the San Marcos wells were again representative of saline wells, with San Marcos having slightly higher ion concentrations noted by the radii of the circles in the diamond areas on the diagrams. The New Braunfels wells B-1, B-2, and C-1 demonstrate the differences in fresh and saline samples.

6. The saline zone for both New Braunfels and San Marcos was saturated with respect to calcite and dolomite. For both sites, both zones were undersaturated with respect to gypsum, anhydrite, celestite, and halite.
7. Cutting descriptions obtained by using the petrographic microscope proved much more accurate than viewing by binocularscope or hand-lense. However, the hand-lense descriptions were very useful during drilling and are recommended as guidelines for those who are drilling wells in the Edwards.
8. Thin section descriptions for each formation in the Edwards Group correlated fairly well between the New Braunfels and San Marcos sites except for minor variations in lithology and constituents.
 - a. In New Braunfels the Georgetown Formation was more of a confining unit than in San Marcos.
 - b. The Cyclic, Marine, Leached and Collapsed Members (undifferentiated) in the Person Formation showed little difference between the two sites. Both sites had low to medium porosity, and an abundant amount of dolomoldic porosity and pore filling sparry calcite. The New Braunfels wells showed an increase in both dolomoldic porosity and pore filling calcite from the saline zone to the fresh zone as well as from the bottom of each well to the top. The Regional Dense Member varied in texture between the two sites. In New Braunfels, the texture of the Regional Dense Member was more of a mud/wackestone, whereas in San Marcos, the texture was more of a wacke/packstone.
 - c. The Grainstone Member of the Kainer Formation in San Marcos was slightly less dolomoldic than in New Braunfels. The Kirschberg and Dolomitic Members (undifferentiated) were the same for each site, except that at the San Marcos site there was more limestone, higher porosity, more dolomoldic porosity, and more pore-filling sparry calcite cement. The Basal Nodular Member between the two sites was very similar except that in San Marcos there was more limestone, less overall porosity, and more dolomoldic porosity. In San Marcos, the Basal Nodular Member could be called a confining unit.

- d. The fact that dolomoldic porosity and pore filling sparry calcite was found in portions of all the wells suggests that at one time a fresh water environment may have existed in the vicinity of all the wells at both sites.
9. Petrophysical analysis showed that changes in lithology, porosity and water quality could be accurately detected. The use of wireline geophysical logs, in conjunction with water chemistry analysis and thin section analysis, fine-tuned the hydrogeological characterization of the sites. The following is a summary of the petrophysical analysis:

- a. Gamma Ray counts increased from the fresh water to the saline water zone in New Braunfels. The gamma ray counts in San Marcos well C were similar to counts found in the New Braunfels well A-1. An increase in gamma ray counts is associated with an increase in shale/clay, which was verified by the thin sections in New Braunfels. Also, both mineralogic changes and oxidation of organic matter by fresh water can cause a reduction in the gamma ray counts (Deike,1990). Thus, the overall imprint of greater diagenesis is more evident in New Braunfels than at the San Marcos site.

The gamma ray counts of the San Marcos well B was similar to the New Braunfels wells B-1, B-2 and C. However, no petrographic analysis was performed on the San Marcos well B, thus, no explanation could be made for the similarities.

- b. Computed lithologies tended to overestimate the amount of shale in the shaly formations and members.
- c. Apparent grain density histograms showed that, overall, the Kainer Formation (without the Basal Nodular Member) tended to be less dolomitic than the Person Formation (without the Regional Dense Member).
- d. Photoelectric Factor (PEF) curve, part of the lithodensity tool, was a good indicator of lithology: A decrease in PEF values occurs from the saline (well A-1) to the fresh (well C-1) zone in New Braunfels. This is an indication that the chert content increased and the shale content decreased from wells A-1 to C-1. A strong correlation existed between the San Marcos wells and the New Braunfels well A-1. The PEF curves also indicated that the main lithology for the Georgetown Formation, Regional Dense Member, and the Grainstone Member for both sites

was limestone. The PEF curves indicated that the lithology for the Basal Nodular Member was limestone in San Marcos but both limestone and dolomite in New Braunfels. The overall lithology for the Person Formation was identified as more dolomitic than for the Kainer Formation (above the Basal Nodular Member). Other histograms and crossplots confirmed these results. A high degree of correlation existed from bed to bed at each site.

- e. A very high correlation exists between lithology and porosity: dolomites (45%) were higher in porosity than limestones (less than 20%). Alternating high and low porosity intervals in the Kainer and Person Formations were due to the interbedded nature of the formations. The Regional Dense Member had the lowest porosity (5-10%). The Georgetown in New Braunfels had the next lowest porosity (10-15%), followed by the Basal Nodular Member. In San Marcos, the Basal Nodular Member had lower porosity than the Georgetown. The Kirschberg and Dolomitic Members (undifferentiated) were next, then the Grainstone Member, and then the Cyclic, Marine, Leached, and Collapsed were the highest. It was found that the Kainer Formation had poorer quality aquifer rocks than the Person Formation (excluding the Regional Dense Member).
- f. A high degree of correlation was found between low porosity and high formation resistivity (low conductivity). In New Braunfels, a decrease in porosity occurred from wells A-1 (saline) to C-1 (mostly fresh). Thus, in the absence of porosity logs, resistivity logs can be used as gross indicators of porosity and lithology.
- g. A high degree of correlation was observed between water resistivities calculated from the logs and those obtained by analysis of water sample. In New Braunfels, wells A-1 and B-1, the Regional Dense Member separates less saline water from underlying more saline water.
- h. In New Braunfels, the very low porosity of the Regional Dense Member makes it a confining bed where it separates less saline water from more saline water. In San Marcos, the low porosities of the Georgetown Formation, the Regional Dense Member, and the Basal Nodular Member, combined with small pore throats make these intervals confining units. As such, should control the down-gradient lateral as well as vertical movement of water.

7.2 DISCUSSION

7.2-1 IMPORTANT LITHOLOGIC CHARACTERISTICS OF THE EDWARDS GROUP

Scientists who have studied the Edwards Aquifer have described the rocks in the saline-water zone as "mostly dolomitic, medium to dark gray or brown, and containing unoxidized organic material, including petroleum, and accessory minerals such as pyrite, gypsum, and celestite" (Maclay and Small, 1980). Similar features were observed at New Braunfels and San Marcos.

The matrix of the rocks in the saline-water zone have also been described as more porous than the stratigraphically equivalent rocks in the fresh-water zone. From the thin section descriptions and well logs, we found this to be true. However, Maclay and Small (1980) have also pointed out that "permeability is restricted in the saline zone and is probably due to much more restricted interconnections between more larger vugs and cavernous openings." The thin section descriptions, well log analysis, and the relatively low transmissivities in San Marcos and the New Braunfels well A-1 (all in the saline zone) concur with this statement. In addition, the restrictive nature of the Regional Dense Member, very low porosity and permeability, at both drill sites, separated less saline water from more saline water. The restrictive low porosities of the Georgetown Formation, Regional Dense Member and Basal Nodular Member, combined with small pore throats seen in thin section, should control the down-gradient lateral movement as well as vertical movement of water in San Marcos.

Maclay and Small (1983) have also described the rocks in the fresh-water zone as "calcitic, light buff or gray to white, strongly recrystallized, dense, and contain little pyrite, no gypsum, and dolomite is extensively replaced by calcite." Similar features were observed at New Braunfels and San Marcos: calcite replacement and cementation as well as a high degree of dolomoldic porosity in the cuttings of all wells.

7.2-2 EFFECTS OF LITHOLOGY ON TRANSMISSIVITY AND STORATIVITY

Maclay and Small (1980) report that "a large portion of the total porosity occurs within the rock matrix. Because the rock matrix constitutes most of the bulk of the aquifer, the interconnected porosity within the rock matrix essentially provides the storage capacity of the aquifer." They conclude that "this porosity provides essentially nothing to the rock's transmissivity." The storage coefficient for the saline zone well (A-1) in New Braunfels was higher than the less

mineralized wells even though the caliper logs, video summary, and thin sections showed correlations between equivalent beds with similar percentages. The transmissivity values increased from the top down to the bottom of each well (paralleling the general trend of increasing salinity with increasing depth). Transmissivity values also increased from the more saline wells to the less saline wells. In San Marcos, the storage coefficient was very low compared to New Braunfels, even though, lithology and porosity percentages were comparable. Transmissivity values were relatively lower in San Marcos than in New Braunfels.

Within the Edwards Aquifer, Maclay and Small (1980) stress that "the bulk volume of large, secondary openings is much less than that of the rock matrix." However, they conclude that "this secondary porosity contributes most to the great capacity of the aquifer to transmit water." In particular, they attribute most of the secondary openings to dissolution and dedolomitization processes. In confirmation of these observations, the video summaries and well logs demonstrated that large cavities were present in the New Braunfels wells, where the transmissivity values were higher than at San Marcos.

7.2-3 IMPORTANT CHEMICAL CONSIDERATIONS FOR THE FRESH/SALINE-WATER INTERFACE

Clement (1989) demonstrates that a strong Na-Cl facies extends from east Bexar through Comal and Hays Counties. Clement further states that as the potentiometric surface declines and the intensity of faulting increases to the east, Na and Cl concentrations also rise. Water samples demonstrated an increase in ionic concentrations between the fresh and saline zone in New Braunfels, and an increase in ionic concentrations from the New Braunfels site toward the San Marcos site.

Along the limestone coast of the Yucatan Peninsula, Mexico, it has been found that caves tend to form at the saline/fresh water interface (Back et al., 1986, and Stoessell, et al., 1989). This phenomenon has also been observed (but not published) in the Edwards Aquifer by Ogden (1992). The caves are formed by the corrosive effect of the mixing of two waters containing different saturation levels of calcite. Drever (1982) points out that:

In general, mixing of two waters of different compositions, both of which are in equilibrium with calcite, is likely to result in a water that is not in equilibrium with calcite. It may be supersaturated or

undersaturated, depending on the particular compositions or the waters involved.

In the case of the EUWD wells in New Braunfels, the fresh-water zone tended to be undersaturated with respect to calcite, while the more mineralized water of the saline zone tended to be more saturated with respect to calcite. Both the wells in San Marcos were also saturated with respect to calcite. In New Braunfels where the fresh water and saline water encountered each other, the two types of waters mixed caves or vugs formed. This occurred at the bottom of all the New Braunfels wells (as noted by the video summaries in Appendix III and in the caliper logs).

7.3 CONCLUSIONS

By drilling the well transects at their respective locations in New Braunfels and San Marcos, the existing saline zone boundary was found to be inaccurately placed. In both instances, the saline zone was found to be much closer to the city supply wells and springs (see Figure Nos. 7-1 and 7-2).

By studying the hydrogeologic and chemical data, the fresh/saline-water interface could be characterized from the well transects. In New Braunfels, specific conductance values of 4000 $\mu\text{S}/\text{cm}$ or greater (or total dissolved solids equal to approximately 3000 mg/l) were observed in the bottom portion of all the wells in the transect, including the LCRA well. Thus, the New Braunfels transect was in a transition zone between the fresh and saline zones.

In San Marcos, the well transect indicates only a zone of high salinity (specific conductance of 14,000 $\mu\text{S}/\text{cm}$ or total dissolved solids equal to 9000 mg/l or greater); no transition zone was observed.

The data available for interpreting whether or not the interface has actually moved was not conclusive. However, several inferences can be made:

The petrographic data for all the wells was consistent, and showed for both sites that at one time in geologic history, the formations may have been exposed to a fresh-water environment.

All the wells in New Braunfels were observed to have large secondary porosity development, relatively medium transmissivities values, and relatively low to medium salinity.



EDWARDS UNDERGROUND WATER DISTRICT

FIGURE NO. 7-1 New Braunfels proposed Fresh/Saline-Water Interface based on study results.

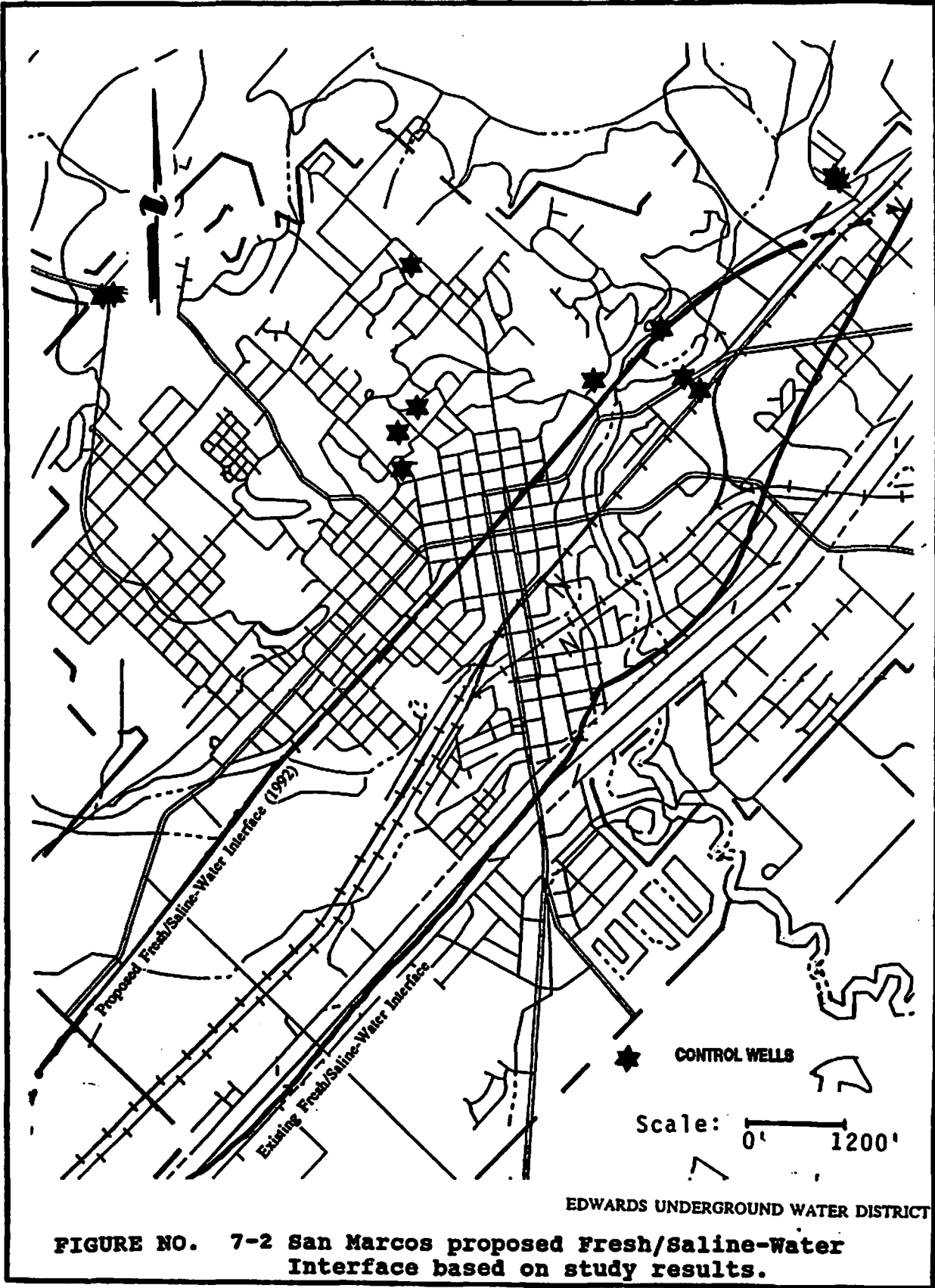


FIGURE NO. 7-2 San Marcos proposed Fresh/Saline-Water Interface based on study results.

Whereas in San Marcos, secondary porosity was not as developed, the transmissivities were lower, and the specific conductance values were high.

During the 9-hour pump test in New Braunfels, these water levels did not drop significantly, and the quality of the water in the pumping well (B-1) increased in specific conductance. It did not increase to the same specific conductance as the A-1 well, but it did increase in specific conductance compared to the fresh water in the C-1 well. The lower portion of the B-1 well produced a higher specific conductance value when packered off and pumped than what was observed in the openhole 9-hour pump test.

The conclusions to be drawn from this test are not definitive with regard to saline water intrusion because the well used as the production well was a transition (contained both fresh and saline waters) well. An increase in specific conductance in the production well could indicate that the interface between the fresh/saline zones moved. This is supported by a low sloping cone of depression during the pump test combined with the ability of water to flow from the saline zone to this transitional well. Furthermore, the well must have also drawn fresh water to it, for the specific conductance values did not increase to the same values observed in the saline zone. However, in New Braunfels, public supply wells are located in this lower block. Thus, an element of caution should be considered due to the possibility that saline water could be directed to the wells by long term pumping or during periods of increased hydrologic stress on the aquifer system in this area.

During the 9-hour pump test at the D well site in San Marcos, the water quality improved by approximately 2000 $\mu\text{S}/\text{cm}$ (from 14,000 to 12,000 $\mu\text{S}/\text{cm}$). The observation wells, B, C/upper zone, and C/lower zone, however, were not apparently affected by the pumping in the D well. Two important observations were made from these results: 1) even though the geophysical logs showed displacement of the formations between the C and D wells, the lack of affect on the B and C wells from the pumping of the D well supports the hypothesis that a fault could exist and could be acting as a semi-barrier between the wells; and 2) also from the geophysical logs, a fault was interpreted to cross the well bore just below the Regional Dense Member, and the decrease in conductivity and increase in transmissivity below this member supports the conclusion that this fault exists. It is, however, inconclusive whether there is communication from the Edwards where the wells were drilled up the San Marcos Fault to the spring orifices.

Maclay and Small (1984) have shown that "vertical displacement of 50% or greater will place the most permeable stratigraphic subdivisions on one side of the fault plane against

relatively impermeable strata on the other side." In New Braunfels, the Edwards is completely displaced by the Comal Springs Fault. Thus, if the flow system in the lower block at the New Braunfels transect is not in direct communication with the flow system in the upper block, then saline intrusion at Comal Springs is unlikely to occur.

The monitoring of the interface between the fresh/saline zones in New Braunfels could also indicate movement of this interface between New Braunfels and San Marcos. First consider that from San Antonio to New Braunfels, the water in the fresh zone diverges into two flow paths created by the Comal Springs Fault. Thus, if the blocks are not communicating at the Comal Springs Fault, then they could combine at some point between New Braunfels and San Marcos (up-gradient from the San Marcos Springs). The movement of the saline zone boundary at this point could then have an effect on the fresh water in San Marcos where the public supply wells and springs are located.

Long term monitoring of the potentiometric surfaces and water quality in and adjacent to the fault blocks, however, would have to be performed in order to determine the direction of and mechanism for any movement along the saline zone boundary.

7.4 RECOMMENDATIONS

A well on the up-thrown side of the San Marcos Fault, up-gradient from the springs, should be drilled to determine if saline water exists on that side of the fault. In addition, the wells drilled by the USGS at the Federal Fish Hatchery along McCarty Lane, and located between New Braunfels and San Marcos, could be used for further studying and testing. The location of another transect between San Antonio and New Braunfels, combined with the one at the Fish Hatchery, would further delineate the flow paths between San Antonio and San Marcos. However, before any wells are further planned for drilling, surface and downhole geophysical surveys should be performed to possibly better delineate the fresh/saline-water interface and more efficiently determine where monitoring wells should be drilled.

In any case, the saline zone boundary has not been detailed in the area described above, and with information from any additional studies, would likely be moved. In addition to studying the Edwards Aquifer from well transect data, tracer tests would increase our knowledge of the fresh-water flow regime and improve the delineation of the saline zone boundary.

BIBLIOGRAPHY

- Abbott, P. L., 1973, The Edwards Limestone in the Balcones Fault zone, south-central Texas: The University of Texas at Austin, Ph.D. Dissertation.
- Allen, U. S., 1989, Model for hydrocarbon migration and entrapment within faulted structures: American Association of Petroleum Geologists, vol. 73/7, pp 803-811.
- Back, B., Hanshaw, B. B., Herman, J. S., and Van Driel, J. N., 1986, Differential dissolution of a Pleistocene reef in the ground-water mixing zone of coastal Yucatan, Mexico: *Geology*, Vol. 14, pp. 137-140.
- Back, W., Hanshaw, B. B., Pyle, T. E., Plummer, L. N., and Weidie, A. E., 1979, Geochemical significance of groundwater discharge and carbonate solution to the formation of Caleta Xel Ha, Quintana Roo: Mexico, *Water Resources Research*, Vol. 15, pp. 1521-35.
- Bathurst, R. G. C., 1986, *Developments in Sedimentology 12, Carbonate Sediments and Their Diagenesis*: Elsevier Scientific Publishing Company, New York, New York.
- Burgess, W. J. 1966, Geologic Evolution of the Mid-Continent and Gulf Coast Areas - A Plate Tectonics View" in *Transactions of the Gulf Coast Association of Geologic Societies*: Vol 26, pp. 132-143.
- Carozzi, A. V., 1989, *Carbonate Rock Depositional Models, A Microfacies Approach*: Prentice Hall, Englewood, Cliffs, New Jersey.
- Clement, T. J., 1989, Hydrochemical facies in the bad-water zone of the Edwards Aquifer, central Texas: The University of Texas at Austin, Masters Thesis.
- DeCook, K. J., 1975, *Geology and groundwater resources of Hays county, Texas*: Texas Board of Water Engineers, Bulletin 6004.
- Deike, R. G., 1990, Dolomite dissolution rates and possible Holocene dedolomitization of water-bearing units of the Edwards Aquifer, South-Central Texas: *Journal of Hydrology*, Vol. 112, pp. 35-373.

Dietz, R. S., and Holden, J. C., 1970, The breakup of Pangea in readings from Scientific American, 1976, Continents adrift and continents aground: W. H. Freeman and Company, San Francisco, California, pp. 126-137.1

Drever, J. I., 1982, Geochemistry of Natural Waters: Prentice-Hall, Engelwood Cliffs, New Jersey.

Dunham, R. J., 1962, Classification of carbonate rocks according to depositional texture: in W. E. Ham, ed., Classification of Carbonate Rocks, American Association of Petroleum Geologist, Memoir 1, Tulsa, Oklahoma.

Ellis, P. M., 1985, Diagenesis of the lower Cretaceous Edwards Group in the Balcones Fault zone, south-central Texas: The University of Texas at Austin, Ph.D. Dissertation.

Everett, B. J., 1990, Identification of flow intervals and pore geometry of a core (TWDB RB-68-11-718) from the middle Trinity Aquifer of southern Kendall County, Texas: University of Texas at San Antonio, Masters Thesis.

Fetter, Jr., C. W., 1980, Applied Hydrogeology: Columbus, Ohio, Charles E. Merrill Publishing Company.

Ferris, J. G., Knowles, D. B., Brown, R. H., and Stallman, R. W., 1962, Theory of aquifer tests: USGS Supply Paper 1536.

Freeze, R. A. and Cherry, J. A., 1979, Groundwater: Engelwood Cliffs, New Jersey, Prentice-Hall.

Groschen, G. E., in review, Analysis of data from test sites along the freshwater/saline-water interface of the Edwards Aquifer, San Antonio, Texas: USGS Water Supply Paper 2336-B.

Guyton, W. F., 1979, Geohydrology of Comal, San Marcos, and Hueco Springs: TDWR Report 234.

_____ 1986, Drilling, construction, and testing of monitor wells for the Edwards Aquifer Bad-Water Line experiment: City Water Board of San Antonio, EUWD, TWDB, and USGS.

Hammond Jr., W. W., 1984, Hydrogeology of the Lower Glen Rose Aquifer, South-Central Texas: University of Texas at Austin, Ph.D. Dissertation.

Hammond Jr., W. W., 1992, personal conversations.

Harden, R. W., 1968, Review of water quality changes in Edwards Reservoir -- especially near the bad water line: William F Guyton and Associates.

Hoyt, J. R., 1982, General geologic overview of the central Texas area in Geology of Central Texas West and Northwest of San Antonio, San Antonio South Texas Geology Society Guidebook, November 5, 6, 7, 1982 Field Trip: The University of Texas at San Antonio, pp 32-45.

_____ 1992, personal conversations.

Jacob, C. E., 1980, The recovery method for determining the coefficient of transmissibility, in Methods of Determining Permeability, Transmissibility and Drawdown: USGS Water Supply Paper 1536, pp. 283-289.

Land, L. F., 1984, Proposed 10-year plan for continuation of hydrologic studies of the Edwards Aquifer, San Antonio Area, Texas: USGS Open-File Report 84-817.

Lozo, F. E., and Smith, C. I., 1964, Revision of Comanche Cretaceous stratigraphic nomenclature, southern Edwards Plateau, southwest Texas: Transactions of the Gulf Coast Association of Geological Societies, v. 14, p. 285-307.

MacCary, L. M., 1978, Interpretation of well logs in a carbonate aquifer: USGS Water-Resources Investigations 78-88.

Maclay, R. W. and Land, L. F., 1986, Simulation of Flow in the Edwards Aquifer, San Antonio Region, Texas, and refinement of storage and flow concepts: USGS Open-File Report 86-532.

Maclay, R. W. and Small, T. A., 1983, Carbonate Geology and Hydrology of the Edwards Aquifer in the San Antonio Area, Texas: USGS Open-File Report 83-537.

_____ 1982, Test-hole data for the Edwards Aquifer in the San Antonio Area, Texas: TDWR LP-171.

Maclay, R. W., Small, T. A., and Rettman, P. L., 1980, Hydrochemical data for the Edwards Aquifer in the San Antonio Area, Texas: TDWR LP-131.

_____ 1980, Water-level, recharge, discharge, specific-capacity well-yield, and aquifer-test data for the Edwards Aquifer in the San Antonio Area, Texas: TDWR LP-133.

_____ 1981, Applications and analysis of borehole data for the Edwards Aquifer in the San Antonio Area, Texas: TDWR LP-139.

Mortimer, C. E., 1975, Chemistry, A Conceptual Approach, 3rd Edition: New York, New York, D. Van Nostrand Company.

Ogden, A. E., 1992, personal conversation.

Ogden, A. E., and Spinelli, A. J., 1985, Hydrologic and hydrochemical data for the Edwards Aquifer in Hays and Comal Counties: Southwest Texas State University, Edwards Aquifer Research and Data Center, San Marcos, Texas.

Pavlicek, D., Small, T. A., and Rettman, P. L., 1987, Hydrogeologic Data from a study of the freshwater zone/saline-water zone interface in the Edwards Aquifer, San Antonio Region, Texas: USGS Open-File Report 87-389.

Pearson Jr., F. J., Rettman, P. L., and Wyerman, T. A., 1975, Environmental tritium in the Edwards Aquifer, central Texas: USGS Open-File Report 74-362.

Perez, R., 1986, Potential for updip movement of saline-water in the Edwards Aquifer, San Antonio, Texas: USGS Water-Resources Investigations Report, 86-4032.

Prezbindowski, D. R., 1981, Carbonate rock-water diagenesis Lower Cretaceous, Stuart City Trend, South Texas: University of Texas at Austin, Ph.D. Dissertation.

Rose, P. R., 1978, Edwards Group, surface and subsurface, central Texas: The University of Texas at Austin, Bureau of Economic Geology Report of Investigations No. 74.

- Scholle, P. A., 1978, A color illustrated guide to carbonate rock constituent, textures, and porosities: The American Association of Petroleum Geologist, Memoir 27, Tulsa, Oklahoma.**
- Scholle, P. A., Bebout, D. G., and Moore, C. H., 1983, Carbonate Depositional Environments: American Association of Petroleum Geologist, Tulsa, Oklahoma.**
- Sheldon, R. A., 1982, Roadside Geology of Texas: Mountain Press Publishing Company, Missoula Montana.**
- Small, T., 1985, Hydrogeologic sections of the Edwards Aquifer and its confining units in the San Antonio Area, Texas: USGS Water-Resources Investigations Report 85-4259.**
- _____ 1992, Personal conversations.**
- Stoessell, R. K., Ward, W. C., Ford, B. H., and Schuffert, J. D., 1989, Water Chemistry and CaCO₃ dissolution in the saline part of an open-flow mixing zone, coastal Yucatan Peninsula, Mexico: GSA Bulletin, Vol. 101, pp 159-169.**
- Todd, K. D., 1980, Groundwater Hydrology, 2nd Edition: New York, New York, John Wiley & Sons.**
- Truesdell, A. H., Plummer, L. N., and Jones, B. F., 1984, WATEQS, a FORTRAN IV versions of WATEQ, a computer program for calculating chemical equilibria of natural waters: USGS Water Resources Paper, 76-13.**
- Veni, G., 1992, Personal conversations.**
- Warren, J. K., 1989, Evaporite Sedimentology: Prentice Hall, Englewood, Cliffs, New Jersey.**
- Wilson, J. L., 1975, Carbonate Facies in Geologic History: Springer-Verlag, New York, New York.**

The terms and symbols used in Plates Nos. 5-1 through 5-5 are define as follows:

Formation. Formations refers to the formations within the Edwards Group, for example: GT = Georgetown; P = Person; and K = Kainer.

Member. Members refers to the members within the Person and Kainer Formations, such as: C, M, L, & C = Cyclic, Marine, Leached, and Collapsed Members; RD = Regional Dense Member; K & D = Kirschberg and Dolomitic Members; and BN = Basal Nodular Member.

Depth (feet). The feet below land surface is indicated by a scale 2.5 inches equal 100 feet.

Lithology. The lithologic column refers to the rock type, such as the following:
limestone = blue with brick pattern; dolomite = purple with a "slanted" brick pattern; mixture of dolomite and limestone = light blue/green brick pattern with a slash in the bottom corner of each brick;

Texture. This column refers to Dunham's (1962) classification system of: mudstone (m); wackestone (w); packstone (p); and grainstone (g). If two lithology were present, such as dolomite and limestone, and thus, two types of textures were present in an interval, then a ";" separates them (c;m). A "/" means that the texture ranges from one rock type to another: a mudstone to a packstone would be designated as "m/p."

Minor Minerals and Structures. The observed accessory minerals were, for example, pyrite or "BRB's" which stands for black round bodies or unidentifiable opaque minerals. The only observed structures were stylolites. Stylolites is sometimes abbreviated as "stylol" and celestite as "celest."

Fossil Content. Very few fossils were specifically classified. Miliolids were the only fossil identified, everything else was identified as either a fossil or an allochem.

Porosity. Porosity was characterized in four ways: n = none visible; l = low, m = medium, and h = high. See "texture" above for explanations on the use of ";" versus "/".

Porosity Type. Two types of porosity were identified: m = moldic; and bp = between particles.

Color. The color of the cuttings were abbreviated to the following: br = brown; g = gray; bl = black; and w = white. Light, medium, or dark were used as adjectives and were abbreviated to: lt, m, and dk, respectively. See "texture" above for explanations on the use of ";" versus "/".

FORMATION	MEMBER	DEPTH (FT)	LITHOLOGY	TEXTURE	MINOR MINERALS & STRUCTURES	FOSSIL CONTENT	POROSITY	POROSITY TYPE	COLOR
AMESON	C L I A R O	550		M/W	BRB'S/CHERT	FOSSILS	L/none	MO	LT G
				M/W	BRB'S/CHERT	FOSSILS	L/none		DK G
				W		FOSSILS	M/L		LT BR/O
				M/P		FOSSILS	L/none		LT G
				P	CHERT	FOSSILS	M/H		LT BR
				P	CHERT		M		BR
				M/P	CHERT		L/none		LT BR
				M	CHERT		L/none		DK G
				C	CHERT		M/H		DK BR
				C	CHERT		L/none		LT G
				M	LAMINATIONS		H		DK BR
				P			none/L		DK BR
				C	CHERT		M/L		LT BR/W
				C	CHERT		M		BR
				M			M	MO	W
W			H	MO	LT BR				
C					LT BR				
C	CHERT		H		LT BR/G				
C			M/H	BP/MO	LT BR				
C	CHERT		H	MO/BP	M/DK BR				
W	CHERT		H		DK/M BR				
M/W/P	CHERT		M		LT G				
M/W			M/L		DK/M BR				
M			none		LT G				
M/W	OIL		L/none		LT G/BR				
M/W			M	MO	LT BR				
W/P			M/L		BR				
W			L		BR				
W			M/H		LT BR				
W	CHERT		H		LT BR				
W/M			L		BR				
M	CLAY		L		LT G/BR				
M			none		LT G				
G			L/none		LT BR/W				
G	CHERT		H		LT BR				
G	CHERT								
C	PYRITE/IRON		L/M/none	BP	M BR/G				
KAI N E R	K G D	800		G		ALLOCHEMS	L/M	MO/BP	LT G/LT BR
				C			M/L		BR
				C			M/H		BR
				C	CELEST/CHERT	FOSSILS	H	MO	LT BR
				M	CELESTITE		L		M G
				C	CELEST/BRB'S		L	BP	LT BR
				W/G	CELEST/BRB'S		H/M	MO/BP	DK BR
				W/G	CELESTITE		none		LT G
				C	CELEST/CHERT		M	BP	LT BR
				W/P	CELESTITE	FOSSILS	none		LT/M G
				W/P		ALLOCHEMS	L/M	BP	M/DK BR
				W/P		ALLOCHEMS	M	BP	M/DK G
				G	CHERT	ALLOCHEMS	M/H	BP	LT BR
				C	CHERT/CHERT	ALLOCHEMS	M	BP	LT G
				C	CHERT		M	BP	M/DK BR
C			M		BR				
P	CHERT		M/L		BR				
P			M		LT BR				
G			L/none	BP	DK G				
G			L		W/LT BR				
G			none		BR/G				
G			M		BR				
C	CHERT		none		LT BR				
C	CHERT		none		DK G				
C	CHERT		M/L		BR				
C			M/L		BR				
C			M/L		BR				
C	PYRITE		L		LT BR				
C			L		LT BR				
C			L		LT BR				
C			L/M		LT BR				
C			L/none		BR				
C			L/M/H		BR				
C			L/M		BR				
C			M		BR				
C			L		BR				
C			L		BR				
C	CELESTITE		M/H	MO/BP	BR				
C	PYRITE/CHERT		M/H	MO/BP	BR				
C	CHERT		L/M	MO	BR				
C	CHERT		M	MO	BR				
W/C: P	BRB'S/CHERT		L/M	MO/BP	DK G; LT BR				
P	BRB'S/CHERT		none		W				
P	BRB'S		L		M BR/G				
P			L/M		BR				

PLATE 5-3

New Braunfels Well No. C-1

Lithologic Descriptions of Rock Cuttings

EDWARDS UNDERGROUND WATER DISTRICT

FORMATION	MEMBER	DEPTH (FT)	LITHOLOGY	TEXTURE	MINOR MINERALS & STRUCTURES	FOSSIL CONTENT	POROSITY	POROSITY TYPE	COLOR	
EDWARDS	G T	400		M/W	PYRITE	MOLUSCAN	M		M G	
				G	PYRITE	MOLUSCAN	H	MO	BR/G	
	C. J. JACO	450		G			ALLOCHEMS	L	MO	BR
				G	CHERT	FOSSILS	M	MO	BR	
				G	CHERT	ALLOCHEMS	M/L	MO	BR/GA	
				G	CHERT		L	MO	DK G	
				G	CHERT		M/H	MO	DK G	
				G	CHERT	ALLOCHEMS	M/L	MO	DK G	
				W	CHERT		M/H	MO	G/BR	
				W/M	CHERT		M/L	MO	BR/G	
				M	CHERT		M	MO	G/DK G	
				G	CHERT		M/L	MO	DK G/BL	
				W	PYRITE/CHERT		M/L		G	
				W	CHERT		L	MO	DK G	
				W	CHERT		L	MO	DK G/BR	
P/W	CHERT	MILIOLIDS	M	MO	BR					
W	CHERT		M/L	MO	DK BR					
W	CHERT		L	MO	BR/M G					
W/M	ALLOCHEMS		L	MO	LT/BR/G					
W	ALLOCHEMS		L/M	MO	BR					
W	CHERT		M		DK G					
W/M			M/H		BR					
P			H	MO	BR					
W			H	MO	BR					
M		FOSSILS	L/none		LT/DK G					
KAINIER	R D	550		M	STYLOLITES		none		M G/W	
				M/W			none		W	
	G				none	MO	BL			
	M/G				M		BR			
	P	CHERT			L		W/BR			
	W/P	CHERT			L		BR			
	W	CHERT			L		W			
	G				L		BR			
	W/P	CHERT			L		BR			
	W/P	CHERT			L		BR			
	G				L		W			
	G				L		BR			
	G				L		BR			
	P	CHERT			L/M	MO	BR			
	W	CHERT			H	MO	BR			
G/P	PYRITE		L		BR					
KAINIER	K & D	700		G			L/M		LT BR	
				G			L		BR	
				G	BRB'S/CHERT		H		BR	
				P	CHERT		H/M		BR/M G	
				P	CHERT		L		G/LT BR	
				P/G			L		W	
				W			L		LT BR	
				G/P			L		BR	
				W			M		BR	
				G/P			M		LT BR	
				W			M		BR	
				G/P	CHERT		M		BR	
				W	CHERT		M		BR	
				G/P	CHERT		M/L		BR	
				M/W			L/M		BR	
W			L		G/DK G					
W/P			M		LT BR					
W/P	CHERT	MILIOLIDS	M/L	MO	BR					
W	CHERT	MILIOLIDS	L/M/H		BR					
W	CHERT	MOLUSCAN	L/M		BR					
W			M/L		LT BR					
P/W/G	CHERT	MILIOLIDS	L/M	MO	BR					
W	CHERT		L		M/DK BR					
W	CHERT		L/M		M BR					
W	CHERT		M		BR					
W/P			L		BR					
G			M/H		BR					
W/P	BRB'S		L/M		BR					
G	BRB'S		L		G					
P	BRB'S		M		BR					
G/P	BRB'S/CELEST		L		BR/G					
G/W	BRB'S/GYPSUM		L/M		BR					
W	BRB'S		L/M		G/W					
G	BRB'S		L/M		BR					
G/P			L		W					
W/M			L		BR					
W/P			L		LT/DK G					
P	BRB'S		L		M/DK G					
W			L		M/DK G					
W			none		BR					
W/M	BRB'S		L		DK G					
P			L		M/DK G					

PLATE 5-4

San Marcos Well No. B

Lithologic Descriptions of Rock Cuttings

EDWARDS UNDERGROUND WATER DISTRICT

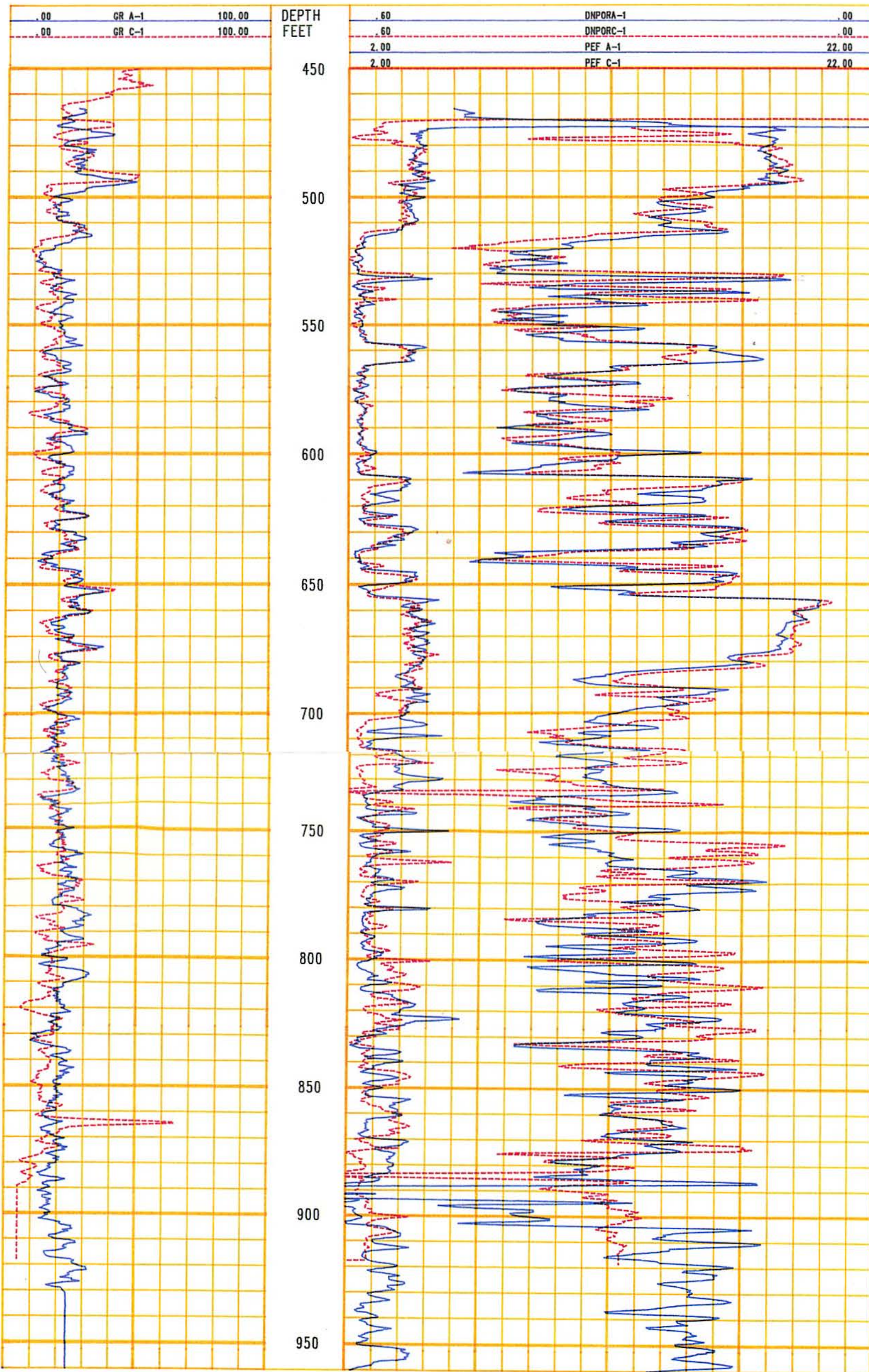
FORMATION	MEMBER	DEPTH (FT)	LITHOLOGY	TEXTURE	MINOR MINERALS & STRUCTURES	FOSSIL CONTENT	POROSITY	POROSITY TYPE	COLOR
DUNSMON	G H D	400							
		450		P	BRB'S	FOSSILS	none		G
			P		FOSSILS	none		MD BR	
		500	P	CHERTY	MILIOLIDS	none		MD BR	
			P	CHERTY	MILIOLIDS	none		MD BR	
		550	P	CHERTY	FOSSILS	L		MD BR	
			P	CHERTY	FOSSILS	L/none		LT/MD BR	
			P	CHERTY	FOSSILS	none		MD BR/G	
		600	M	STYLOLITES	FOSSILS	none		DK G	
			P		FOSSILS	L		LT BR	
KAINER	G K D			P	CHERTY	FOSSILS	none		LT/MD BR
			P/G	CHERTY	FOSSILS	none		BR	
		650	G	CHERTY	MILIOLIDS	L		LT BR	
			P/G	CELESTITE	MILIOLIDS	L/M		DK G	
		700	P	CHERTY/CELEST	FOSSILS	L/M		DK BR	
			P/G	CHERTY/CELEST	FOSSILS	L/M/H		LT/DK BR	
		750							
		800							

PLATE 5-6

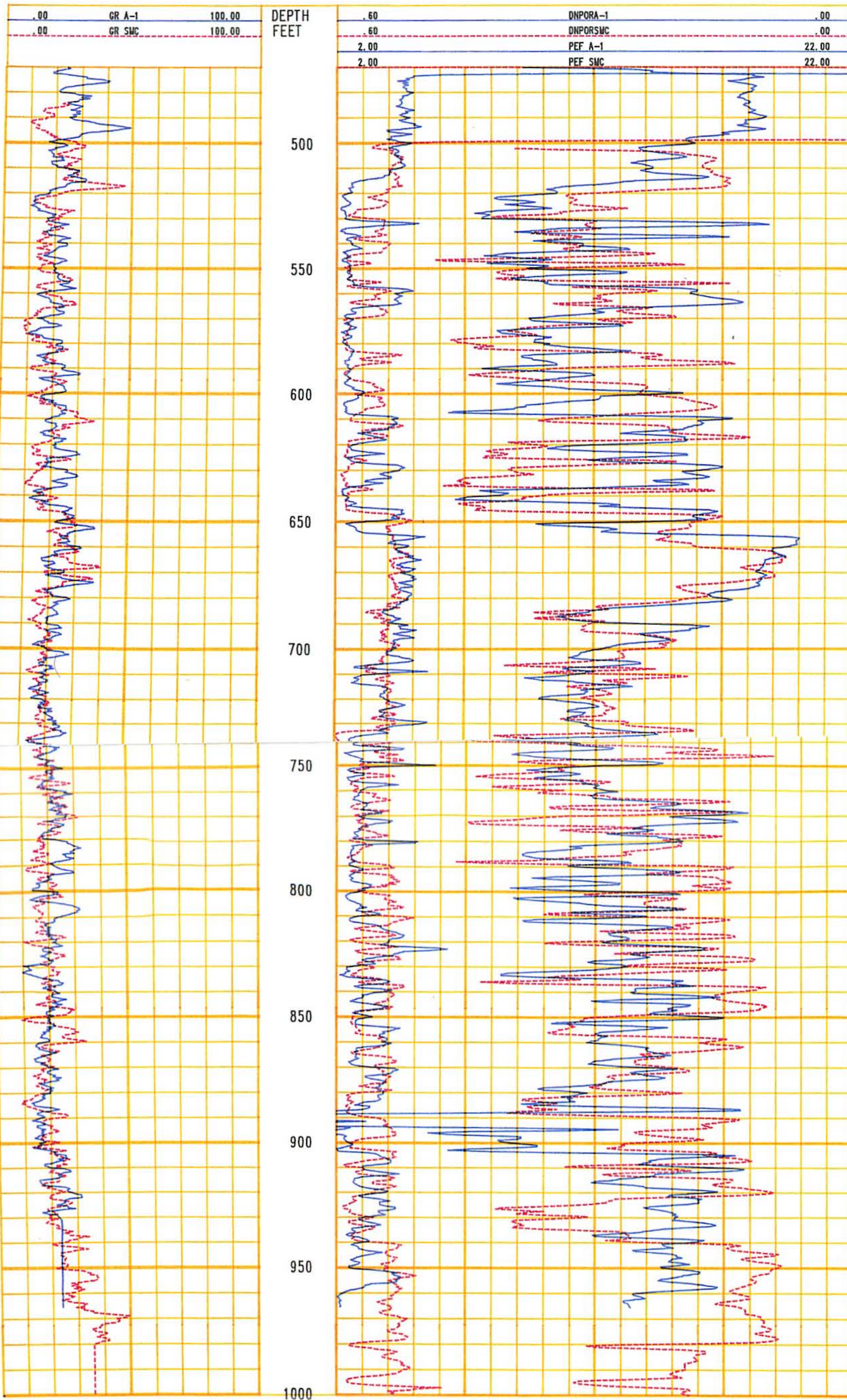
San Marcos Well No. D

Lithologic Descriptions of Rock Cuttings

EDWARDS UNDERGROUND WATER DISTRICT



COMPOSITE PLATE 6-1, NB A-1 AND C-1. An overlay of the gamma ray (GR), density-neutron crossplot porosity (DNPOR) and photoelectric factor (PEF) curves from the New Braunfels A-1 and C-1 wells. The curves from the two wells were correlated to the New Braunfels B-1 well and hung on the Regional Dense Member. The depths on the log correspond to the B-1 well.



COMPOSITE PLATE 6-2, NB A-1 AND SM C.

An overlay of the gamma ray (GR), density-neutron crossplot porosity (DNPOR) and photoelectric factor (PEF) curves from the New Braunfels A-1 and San Marcos C wells. The curves from the two wells were correlated to the New Braunfels B-1 well and hung on the Regional Dense Member. The depths on the log correspond to the B-1 well.

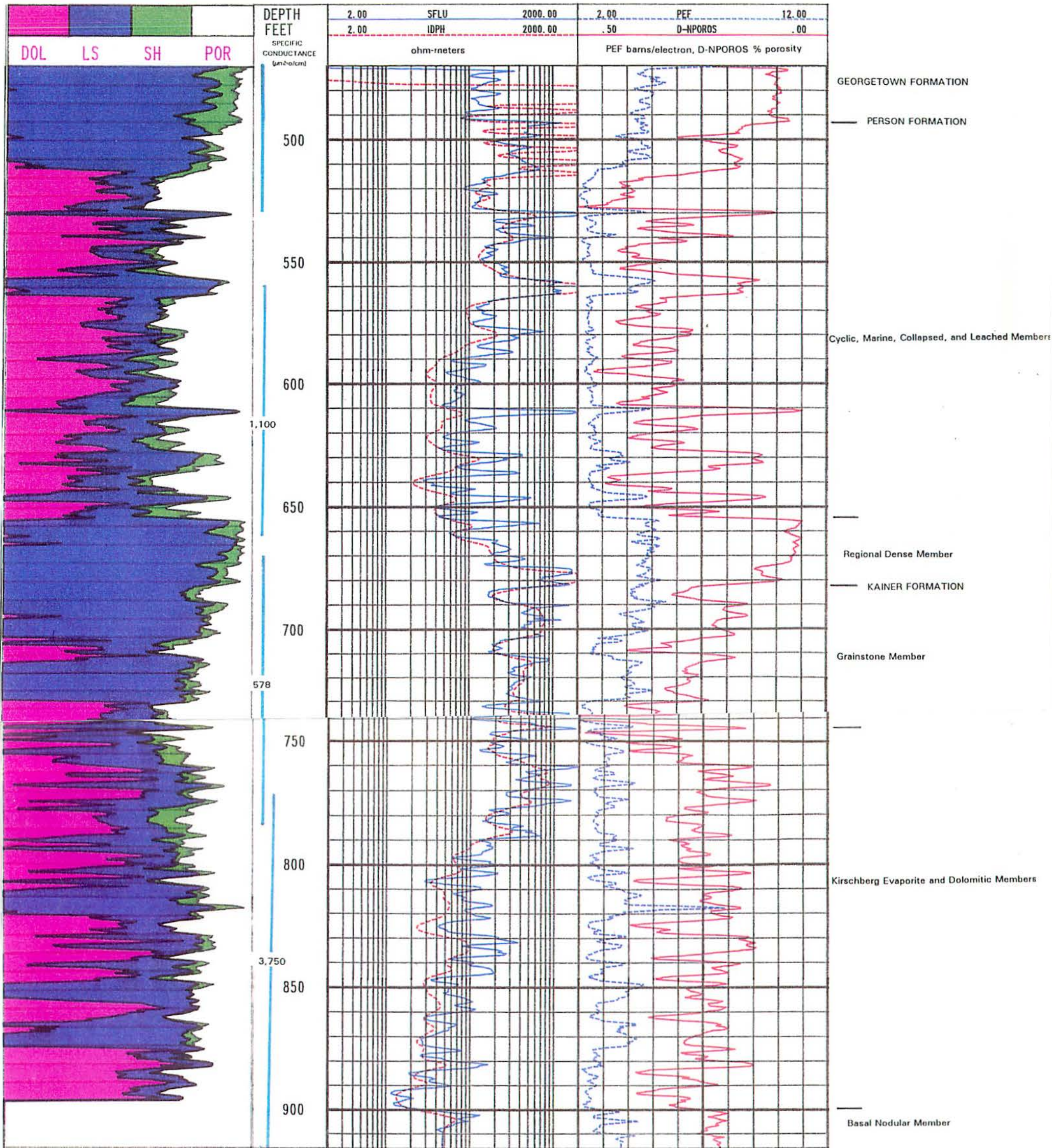


PLATE 6-3, NB B-1. Track 1 contains a lithology-porosity column. Track 2 contains unaveraged spherically focused (SFLU) and deep phasor induction (IDPH) logs. Track 3 contains photoelectric factor (PEF) and density-neutron crossplot porosity (D-NPOROS) curves. The depth column contains depth intervals and specific conductances of selected water samples collected during the drilling. Formation and member boundaries are marked to the right of Track 3. Bit size is 7 7/8 inches. At the time of logging the borehole was filled with formation water and the bottomhole temperature was 75° F. The bottom of surface casing is at 470 feet and the logger's T.D. is 916 feet. The well was logged 11/21/89.

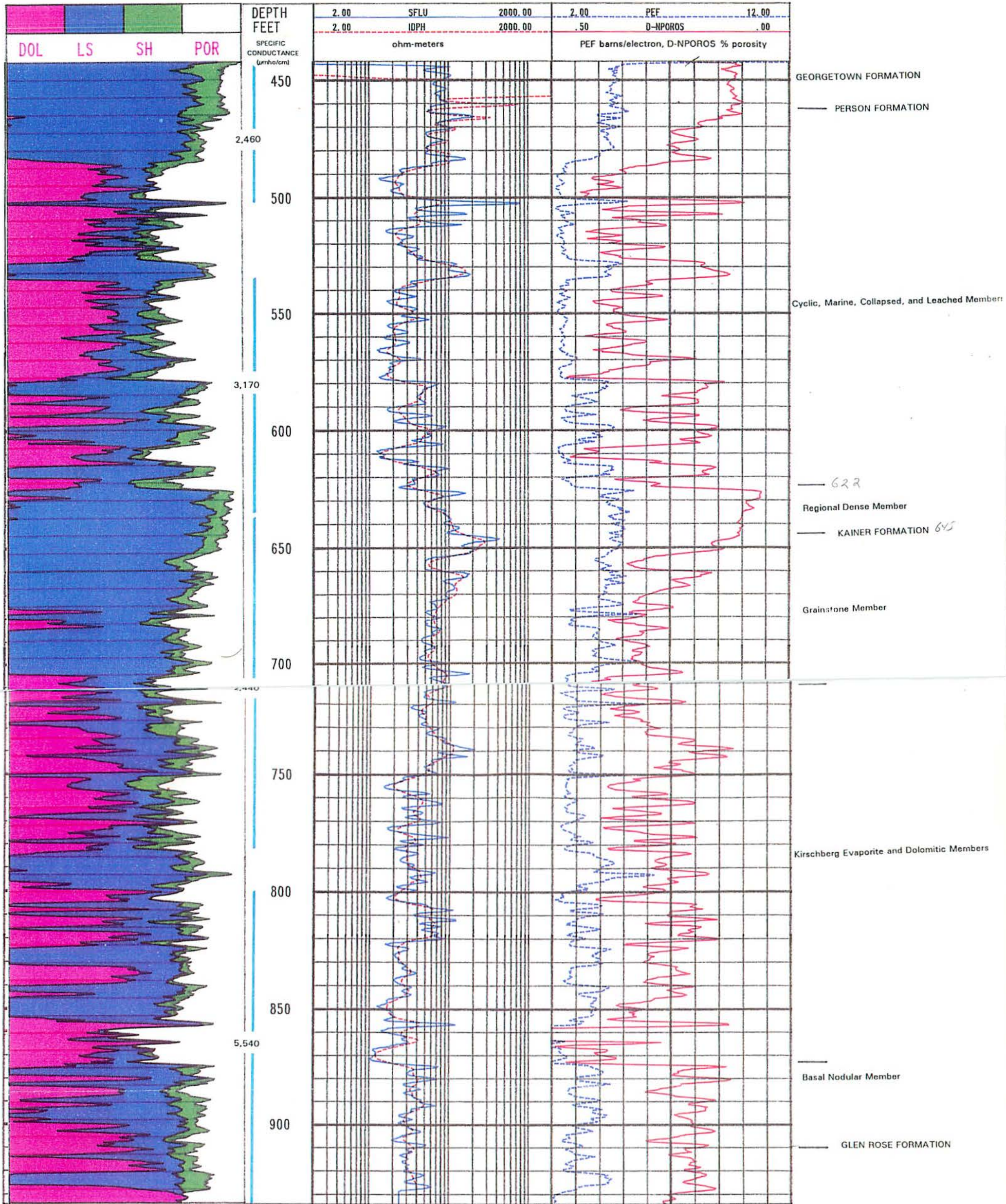


PLATE 6-4, NB A-1. Track 1 contains a lithology-porosity column. Track 2 contains unaveraged spherically focused (SFLU) and deep phasor induction (IDPH) logs. Track 3 contains photoelectric factor (PEF) and density-neutron crossplot porosity (D-NPOROS) curves. The depth column contains depth intervals and specific conductances of selected water samples collected during the drilling. Formation and member boundaries are marked to the right of Track 3. Bit size is 7 7/8 inches. At the time of logging the borehole was filled with formation water and the bottomhole temperature was 73° F. The bottom of surface casing is at 442 feet and the logger's T.D. is 934 feet. The well was logged 11/20/89.

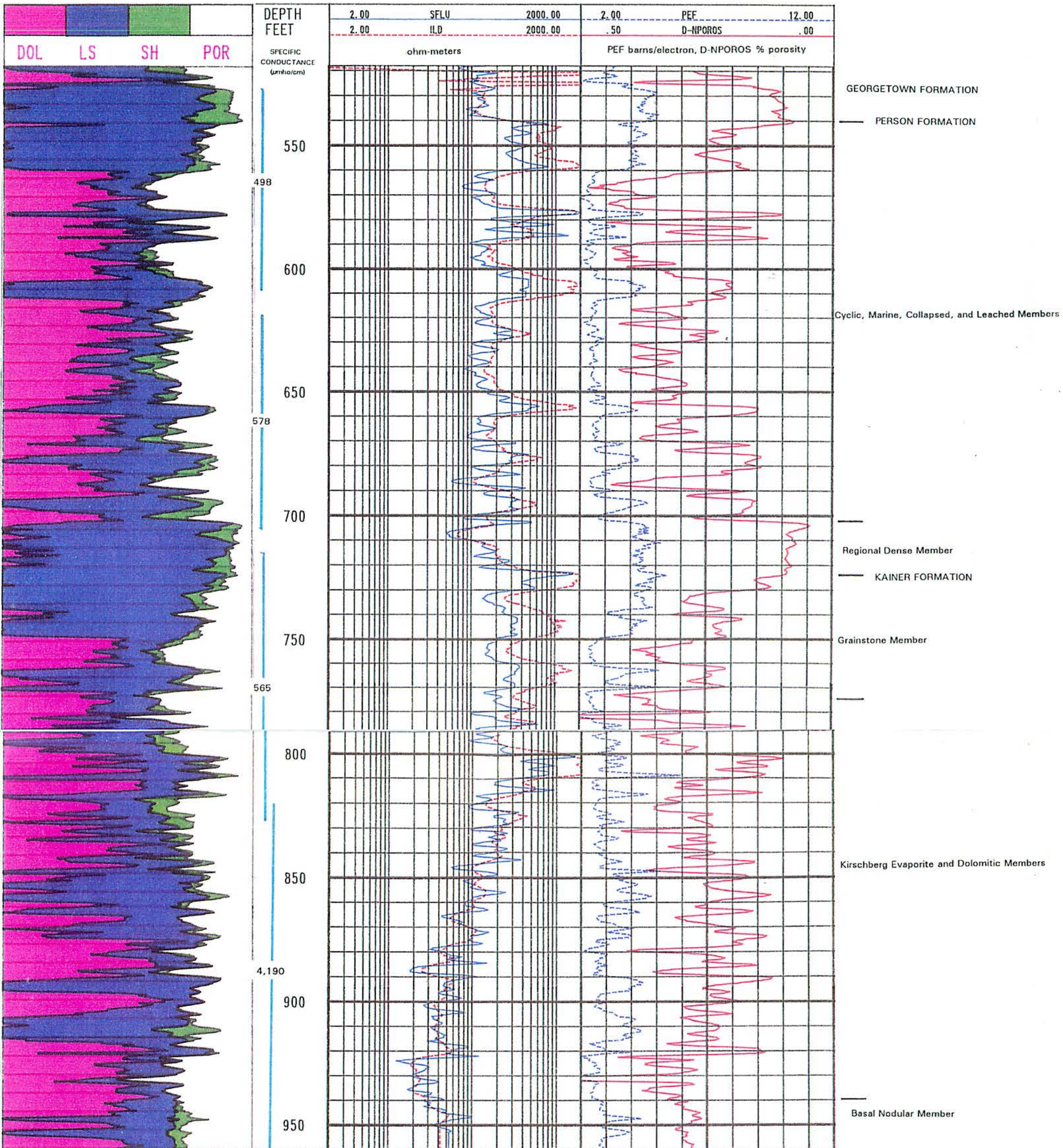


PLATE 6-5, NB C-1. Track 1 contains a lithology-porosity column. Track 2 contains unaveraged spherically focused (SFLU) and deep induction (ILD) logs. Track 3 contains photoelectric factor (PEF) and density-neutron crossplot porosity (D-NPOROS) curves. The depth column contains depth intervals and specific conductances of selected water samples collected during the drilling. Formation and member boundaries are marked to the right of Track 3. Bit size is 7 7/8 inches. At the time of logging the borehole was filled with formation water and the bottomhole temperature was not recorded. The bottom of surface casing is at 518 feet and the logger's T.D. is 960 feet. The well was logged 2/21/90. No standoff was used on the dual induction tool.

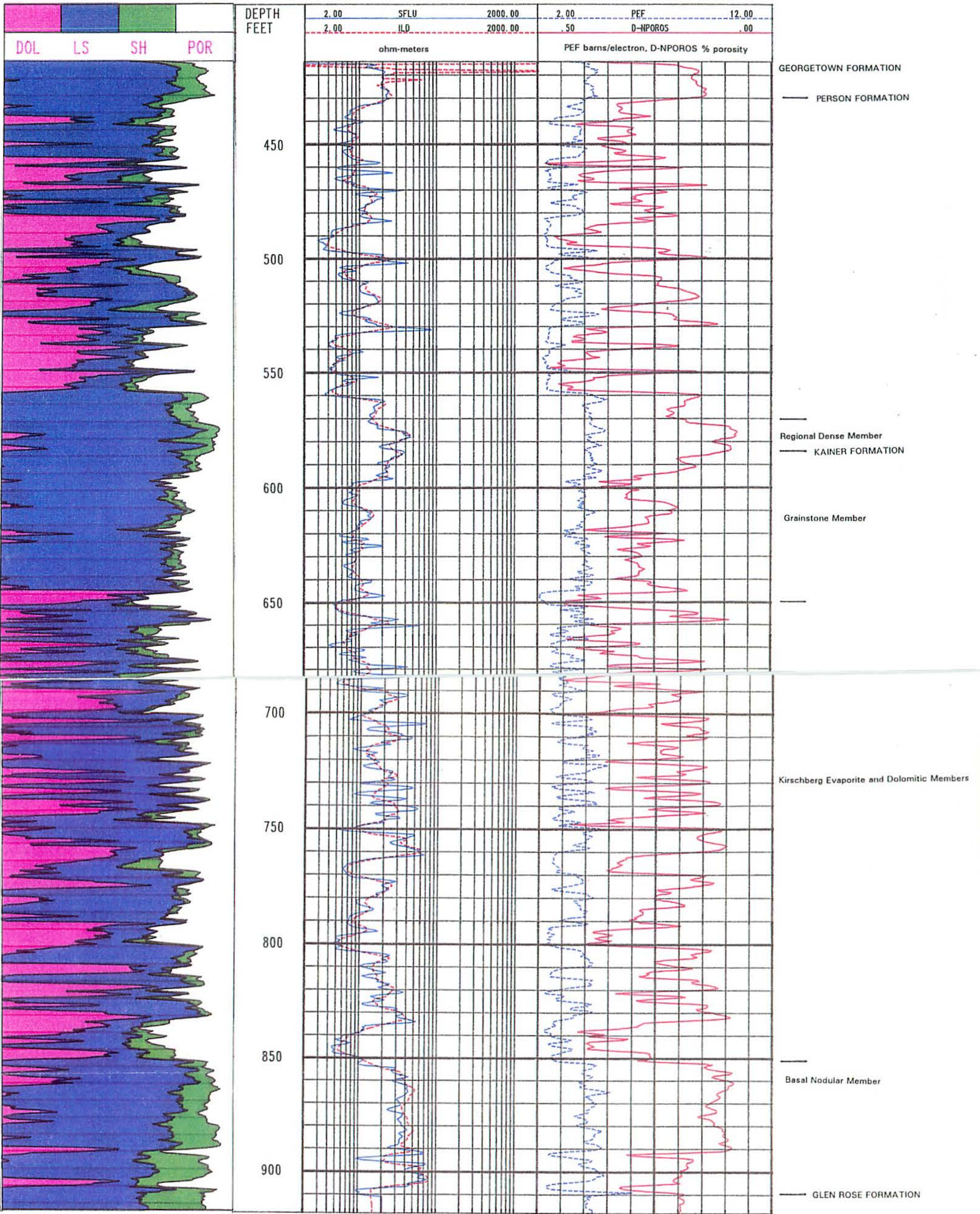


PLATE 6-6, SM C. Track 1 contains a lithology-porosity column. Track 2 contains unaveraged spherically focused (SFLU) and deep induction (ILD) logs. Track 3 contains photoelectric factor (PEF) and density-neutron crossplot porosity (D-NPOROS) curves. Formation and member boundaries are marked to the right of Track 3. Bit size is 7 7/8 inches. At the time of logging the borehole was filled with formation water and the bottomhole temperature was 90°. The bottom of surface casing is at 414 feet and the logger's T.D. is 918 feet. The well was logged 7/25/90.

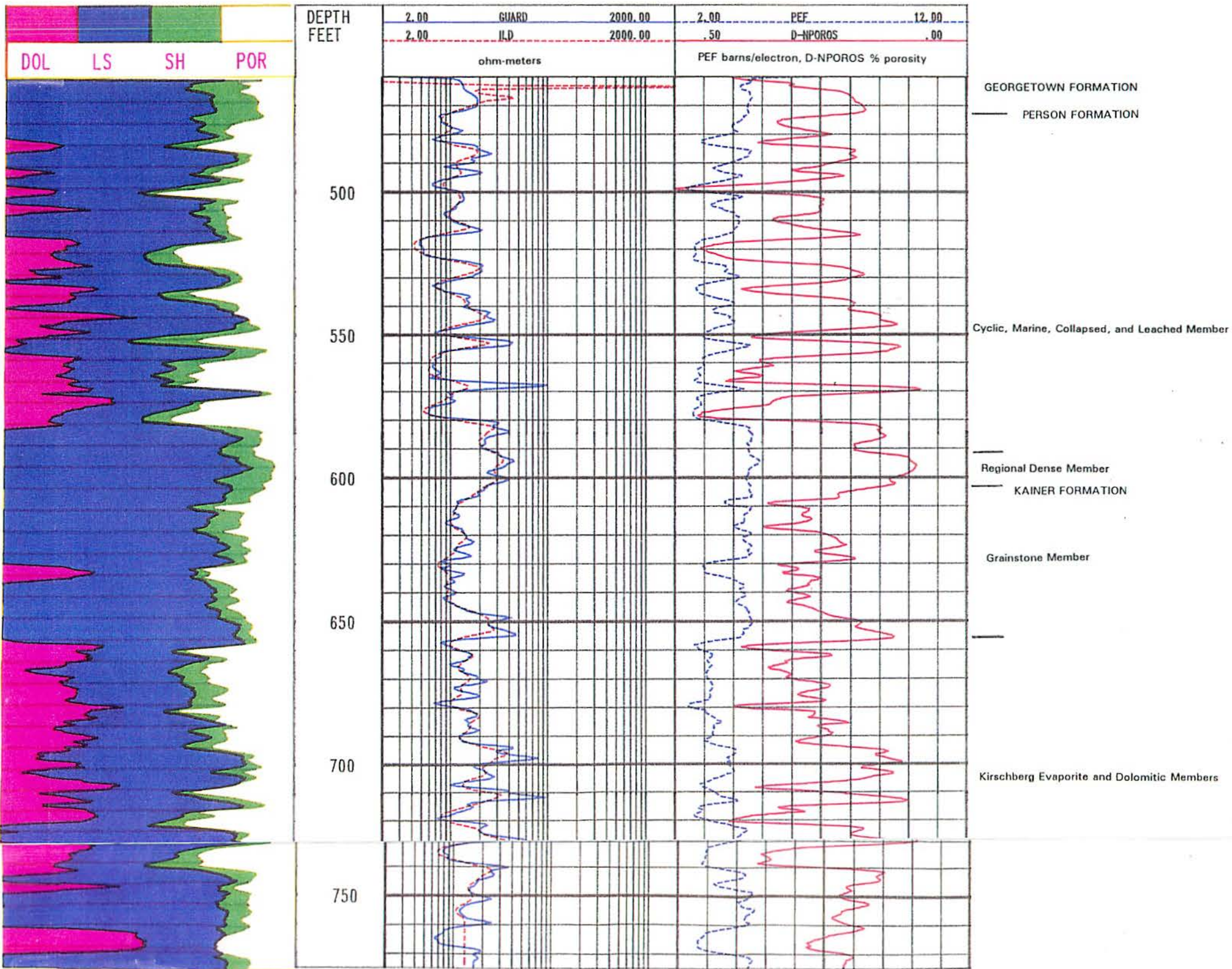


Plate 6-7 SMD. Track 1 contains a lithology-porosity column. Track 2 contains guard and deep induction (ILD) logs. Track 3 contains photoelectric factor (PEF) and density-neutron crossplot porosity (D-NPOROS) curves. Formation and member boundaries are marked to the right of Track 3. Bit size is 7 7/8 inches. At the time of logging the borehole was filled with formation water and the bottomhole temperature was 92° F. The bottom of surface casing is at 460 feet and the logger's T.D. is 775 feet. The well was logged 3/1/92.

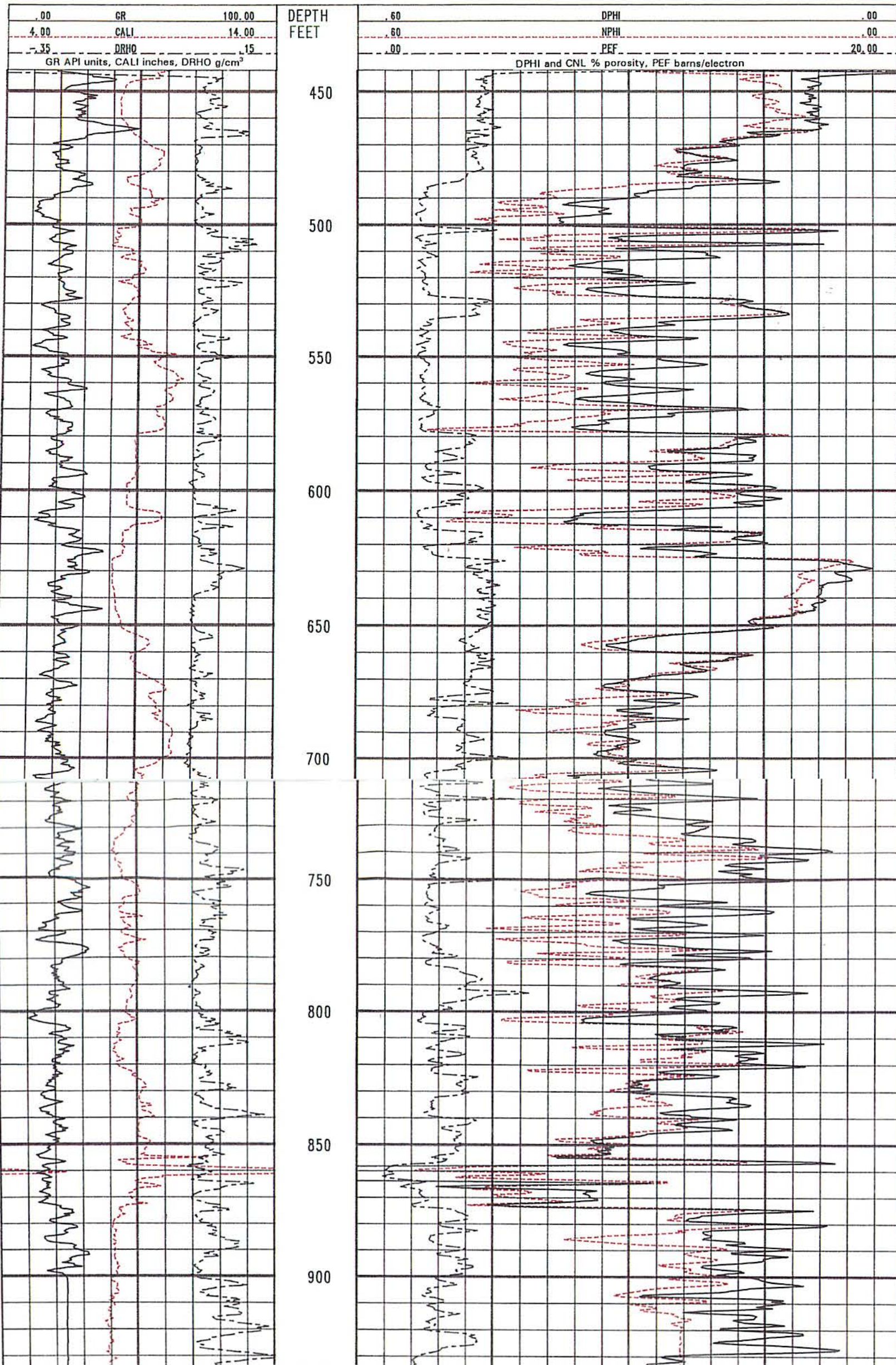


PLATE 6-8, NB A-1. Track 1 contains three logs: gamma ray (GR), caliper (CALI), and Δ rho (DRHO). Tracks 2 and 3 contain three logs: density porosity (DPHI), neutron porosity (NPHI), and photoelectric factor (PEF). The density and neutron porosities were computed with a limestone matrix.

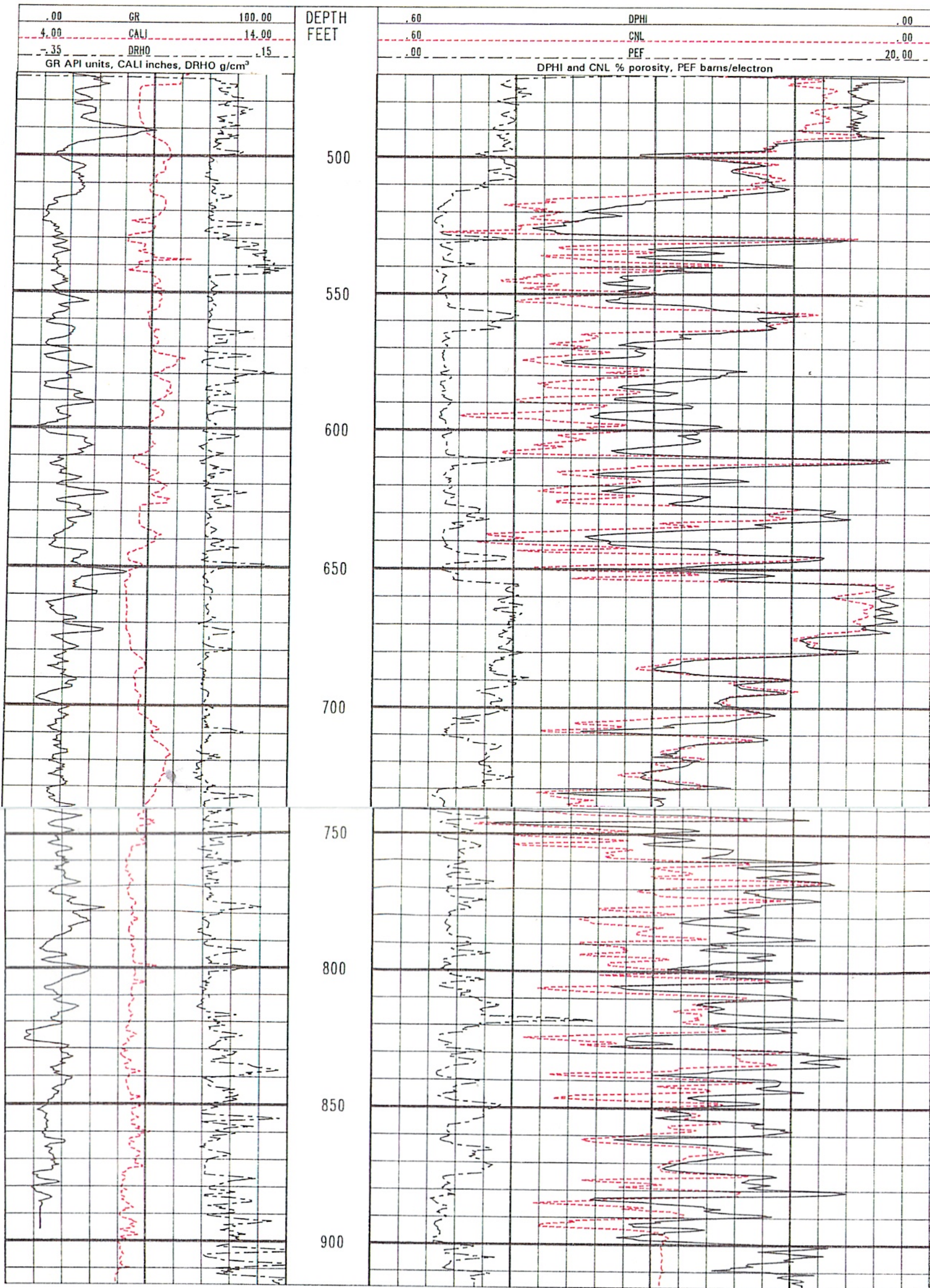


PLATE 6-9, NB B-1. Track 1 contains three logs: gamma ray (GR), caliper (CALI), and Δ rho (DRHO). Tracks 2 and 3 contain three logs: density porosity (DPHI), neutron porosity (NPHI), and photoelectric factor (PEF). The density and neutron porosities were computed with a limestone matrix.

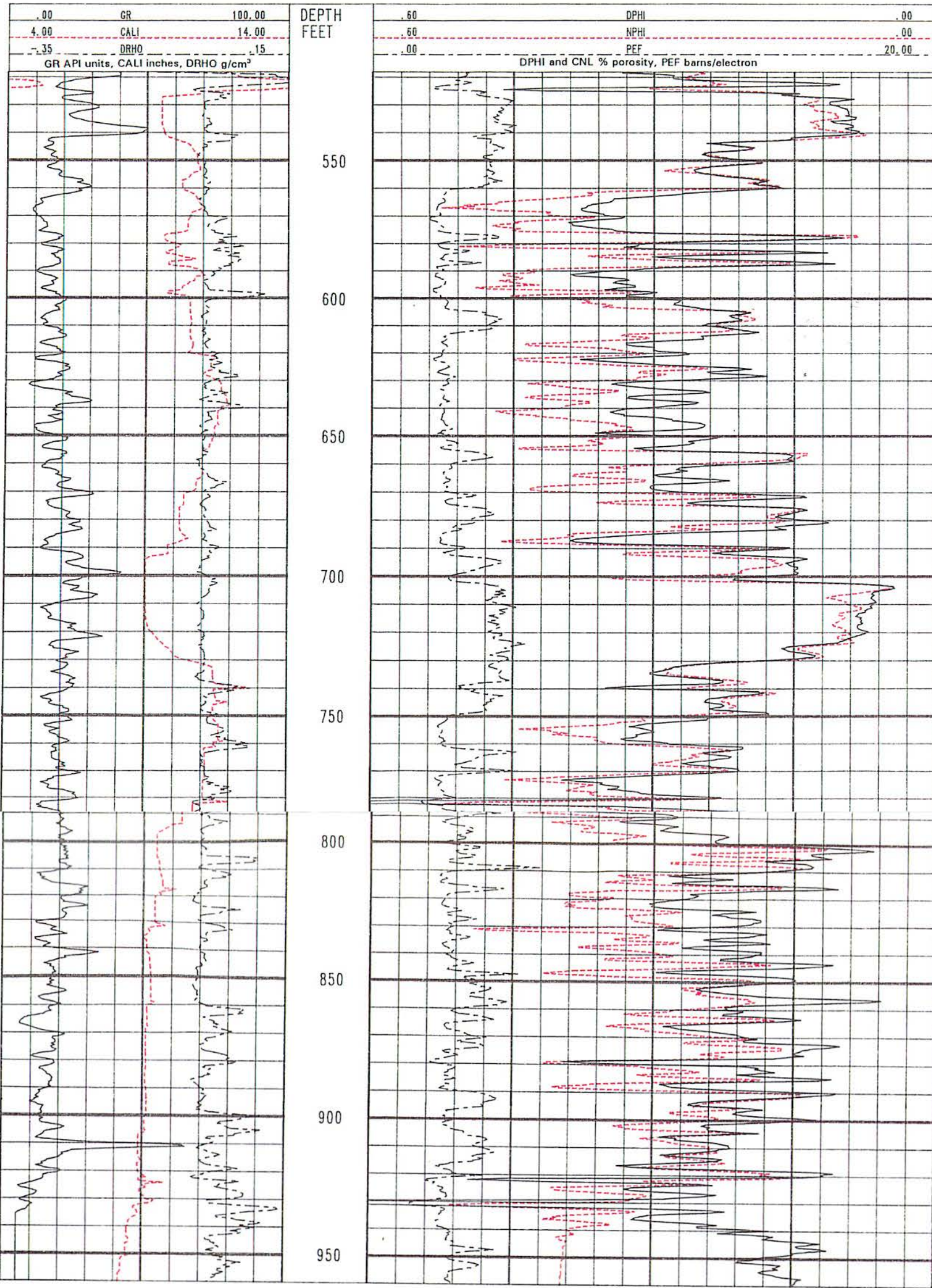


PLATE 6-10, NB C-1. Track 1 contains three logs: gamma ray (GR), caliper (CALI), and Δ rho (DRHO). Tracks 2 and 3 contain three logs: density porosity (DPHI), neutron porosity (NPHI), and photoelectric factor (PEF). The density and neutron porosities were computed with a limestone matrix.

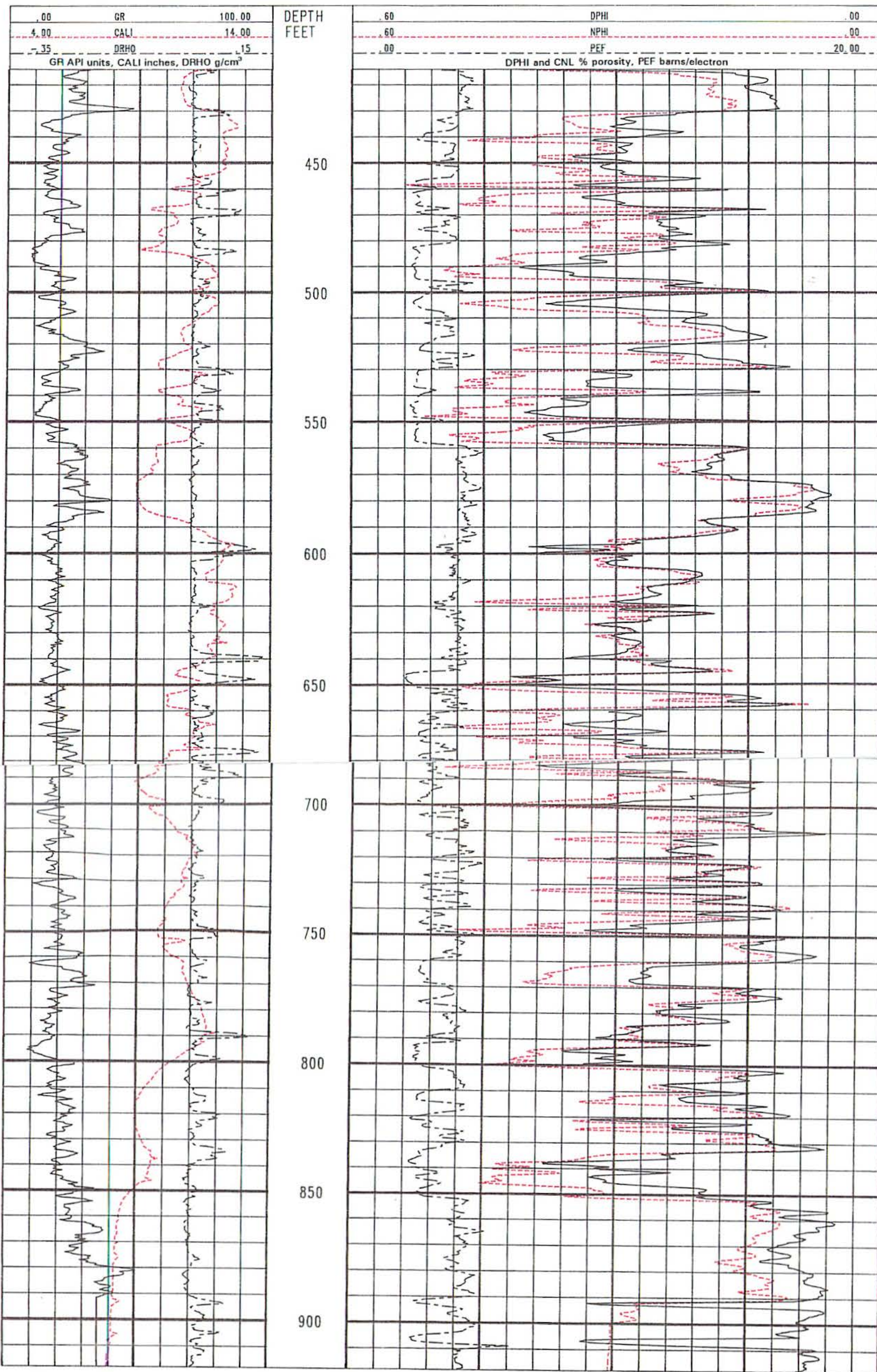


PLATE 6-11, SM C. Track 1 contains three logs: gamma ray (GR), caliper (CALI), and Δ rho (DRHO). Tracks 2 and 3 contain three logs: density porosity (DPHI), neutron porosity (NPHI), and photoelectric factor (PEF). The density and neutron porosities were computed with a limestone matrix.

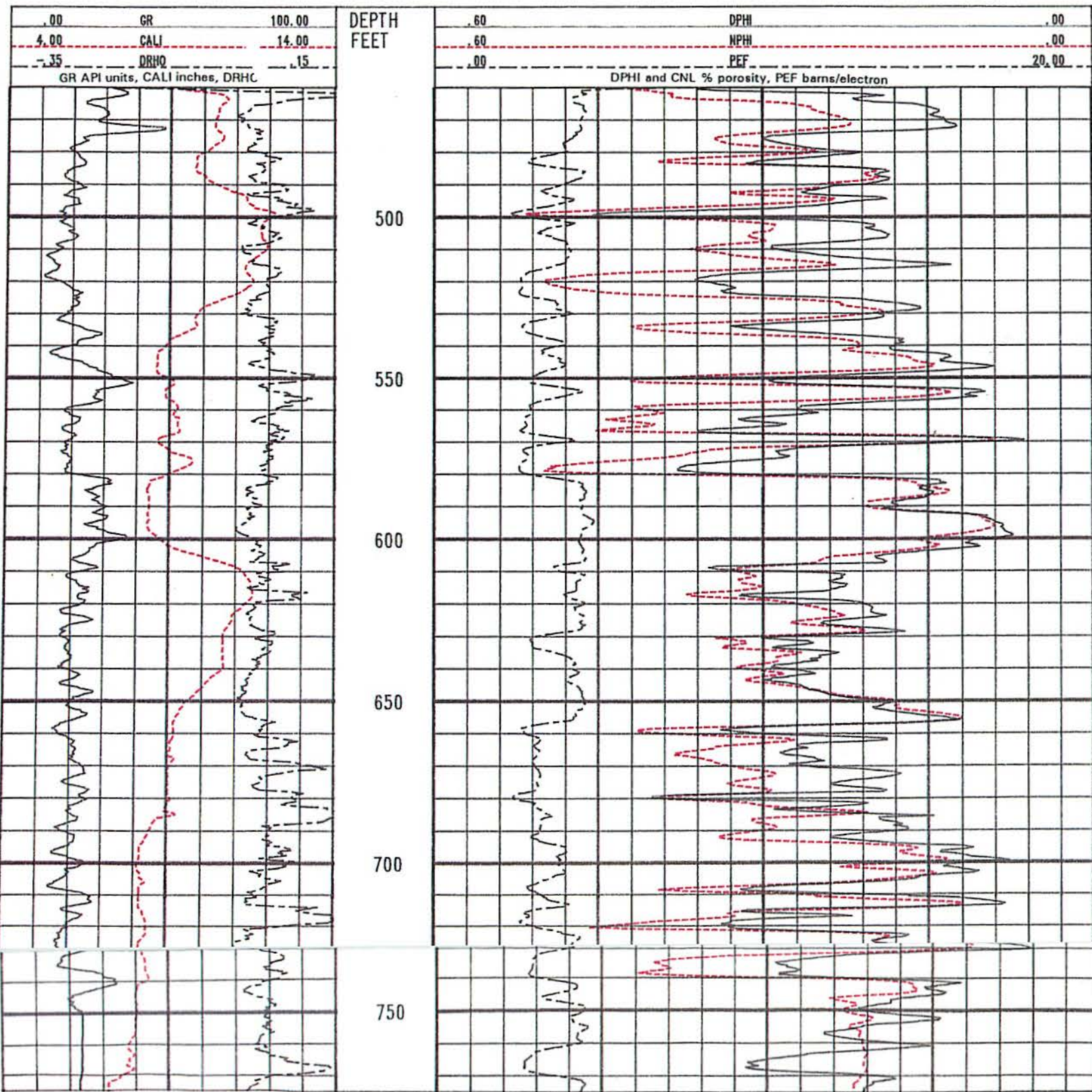


Plate 6-12 S M D. Track 1 contains three logs: gamma ray (GR), caliper (CALI), and Δ rho (DRHO). Tracks 2 and 3 contain three logs: density porosity (DPHI), neutron porosity (NPHI), and photoelectric factor (PEF). The density and neutron porosities were computed with a limestone matrix.

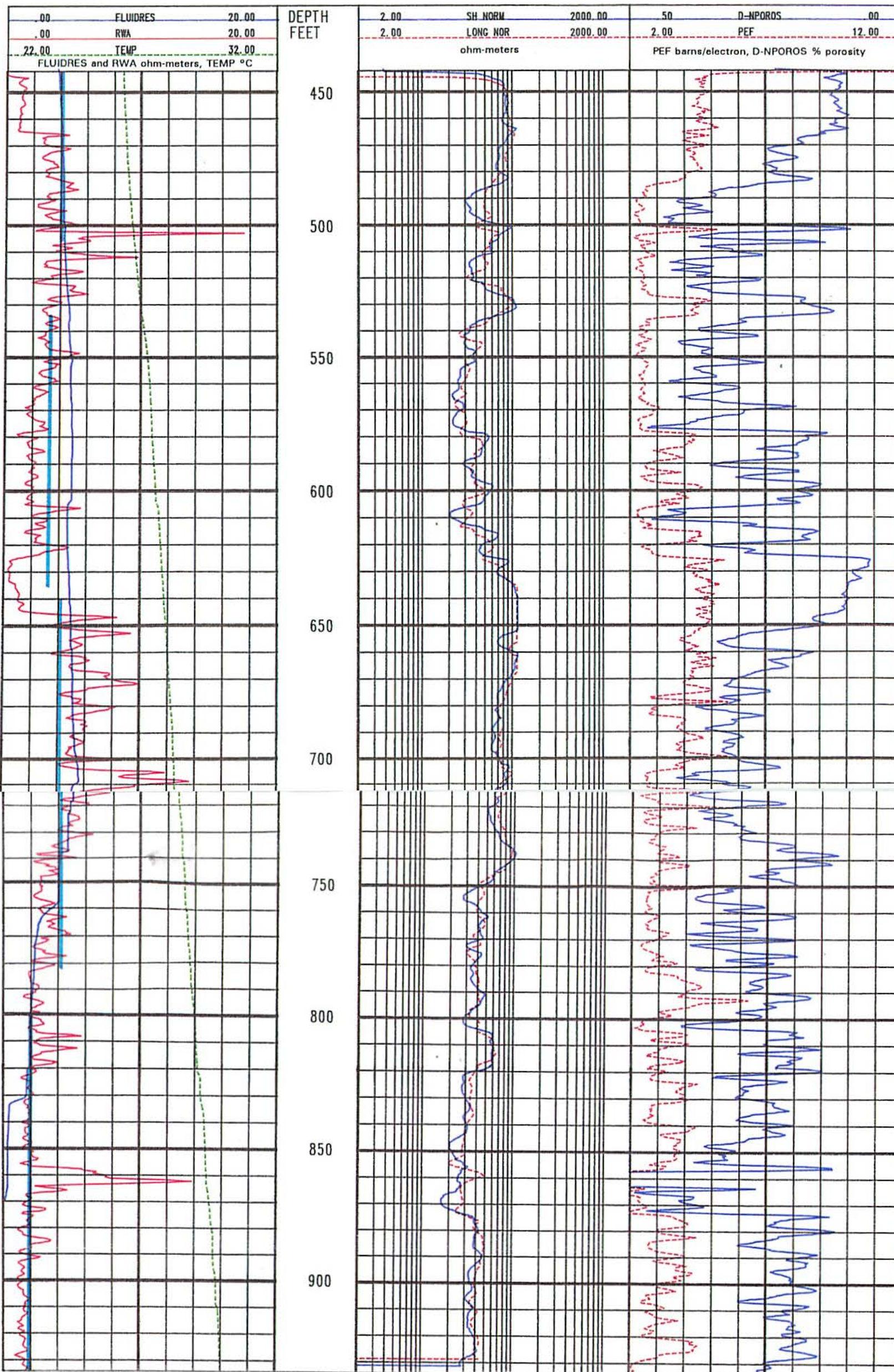


PLATE 6-13, NB A-1. Track 1 contains fluid resistivity (FLUIDRES) and temperature (TEMP) logs, along with an apparent formation water resistivity (RWA) curve. The RWA curve was calculated from the equation: $RWA = Rt(Porosity)^2$, where Rt is the SFLU curve and Porosity is the density-neutron crossplot porosity. Track 1 also contains depth intervals (blue lines) and resistivities of selected water samples collected during pump tests. Track 2 contains 16 inch short normal (SH NORM) and 64 inch long normal (LONG NOR) logs. Track 3 contains density-neutron crossplot porosity (D-NPOROS) and photoelectric factor (PEF) curves. The FLUIDRES, TEMP, SH NORM, and LONG NOR curves were digitized from the hard copies. At 635 to 652 feet on the normal logs the curves flat top because the curves went off scale on the hard copy.

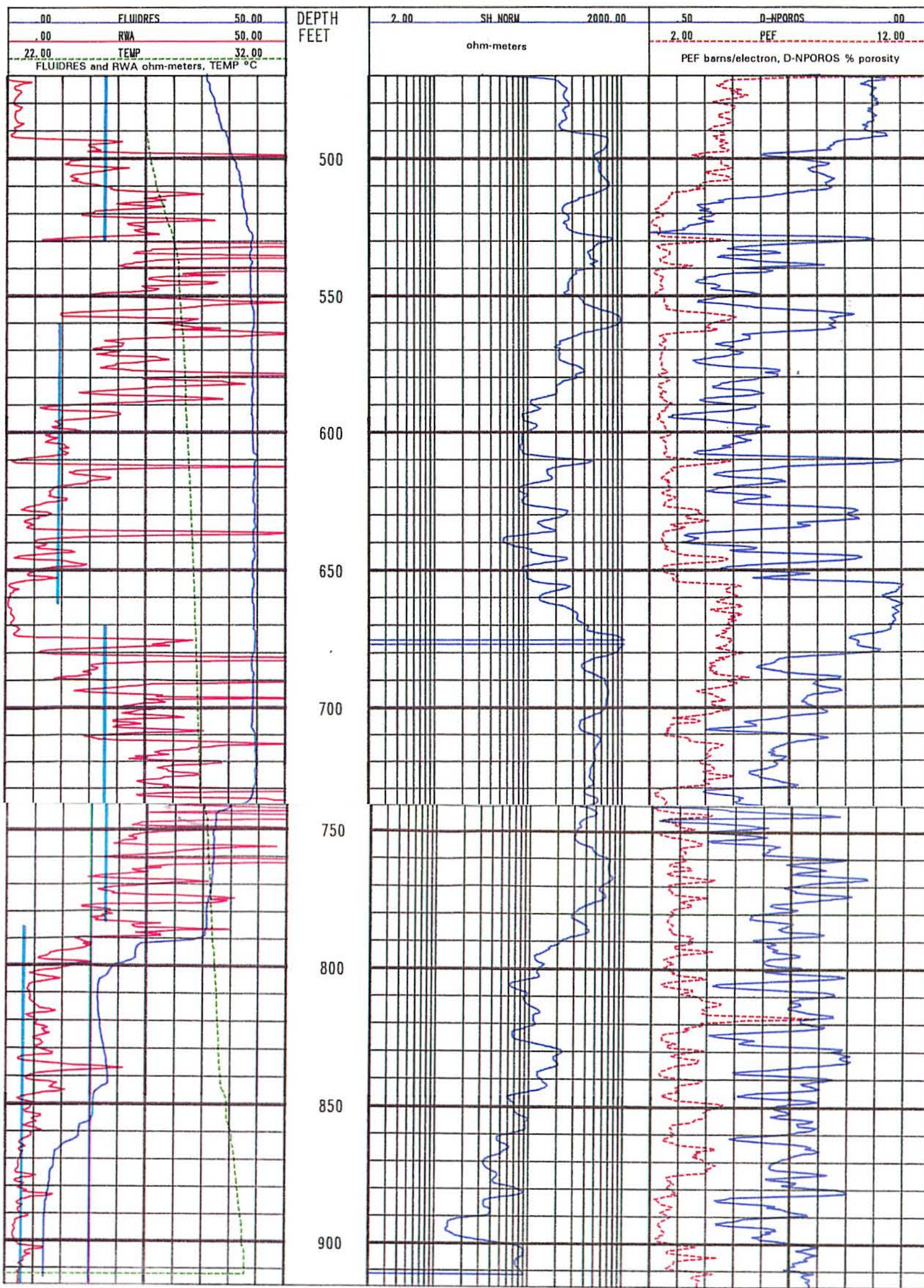


PLATE 6-14, NB B-1. Track 1 contains fluid resistivity (FLUIDRES) and temperature (TEMP) logs, along with an apparent formation water resistivity (RWA) curve. The RWA curve was calculated from the equation: $RWA = Rt(\text{Porosity})^2$, where Rt is the SFLU curve and Porosity is the density-neutron crossplot porosity. Track 1 also contains depth intervals (blue lines) and resistivities of selected water samples collected during pump tests. Track 2 contains a 16 inch short normal (SH NORM) log. Track 3 contains density-neutron crossplot porosity (D-NPOROS) and photoelectric factor (PEF) curves. The FLUIDRES, TEMP, and SH NORM curves were digitized from the hard copies. The interval on the short normal curve at 685 feet that goes to zero is where the curve went off scale on the hard copy.

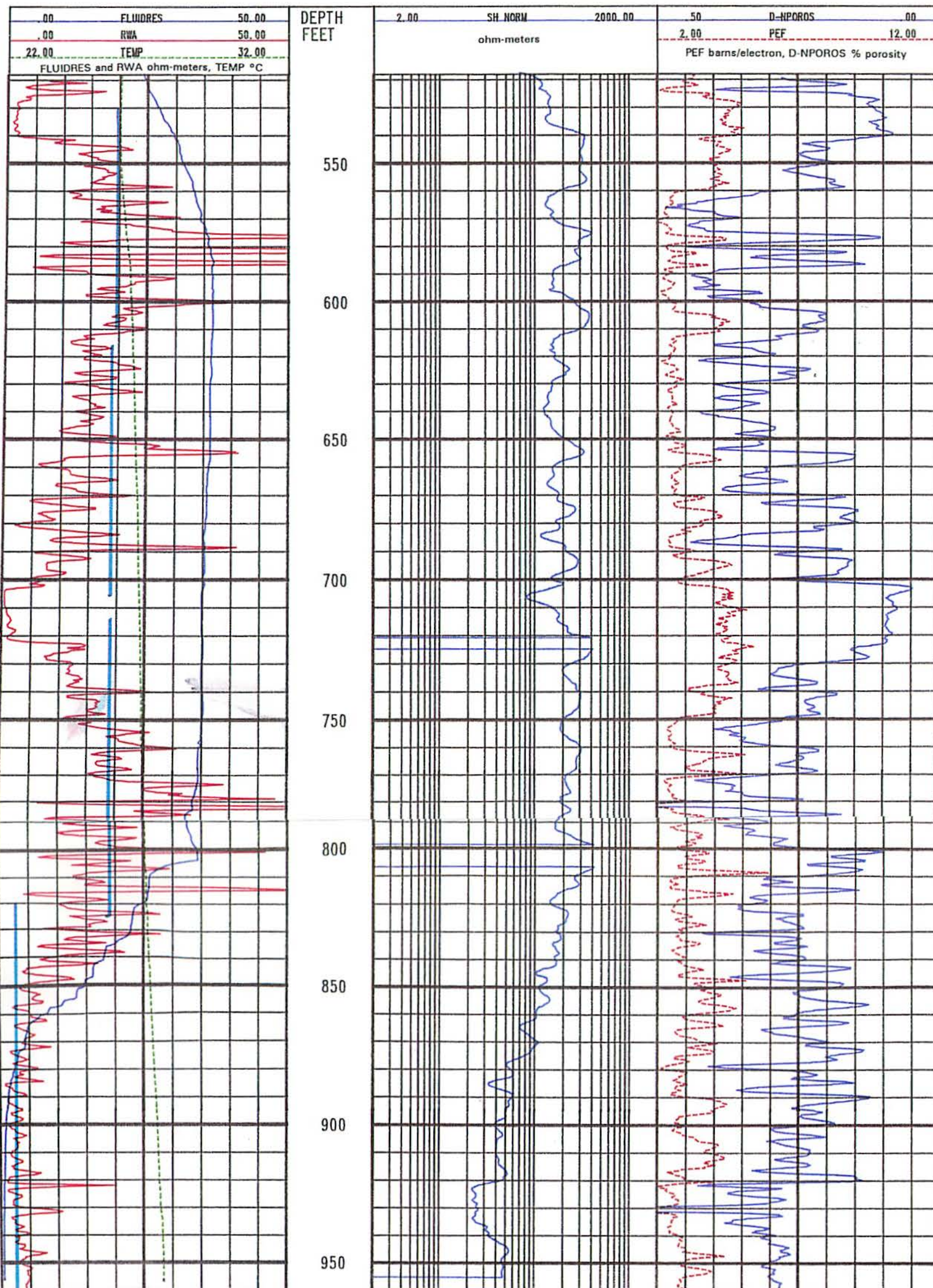


PLATE 6-15, NB C-1. Track 1 contains fluid resistivity (FLUIDRES) and temperature (TEMP) logs, along with an apparent formation water resistivity (RWA) curve. The RWA curve was calculated from the equation: $RWA = Rt(\text{Porosity})^2$, where Rt is the SFLU curve and Porosity is the density-neutron crossplot porosity. Track 1 also contains depth intervals (blue lines) and resistivities of selected water samples collected during pump tests. Track 2 contains a 16 inch short normal (SH NORM) curve. Track 3 contains density-neutron crossplot porosity (D-NPOROS) and photoelectric factor (PEF) curves. The FLUIDRES, TEMP, and SH NORM curves were digitized from the hard copies. Intervals on the short normal curve that go to zero are where the curve went off scale on the hard copy.

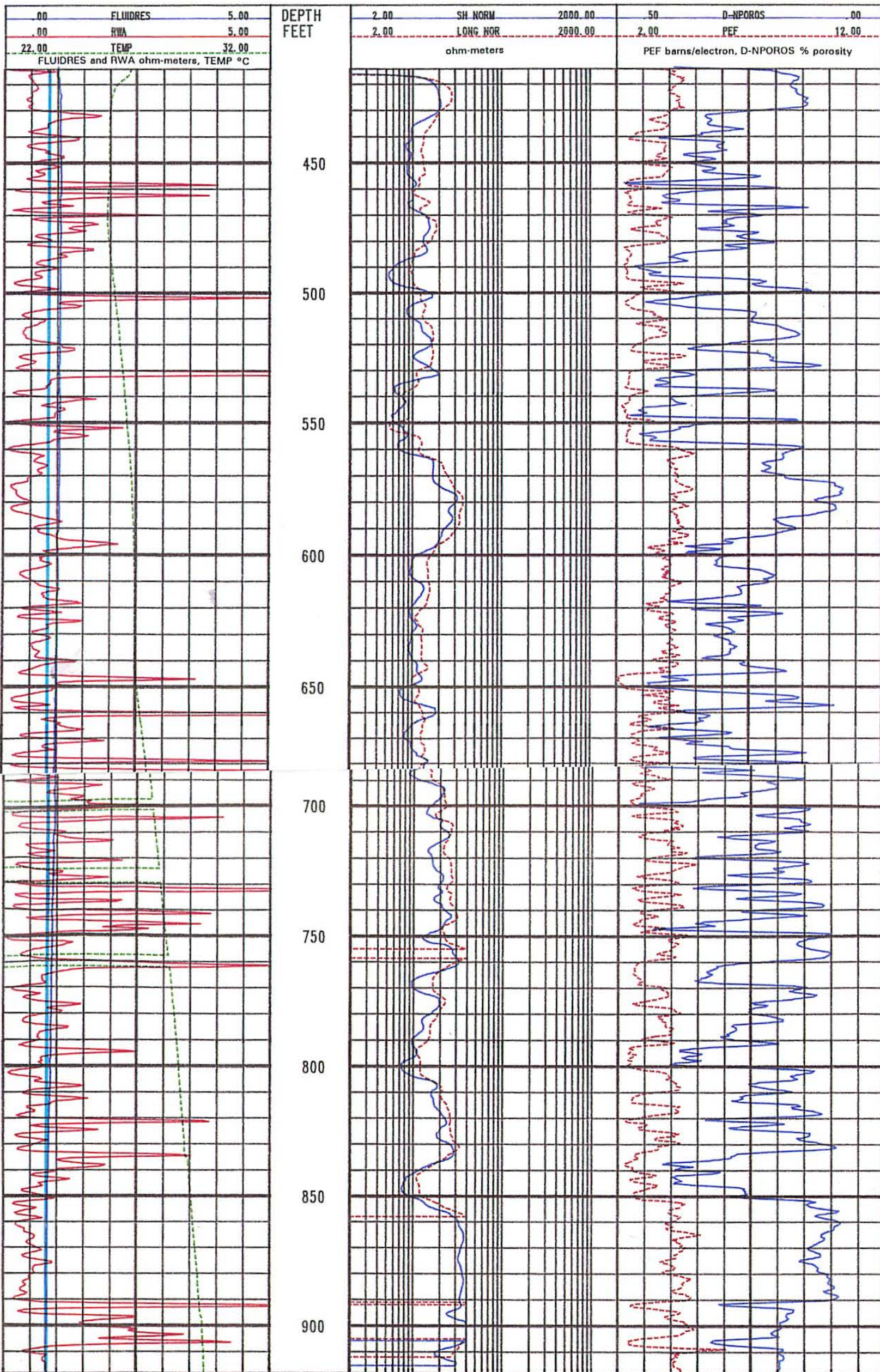


PLATE 6-16, SM C. Track 1 contains fluid resistivity (FLUIDRES) and temperature (TEMP) logs, along with an apparent formation water resistivity (RWA) curve. The RWA curve was calculated from the equation: $RWA = Rt(Porosity)^2$, where Rt is the SFLU curve and Porosity is the density-neutron crossplot porosity. Track 1 also contains depth intervals (blue lines) and resistivities of selected water samples collected during pump tests. Track 2 contains 16 inch short normal (SH NORM) and 64 inch long normal (LONG NOR) curves. Track 3 contains density-neutron crossplot porosity (D-NPOROS) and photoelectric factor (PEF) curves. The FLUIDRES, TEMP, SH NORM, and LONG NOR curves were digitized from the hard copies. Intervals on the temperature curve that go to zero are where there was no data recorded on the hard copy and are an artifact of the digitizing process. Intervals on the long normal curve that go to zero are where the curve went off scale on the hard copy.

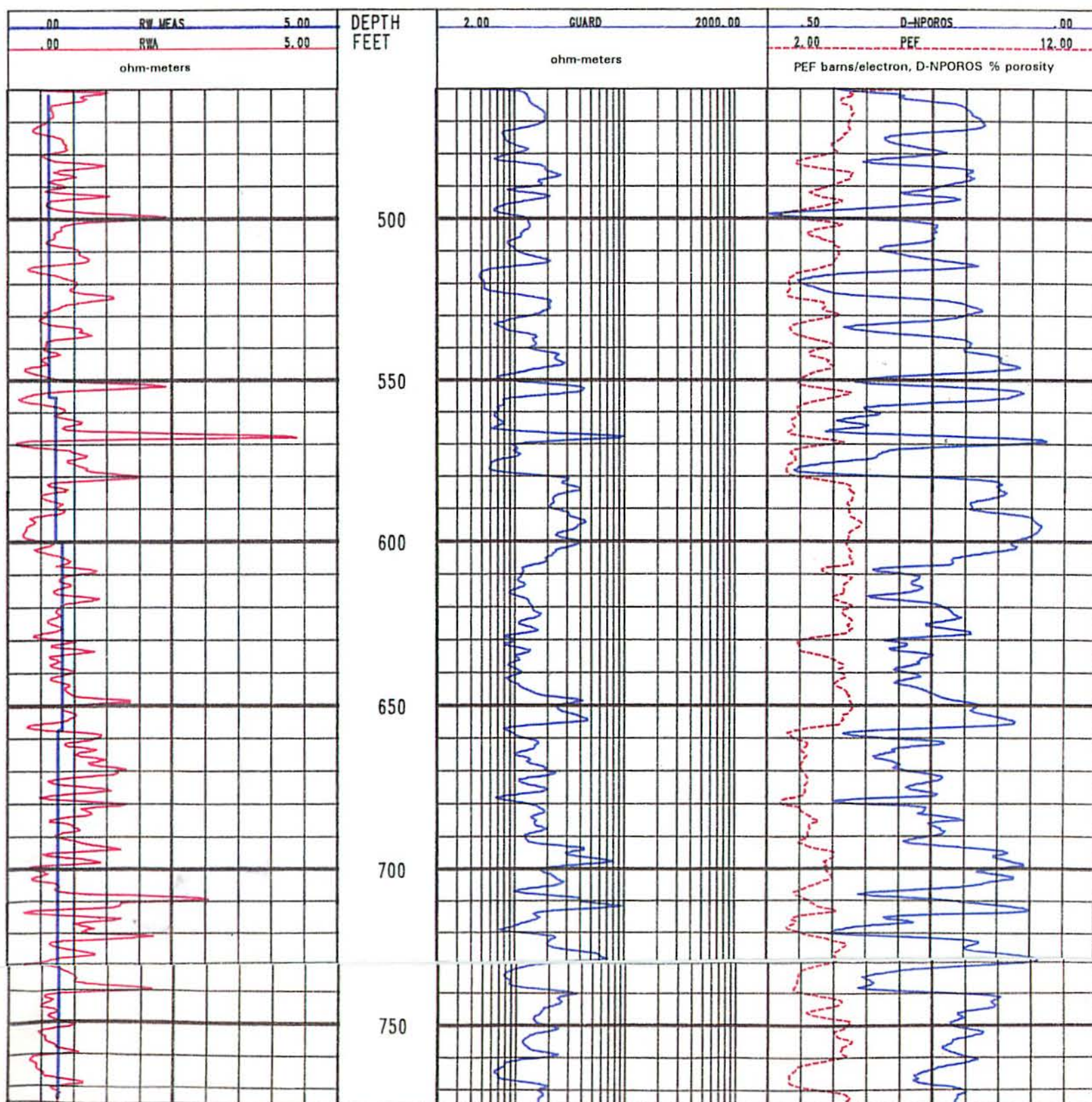


Plate 6-17 SM D. Track 1 contains an apparent formation water resistivity (RWA) curve. The RWA curve was calculated from the equation: $RWA = Rt (Porosity)^2$, where Rt is the guard curve and Porosity is the density-neutron crossplot. Track 1 also contains depth intervals (blue lines) and resistivities of selected water samples collected during pump tests (RW MEAS). Track 2 contains a guard curve. Track 3 contains density-neutron crossplot porosity (D-NPOROS) and photoelectric factor (PEF) curves.

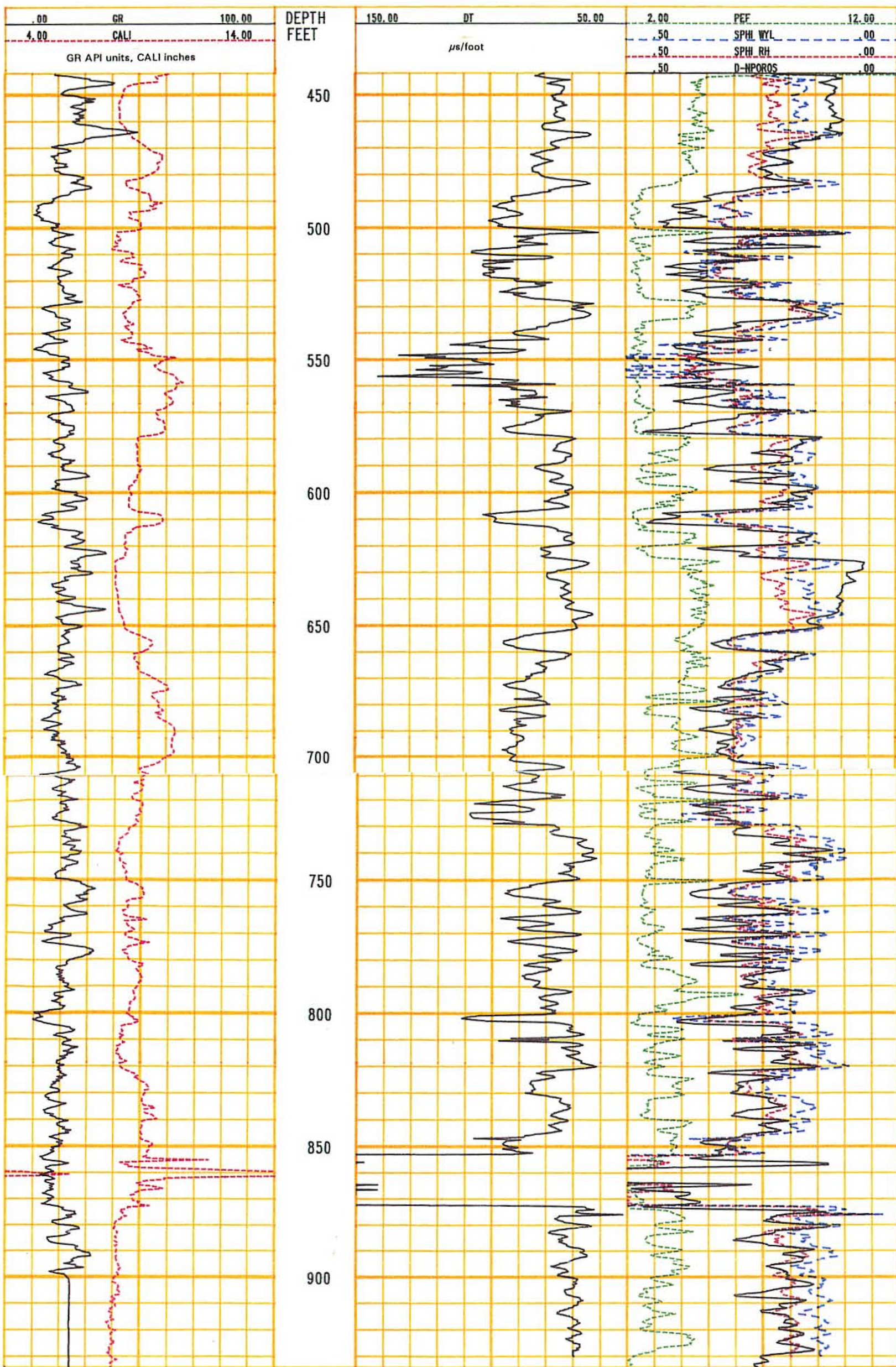


PLATE 6-18 NB A-1. A comparison of sonic and density-neutron crossplot porosities. Track 1 contains gamma ray (GR) and caliper (CALI) curves. The caliper is from the density-neutron log. Track 2 contains the interval transit time (DT). Track 3 contains photoelectric factor (PEF), sonic porosity calculated from the Wyllie equation (Sphi WYL), sonic porosity calculated from the Raymer-Hunt equation (Sphi RH), and density-neutron crossplot porosity (D-NPOROS). The sonic porosities were calculated with a limestone Δt_{matrix} of 47.5 $\mu s/ft$ and a Δt_{fluid} of 206 $\mu s/f$.

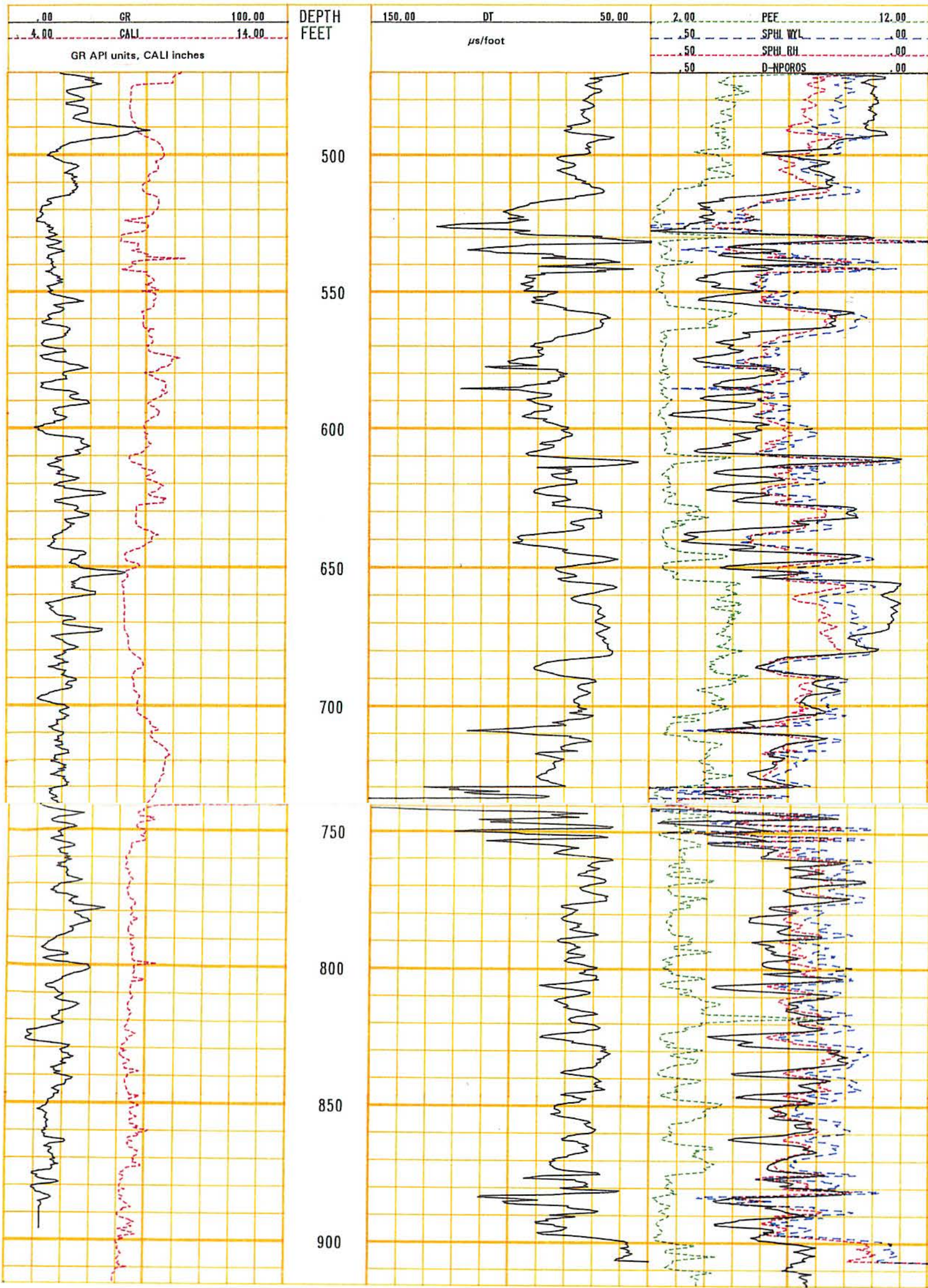


PLATE 6-19 NB B-1. A comparison of sonic and density-neutron crossplot porosities. Track 1 contains gamma ray (GR) and caliper (CALI) curves. The caliper is from the density-neutron log. Track 2 contains the interval transit time (DT). Track 3 contains photoelectric factor (PEF), sonic porosity calculated from the Wyllie equation (SPHI WYL), sonic porosity calculated from the Raymer-Hunt equation (SPHI RH), and density-neutron crossplot porosity (D-NPOROS). The sonic porosities were calculated with a limestone Δt_{matrix} of 47.5 $\mu\text{s}/\text{ft}$ and a Δt_{fluid} of 206 $\mu\text{s}/\text{f}$.